Modeling phenotypic plasticity as an indicator of adaptability in beef cattle

by

William Ryan Shaffer

B.S., Oklahoma State University, 2017

A THESIS

submitted in partial fulfillment of the requirements for the degree

MASTER OF SCIENCE

Department of Animal Sciences and Industry
College of Agriculture

KANSAS STATE UNIVERSITY
Manhattan, Kansas

2022

Approved by:

Major Professor
Dr. Megan Rolf

Copyright

Abstract

Adaptability is an ambiguous term that has taken on several definitions over the history of the field of genetics. At its most simple definition, adaptability refers to the ability of the organism in question to prosper or adjust to a new environment, which also implies the possibility of genetic-by-environment effects (i.e., alleles conferring different value depending on the environment; G×E). However, what this definition entails has grown ever more complex as our understanding of genetics has evolved. Initially, it was simply the consequence of selection, either natural or artificial, changing allele frequencies to match the species to the environment. In livestock production, however, local adaptation, whereby individuals or subpopulations are adjusted to a specific environment, and phenotypic plasticity, or the ability of an individual to perform across a wide variety of environments, are also relevant. Local adaptation can merely be thought of as an extension of selection for subpopulations in different environments. Phenotypic plasticity, however, involves consistency of performance across diverse environments.

Phenotypic plasticity, which can also be thought of as a lack of environmental sensitivity to performance, may be important to livestock producers given the extensive use of seedstock across the United States and world via artificial insemination. However, it is unknown whether it is better to produce many sires suited for a particular environment, which would reduce selection intensity, or many sires selected for phenotypic plasticity, which would allow for an increase in selection intensity. However, selecting for increased phenotypic plasticity would likely have tradeoffs on other selection criteria. Furthermore, how to define, model, and select on phenotypic plasticity is still debatable.

Local adaptation has traditionally been modeled via multi-trait animal models, where each trait is merely the phenotypic records for the trait of interest in different categories of the environment. As an example, yearling weight could be measured in many regions of the United States and the weaning weights in each region would be different traits. Each region then has a genetic correlation, which would correspond to the degree of G×E effects and environmental sensitivity. Phenotypic plasticity, however, can be thought of as an infinite number of "regions" or environments. In such a case, it may be better to characterize the environments, which can be classified by a continuous variable like temperature, by a function. Thus, random regression, which allows for random intercepts and slopes (or higher order polynomials) is the natural extension of a categorical variable into a continuous case for individuals, much like ANOVA and regression are represented by ANCOVA. Individuals with a random slope that counteracts the population expectation to move it towards zero would be considered more phenotypically plastic. The slope variance indicates the degree of G×E effects and variance. Furthermore, the random intercept (which can intuitively be centered around a baseline environment of interest) and random slope share a covariance structure, which define the relationship between baseline production and environmental sensitivity.

Random regression has thus far been applied to evaluate G×E and life cycle or growth curves. The applications to G×E remain limited in the literature and focus mostly on dairy cattle with a few applications to beef cattle. With some notable exceptions, the prevailing trend appears to be an unfavorable relationship between baseline (intercept) performance and environmental sensitivity (slope) in most traits.

Dry matter intake (DMI) and respiration rate were modeled as a function of water restriction (WR) and estimated breeding values (EBV) for the intercept and slope of WR were

computed. Genetic correlations between the intercept and slope, permanent environment (PE) parameters, WR-specific genetic variances, WR-specific PE variances, WR-specific heritabilities, genetic correlations between different levels of WR were computed. Spearman rank correlations between EBVs from different levels of WR, and Beef Improvement Federation (BIF) accuracy at different levels of WR were also examined. Finally, a genome-wide association study was conducted on the intercept and slope traits to evaluate biological pathways and processes that might be contributing to each trait.

The population slope for DMI under WR was -4.10 kg DMI per 100% WR. This indicated that DMI decreased on average as WR increased. Therefore, selection for positive slope EBVs is warranted to increase phenotypic plasticity. The slope variance was great enough at 3.16 $(\frac{kg\ DMI}{100\%\ WR})^2$ such that the phenotypic mean could easily be moved towards zero change in DMI as WR increased. However, the genetic correlation between the intercept, which represents DMI under normal, non-restricted conditions, was highly negative at -0.75. This indicates selection to increase phenotypic plasticity will decrease DMI under ad libitum conditions, which would result in a production loss under normal management. While it was log-transformed, respiration rate followed a similar trend with a much greater magnitude of genetic correlation between the intercept and slope at -0.98. This is interesting as respiration rate is predicted to decrease as WR increases. However, respiration rate may be a proxy for shedding metabolic heat generated from production (e.g., milk yield or muscle deposition and weight gain), which would explain this apparent conundrum.

In general, estimated genetic variance decreased by nearly half from just greater than two $kg\ DMI^2$ at 0% WR to less than one $kg\ DMI^2$ at 50% WR; however, uncertainty was large. There was no evidence of a PE effect until about 40% or greater WR and, even then, the

estimated variance was relatively small compared to the genetic variance. Log-transformed respiration rate variances were not shown for respiration rate given the difficulty in interpreting a transformed variable. Heritabilities of DMI and respiration rate varied by group, due to the inclusion of heterogeneous variances by group. Dry matter intake heritability followed a similar trend as the genetic variance, with estimates at 0% WR between 0.25 and 0.40. However, the declining trend was much smaller. It is worth noting the 95% credible intervals highly overlapped, indicating there may be little probability for a difference in heritability as WR increases. Interestingly, the trend for the DMI repeatability was even less steep, likely due to the evidence for PE effects as WR increased. Respiration rate WR-specific heritabilities and repeatabilities followed a similar pattern. However, there was little evidence for a heritable component past approximately 25% WR as the 95% credible intervals overlapped zero. Therefore, genetic correlations and accuracies of respiration rates were not considered past 25% WR for respiration rate.

In general, the Spearman correlations between the EBVs at different levels of WR and genetic correlations between different levels of WR were in near agreeance. This is generally to be expected. Genetic correlations for DMI between different water restricted environments were generally high except at the most divergent WR values (e.g., 0% and 40% or 50%). Genetic and Spearman correlations between the most divergent environments for DMI were as low as 0.80, which is high and indicates small/few G×E effects and predictions in one environment should be accurate in others. The correlations for respiration rate at divergent WR values were even greater, only reaching as low as 0.975. However, this was only between 0% and 25% WR due to a lack of heritability beyond this point. While the correlations generally indicate selection based on non-restricted environments is an accurate indicator of performance in water restricted

environments, it is worth noting the decreasing genetic variance is still potentially of concern for long term genetic improvement. Finally, the BIF accuracies generally increased as WR increased (with large 95% credible intervals) for both DMI and respiration rate. This is likely because of the greater amount of data present at higher WR levels or decrease in overall variance, which would likely have greater influence on the EBVs.

Finally, GWAS was performed for both the intercept and slope of DMI and respiration rate. For DMI, metabolic signaling and exocytosis pathways and biological gene ontology (GO) terms were enriched for the intercept. In contrast, the slope for DMI was mostly related to central metabolism, including fat metabolism. A previous, traditional GWAS (i.e., no G×E included) also identified fat metabolism pathway genes for DMI, which may indicate models not accounting for G×E pick up signals from both the intercept and slope that are strong enough in both. This would corroborate with the high genetic correlation between the intercept and slope. Due to the lack of a heritable component at most values of WR, respiration rate GWAS was not conducted.

Respiration rate and DMI were also modeled in a random regression model with a temperature humidity index (THI) as a covariate to model heat stress. Analyses mirror the WR covariate. However, there was less data available for respiration rate as two of the seven groups did not reach high enough THI levels. The population slope for DMI was -0.046 $\frac{kg\ DMI}{1\ unit\ THI}$, indicating daily DMI decreases, on average, as THI increases. This would be expected a priori and corresponds to a nearly one kg DMI decrease as THI approaches 90. Multiplied across an entire feedlot population, this represents a serious loss of production. Fortunately, the point estimate and bounds of the 95% credible interval for the slope variance indicate there is ample room for selection to improve phenotypic plasticity and move the population slope towards zero.

Consistent with the G×E literature, there is an unfavorable genetic correlation of -0.78 between selection for increased production under thermoneutrality (the intercept) and environmental sensitivity (the slope). This indicates there is a tradeoff in selecting for phenotypic plasticity and productivity under optimal conditions.

The population slope for the log-transformed respiration rates was positive, which would be expected as a response to heat stress a priori. While there was a great amount of uncertainty, the genetic correlation between the respiration rate intercept and slope under THI was negative at both bounds of the 95% credible interval. This is initially strange, as selection to reduce respiration rate under thermoneutral conditions would be expected to increase environmental sensitivity and decrease phenotypic plasticity whereas selection to increase respiration rate under thermoneutral conditions would apparently increase phenotypic plasticity. However, respiration rate under thermoneutral conditions has been associated with shedding metabolic heat generated from production. Thus, selection to increase respiration rate (and possibly production) in thermoneutral conditions would appear to decrease environmental sensitivity. In reality, selection to increase respiration rate in thermoneutral conditions would likely change the frequency of alleles associated with production. Therefore, the seemingly nonsensical relationship between the additive genetic intercept and slope is not favorable and selection to increase respiration rate/production in thermoneutral conditions would decrease production in heat-stressed conditions and increase environmental sensitivity.

The THI-specific genetic variance for DMI rapidly decreased as THI increased, but appeared to stabilize past 80 THI at about 50% of thermoneutral conditions. At lower levels of THI, there was no evidence of a PE effect, but there was evidence for moderate PE effects at higher THI. The heritability and repeatability of DMI within each group reflected the trends of

the variance components with heritability point estimates ranging from 0.3-0.4; but a great degree of overlap of the 95% credible intervals made it difficult to determine whether the decrease in heritability and repeatability was meaningful. As would be expected, the repeatability was similar to heritability at low THI, but declined less than heritability at high THI due to the additional PE variance. Respiration rate was very lowly heritable, with point estimates ranging from 0.02 to 0.04 at 70 THI for the different groups. However, uncertainty placed the point estimates anywhere from just above 0 to 0.08, indicating respiration rate is lowly heritable under varying THI.

Genetic correlations between different levels of THI for DMI or respiration rate were both low. Genetic correlations for DMI and respiration rate between 70 and the upper bound of THI (85 for DMI and 80 for respiration rate) were 0.50 and 0.40, respectively. This is low and indicates performance at thermoneutrality is not a great indicator of performance in heavily heat stressed environments. Spearman correlations between the EBVs at the same THI levels were likewise low, with Spearman correlations between THI levels of 0.40 and 0.20 for DMI and respiration rate, respectively. Therefore, phenotypic plasticity likely plays a large role in environments with high THI. The BIF accuracies for EBVs at different levels of THI generally increased as THI increased. However, past 75 THI, there was no increase in accuracy observed.

The GWAS for DMI intercept and slope under THI identified several variants associated with the traits. The intercept seemed to be mostly associated with energy balance signaling to generate adenosine triphosphate generation, whereas the slope was associated with a variety of pathways, including gastric acid secretion, cAMP signaling, Ras signaling, and fat metabolism. Most of these are growth pathways, but fat metabolism has been implicated in previous studies

and provides a connection to pathways identified for the intercept, because energy balance signaling may be related.

The intercept for respiration rate was the most interesting, as cardiomyopathy and heart function were the primary GO terms and pathways implicated. Cardiomyopathy and heart function are interesting, as high-altitude disease pulmonary arterial pressure and similar issues in the feedlot are thought to be related. A high-altitude disease GWAS identified similar gene candidates that were associated with heart function and cardiomyopathies. This may indicate respiration rate in thermoneutral environments could be related to either the ability of the animal to properly supply oxygen or a relationship between heart issues in the feedlot and high-altitude disease. The associated variants for the slope, however, were associated with GO terms and pathways related to metabolic signaling and metabolism. This strengthens the previous untested hypothesis relating respiration rate to increased metabolic heat.

Table of Contents

List of Figures

List of Tables

Chapter 1 - An Introduction to Climate Adaptability and Applications in the Genetic Evaluation of Beef Cattle

Introduction

Adaptability refers to the ability of an organism to adjust to new environments (Adger *et al.*, 2005). Adaptability can refer to the evolution of populations due to selection pressure (classical adaptation or classical response to selection), selecting individuals more suited for a specific, often extreme environment (local adaptation), or selecting individuals who can maintain phenotypic stability across environments (phenotypic plasticity; Scheiner and Lyman, 1989; Jensen *et al.*, 2008; West-Eberhard, 2008; Grandin and Deesing, 2013; Berry, 2018). Unlike classical adaptation, local adaptation and phenotypic plasticity imply the value of genetics differs as the environment changes, or genetic-by-environment interaction effects (G×E; Falconer and Mackay, 1996). The objectives of this review were to discuss:

1) the background of adaptability and different modes of adaptation

2) the biological basis of adaptation

3) what mode of adaptation is "best" for the beef industry

4) the current inclusion of genetic evaluation usage in the beef industry and likely obstacles to implementing adaptability

5) modelling local adaptation and phenotypic plasticity

6) the genetic architecture of phenotypic plasticity

7) current literature modelling local adaptation and phenotypic plasticity.

Overview of Modes of Adaptation

Quantitative and population geneticists traditionally focused on classical adaptation. However, each tended to study classical adaptation slightly differently. Population geneticists often studied the change in genetic variation through long term selection experiments (Yoo *et al.*, 1980; Berry, 2018). Quantitative geneticists, on the other hand, were more interested in short-term selection response in populations and the rate of genetic gain. This interest in the response to selection led to the advent of tools such as the breeder's equation (Falconer and Mackay, 1996). This is not necessarily different from a population geneticist's point of view, however, as the rate of selection process is directly related to the amount of genetic variance available (Bourdon, 2000). However, classical adaptation fails to account for environment-specific differences. Selection differing by environment constitutes G×E (Falconer and Mackay, 1996).

A G×E exists when the difference in performance between genotypes or alleles changes across environments (Figure 1.1; Falconer and Mackay, 1996). Genetic-by-environment interactions can be characterized in different formats. Assuming categorical environments and genotypes, Figures 1.1A and 1.1B demonstrate G×E where the relative performance of two alleles differs between two environments. Figure 1.1A demonstrates locus-level, categorical G×E with alleles showing re-ranking of performance. Figure 1.1B demonstrates categorical G×E whereby the ranking of alleles is preserved between environments, but the magnitude of their differential effects on performances changes. Figure 1.1C demonstrates categorical G×E with re-ranking at the genotype level. Figure 1.1 demonstrates G×E at a single locus, but local adaptation and phenotypic plasticity are generally characterized genome wide (Klingenberg, 2019; Durbin, 2020). Fundamentally, G×E are driven by the inclusion or exclusion of loci with differential effects on performance as the environment changes (Via and Lande, 1985; Schou *et al.*, 2019).

When the cumulative differential effects across many loci become large enough, the resulting genotypes show environment-specific advantages and re-rankings of genotypes (e.g., Figure 1.1).

Local adaptation emphasizes selection in an "extreme" or specific (Hartl and Clark, 2018) environment (e.g., Jensen *et al.*, 2008; Crawford *et al.*, 2016). As an example, high altitude disease is a selection concern in mountainous areas (Crawford *et al.*, 2016), but is generally not a concern at lower elevations. Local adaptation traits are typically evaluated in conjunction with economically relevant traits (ERTs) in animal breeding, or traits which are selected on to increase profit. This implies a multi-trait model to assess the genetic correlations between the ERT and adaptation trait (e.g., Prayaga *et al.*, 2009; Crawford *et al.*, 2016). However, the genetic correlation between the locally adapted trait and the ERT are likely different in environments where the locally adapted trait is less of an issue (Prayaga *et al.*, 2009; Schou *et al.*, 2019). Different genetic correlations between traits across environments imply different genetic effects in different environments, or G×E (Falconer, 1952; Via and Lande, 1985; Falconer and Mackay, 1996). In particular, genetic correlations between a trait in two discrete environments constitute a direct measure of G×E on a "single" trait (Falconer, 1952; Via and Lande, 1985; Falconer and Mackay, 1996).

Meanwhile, phenotypic plasticity, unlike local adaptation, describes how a trait changes over an environmental continuum through a reaction norm (Klingenberg, 2019). In a reaction norm, the phenotypic performance of a genotype (e.g., strains of plants, breeds, individuals, genotypes at a locus, etc.) is regressed on an environmental covariate (Klingenberg, 2019). The slope of the reaction norm characterizes the environmental sensitivity or response of a genotype to different environments and characterizes the effects of G×E (Falconer and Mackay, 1996; de Jong and Bijma, 2002). To be explicit, the difference between phenotypic plasticity and local

adaptation is that phenotypic plasticity is concerned with an environmental continuum, whereas local adaptation is concerned with categorical environments. This will be an important distinction in the discussion on model specification.

Classical Adaptation in Natural Populations and Genetic Variation

In the past, adaptability typically referred to "classical adaptation" where the maintenance of genetic variation and the influence of effective population size on a population's ability to adapt to environmental changes were key components of studies (Jensen *et al.*, 2008; Berry, 2018). Maintaining genetic variance is important, as it enables the ability of a population to respond to greater environmental pressures or to migrate to new environments (Jensen *et al.*, 2008; Chevin *et al.*, 2010). For many species, climate change creates selective pressure as environments change (Hoffmann and Sgrò, 2011), which is why population geneticists are often interested in classical adaptation.

Genetic change, or the rate of adaptation, is dependent on the selection pressure by the environment, the genetic variation, and the accuracy of selection (Falconer and Mackay, 1996; Pritchard and Rienzo, 2010). Under natural selection, the accuracy of selection is the heritability (Bourdon, 2000). Furthermore, long term selection does not seem to appreciably exhaust genetic variation (Berry, 2018; Martinez *et al.*, 2000), assuming the trait is well described by the infinitesimal model (Falconer and Mackay, 1996; Hill, 1998), and that linkage patterns break up through recombination (Barton and Charlesworth, 1998). This has been demonstrated by 60 years of selection (roughly 12-15 generations) on Holstein milk production, which still today shows a linear trend in genetic potential (CDCB, 2020). Further, various *Drosophila melanogaster* experiments over nearly 90 generations (Yoo *et al.*, 1980) reported similar

conclusions, although genetic correlations with fitness eventually prevented further selection (Yoo *et al.*, 1980; Hartl and Clark, 2018). Variants of relatively large effect, however, may be under greater selection and fix at a rate similar to simple Mendelian selection (Pritchard and Rienzo, 2010). The rapid fixation of large effect, de novo alleles entering a population is often referred to as a selective sweep in population genetics (Pritchard and Rienzo, 2010). The selection pressures can vary by local environmental conditions in demes, meaning different variants may be under selection (Falconer and Mackay, 1996; Hartl and Clark, 2018). In local environments, it is thus possible to imagine how genetic variant effects or the number of genetic variants themselves may be different. This will be explained in greater detail in the discussion of genetic covariances and correlations.

Given the propensity to maintain genetic variance, populations are expected to continuously make genetic progress towards the direction of selection barring bottlenecks/extreme drift, unfavorable correlations with fitness, and an environment permissive to life (Brotherstone and Goddard, 2005; Zhang *et al.*, 2002; Zhang *et al.*, 2004). The assumptions of the infinitesimal model are not completely realistic, however, so allele frequencies are expected to slowly move towards fixation due to selection and drift (Falconer and MacKay, 1996; Hartl and Clark, 2018). For genetic variance to be maintained or increase, new genetic variation must be entering the population through mutations at a rate equal to or greater than fixation due to selection and drift (Lynch and Walsh, 1998). In the context of G×E, this provides a basis for divergent selection within population demes, whereby populations may become locally adapted (Falconer and Mackay, 1996; Hartl and Clark, 2018). Overall, the genetic variance for quantitative traits is not expected to decrease with selection, but different subsets of genetic variation may be under selection and different variants may fix or approach

fixation. This will be of great importance in the discussion of the development and decay of genetic correlations related to G×E.

Animal Breeding, G×E in Quantitative Genetics, and the Volatility of Genetic Covariances Between Traits in Different Environments

In animal breeding programs, selection is imposed on artificial characters rather than fitness. The selection pressure applied to a trait in animal breeding programs is dependent on economic benefit or personal goals, rather than an adaptive advantage (Hazel,1943). Generally, selection is simultaneously applied to many economically important traits breeders wish to improve (Bourdon, 2000), rather than fitness. In genetic evaluations, genetic covariances provide a measure of shared genetic background between traits, which indicates whether selection of one trait would be expected to impact the other (Bourdon, 2000). A genetic correlation indicates the strength of this relationship and allows information for one trait to contribute towards the estimate of another trait, which increases the accuracy of prediction (Henderson and Quaas, 1976).

In many genetic evaluations, however, genetic correlations between traits in one environment, or even when many environments are represented, are often erroneously assumed to be representative of all environments (Schou *et al.*, 2019). Genetic correlations between traits, including fitness, tend to change over time and across environments (Schou *et al.*, 2019). This can be explained by the inclusion of new variation (i.e., genetic mutations) for each trait, the fixation of pleiotropic variants contributing to the covariance, the decay or formation of linkage disequilibrium, and the inclusion of new physiological pathways as environments change (Hazel,

1943; Via and Lande, 1985; Falconer and Mackay, 1996; Hartl and Clark, 2018; Schou *et al.*, 2019). Indeed, as environments become more dissimilar, different subsets of variants in other physiological/biochemical pathways and differential regulation of gene expression become relevant, leading to weaker genetic correlations (de Jong, 1995; Falconer and Mackay, 1996; Sgrò and Hoffman, 2004; Schou *et al.*, 2019). Genetic correlations have also been shown to vary within location as seasonal differences change the environment, leading to further volatility in genetic correlations (Prayaga *et al.*, 2009). As a result, variability of genetic correlations between traits may lead to decreased accuracy of selection (Bourdon, 2000) across environments, which would be detrimental towards genetic progress.

The Role of Adaptability in Beef Cattle Selection

In beef cattle, the relatively few adaptability studies tend to focus on local adaptation rather than phenotypic plasticity (e.g., Prayaga *et al.*, 2009; Durbin, 2020; Speidel *et al.*, 2020). In other words, most development has been focused on traits considered important in a subset of environments, the development of breeds that excel in locally adapted traits, and on the assessment of genetic correlations of local adaptation traits with ERTs. A brief list of examples includes genetic correlations between traits such tick load, fecal egg count, fly load, and rectal temperature (Prayaga *et al.*, 2009), hair shedding (Durbin, 2020), and pulmonary arterial pressure (PAP; Crawford *et al.*, 2016) with ERTs. Recently, some local adaptation expected progeny differences (EPDs) have also been recently introduced in national genetic evaluations. Currently, the American Angus Association has developed and released genetic evaluations for PAP and hair shedding EPDs (American Angus Association, 2020).

Historically, the focus on locally adapted traits seems to have been driven by seedstock producers selling germplasm locally. However, this is hard to verify explicitly. Artificial insemination (AI), however, allowed breeders to use sires from across the world raised in very different environments (Banos and Sigurdsson, 1996; Brotherstone and Goddard, 2005). Furthermore, scalability of beef cattle studies and, until recently, computational power (Robinson, 1991) has limited or continue to limit studies of G×E. Given the beef industry has begun to adopt AI techniques in many of the larger operations, with as many as 29-53% of the larger operations adopting AI (Beef Magazine, 2013; USDA APHIS, 2017), sires are likely being used in an extensive array of environments. Therefore, G×E may need to be considered for accurate selection, similar to the suggestion by Schou *et al.* (2019) for dairy cattle.

With growing access to AI, a handful of elite sires are often used extensively across the country and the globe (Brotherstone and Goddard, 2005; Mulder *et al.*, 2006). Even for commercial herds not utilizing AI, sires may be sourced from AI herds or are progeny from commercial sires/grandsires who were conceived using AI. Therefore, it may be more prudent to select for more phenotypically plastic individuals who can perform at a high level in a wide variety of environments, rather than those adapted to a specific environment. Such individuals would be considered "adaptable" to a wide variety of environments. However, it is unclear whether G×E effects are sufficiently large to warrant inclusion in genetic evaluation. Furthermore, if G×E effects are sufficiently large, it remains unclear whether local adaptation, phenotypic plasticity, or a mixture of the two would be ideal in the beef industry. This is a problem not currently addressed in literature. In environments where local adaptation is considered necessary (e.g., the PAP trait), selection for local adaptation traits can be integrated

into a system where selection emphasis is also placed on phenotypic plasticity. This clearly indicates the two methods do not need to be mutually exclusive.

In United States beef breed genetic evaluations, records from all environments are used and the EPD is assumed to represent the best or average prediction of an individual's general performance across all environments where records are sourced (Mulder and Bijma, 2005; Dominik and Kinghorn, 2008). In other words, the genetic effect is averaged over environmental effects present. However, if environments are diverse and the effects of G×E are large, then an EPD averaged over all environmental factors is likely a poor representation for many environments. One possible solution is to implement regional genetic evaluations for ERTs impacted by G×E. This poses its own set of difficulties, however, including the potential for large sacrifices in producer confidence, accuracy of prediction if the number of records for each environment is low, and tractability of the genetic evaluation.

Producer Confidence and Genetic Evaluation Tractability

In a 2014 survey comprising 839 *BEEF* magazine subscribers, most respondents required birth weight EPDs to make bull purchasing decisions, with the percentage increasing from ~68% for herds less than 50 head of cattle to ~76% for herds of 500 head of cattle or more (Beef Magazine, 2013). Meanwhile, requests of genetic information for purchasing decisions rapidly dropped with herd size for the weaning Weight EPD (ranging from 46.1% to 59.1%), for the milking ability EPD (39.5% to 56.4%), and for the calving-ease direct EPD (58.5% to 61.8%). Other traits and tools, such as economic indices, carcass traits, docility, scrotal circumference, stayability, and the heifer pregnancy EPDs showed less than ~50% usage, particularly in larger herd for which economic indices, heifer pregnancy, and stability EPDs showed less than 30%

usage (Beef Magazine, 2013). Nonetheless, it is worth noticing the survey group potentially represents a more sophisticated sub-population of producers, thus likely yielding upwardly biased usage estimates relative to the general population. The failure to adopt many EPDs and indices could indicate diverse breeding objectives rather than a failure to adopt the technology entirely; however, producers might also only trust certain EPDs or have a narrow range of focus in their breeding objectives. The low usage of economic indices might indicate a lack of comprehension or trust in current technologies.

These findings are consistent with the conclusions of a review by Turner *et al.* (2004), whereby producers seemed to value birth weight EPDs highly but tended to put more trust in phenotypic measurements for other traits. Given the average age of American producers is 57.5 years (USDA NASS, 2017), which is similar to the *BEEF* magazine survey, most producers would have likely sought post-secondary education (if they received any) in the early 1980s. Animal breeding curricula may not have included much information about EPDs during this time period. Therefore, most education was probably obtained through word-of-mouth or extension resources. Overall, the data indicates scarce EPD usage, which may or may not be due to issues with confidence in and/or understanding of EPDs and economic indices, as well as with developing comprehensive breeding objectives. This is concerning, given EPDs are arguably the best prediction tool available to producers to predict genetic merit (Bourdon, 2000).

This data is concerning, as there is the potential implication of incorporating G×E introducing additional knowledge barriers to producers. However, it may be that producers also lack confidence due to recognizing the EPD averaged over environmental factors does not represent their environmental conditions. In such a case, adoption of genetic tools may increase. Overall, it remains unclear whether tractability and confidence in EPDs remains an issue,

whether the introduction of G×E would introduce knowledge barriers, or if the inclusion of G×E might improve producer confidence.

Current Practices in Production and Research

Genetic variances and covariances derived from one or a subset of environments are extended to most, if not all, environments (Schou *et al.*, 2019) and resulting selection decisions and EPDs are assumed to be an accurate representation. In other words, contemporary groups or other group factors capturing environmental variance represent the environments from which they are derived. Within beef breed association genetic evaluations, this likely is not a large problem as contemporary groups cover a wide range of environments and estimates would be unbiased, even if the estimates are averaged over environments. The issue, however, is likely much more pervasive in genetic evaluations not performed by large, multi-institutional collaborations or in prototype genetic evaluations where few, non-random environments are represented (Tempelman, 2010). If genetic variances and covariances change across environments, it may account for some of the discrepancies between estimates across studies utilizing the same populations (e.g., female fertility estimates in Upshaw *et al.*, 2021). Oftentimes, the data utilized is derived from a highly limited set of environments or a specific region; therefore, estimates of (co)variances and functions of (co)variances are only reflective of the represented region. Within classroom instruction, commercial evaluation, and extension efforts, however, G×E is commonly assumed to be zero or inconsequential, and genetic correlations and predictions may be treated as representative of other populations.

If G×E effects are non-negligible, then adaptability addresses this oversight. The little attention adaptability receives, however, tends to be centered around local adaptation, which

often addresses the problem in a single, potentially extreme environment as previously discussed. For G×E that affects evaluations of traits relevant across an environmental continuum, adaptability should be centered on phenotypic plasticity. Animals are often raised in diverse environments across the US and then transported to a relatively homogeneous set of environments for the feedlot phase of production. For local adaptation, the beef industry has relied on breed development and recent local adaptation EPDs to develop locally adapted herds rather than selecting for locally adapted traits from current, high-performance breeds (Hoffman, 2010; Naskar *et al.*, 2012). Given the lack of consideration of G×E in commercial evaluation, it is unclear whether breed development to suit individual environments or selection of environmentally insensitive (phenotypically plastic) individuals within high-performing breeds is the best strategy to maximize production efficiency with the current structure of the beef industry. It is possible the best solution is a combination of the two approaches, which will still allow breeders to capitalize on crossbreeding different lines to achieve breed complementarity and heterosis for their environment. This approach would allow for selecting locally adapted breeds while identifying environmentally insensitive individuals.

Evaluating G×E in a Multi-Trait Model

The relatively few adaptability genetic evaluations in beef cattle production have centered around local adaptation, where the adaptability trait (such as PAP) is genetically correlated with ERTs in the environment. The genetic correlations between the local adaptation trait and the ERT across different pairwise environments can be used to evaluate the extent of G×E and whether the local adaptation trait is truly environmentally specific. Similarly, G×E used to be assessed by analyzing the genetic correlations of a single ERT between discrete

environments or regions in a multi-trait genetic evaluation (Falconer, 1952; Falconer and Mackay, 1996; Via and Lande, 1985). For brevity, this type of evaluation will be referred to as a multivariate G×E genetic evaluation or model throughout. In the multivariate G×E evaluation, a single ERT in each discrete environment would be considered a separate trait and a genetic covariance between the ERT in different environments would be estimated. This methodology, however, requires the specification of the discrete environments (and enough data present within each environment for a separate evaluation), which is often not intuitive or easily determined. It also generates as many predictions for one trait as there are defined regions, potentially leading to further confusion for producers and a lack of tractability. The criteria likely used to define discrete environments will likely change as the context of the evaluation or study changes. No beef breeds within the United States have implemented a multi-trait G×E evaluation. While this approach is likely not useful for large-scale genetic evaluation or modeling phenotypic plasticity, it remains a useful approach for local adaptation studies that seek to understand the impact or extent of G×E.

To gauge the extent of G×E between the discrete environments, the magnitude of the genetic correlations between a trait in different environments can be assessed. If the magnitude of the genetic correlation is closer to zero, then G×E effects are meaningful and local adaptation or phenotypic plasticity should be considered, depending on the environmental differences between regions and the traits in the genetic correlations. A genetic correlation closer to one indicates little G×E (Falconer, 1952; Via and Lande, 1985; Falconer and Mackay, 1996) and local adaptation and phenotypic plasticity would likely not be as important to consider. For a more in-depth review of the theory and implementation of multivariate G×E genetic models, see Falconer (1952), Via and Lande (1985), and Weigel (2001).

Multivariate G×E genetic models appear to be somewhat uncommon in the literature. Namely, studies tend to have diverse titles and descriptions, making identification with search parameters difficult. However, this methodology was used recently in a dissertation studying the hair shedding local adaptation trait (Durbin, 2020), by Fennewald *et al.* (2018), and by Bertrand *et al.* (1987). The same methodology has been used to characterize changes in genetic variation associated with different stages of production in studies utilizing dairy lactation data (each lactation is treated as a separate trait; Rothschild and Henderson, 1979; Tong *et al.*, 1979; Standberg and Danell, 1988). Characterizing differences between various stages of production or life stages generally isn't considered G×E, however, as all animals tend to be subjected to the same production stages.

Durbin (2020) utilized Angus weaning weight performance records to evaluate the effects of G×E on weaning weight performance. Environments constituting the different "traits" in the multi-trait analysis were determined via k-means clustering on mean temperature, mean precipitation, and elevation; importantly, all environments were solely compared to the "High Plains" environment (constituting Nebraska up to North Dakota and parts of Montana) in bivariate analyses to estimate genetic correlations. Given the size of the dataset, 100,000 individuals were randomly chosen per environment for the bivariate models. This process sampling process was repeated 10 times to compare the magnitude of genetic correlations across sample iterates. Durbin (2020) concluded the mean direct genetic correlations between other ecoregions (including the fescue belt) to the High Plains environment across iterations ranged from 0.85 to 0.87. Maternal genetic effects were included in the model and the mean genetic correlations between the other eight environments and the High Plains environment ranged from 0.77 to 0.86, indicating G×E is more influential for the maternal component of weaning weight.

Genetic correlations across iterations were quite different, and differences between the minimum and maximum correlations ranged from 0.13-0.29. This implied variation between subsets of animals.

Fennewald *et al.* (2018) used a similar approach, but defined nine regions based on common map-based splits to identify differences in Red Angus stayability across regions. Heritability ranged from 0.10-0.57, depending on the region, but standard errors tended to be almost as large as many of the estimates. Genetic correlations between regions ranged from 0.32-0.87, indicating G×E may be quite influential for stayability, but measures of uncertainty were not provided (Fennewald *et al.*, 2018). Bertrand (1987) identified inter-regional genetic correlations ranging from 0.55-0.81 for birth weight and weaning weight in Limousin cattle. Overall, there appears to be at least some variability in genetic potential between different regions in the United States. This would at least support exploratory studies into phenotypic plasticity.

Lactation yield is perhaps the most common application of multi-trait models to distinguish differences in genetic variance across a defined category. Genetic correlations for milk yield between the first and second lactations range from 0.80-0.92 (Rothschild and Henderson, 1979; Tong *et al.*, 1979; Standberg and Danell, 1988). Genetic correlations between the first and third lactations range from 0.80-0.84 (Tong *et al.*, 1979; Strandberg and Danell, 1988). Genetic correlations between the second and third lactation range from 0.80-0.97 (Tong *et al.*, 1979; Strandberg and Danell, 1988). Similar ranges and trends have been noted for milk protein and fat (Tong *et al.*, 1979; Strandberg and Danell, 1988). However, as noted earlier, this is not typically considered G×E.

In all cases discussed using the multi-trait model, except Bertrand *et al.* (1987) and Fennewald *et al.* (2018), the genetic correlations were not considered low enough in cursory analyses to warrant the extra labor, time, and computational power/time needed to conduct the evaluations at the time. For Bertrand *et al.* (1987) and earlier evaluations, computational power and industry implementation would likely have been a limitation regardless. It is also worth noting there is sometimes relatively little reranking of individuals even if genetic correlations are less than unity (Calus and Veerkamp, 2003). However, minor differences in breeding values and genetic variances across environments can lead to more reranking in economic indices when weighted (Calus and Veerkamp, 2003). Furthermore, no economic impact analysis appears to have been conducted to directly quantify the impact of ignoring genetic correlations less than one or the cost of implementing G×E multi-trait analyses to determine an appropriate threshold for inclusion in evaluations. Until such analyses are done on a case-by-case basis, it is difficult to determine what genetic correlation threshold warrants implementation.

Evaluating G×E with Fixed Effect Reaction Norms

Another method to evaluate the extent of G×E is the use of reaction norms. Reaction norm models are useful to characterize the changes in phenotype of known genotypes as the environment (Figure 1.2) or another continuous variable changes. In this case, genotype colloquially refers to a genetic group, such as a clonal line of plants (strain), breed, individual, or genotype at a single locus. Fixed effect reaction norm models have traditionally been utilized to compare groups, such as breeds or clonal lines of plants, but have extremely limited uses in individual prediction due to population structure (Klingenberg, 2019). In other words, accounting

for non-independence (i.e., relationships) between individuals is important. Fixed effect reaction norm models fit a regression line for each genotype, allowing for a different intercept (performance at a baseline environment) and slope (response to the environmental continuum, usually referred to as environmental sensitivity or phenotypic plasticity) for each genotype (e.g., Figure 1.2). Fitting genotype as a fixed effect is considered acceptable when inference is only desired between a set number of known genotypes, such as comparing strains of wheat (Pennekamp *et al.*, 2014). If the genotypes in question represent a sample of a population and inference to the population is desired or genotypes are non-independent (implying relatedness/population structure), mixed models/hierarchical models should be utilized (Klingenberg, 2019).

If the G×E is assumed or known to be zero, then the difference in performance between genotypes should remain constant as the environment changes. In other words, the only difference between the functions for each genotype should be the difference between the intercepts, which is maintained throughout the regression line or curve (e.g., Figure 1.2A). In a fixed effects regression model, discrete genotypes (such as breeds of cattle) can be modeled over the environmental continuum with no G×E in an ANCOVA with homogeneous slopes. For the example of modeling genotypes across an environment with a common slope (no G×E), a base linear model would have the form $y_{ij} = \eta + \alpha_i + \beta_1 x_{ij} + e_{ij}$ (Littell *et al.*, 2006a). Here, y_{ij} represents the j^{th} observation for genotype i (indicates subsampling or multiple records for each genotype), η represents the overall intercept, α_i represents the differential effect for the i^{th} genotype relative to η or the deviation from the overall intercept for the i^{th} genotype, β_1 represents the common phenotypic regression coefficient (slope) for the regression of $\boldsymbol{y}$ on $\boldsymbol{x}$ (Schaeffer, 2004), x_{ij} represents the j^{th} environmental observation for the i^{th} genotype, and e_{ij}

represents the residual for each observation with standard assumptions of distribution and independence (Littell *et al.*, 2006a).

Factor-level effects models are commonly employed in many statistical software utilizing a set-to-zero restriction for fixed effect models. When fitting an overall mean or intercept (i.e., a column of ones in the incidence matrix), class dummy variables lead to a singular matrix by definition. This is due to the incidence columns for a given factor summing to the intercept/mean column. In a set-to-zero restriction, one level of each factor (typically the last for simplicity) is replaced with a zero vector with a number of elements equal to the number of rows and dropped from the corresponding incidence matrix. This in turn allows the intercept to absorb the effect of all dropped factor levels and is the base or "anchor" to which other estimates are relative (Saeed *et al.*, 2014). This is the basis for estimable functions. In the above factor-level effects model, the overall intercept, η, consists of the dropped level of genotype, α_{i^*}, and simple linear regression (SLR) intercept, β_0. More explicitly in the basic model presented, $\eta = \alpha_{i^*} + \beta_0$, where β_0 represents the phenotypic intercept (Schaeffer, 2004) in a SLR. As can be seen in Figure 1.2A, the regression lines for each breed are parallel, indicating no G×E.

The above model can be expanded to include a differential slope effect for each genotype, $y_{ij} = \eta + \alpha_i + \beta x_{ij} + \alpha\beta_i x_{ij} + e_{ij}$, yielding an ANCOVA with heterogeneous slopes (Figure 1.2B; Littell *et al.*, 2006a). Most terms in common with the homogeneous slopes model are interpreted the same. The addition of $\alpha\beta_i$ represents the deviation from the overall slope, β, of the i^{th} genotype. Similar to the intercept, β represents the phenotypic slope in a SLR plus the slope of the dropped level of the cross product of alpha and beta (in a set-to-zero restriction). More explicitly, it absorbs $\alpha\beta_{i^*}$, such that $\beta = \beta_1 + \alpha\beta_{i^*}$, where β_1 is the phenotypic slope

(Schaeffer, 2004) in a SLR. Thus, the overall regression line, $\eta + \alpha_i + \beta x_{ij} + \alpha\beta_i x_{ij}$, or $(\eta + \alpha_i) + (\beta + \alpha\beta_i)x_{ij}$, represents the phenotypic trajectory for genotype i (Schaeffer, 2004; Littell *et al.*, 2006a). While only linear relationships have been presented here, higher order polynomial coefficients can be incorporated to account for non-linear relationships, similar to expanding SLR to a higher order model (Littell *et al.*, 2006a). Furthermore, it is common to encounter heteroscedasticity/heterogeneity of residual variances (heterogeneous environmental variances) in evaluations of G×E. While not explicitly discussed here, heteroskedasticity must be addressed, if present, for inference to be valid (Littell *et al.*, 2006a; Mota *et al.*, 2016).

To summarize, an ANCOVA with homogeneous slopes assumes a constant difference in performance between genotypes (Figure 1.2A) without any dependency on the continuous (environmental) variable (i.e., no G×E). The ANCOVA with heterogenous slopes (Figure 1.2B) specification allows for the slope to vary as a function of the genotype and the environment, and therefore allows for G×E (Pennekamp *et al.*, 2014). Slopes will, however, remain the same across genotypes if there are no G×E effects. Because this is a fixed effects regression model, inferences should only be drawn between genotypes in the model. Inference between individuals in populations with structure (i.e., relatedness between individuals) or inference extended to a population of genotypes from the genotypes in the ANCOVA models would be erroneous. Briefly, fixed effects are used for independent genotypes (i.e., no structure or covariance) when inference between the evaluated genotypes is desired, but not extended to unrepresented genotypes (i.e., the genotypes are not a sample of a population). Pennekamp *et al.* (2014) utilizes a fixed effects regression model in a plant G×E study and provides further explanation for whether genotypes should be considered as fixed or random effects.

Evaluating G×E with Random Effect Reaction Norms (Random Regression)

As discussed, fixed effect reaction norm models are insufficient to model genotypes which represent a sample of a population (and thus imply inference on population parameters or to a population of genotypes) or have shared variance. The base animal model has the general form $y_i = \boldsymbol{x_i\beta} + a_i + e_i$, where y_i is the phenotypic observation for animal i, $\boldsymbol{x_i\beta}$ is the sum of fixed effects for animal i, a_i is the random additive genetic deviation from the expected value of y_i for the i^{th} animal across represented environments, and e_i is the residual for the i^{th} animal with standard assumptions of its distribution and independence (Quaas and Pollak, 1980). Importantly, a_i is relative to the expectation of the phenotype and the expectation of the residual is zero, which also implies it is relative to the overall mean. Therefore, the additive genetic value is the average additive genetic value with respect to represented environments.

Furthermore, the animal effect is assumed to be distributed $\boldsymbol{a} \sim N(0, \sigma_a^2 \boldsymbol{A})$, where $\boldsymbol{A}$ captures the expected genetic relatedness between individuals and thus handles structure and accounts for selection (Henderson, 1975; Quaas and Pollak, 1980; Kennedy *et al.*, 1988; Cardoso and Tempelman, 2003, Kang *et al.*, 2010). Fixed effects, such as differences due to sex, are represented by $\boldsymbol{x_i\beta}$, where $\boldsymbol{\beta}$ is a vector of fixed effects and $\boldsymbol{x_i}$ is a row vector of the incidence matrix, $\boldsymbol{X}$, connecting fixed effect estimates to an observation (sum of fixed effects for the i^{th} animal). For the sake of simplicity and clarity, fixed effects aside from regression coefficients for a covariate will not be included and matrix/vector notation will not be used in the following model expressions.

In a random effects model with a covariate, a_i would serve as a random intercept (value when the covariate is 0) when included in a random intercepts model and is, in fact, the additive

genetic random intercept (genetic deviation from the mean or expectation). In the following model, $y_{ij} = \beta_0 + \beta_1 x_{ij} + a_i + e_{ij}$, where a_i and e_{ij} maintain the same distribution and assumptions as before, β_0 serves as the phenotypic intercept for the regression of $\boldsymbol{y}$ on covariate $\boldsymbol{x}$, β_1 represents the phenotypic slope for the regression, and a_i represents the additive genetic intercept and genetic deviation from the phenotypic intercept, β_0. More succinctly, the model can be written as $y_{ij} = (\beta_0 + a_i) + \beta_1 x_{ij} + e_{ij}$, where the term in parentheticals represents the intercept for genotype i (Littell *et al.*, 2006c; Mota *et al.*, 2016). The random intercepts model assumes there is no additive genetic interaction with the environmental variable (i.e., no G×E), so the difference between two genotypes is a function of the random intercepts. The random intercepts model notably has a similar appearance, structure, and intention as an ANCOVA with homogenous slopes, but includes the benefits of modeling random effects by incorporating a variance or covariance structure. For a more detailed explanation on the implications of fixed versus random effects, see Littell *et al.* (2006d), Pennekamp *et al.* (2014), or similar works.

Extending further, mixed models with random slopes allow for the modeling of heterogeneous slopes by subject. Such models are coined random regression models, which allow for random slopes and intercepts, incorporate covariance structures, and allow for inference to populations (Littell *et al.*, 2006d). If the random intercepts model is comparable to an ANCOVA with homogeneous slopes, then a random regression model is comparable to an ANCOVA with heterogenous slopes. The random regression model has the base form $y_{ij} = \beta_0 + \beta_1 x_{ij} + a_i + b_i x_{ij} + e_{ij}$, with y_{ij}, β_0, β_1, x_{ij}, and e_{ij} interpreted the same as the random intercepts model. In addition, a_i represents the random effect for the i^{th} subject and is the random intercept (value when the covariate is 0) of the subject deviated from the fixed intercept (β_0), and b_i represents the random slope for the i^{th} subject (Littell *et al.*, 2006c) deviated from

the fixed slope (β_1). Unlike the random intercepts model, a_i and b_i are distributed $\begin{bmatrix}\boldsymbol{a}\\ \boldsymbol{b}\end{bmatrix} \sim N\left(\begin{bmatrix}0\\0\end{bmatrix}, \begin{bmatrix}\sigma_a^2 & \sigma_{ab}\\ \sigma_{ab} & \sigma_b^2\end{bmatrix} \otimes \boldsymbol{I}\right)$, accounting for the covariance, and hence the correlation, between the random intercept and slope. The random regression model can be more succinctly written as $y_{ij} = (\beta_0 + a_i) + (\beta_1 + b_i)x_{ij} + e_{ij}$, where the two parentheticals represent the intercept and slope for a subject, respectively. The fixed regression parameters, β_0 and β_1, represent the intercept and slope, respectively, for the regression of $\boldsymbol{y}$ on $\boldsymbol{x}$ and the random terms, a_i and b_i, represent the subject deviations from the fixed intercept and slope, respectively.

When the random regression model is put in the context of the animal model, a_i is the random additive genetic intercept for individual i (additive genetic deviation from the phenotypic intercept) and b_i is the random additive genetic slope for individual i, also expressed as a deviation from the phenotypic slope. It then follows $a_i + b_i x_{ij}$ is the additive genetic deviation from the population environmental mean, $\beta_0 + \beta_1 x_{ij}$ (similar to the overall mean of μ or $\boldsymbol{X\beta}$ in a standard animal model), for a given value of the environmental covariate, x (e.g., Figure 1.3). Furthermore, a_i and b_i are similarly distributed $\begin{bmatrix}\boldsymbol{a}\\ \boldsymbol{b}\end{bmatrix} \sim N\left(\begin{bmatrix}0\\0\end{bmatrix}, \begin{bmatrix}\sigma_a^2 & \sigma_{ab}\\ \sigma_{ab} & \sigma_b^2\end{bmatrix} \otimes \boldsymbol{A}\right)$, where $\otimes$ is the Kronecker product connecting variances and covariances to the genetic relatedness matrix, $\boldsymbol{A}$ (or some type of relatedness matrix). This covariance structure defines the genetic relationship between the intercept and the slope traits (Mota *et al.*, 2016). The rearranged form $(\beta_0 + a_i) + (\beta_1 + b_i)x_{ij}$ represents an animal's phenotypic trajectory, where $\beta_0 + a_i$ is an animal-specific intercept and $\beta_1 + b_i$ is an animal specific slope (e.g., Figure 1.3). If a covariate value of zero is nonsensical or uninteresting, the covariate can be centered or adjusted to provide a more meaningful intercept (i.e., $x_{ij} - \bar{x}$ or $x_{ij} - \delta$, where delta represents an arbitrary center).

With this approach, the random, additive genetic slope determines the extent of phenotypic plasticity (Mota *et al.*, 2016). Furthermore, if σ_b^2 is non-zero, it implies animal-specific slopes are different, relative differences between animals' BV change as the environment changes, and G×E effects exist (Schaeffer, 2004). However, the additive genetic slope is a deviation from the population slope, as previously mentioned. With this information, an additive genetic slope (i.e., b_i) of the same magnitude, but opposite sign, of the population phenotypic slope (i.e., β_1) would indicate a completely environmentally insensitive (phenotypically plastic) individual. This is due to the additive genetic component neutralizing any non-zero population trends, thus stabilizing phenotypic performance and giving a phenotypic slope of zero for the individual. This is most closely demonstrated by the phenotypic trajectory for animal two in Figure 1.3. The additive genetic intercept, on the other hand, represents the baseline performance. This can be the performance at an environmental value of zero when the covariate is uncentered, but is otherwise the performance at an environmental value of $\bar{x}$ or δ if centered. A possible centering value could be a neutral or optimal environment (e.g., the threshold at which heat stress begins).

The genetic correlation, $r_{ab} = \frac{\sigma_{ab}}{\sqrt{\sigma_a^2+\sigma_b^2}}$, represents the genetic relationship between the additive genetic baseline performance and phenotypic plasticity (Mota *et al.*, 2016). The genetic correlation determines the impact of phenotypic plasticity selection on baseline performance and vice-versa. Other effects, such as a permanent environmental effect or maternal effect, should also be included and specified to have their own random intercepts and slopes (Mota *et al.*, 2016) if they are appropriate to the data being fitted. Like fixed effects regression, random regression models are not limited to being linear and higher orders for the random and fixed components of

the model can be specified. For a more detailed overview of non-linear random regression models, see Schaeffer (2004). Furthermore, for a more detailed overview of the evolution of random regression models from multi-trait models and repeatability models (and the limitations of each), nuances of statistical implementation, and usage outside of the context of G×E, see Oliveira *et al.* (2019).

Random regression models additionally offer the flexibility to determine environment-specific genetic variances, genetic covariances between the trait in different environments, and any resulting functions, such as repeatability (if a permanent environment effect is modeled) and heritability (Mota *et al.*, 2016). The genetic variance for a given environment, x, in the base model presented above is $\sigma_u^2|x = var(a_i + b_i x) = \sigma_a^2 + x^2\sigma_b^2 + 2x\sigma_{ab}$, where $\sigma_u^2|x$ is the additive genetic variance at a given value of x and other terms are as defined previously. Thus, the narrow-sense heritability for environment x is $h^2|x = \frac{\sigma_u^2|x}{\sigma_u^2|x+\sigma_e^2}$, assuming homogeneous residual variance and no other variance components. The additive genetic covariance between two environments is $\sigma_{u|x_1,u|x_2} = cov(a_i + b_i x_1, a_i + b_i x_2) = \sigma_a^2 + x_1 x_2 \sigma_b^2 + (x_1 + x_2)\sigma_{ab}$ and the additive genetic correlation between two environments follows as $r_{u|x_1,u|x_2} = r(a_i + b_i x_1, a_i + b_i x_2) = \frac{\sigma_{u|x_1,u|x_2}}{\sqrt{(\sigma_u^2|x_1)(\sigma_u^2|x_2)}}$ (Mota *et al.*, 2016). Random regression models are highly flexible tools allowing for the analysis of phenotypic plasticity via the slope of the regression, performance in a baseline environment via the intercept, functions of covariances across environments (correlation, heritability, repeatability, etc.) and between the slope and intercept (phenotypic plasticity and baseline performance), and the estimation of breeding values across the environment. Thus, their importance to adaptability is immediately clear, given the variety of questions they can answer.

Random regression models can generally be thought of as an extension of a repeated measures model to longitudinal traits (i.e., traits measured more than once over time). In a repeated measures model, effects are only computed for a few "environments" and the relationship between each environment is determined by a covariance structure (Littell *et al.*, 2006b). Random regression models assume an infinite number of environments (hence why they are often described as "infinite dimensions" models), which are related by a polynomial (i.e., a line or curve) rather than point estimates with a co-variance structure (Littell *et al.*, 2006b; Littell *et al.*, 2006d). However, as noted previously for random regression models, variances for any point and covariances between any two points can be calculated as a function of the polynomial (co)variance components. Furthermore, repeatability models assume the genetic variance is the same between each measurement, which is often erroneous in growth or time-based longitudinal traits and certainly erroneous in the context of G×E (Jensen, 2001; Oliveira *et al.*, 2019). In addition, random regression models tend to provide greater accuracies than multi-trait G×E and repeated measures models when the dimensions are relatable by a suitable function (Tier and Meyer, 2004; Baldi *et al.*, 2010; Oliveira *et al.*, 2019). Given the reasons above, it is clear random regression models should be the gold standard for modeling and studying G×E when the environmental covariate can be represented by polynomials.

Random Regression and Similar Models Applied to Beef and Dairy Cattle

Random regression has been extensively used in dairy cattle and modestly used in beef cattle animal breeding research (e.g., Jensen, 2001; Oliveira *et al.*, 2019) to evaluate the environmental sensitivity (i.e., phenotypic plasticity or G×E) for ERTs in the context of environmental covariates. In particular, random regression has been extensively applied to milk

production or milk content (e.g., protein content, fat, etc.) under a test-day covariate in dairy cattle (Jensen, 2001; Oliveira *et al.*, 2019). In the case of test-day or similar covariates, the additive genetic variance is modeled as a function of time (usually days in milk). However, random regression random models are typically not interpreted as G×E for prediction of lactation or growth trajectories with a time covariate (Oliveira *et al.*, 2019), as every animal is arguably subjected to the same "environments" (e.g., lactation cycles, growth cycles, or developmental stages from juvenile to various production stages). Each stage of the production cycle can be considered a different temporal aspect that all animals experience, but the same concepts of genetic variation and genetic correlations in the context of G×E apply (Jensen, 2001; Schaeffer, 2004; Oliveira *et al.*, 2019). While the concepts of G×E apply, it is worth noting different stages of production are not considered environments. As Oliveira *et al.* (2019) emphasized, random regression models differ from repeatability models by relaxing the assumption of a genetic correlation of one between any two environments. Given test-day models model production of different stages of production, different alleles (i.e., genetic variation) are involved in different stages of production (i.e., time), which is why random regression can be appropriate.

One consequence of production cycle covariates is fixed phenotypic trajectories are often nested within contemporary groups or other group factors to account for differences in the environment between groups (Schaeffer, 2004; Oliveira *et al.*, 2019). Given the interest is between different stages of production or production over time in a cycle, it is logical to remove other sources of environmental effects when possible. Schaeffer (2004) also recommends nesting phenotypic trajectories within other classifications, such as sex or breed, to account for different phenotypic trajectories. This is similar to fitting breed or sex as a classification fixed effect in a

base animal model. In some G×E analyses, nested fixed trajectories may not be needed or may be confounded (Ravagnolo and Misztal, 2000; Schaeffer, 2004; Mota *et al.*, 2016).

A mentioned previously, random regression has been applied extensively to test-day lactation curves based on a time-based covariate, such as days in milk (as summarized by Jensen, 2001; Schaeffer, 2004; Oliveira *et al.*, 2019). The use of Legendre Polynomials (a type of orthogonal polynomial) to reduce correlations between regression coefficients of 2nd order and higher polynomials on days in milk/time has been widely accepted as standard practice in test-day random regression models (Schaeffer, 2004). Reducing correlations gives greater numerical stability. However, for first order (linear) functions, orthogonal polynomials are not needed to reduce correlations (Schaeffer, 2004). In addition to univariate analyses, multivariate analyses including different parities as different traits, milk components, such as volume, fat, and protein content, somatic cell score, fertility, and various growth and feed efficiency traits have been analyzed under test day models (Jensen, 2001; Schaeffer, 2004; Oliveira *et al.*, 2019).

In both beef and dairy cattle, random regression, repeatability, and similar models have been used to study temperature-humidity index (THI) as an environmental covariate related to heat stress. There are many ways to derive THI, depending on the context (Bohmanova *et al.*, 2007), but the most common in beef and dairy cattle is a THI formula developed for cattle (NOAA, 1976; Bohmanova *et al.*, 2007) that is used in the subsequent studies. In dairy cattle, Ravagnolo and Misztal (2000) looked at the effect of THI greater than 72 (onset of heat stress) on milk yield and component traits in a test day model. Total additive heritabilities for each trait tended to change by less than 0.05 across the THI continuum (72 - 92). However, the environmental sensitivity genetic variance became equal to the baseline production genetic variance at a THI greater than 88-92 for all traits and the genetic correlation between baseline

production and environmental sensitivity was approximately -0.3 for all traits. Ravagnolo and Mistzal (2000) concluded that continual selection for baseline performance would result in greater sensitivity to heat stress.

Brügemann *et al.* (2011) found genetic correlations of >0.90 looking at milk protein and THI using a random regression model and concluded there was little evidence for G×E. While Brügemann *et al.* (2011) found genetic variance to be greatest in THI-neutral zones for milk protein, Ravagnolo and Mistzal (2000) found genetic variance to be greatest at high THI for milk protein. Aguilar *et al.* (2009) reported that genetic variance for environmental sensitivity increased as parity increased (i.e., as cows moved to higher production lactations) and the genetic correlations between baseline performance and environmental sensitivity were highly negative, ranging from -0.30 to -0.50. This agrees with Ravagnolo and Mistzal (2000) that selection for higher baseline performance is detrimental to production in heat stressed environments. Interestingly, the baseline performance genetic correlations between parities for all milk traits considered were ≥ 0.84, but the environmental sensitivity genetic correlations between parities ranged from 0.56-0.79 (Aguilar *et al.*, 2009). This would imply genetic variance influencing phenotypic plasticity may be dependent on production or developmental stage, which supports the notion that temporal factors in production/developmental stages should be accounted for. While not a perfect solution, this would point towards nesting fixed regressions within different production stages.

Using the same heat stress threshold methodology (and THI calculations) as Ravagnolo and Misztal (2000), Bradford *et al.* (2016) modeled the effects of heat stress on Angus weaning and yearling weight using threshold values of 75 and 70, respectively. Values greater than the threshold were assigned to head load categories ranging from one to ten. In general, direct

heritabilities decreased as heat load increased, which is consistent with Brügemann *et al.* (2011). Interestingly, the maternal heritability point estimates tended to increase. However, it should be noted the large measures of uncertainty around the different heritability estimates would likely indicate the confidence intervals for differences between different levels of heat load overlap zero, potentially implying no evidence for a difference (Bradford *et al.*, 2016). Furthermore, unlike the previous random regression studies discussed, Bradford *et al.* (2016) reported favorable, positive genetic correlations between the intercept and slope additive genetic parameters. This indicated selection for growth in the absence of heat stress was indicative of selection for growth in heat stress. This would indicate selection for increased growth in thermoneutral environments would increase phenotypic plasticity. Direct genetic correlations between the intercept and slope (SD) were 0.30 (0.002) and 0.71 (0.06) for weaning weight and yearling weight, respectively, while maternal genetic correlations were 0.87 (0.001) and 0.96 (0.07) for maternal weaning weight and yearling weight, respectively (Bradford *et al.*, 2016). To quantify the effects of G×E on selection, Spearman rank correlations were generated between various heat loads. Spearman rank correlations for yearling weight maternal genetic correlations between different heat loads were generally high (0.99), with direct Spearman rank correlations dropping as far as 0.91. Spearman rank correlations for weaning weight maternal between head loads were all high as well (≥0.97). The Spearman rank correlations for direct weaning weight were high between low and moderate heat loads, but were as low as 0.71 between low to moderate and high heat loads (Bradford *et al.*, 2016). This indicates that reranking tends to occur in the most extreme environments rather than intermediates. This may be evidence for local adaptation selection rather than selection over a continuous environment.

Mateescu *et al.* (2020) used random regression to identify G×E in admixed groups of *Bos taurus* and *Bos indicus* cattle. Groups of roughly 50 cattle ranging from 0-100% Brahman and Angus were included in the analysis. Environmental sensitivity to heat stress was evaluated using body temperature. As might be expected, groups with a greater percentage of *Bos indicus* admixture had lower baseline body temperatures and a decreased sensitivity to high THI relative to individuals with a greater proportion of *Bos taurus* ancestry (Mateescu *et al.*, 2020). However, the covariances between groups were assumed zero with a common between-group variance, and the animal slopes and intercepts were assumed zero and independent (Mateescu *et al.* 2020). Given these are admixed breed groups and are not independent, the information shared between groups is likely not being accounted for in each group. Furthermore, the previously discussed random regression studies clearly indicate the slope and intercept do not appear to be independent. Thus, not accounting for shared information may not be allowing for appropriate flow of information.

Random regression models have also been applied to model growth as a function of time across various life and production stages (Meyer, 2000; Schenkel 2002; Baldi *et al.*, 2010), to model G×E at the level of individual quantitative trait loci (QTL; Yang *et al.*, 2015), and to model various traits using an aggregate environmental covariate, such as contemporary group estimates or progeny means (Maricle, 2008; Cardoso and Tempelman, 2012; Mota *et al.*, 2016).

Baldi *et al.* (2010) modeled weight curves with Legendre Polynomials from birth to adulthood. Meyer (2000) conducted a similar analysis, but used cows at mature weight and modeled cyclical seasonal effects on body weight, rather than different production stages. Schenkel *et al.* (2002) modeled weight gain of station-tested beef bulls using time as a covariate and Legendre Polynomials. In a fairly novel approach, Mota *et al.* (2016) and Cardoso and

Tempelman (2012) used random contemporary group estimates as the environmental covariate to examine log-transformed tick loads and post-weaning gain, respectively. The logic here is that random contemporary group estimates captures a variety of local environmental effects into one estimate (albeit, with shrinkage as they were fit as random effects), unlike a single environmental covariate. Maricle (2008) used herd or farm progeny means for birth, weaning, and yearling weight as the environmental covariate in each random regression analysis. Yang *et al.* (2015) extended random regression genomic prediction models to individual SNPs, rather than individuals, which produced SNP-specific intercepts and slopes. This is perhaps exceedingly interesting as it has the potential to answer a variety of questions related to the genetic architecture. For example, it could answer which SNPs are contributing towards the baseline performance and/or environmental sensitivity and which are contributing towards reduced environmental sensitivity and increased phenotypic plasticity. This methodology would allow the distributions of SNP effects to be characterized rather than animal effects.

Clearly, most random regression studies discussed here applies primarily to production cycles and stages. However, there are some studies which explicitly modeled G×E using an environmental or aggregate environmental covariate. Unfortunately, the literature still seems to be rather sparse for these types of analyses, indicating there is likely much work to be done to characterize phenotypic plasticity for a variety of traits.

Modern Genome-Wide Association Study Methodologies

In livestock, a genome-wide association study/analysis (GWAS) is a popular method to detect genomic regions or loci correlated with quantitative traits or complex diseases (Hästbacka *et al.*, 1992). Since the earliest implementations, GWAS has evolved to include genotyping

arrays and sequence data covering the entirety of the genome. Implementing alternative genetic architectures (distributions of SNP effects and variance) in a Bayesian analysis (Bayes alphabet approaches; Meuwissen *et al.*, 2001; Habier *et al.*, 2011) and implementing genotypes in genomic best linear unbiased prediction (GBLUP) and single-step GBLUP (ssGBLUP; Strandén and Garrick, 2009; Wang *et al.*, 2012; Zhang *et al.*, 2016) are all modern approaches to GWAS. The latter case, where genotypes are used directly in a genetic relatedness matrix (GRM) in BLUP, allows for the post-hoc computation of marker effects and distributions. The detection of QTL, or regions associated with a trait, largely depends on linkage disequilibrium (LD) between the causal mutation and markers usually in the form of SNPs (Hästbacka *et al.*, 1992; Hirschhorn and Daly, 2005). The design of genotyping arrays, models (e.g., adequately accounting for various design effects or population structure), and control of false positives (controlling Type-I error at the expense of power) are equally important considerations in a GWAS (Hirschhorn and Daly, 2005).

Mixed models have been a staple in modern GWAS methodologies used in animal breeding contexts (Korte and Farlow, 2013). Mixed model GWAS methodology accounts for population structure, inbreeding, and selection with a genomic or blended relationship matrix (Henderson, 1975; Quaas and Pollak, 1980; Kennedy *et al.*, 1988; Cardoso and Tempelman, 2003, Kang *et al.*, 2010). The GRM accounts for the lack of independence between subjects by accounting for the genetic relationships scaled by the additive genetic variance (giving the genetic covariance) between individuals. The pedigree-based GRM (**A**) gives the expected relationships based off expectation of Mendelian sampling, whereas the genomics-based GRM (**G)** accounts for Mendelian sampling (Yu *et al.*, 2017). The inclusion of the GRM in mixed model approaches has drastically reduced spurious associations (Type-I error) and highlighted

QTL with strong effects (Korte and Farlow, 2013). Single nucleotide polymorphism effects are now often computed post-hoc from GBLUP in software such as the BLUPF90 suite (Zhang *et al.*, 2016) using liner algebra. The methods originally employed to compute SNP effects from GBLUP (Strandén and Garrick, 2009; Zhang *et al.*, 2016) implicitly assumed an infinitesimal genetic architecture (distribution of marker effects and variance), which generally fits the genetic architecture of many polygenic/quantitative traits commonly found in livestock quite well (Cole *et al.*, 2009; Pritchard and Rienzo, 2010; Su *et al.*, 2010).

In the case of traits with large effect loci, however, the infinitesimal model is not an accurate descriptor of the genetic architecture. Traits which do not fit infinitesimal assumptions well typically include Mendelian traits/diseases or complex diseases such as Chron's disease or some cancers (Gibson, 2009). Complex diseases, for example, are typically influenced by many additive and non-additive genetic factors, the environment, and G×E effects (Gibson, 2009). Bayesian models, such as the Bayes alphabet (Meuwissen *et al.*, 2001; Habier *et al.*, 2011) may be more useful and flexible models for different distributions of SNP effects, though these models have some drawbacks related to time and computational efficiency. The various Bayesian models allow for the specification of different genetic architectures, which can model traits with varying effect sizes well; however, new frequentist approaches also allow for individual weights to be applied to SNPs to alleviate the limitations of more traditional frequentist approaches (weighted GBLUP/ssGBLUP, WGBLUP/WssGBLUP; VanRaden, 2008; Zhang *et al.*, 2016). Overall, the choice of methodology depends on the genetic architecture of the trait and computational limitations.

Genetic Architecture of Phenotypic Plasticity

Genome-wide association analysis/study is a useful tool to elucidate the genetic architecture of phenotypic plasticity (environmental sensitivity) as well as to discover QTL associated with baseline performance and phenotypic plasticity in random regression models (Lillehammer *et al.*, 2009; Streit *et al.*, 2013; Oliveira *et al.*, 2019). The genetic architecture of phenotypic plasticity traits (slope of the random regression model) is largely unknown in beef cattle populations because not many traits have been explored. However, QTL associated with baseline performance and changes amongst different stages of production have been found in dairy milk production using test-day as an environmental covariate (Lillehammer *et al.*, 2009; Hayes *et al.*, 2009). In this case, most QTL exhibited an unfavorable (positive) relationship between the baseline performance for milk production and the environmental sensitivity of milk production. In other words, most QTL increasing baseline performance of milk production increased the environmental sensitivity (slope) of milk production. Approximately 1/3 of identified QTL were favorably (negatively) related, however, indicating selection to improve the baseline performance of milk yield and decrease the production stage sensitivity of milk yield would be possible in this population (Lillehammer *et al.*, 2009). However, Lillehammer *et al.* (2009) utilized test-day as a covariate. It was previously discussed that test-day as a covariate may not be a suitable, or at least complete, indicator of G×E as it's modeling production stages. It is possible test-day is confounded with environmental effects, but it is not clear whether this is G×E or not.

It should be noted a genetic correlation generally viewed as unfavorable may not be detrimental in populations and species managed in carefully controlled environments. In fact, greater environmental sensitivity may be favorable in certain production scenarios where the

environment can be controlled to maximize production (i.e., to maximize production in a pre-defined environment), which tends to be common in pork and poultry production. However, these relationships will likely be less manageable for species reared and housed in diverse and extensive environments, such as beef cattle, and would be considered unfavorable.

Furthermore, variation discovered through GWAS in dairy cattle seems to indicate QTL for milk production tend to change sign across the environmental continuum (Lillehammer *et al.*, 2007). In other words, QTL favorable in one environment are not necessarily favorable in another (or may have negligible effects). This may contribute to differences in genetic correlations, variances, and heritabilities between studies conducted in different environments. Lillehammer *et al.* (2007) posits this as one possible reason for the failure to fix large effect QTL through selection. In addition, several studies (Lillehammer *et al.*, 2007; Lillehammer *et al.*, 2009; Hayes *et al.*, 2009) indicated an increased ability to discover additional QTL influencing the trait of interest when the slope (environmental sensitivity) was included in the GWAS models, as opposed to those that do not consider an environmental covariate. This is likely due to the identification of QTL which may only be important under certain environmental conditions (such as when stress-related physiological pathways are utilized), providing further evidence that genetic variances and covariances change across an environmental continuum.

Genome wide association analyses have their limitations, however. Loci with small effects, rare variants (low minor allele frequency), or causative loci in linkage equilibrium with many markers are difficult or impossible to detect in most GWAS (Korte and Farlow, 2013). Even traits considered to be Mendelian in nature, such as eye color, often have a partial polygenic architecture with small effects that are hard to detect without large sample sizes (Simcoe *et al.*, 2021). Adaptability is thought to be mostly polygenic (Pritchard and Rienzo,

2010), so these limitations would certainly apply. Because of these limitations, there is often insufficient power to detect large numbers of QTL in GWAS.

Dry Matter Intake, Respiration Rate, and Water Intake in the Context of Adaptability

Traits are often not considered in the context of an environmental covariate. When they are, a repeatability model is often used (e.g., Ravagnolo and Misztal, 2000; Luo *et al.*, 2021), which implicitly assumes (co)variance components are constant across the environment measured or the environmental covariate is constant. As discussed previously, this may not be the most appropriate model, as it ignores G×E and may fail to capture key trends in (co)variances or functions of (co)variance (heritability, repeatability, correlations, etc.) and breeding values. Respiration rate is not widely studied, but studies in the literature for respiration rate often utilize a repeatability model. Luo *et al.* (2021) measured respiration rate categorically in dairy cattle and estimated the heritability at 0.04 (0.01) and the repeatability at 0.14. The temperature humidity index (THI) conditions ranged from 70.5-90.2, with a mean of 80.77. However, respiration rate (measured categorically as a score) was moderately genetically correlated with production traits, such as milk yield, milk fat, and milk protein across parities, with point estimates ranging from 0.04 to 0.33 (with standard errors ranging from 0.06-0.07; Luo *et al.*, 2021). This is unexpected, as genetic variants increasing respiration rate (a measure of heat stress and energy expenditure) would not initially be expected to increase production. However, this apparent paradox might be explained by increased metabolic processes, which generates more body heat that must be expelled (Carabaño *et al.*, 2014). This would indicate higher producing animals will experience

more heat stress and hence would have a greater respiration rate. Carabaño *et al.* (2014) suggest this is evidence of selection for production increasing environmental sensitivity to heat stress.

Dry matter intake (DMI) has been used in random regression models, but usually under the context of a lactation or growth curve (e.g., Veerkamp and Thompson, 1999; Kramer *et al.*, 2008). However, as mentioned previously, production cycles or stages are generally not discussed in the context of adaptability and G×E, given each animal is subjected to the same stages or cycle. Water intake follows a similar trend, where it is evaluated relative to production stages (e.g., Kramer *et al.*, 2008). Thus far, there does not appear to be much literature regarding DMI, water intake, and respiration rate in the context of adaptability.

Ahlberg *et al.* (2019) determined water intake had a heritability of 0.39 (0.07) in crossbreed *Bos taurus* feedlot steers, indicating water intake is moderately to highly heritable. Water to gain ratio (similar calculation to feed to gain or feed conversion ratio) had a heritability of 0.39 (0.05), indicating it is moderately to highly heritable as well. The genetic correlation between water intake and water to gain was 0.99 (0.57). Normally, this would indicate water intake breeding values are a near-perfect indicator of water to gain ratio breeding values, but the high standard error renders this interpretation unclear (Ahlberg *et al.*, 2019). The genetic correlation between water intake and dry matter intake was 0.34 (0.27), between water intake and residual water intake (similar in calculation to residual feed intake) was 0.88 (0.33), between water intake and residual feed intake was 0.33 (0.11), and between water intake and feed to gain ratio was 0.90 (0.85). Water intake may be genetically related (unfavorably) to feed intake and feed efficiency traits, but high standard errors mean it is hard to determine the exact interpretation.

Pereira *et al.* (2021) reported a similar heritability estimate of 0.37 for water intake (95% highest probability density, HPD, 0.20-0.56) in Senepol cattle. Genetic correlation estimates for water efficiency traits, such as residual water intake and water to gain ratio) had similar interpretations as Ahlberg *et al.* (2019), given the estimate uncertainties were large (Pereira *et al.*, 2021). Thus far, there does not appear to be a large amount of work done with the genetics of water efficiency in a traditional animal model or in the context of adaptability.

Conclusion

Adaptability is a complex concept with variable definitions, but can be characterized by modeling G×E in livestock. In the beef industry, due to the opportunities for selling germplasm to an increasingly global market, selection for phenotypic plasticity may be beneficial for increasing the accuracy of selection and stability of progeny performance in disparate environments; however, it remains unclear whether producers would adopt such technology. Random regression analysis lends itself nicely to this type of problem, given its flexibility and the assortment of research questions it can answer, provided the environmental continuums affecting the trait are known. Alternatively, local adaptation may be a better choice for traits which are only expressed in some environments, continuous environments where genetic correlations only decay at extreme values, or for producers that only sell locally. Local adaptation can be facilitated within random regression or in conjunction with random regression, however, meaning local adaptation and phenotypic plasticity do not have to be mutually exclusive in terms of modeling.

Random regression can answer a variety of questions, including (but not limited to) environment-specific variances, environment-specific estimated breeding values, genetic

correlations between a trait in different environments, the environmental sensitivity, and the relationship between a trait in a baseline/neutral environment and its environmental sensitivity. Random regression thus far has been used in a wide variety of applications, including heat stress, production curves, growth curves for various production stages, modeling cyclical environmental events over time, characterizing breed or admixture heat stress differences, characterizing many environmental effects simultaneously with a single covariate, and modeling SNP-specific G×E. One common theme in random regression applied to G×E problems is the apparent antagonism between selection for baseline performance and phenotypic plasticity. Random regression clearly lends itself to answering a large variety of research questions, but its potential applications are likely not fully explored in the beef industry. Much work needs to be done to establish best practices within beef genetic evaluation and to identify robust ways to describe the environmental continuum.

Biological discovery and characterization of the genetic architecture of traits, usually through GWAS-type approaches, can also be integrated within and enhanced by random regression analysis. However, applications of random regression for biological discovery remain underutilized and underexplored in literature. Thus, the genetic architecture of phenotypic plasticity/environmental sensitivity for many traits under various environmental continuums remains unclear. Much work remains to understand the underlying biological mechanisms driving phenotypic changes.

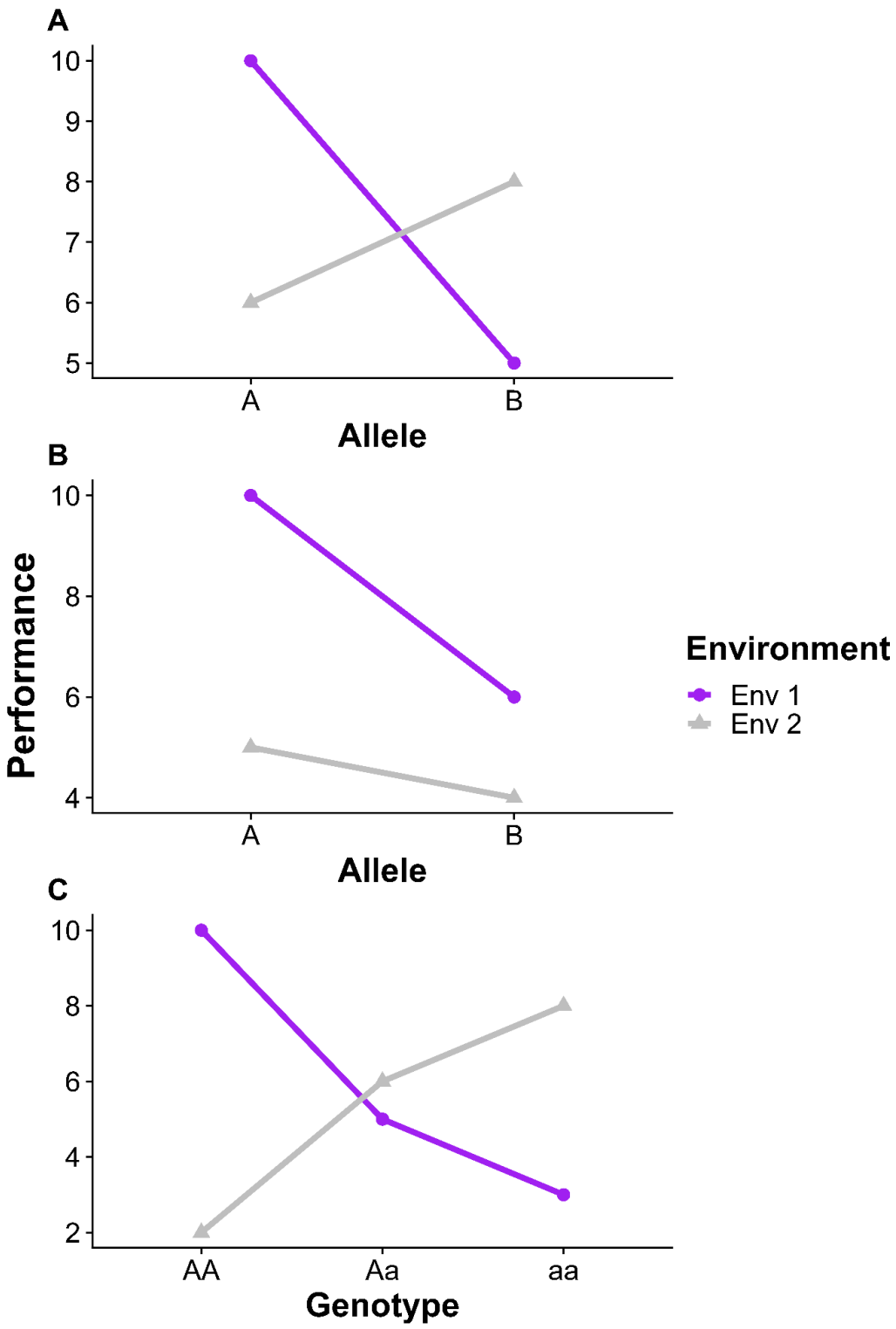

Figure 1.1 G×E at a single locus. (A) An allelic G×E for a given locus. (B) An allelic G×E for a given locus without re-ranking of the "best" allele. (C) A genotypic G×E for the A locus.

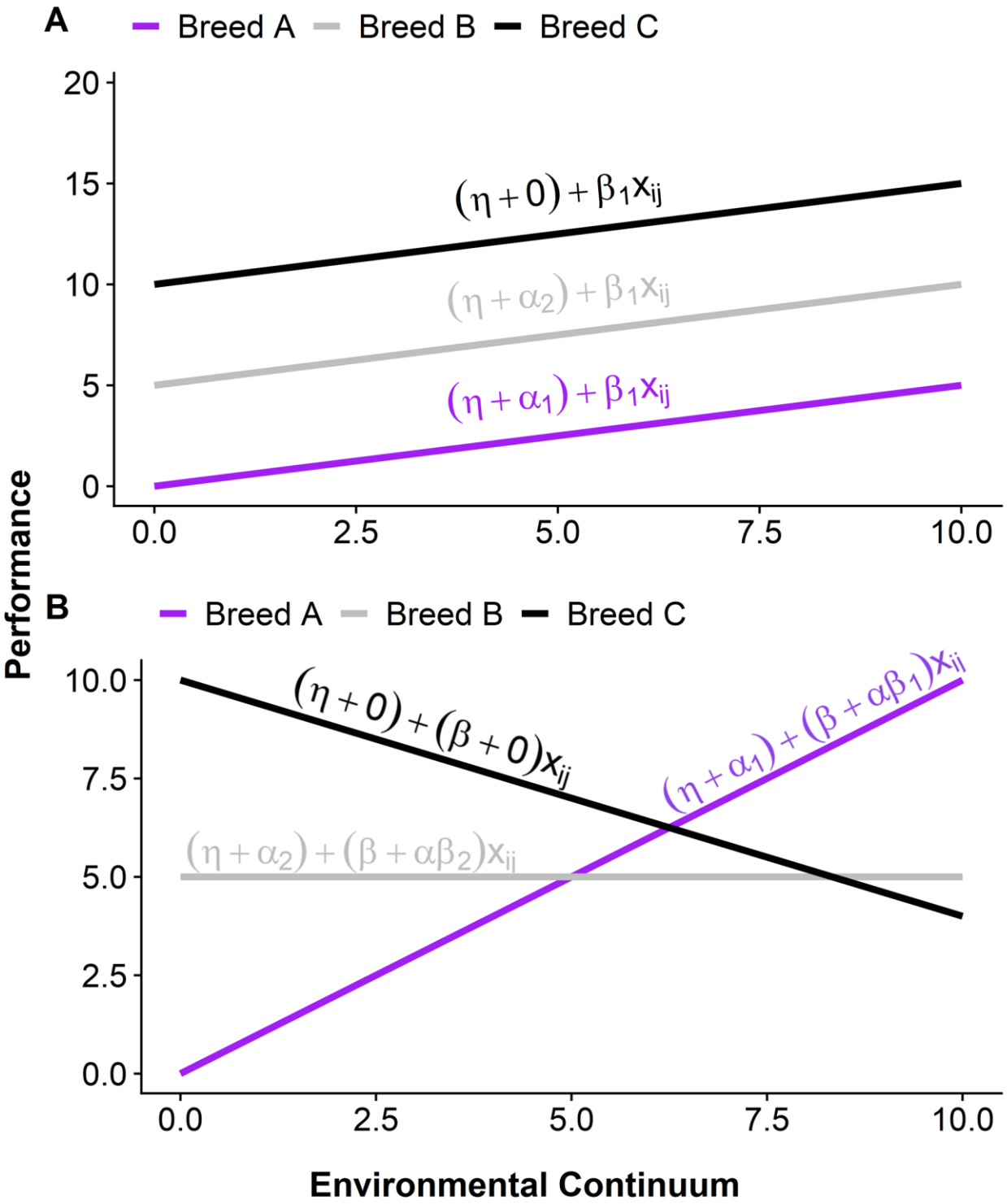

Figure 1.2 Reaction norm examples with the differences between slopes and intercepts for each genotype represented in statistical form. (A) A reaction norm with homogeneous slopes (no G×E). (B) A reaction norm with heterogeneous slopes, thus exhibiting G×E.

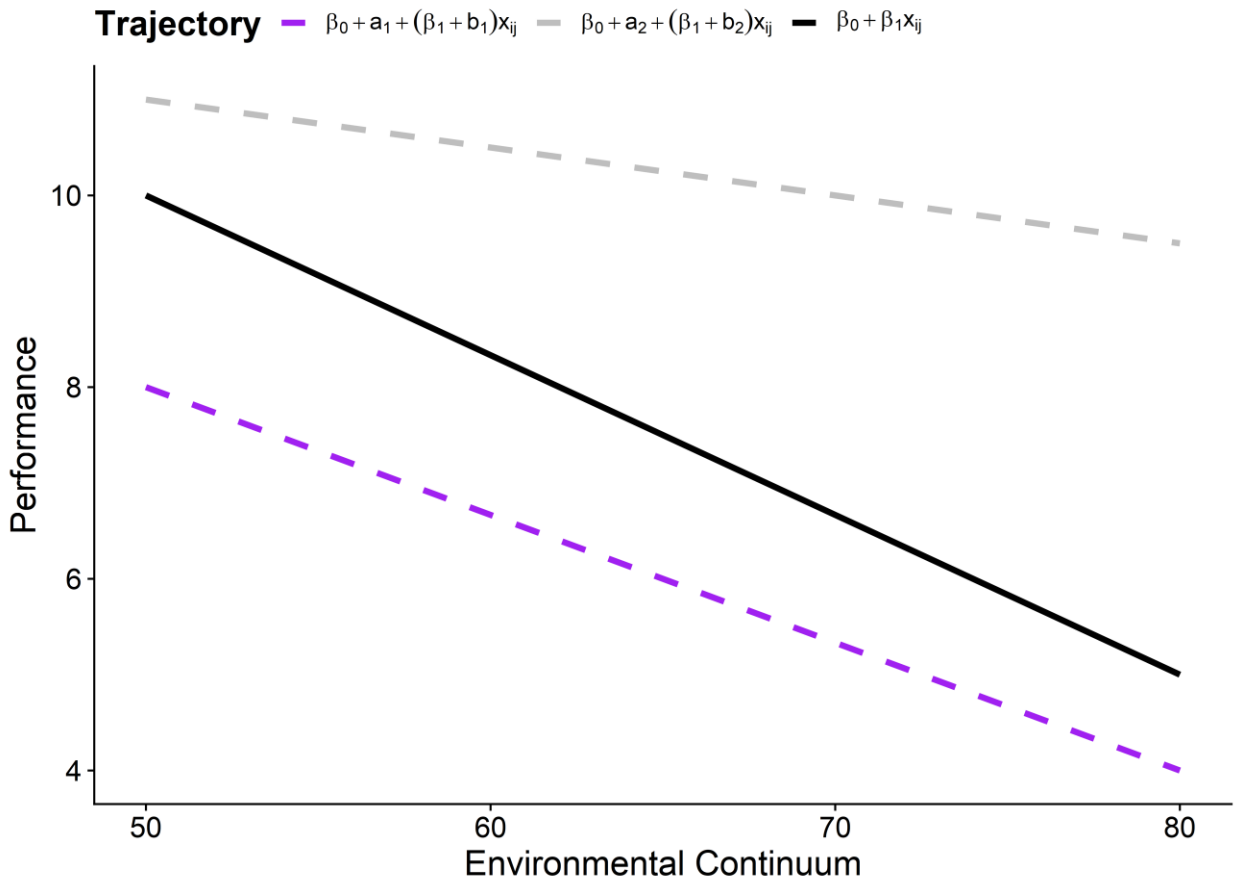

Figure 1.3 Random regression of performance on an environmental variable with an overall phenotypic trajectory (black line) and two animal specific phenotypic trajectories (gray and purple dashed lines).

References

Adger, N. W., N. W. Arnell, and E. L. Tompkins. 2005. Successful adaptation to climate change across scales. Glob. Environ. Change 15:77-86.

Aguilar, I., I. Misztal, and S. Tsuruta. 2009. Genetic components of heat stress for dairy cattle with multiple lactations. J. Dairy Sci. 92:5702-5711.

Ahlberg, C. M., K. Allwardt, A. Broocks. K. Bruno, A. Taylor, L. Mcphillips, C. R. Krehbiel, M. Calvo-Lorezno, C. J. Richards, S. E. Place, U. Desilva, D. L. Vanoverbeke, R. G. Mateescu, L. A. Kuehn, R. Weaber, J. Bormann, and M. M. Rolf. 2019. Characterization of water intake and water efficiency in beef cattle. J. of Anim. Sci. 97:4770-4782.

American Angus Association. 2020. EPD and $Value definitions. https://www.angus.org/Nce/Definitions.aspx (Accessed 8 June 2020.)

Baldi, F., L. G. Albuquerque, and M. M. Alencar. 2010. Random regression models on Legendre polynomials to estimate genetic parameters for weights from birth to adult age in Canchim cattle. J. Anim. Breed. and Genet. 127:289-299.

Banos, G., and A. Sigurdsson. 1996. Application of contemporary methods for the use of international data in national genetic evaluations. J. Dairy Sci. 79:1117-1125.

Barton, N. H., and B. Charlesworth. 1998. Why sex and recombination? Science 281:1986-1990.

Beef Magazine. 2013. BEEF 2014 Genetics. Penton Media, Overland Park, Kansas.

Berry, D. P. 2018. Symposium review: Breeding a better cow—Will she be adaptable? J. Dairy Sci. 101:3665–3685.

Bertrand, J. K., J. D. Hough, and L. L. Benyshek. 1987. Sire × environment interactions and genetic correlations of sire progeny performance across regions in dam-adjusted field data. J. Anim. Sci. 64:77-82.

Bohmanova, J., I. Misztal, and J. B. Cole. 2007. Temperature-humidity indices as indicators of milk production losses due to heat stress. J. Dairy Sci. 90:1947-1956.

Bourdon, R. M. 2000. Factors affecting the rate of genetic change. In: Understanding animal breeding. Prentice Hall, Upper Saddle River, NJ.

Bradford, H. L., B. O. Fragomeni, J. K. Bertrand, D. A. L. Lourenco, and I. Misztal. 2016. Genetic evaluations for growth heat tolerance in Angus cattle. J. Anim. Sci. 94:4143-4150.

Brotherstone, S., and M. Goddard. 2005. Artificial selection and maintenance of genetic variance in the global dairy cow population. Phil. Trans. R. Soc. B. 360:1479-1488.

Brügemann, K., E. Gernand, U. U. von Borstel, and S. König. 2011. Genetic analyses of protein yield in dairy cows applying random regression models with time-dependent and temperature x humidity-dependent covariates. J. Dairy Sci. 94:4129-4139.

Calus, M. P. L., and R. F. Veerkamp. 2003. Estimation of environmental sensitivity of genetic merit for milk production traits using a random regression model. J. Dairy Sci. 86:3756-3764.

Carabaño, M. J., K. Bachagha, M. Ramón, and C. Díaz. 2014. Modeling heat stress effect on Holstein cows under hot and dry conditions: Selection tools. J. Dairy Sci. 97:7889-7904.

Cardoso, F. F., and R. J. Tempelman. 2003. Bayesian inference on genetic merit under uncertain paternity. Genet. Sel. Evol. 35:469-487.

The Council of Dairy Cattle Breeding. 2020. Genotypic and phenotypic trends. https://queries.uscdcb.com/eval/summary/trend.cfm (Accessed 8 June 2020.)

Chevin, L. M., R. Lande, and G. M. Mace. 2010. Adaptation, plasticity, and extinction in a changing environment: towards a predictive theory. PLoS Biol. 8:e1000357.

Cole, J. B., P. M. VanRaden, J. R. O'Connell, C. P. Tassell, T. S. Sonstegard, R. D. Schnabel, J. F. Taylor, and G. R. Wiggans. 2009. Distribution and location of genetic effects for dairy traits. J. Dairy Sci. 92:2931-2946.

Crawford, N. F., M. G. Thomas, T. N. Holt, S. E. Speidel, and R. M. Enns. 2016. Heritabilities and genetic correlations of pulmonary arterial pressure and performance traits in Angus cattle at high altitude. J. Anim. Sci. 94:4483-4490.

de Jong, G. 1995. Phenotypic plasticity as a product of selection in a variable environment. The Am. Nat. 145: 493-512.

de Jong, G., and P. Bijma. 2002. Selection and phenotypic plasticity in evolutionary biology and animal breeding. Livest. Prod. Sci. 78:195-214.

Dominik, S., and B. P. Kinghorn. 2008. Neglecting genotype × environment interaction results in biased predictions from selection index calculations. Livest. Sci. 114: 233-240.

Durbin, H. J. 2020. Genomics of seasonal hair shedding and ecoregion-specific growth to identify environmentally-adapted beef cattle. PhD Diss. Univ. Missouri, Columbia.

Falconer, D. S. 1952. The Problem of Environment and Selection. Am. Nat. 86:293–298.

Falconer, D. S., and T. F. Mackay. 1996. Introduction to Quantitative Genetics. 4th ed. Rev. Pearson, New York, NY.

Fennewald, D. J., R. L. Weaber, and W. R. Lamberson. 2018. Genotype by environment interaction for stayability of Red Angus in the United States. J. Anim. Sci. 96:422-429.

Gibson, G. 2009. Decanalization and the origin of complex disease. Nat. Rev. Genet. 10:134-140.

Grandin, T., and M. J. Deesing. 2013. Genetics and the Behavior of Domestic Animals. Academic Press.

Habier, D., R. L. Fernando, D. Kizilkaya, and D. J. Garrick. 2011. Extension of the Bayesian alphabet for genomic selection. BMC Bioinform. 12:168.

Hartl, D. L., and A. G. Clark. 2018. Principles of Population Genetics. 4th ed. Oxford University Press, New York, NY.

Hästbacka J., A. de la Chapelle, I. Kaitila, P. Sistonen, A. Weaver, and E. Lander. 1992. Linkage disequilibrium mapping in isolated founder populations: diastrophic dysplasia in Finland. Nat. Genet. 2:204-211.

Hayes, B. J., P. J. Bowman, A. J. Chamberlain, K. Savin, C. P. van Tassell, T. S. Sonstegard, and M. E. Goddard. 2009. A validated genome wide association study to breed cattle adapted to an environment altered by climate change. PLoS ONE 4:e6676.

Hazel, L. N. 1943. The genetic basis for constructing selection indexes. Genetics 28:476-490.

Henderson, C. R. 1975. Best linear unbiased estimation and prediction under a selection model. Biometrics 31:423–447.

Henderson, C. R., and R. L. Quaas. 1976. Multiple trait evaluation using relatives' records. J. Anim. Sci. 43:1188-1197.Hill, W. G. 2000. Maintenance of quantitative genetic variation in animal breeding programmes. Livest. Prod. Sci. 63:99-109.

Hirschhorn, J. N., and M. J. Daly. 2005. Genome-wide association studies for common diseases and complex traits. Nat. Rev. Genet. 6:95-108.

Hoffman, I. 2010. Climate change and the characterization, breeding and conservation of animal genetic resources. Anim. Genet. 41:32-46.

Hoffmann, A. A., and C. M. Sgrò. 2011. Climate change and evolutionary adaptation. Nature. 470:479–485.

Jensen, J. 2001. Genetic evaluation of dairy cattle using test-day models. J. Dairy Sci. 84:2803-2812.

Jensen, L. F., M. M. Hansen, C. Pertoldi, G. Holdensgaard, K.-L. D. Mensberg, and V. Loeschcke. 2008. Local adaptation in brown trout early life-history traits: implications for climate change adaptability. Proc. Biol. Sci. 275:2859–2868.

Kang, M. K., J. H. Sul, S. K. Service, N. A. Zaitlen, S. Kong, N. B. Freimer, C. Sabatti, and E. Eskin. 2010. Variance component model to account for sample structure in genome-wide association studies. Nat. Genet. 42:348-354.

Kennedy, B. W., L. R. Schaeffer, and D. A. Sorensen. 1988. Genetic properties of animal models. J. Dairy Sci. 71:17-26.

Klingenberg, C. P. 2019. Phenotypic plasticity, developmental instability, and robustness: the concepts and how they are connected. Front. Ecol. Evol. 7:56.

Korte, A., and A. Farlow. 2013. The advantages and limitations of trait analysis with GWAS: a review. Plant Methods 11:259-272.

Kramer, E., E. Stamer, K. Mahlkow, W. Lüpping, and J. Krieter. 2008. Relationship between water intake, dry matter intake and dairy milk yield on a German research farm. Livest. Sci. 115:99-104.

Lillehammer, M., M. Árnyasi, S. Lien, H. G. Olsen, E. Sehested, J. Ødegård, and T. H. E. Meuwissen. 2007. A genome scan for quantitative trait locus by environment interactions for production traits. J. Dairy. Sci. 90:3482-3489.

Lillehammer, M., B. J. Hayes, T. H. E. Meuwissen, and M. E. Goddard. 2009. Gene by environment interactions for production traits in Australian dairy cattle J. Dairy Sci. 8:4008-4017.

Littell, R. C., G. A. Milliken, W. W. Stroup, R. D. Wolfinger, and O. Schabenberger. 2006a. Analysis of covariance. In: SAS for mixed models. 2nd ed. SAS Institute Inc., Cary, NC. p. 244-250.

Littell, R. C., G. A. Milliken, W. W. Stroup, R. D. Wolfinger, and O. Schabenberger. 2006b. Analysis of repeated measures data. In: SAS for mixed models. 2nd ed. SAS Institute Inc., Cary, NC. p. 244-250.

Littell, R. C., G. A. Milliken, W. W. Stroup, R. D. Wolfinger, and O. Schabenberger. 2006c. Random coefficient models. In: SAS for mixed models. 2nd ed. SAS Institute Inc., Cary, NC. p. 317-325.

Littell, R. C., G. A. Milliken, W. W. Stroup, R. D. Wolfinger, and O. Schabenberger. 2006d. Random effects models. In: SAS for mixed models. 2nd ed. SAS Institute Inc., Cary, NC. p. 58-61.

Luo, H., L. F. Brito, X. Li, G. Su, W. Xu, X. Yan, H. Zhang, G. Guo, L. Liu, and Y. Wang. 2021. Genetic parameters for rectal temperature, respiration rate, and drooling score in Holtein cattle and their relationships with various fertility, production, body conformation, and health traits. J. Dairy Sci. 104:4390-4403.

Lynch, M., and J. B. Walsh. 1998. Genetics and Analysis of Quantitative Traits. Sinauer Associates Inc., Sutherland, MA.

Maricle, E. A. 2008. Genotype by environment interaction estimated by using reaction norms in cattle. MS Thesis. Univ. Missouri, Columbia.

Mateescu, R. G., K. M. Sarlo-Davila, S. Dikmen, E. Rodgriguez, and P. A. Oltenacu. 2020. The effect of Brahman genes on body temperature plasticity of heifers on pasture under heat stress. J. Anim. Sci. 98:1-9.

Martinez, V., L. Bünger, and W. G. Hill. 2000. Analysis of response to 20 generations of selection for body composition in mice: fit to infinitesimal model assumptions. Genet. Sel. Evol. 32:3–21.

Meuwissen, T. H. E., B. J. Hayes, and M. E. Goddard. 2001. Prediction of total genetic value using genome-wide dense marker maps. Genetics 157:1819-1829.

Meyer, K. 2000. Random regressions to model phenotypic variation in monthly weights of Australian beef cows. Livest. Prod. Sci. 65:19-38.

Mota, R. R., R. J. Tempelman, P. S. Lopes, I. Aguilar, F. F. Silva, and F. F. Cardoso. 2016. Genotype by environment interaction for tick resistance of Hereford and Braford beef cattle using reaction norm models. Genet. Sel. Evol. 48.

Mulder, H. A., and P. Bijma. 2005. Effects of genotype × environment interaction on genetic gain in breeding programs. J. Anim. Sci. 83: 49-61.

Mulder, H. A., R. F. Veerkamp, B. J. Ducro, J. A. M. van Arendonk, and P. Bijma. 2006. Optimization of dairy cattle breeding programs for different environments with genotype by environment interaction. J. Dairy. Sci. 89:1740-1752.

Naskar, S., G. R. Gowane, A. Chopra, C. Paswan, and L. L. Prince. 2012. Genetic adaptability of livestock to environmental stresses. In: V. Sejian, S. M. K. Naqvi, T. Ezeji, J. Lakritz, R. Lal, editors, Environmental stress and amelioration in livestock production. Springer Berlin Heidelberg, Berlin, Heidelberg. p. 317-378.

National Oceanic and Atmospheric Administration. 1976. Livestock hot weather stress. US Dept. Commerce, Natl. Weather Serv. Central Reg., Reg. Operations Manual Lett. C-31-76. US Govt. Printing Office, Washington, DC.

Oliveira, H. R., L. F. Brito, D. A. L. Lourenco, F. F. Silva, J. Jamrozik, L. R. Schaeffer, and F. S. Schenkel. 2019. *Invited review*: Advances and applications of random regression models: From quantitative genetics to genomics. J. Dairy Sci. 102:7664-7683.

Pennekamp, F., K. A. Mitchell, A. Chaine, and N. Schtickzelle. 2014. Dispersal propensity in Tetrahymena thermophila ciliates – a reaction norm perspective. Evolution 68:2319-2330.

Pereira, G. M., A. A. Egito, R. C. Gomes, M. N. Ribas, R. A. A. Torres Junior, J. A. Fernandes Junior, and G. R. O. Menezes. 2021. Water requirements of beef production can be reduced by genetic selection. Animal 15:100142.

Prayaga, K. C., N. J. Corbet, D. J. Johnston, M. L. Wolcott, G. Fordyce, and H. M. Burrow. 2009. Genetics of adaptive traits in heifers and their relationship to growth, pubertal and carcass traits in two tropical beef cattle genotypes. Anim. Produc. Sci. 49:413–425.

Pritchard, J. K., and A. D. Rienzo. 2010. Adaptation – not by sweeps alone. Nat. Rev. Genet. 11:665-667.Quaas, R. L., and E. J. Pollak. 1980. Mixed model methodology for farm and ranch beef cattle testing programs. J. Anim. Sci. 51: 1277-1287.

Ravagnolo, O., and I. Misztal. 2000. Genetic component of heat stress in dairy cattle, parameter estimation. J. Dairy Sci. 83:2126-2130.

Robinson, G. K. 1991. That BLUP is a good thing: the estimation of random effects. Stat. Sci. 6:15-51.

Rothschild, M. F., and C. R. Henderson. 1979. Maximum likelihood estimates of parameters of first and second lactation milk records. J. Dairy. Sci. 62:990-995.

Saeed, B. I. I., S. K. Appiah, N. N. N. Nsowah-Nuamah, L. Munyakazi, and A. A. I. Musah. 2014. Model equivalence in general linear models: set-to-zero, sum-to-zero restrictions, and extra sum of squares method. Int. J. of Stat. and Probab. 3:42-53.Schaeffer, L. R. 2004. Application of random regression models in animal breeding. Livest. Prod. Sci. 86:35-45.

Scheiner, S. M., and R. F. Lyman. 1989. The genetics of phenotypic plasticity I. Heritability. J. Evol. Biol. 2:95–107.

Schenkel, F. S., S. P. Miller, J. Jamrozik, and J. W. Wilton. 2002. Two-step and random regression analyses of weight gain of station-tested beef bulls. J. Anim. Sci. 80:1497-1507.

Schou, M. F., A. A. Hoffmann, and T. N. Kristensen. 2019. Genetic correlations and their dependence on environmental similarity-Insights from livestock data. Evolution. 73:1672–1678.

Sgrò, C. M., and A. A. Hoffman. 2004. Genetic correlations, tradeoffs, and environmental variation. Heredity. 93: 241-248.

Simcoe, M., A. Valdes, F. Liu, N. A. Furlotte, D. M. Evans, G. Hemani, S. M. Ring, G. D. Smith, D. L. Duffy, G. Zhu, S. D. Gordon, S. E. Medland, D. Vuckovic, G. Girotto, C. Sala, E. Catamo, M. P. Concas, M. Brumat, P. Gasparini, D. Toniolo, M. Cocca, A. Robino, S. Yazar, A. Hewitt, W. Wu, P. Kraft, C. J. Hammond, Y. Shi, Y. Chen, C. Zeng, C. C. W. Klaver, A. G. Uitterlinden, M. A. Ikram, M. A. Hamer, C. M. van Duijn, T. Nijsten, J. Han, D. A. Mackey, N. G. Martin, C. Y. Cheng, 23and Me Research Team, International Visible Trait Genetics Consortium, D. A. Hinds, T. D. Spector, M. Kayser, and P. G. Hysi. 2021. Genome-wide association study in almost 195,000 individuals identifies 50 previously unidentified genetic loci for eye color. Sci. Adv. 7:eabd1239.

Speidel, S. E., M. G. Thomas, T. N. Holt, and R. M. Enns. 2020. Evaluation of the sensitivity of pulmonary arterial pressure to elevation using a reaction norm model in Angus cattle. J. Anim. Sci. 98:1-9.

Strandberg, E., and B. Danell. 1989. Genetic and phenotypic parameters for production and days open in the first three lactations of Swedish dairy cattle. Acta Agric. Scand. 39:203-215.

Strandén, I., and D. J. Garrick. 2009. Technical note: Derivation of equivalent computing algorithms for genomic predictions and reliabilities of animal merit. J. Diary. Sci. 92: 2971-2975.

Streit, M., R. Wellmann, F. Reinhardt, G. Thaller, H. Piepho, and J. Bennewitz. 2013. Using genome-wide association analysis to characterize environmental sensitivity of milk traits in dairy cattle. J. Anim. Sci. 3:1085-1093.

Su, G., B. Guldbrandsten, V. R. Gregersen, and M. S. Lund. 2010. Preliminary investigation on reliability of genomic estimated breeding values in the Danish Holstein population. J. Dairy Sci. 93:1175-1183.

Tempelman, R. J. 2010. Addressing scope of inference for global evaluation of livestock. R. Bras. Zootec. 39.

Tier, B., and K. Meyer. 2004. Approximating prediction error covariances among additive genetic effects within animals in multiple-trait and random regression models. J. Anim. Breed. and Genet. 121:77-89.

Tong, A. K. W., B. W. Kennedy, and J. E. Moxley. 1979. Heritabilities and genetic correlations for the first three lactations from records subject to culling. J. Dairy Sci. 62:1784-1790.

Turner, T., K. C. Dhuyvetter, T. L. Marsh, and R. D. Jones. 2004. Estimating the economic values associated with EPDs for Angus bulls at auction. Proc. West. Agric. Econ. Assoc.

Upshaw, K., M. Butler, J. Henderson, W. Shaffer, and M. M. Rolf. 2021. Utilization of genomic testing for the selection of desirable traits in cattle. Pages Unknown – editing stage. In: Bovine Reproduction. Edited by Richard Hopper. Wiley.

USDA Animal and Plant Health Inspection Service. 2017. Beef cow-calf management practice in the United States, 2017. Beef 2017.

USDA National Agricultural Statistics Service. 2017. 2017 Census of Agriculture. https://www.nass.usda.gov/Publications/AgCensus/2017/Full_Report/Volume_1,_Chapter_1_US/ (Accessed 3 March 2021.)

VanRaden, P. M. 2008. Efficient methods to compute genomic predictions. J. Dairy Sci. 91:4414-4423.

Veerkamp, R. F., and R. Thompson. 1999. A covariance function for feed intake, live weight, and milk yield estimated using a random regression model. J. Dairy Sci. 82:1565-1573.

Via, S., and R. Lande. 1985. Genotype-environment interaction and the evolution of phenotypic plasticity. Evolution. 39:505–522.

Wang., H., I. Misztal, I. Aguilar, A. Legarra, and W. M. Muir. 2012. Genome-wide association mapping includes phenotypes from relatives without genotypes. Genet. Res. Camb. 94:73-83.

Weigel, K. A., R. Rekaya, N. R. Zwald, and W. F. Fiske. 2001. International genetic evaluation of dairy sires using a multiple-trait model with individual animal performance records. J. Dairy Sci. 12:2789-2795.

West-Eberhard, M. J. 2008. Phenotypic plasticity. In: Encyclopedia of ecology. 1st ed. Elsevier, Amsterdam, Netherlands. p. 2701-2707.

Yang, W., C. Chen, J. P. Steibel, C. W. Ernst, R. O. Bates, L. Zhou, and R. J. Tempelman. 2015. A comparison of alternative random regression and reaction norm models for whole genome predictions. J. Anim. Sci. 93:2678-2692.

Yoo, B. H., F. W. Nicholas, and K. A. Rathie. 1980. Long-term selection for a quantitative character in large replicate populations of Drosophila melanogaster. Theor. Appl. Genet. 57:113-117.

Yu, H., M. L. Spangler, R. M. Lewis, and G. Morota. 2017. Genomic relatedness strengthens genetic connectedness across management units. G3 10:3543-3556.

Zhang, X. S., J. Wang, and W. G. Hill. 2002. Pleiotropic model of maintenance of quantitative genetic variation at mutation-selection balance. Genetics 161:419-433.

Zhang, X. S., J. Wang, and W. G. Hill. 2004. Redistribution of gene frequency changes of genetic variation following a bottleneck in population size. Genetics 167:1475-1492.

Zhang, X., D. Lourenco, I. Aguilar, A. Legarra, and I. Misztal. 2016. Weighting strategies for single-step genomic BLUP: An iterative approach for accurate calculation of GEBV and GWAS. Front. Genet. 7:151.

Chapter 2 - Phenotypic Plasticity of Dry Matter Intake and Respiration Rate Under Water Restriction

Abstract

Climate change and growing demands for resources are expected to impact quality freshwater availability. It is currently unclear how selection under ad libitum freshwater availability may impact genetic potential in water restricted environments. Selection for phenotypically plastic individuals would alleviate issues associated with divergent genetic potential. Here, we explore the ramifications of selection for dry matter intake (DMI) and respiration rate with ad libitum water intake (WI) on the genetic potential water restricted environments using random regression methodology. First, the genetic correlation between DMI or respiration rate at ad libitum WI (intercept) and the environmental sensitivity (slope) were evaluated. Furthermore, genetic-by-environment interaction (G×E) effects on selection were evaluated with genetic correlations between DMI or respiration rate at various levels of water restriction (WR) and Spearman correlations between estimated breeding values (EBV) of DMI or respiration rate at different levels of WR. The heritability and repeatability of each trait was computed for 0% to 50% WR were calculated, and, finally, the genetic architecture of DMI and respiration rate under ad libitum WI and the environmental sensitivity of each trait were explored with a genome-wide association study (GWAS). The population trajectory slope was negative for both DMI and respiration rate, indicating DMI and respiration rate decrease as WR increases phenotypically. The genetic correlation between the additive genetic intercept and slope was strongly negative for DMI and respiration rate (-0.74 and -0.98, respectively), implying selection to increase either trait under ad libitum WI will increase the environmental sensitivity to WR as the magnitude of the population slope would increase. Initially, this seems favorable for

respiration rate, but respiration rate was previously identified to be positively correlated with production traits, such as milk yield. This would indicate the relationship may not be favorable as selection to increase respiration rate may be analogous to increasing production. Genetic correlations between DMI or respiration rate at divergent levels of WR were strong (≥ 0.78), indicating genetic potential at ad libitum WI is a good indicator of genetic potential in WR environments. The DMI intercept, representing selection with ad libitum WI, was strongly associated with metabolic signaling pathways in the GWAS. The DMI slope, or environmental sensitivity, was strongly associated with metabolic pathways such as glycolysis/gluconeogenesis, amino acid metabolism, fatty acid metabolism, and propionate metabolism. Overall, there was sufficient genetic variance to meaningfully select for more phenotypically plastic cattle. However, genetic correlations between different levels of WR and Spearman correlations between the EBVs at different levels of WR were generally high, indicating G×E effects are not large and there may not currently be a need for selection. Variances and especially covariances are not static in time, however, and this may change over generations.

Introduction

Climate change and increasing water usage may severely impact freshwater availability and cost in the future (Nardone *et al.*, 2010). In the past few years alone, drought has severely impacted much of the United States, including areas where many feedlots are housed, and will likely continue to do so (Nardone *et al.*, 2010). Furthermore, adequate water consumption is dependent on water quality (Golher *et al.*, 2020). If the availability of freshwater becomes limited, freshwater quality deteriorates, or the costs associated with supplying freshwater are

prohibitive, selection for individuals adaptable to environments with varying freshwater availability may be important.

Beef and dairy sires collected for artificial insemination (AI) are often used in a wide variety of environmental conditions across the country and globe (Banos and Sigurdsson, 1996; Brotherstone and Goddard, 2005). In addition, commercial herd sires not conceived through AI are often descendants from progeny of AI sires. Progeny from commercial operations destined for the supply chain are often raised in diverse environments. However, many of the large feedlots in the United States are located in arid environments (Grandin, 2016), where quality freshwater may become scarce, in addition to numerous other environmental differences. Therefore, selection for stable performance across diverse environments may be more prudent than selection for reduced or optimal water intake (WI). Stable performance can be defined as phenotypic plasticity, whereby changes to the transcriptome, proteome, epigenome, and interactions between the three are responsible for maintaining performance as environmental conditions change (West-Eberhard, 2008). This implies heritable components may influence phenotypic plasticity.

Random regression methodology facilitates selection for stable performance, or phenotypically plastic individuals, over an environmental continuum (Schaeffer, 2004; Mota *et al.*, 2016) and the variance of the non-intercept parameters indicates the level of genetic-by-environment interaction (G×E) effects. If there are G×E effects influencing production across varying levels of WI, then selection for phenotypically plastic individuals may be important as sires may rerank and accuracy of selection would be lost. Furthermore, relatively little work has been done to elucidate the genetic architecture and biological relationship between performance in an optimal environment and the environmental sensitivity (Lillehammer *et al.*, 2007;

Lillehammer *et al.*, 2009; Hayes *et al.*, 2009). The objectives of this study were to determine: 1) the impact of G×E on dry matter intake (DMI) and respiration rate in a water restricted environment, 2) the consequences of selection with ad libitum WI on the environmental sensitivity and phenotypic plasticity of the population, and 3) explore the genetic architecture of phenotypic plasticity with respiration rate and DMI under WR environments.

Materials and Methods

Study Population

Full details of the initial study design, ration, rationale, and processing are described in Ahlberg *et al.* (2019). Briefly, 830 steers were sourced from the south and great plains sale barns and Oklahoma State University herds. Animals with observable attributes of heavy *Bos indicus* (such as excessively loose skin and large, elongated ears) or dairy ancestry were excluded from the study due to known relationships between tropical adaptation and water intake (Winchester and Morris, 1956; Brew *et al.*, 2011). Animals were obtained over time, forming seven cohorts, that were on trial between May 2014 and July 2018 (Table A.1) at the Willard Sparks feedlot at Oklahoma State University. Animals were housed in pens containing Insentec (Hokofarm Group, The Netherlands) feed and water intake bunks. All procedures involving animals were approved by Institutional Animal Care and Use Committee at Oklahoma State University (protocol AG13-18) in compliance with the Federation of Animal Science Societies (FASS, 2010) guidelines.

Animal Pre-Processing, Pen Assignment, and Acclimation Procedures

During processing, steers were weighed and implanted with Compudose (Elanco Animal Health, Greenfield, IN), an estradiol 17ß (E2 ß) implant, as part of the Willard Sparks feedlot's

standard processing. Following processing, animals spent a variable amount of time in large feedlot pens adjusting to the facility, feedlot ration, and recovering from travel and processing. After the adjustment period, animals were grouped by initial weight into a light and heavy group and half of each weight group was randomly assigned to one of four pens, with approximately 35 steers per pen. Splitting by initial weight, as a proxy for size, was a management consideration so that bunk gates could be set appropriately for smaller steers. If animals were not separated by size, larger steers could access feed bunks where gates were set lower to allow access to smaller animals without reading their tag and registering the intake event. Animals were subsequently allowed a 21-day acclimation period in their pens prior to beginning the trial. Animals who failed to adapt to the Insentec system were removed from the study. Acclimation period data was not included in the study.

Ration Information

For the duration of the trial, cohorts were fed a ration consisting of approximately 15% cracked corn, 28.44% prairie hay, 51.36% wet corn sweet bran, and 5.20% supplement. Ration analysis was conducted by Dairy One, Inc. (Ithaca, New York) to determine the dry matter and gross energy estimates. There was variation in diet ingredient quality between cohorts, leading to slight variation in the dry matter and gross energy composition of the ration for each cohort. The gross energy values ranged from 18.26 to 19.91 MJ/kg of dry matter and dry matter ranged from 0.70 to 0.74 in all cohorts. Importantly, feed was fed using a slick protocol, where the amount of feed was increased once animals were able to clear the feed bunk, for cohorts 1-3, whereas animals were fed ad libitum feed in groups 4-7.

Study Design

Animals were offered water at ad libitum amounts the first 70 days of the trial (BASE), to determine individual baseline WI (bWI). The bWI was computed as the mean daily WI from BASE. After BASE, the daily water allowance was increasingly restricted based on a percentage of the bWI for each animal. Restriction was increased weekly in 10% increments from 10% to 50% of the bWI and daily allotments would reset at midnight. Restriction periods prior to 50% will be referred to as REST from here on out. Once 50% restriction was achieved, it was maintained for 42 days, subsequently referred to as the EREST period, for a total restriction length of 70 days. The restriction procedure was previously validated and described in Allwardt *et al.* (2017). The system, however, was not able to continuously monitor WI (only final and initial bunk weights), so animals could not be removed from the bunk immediately upon reaching their exact daily intake allotment (Allwardt *et al.*, 2017). Thus, the percentage of water restriction achieved varied slightly each day. The goal, however, was for the average to reach the intended restriction level. A summary of water restriction minimums, maximums, and quartiles by restriction period is presented in Table 2.1, detailing the effectiveness of restriction.

Phenotype Collection, Quality Filtering, and Water Restriction

Feed and WI events records were recorded, in kilograms, for the duration of the 140-day trial on a per animal basis using electronic identification tags and the automated Insentec bunk system. Animals were allowed to visit the bunks as many times as wanted, unless their daily WI limit had been reached during REST or EREST. Individual water intake and FI events were filtered as detailed in Allwardt *et al.* (2017). Briefly, records with a greater end weight than start weight were removed, end weights and start weights outside of a range involving the bunk

sensitivity and programmed maximum were removed, and a length of time in bunk shorter than 5s or longer than 3600 seconds were removed. Intake events with negative intakes were considered erroneous records and intake events outside of the specified time frame were also erroneous the vast majority of the time. Any time an animal became ill and needed treatment, the records pertaining to the day before, day of, and day after treatment were removed. All records were removed for processing days, days where equipment errors occurred, and any day where an event may have interfered with ad libitum intake or restriction implementation.

Intake event records were collected for each animal for 140 days, with 70 days for BASE, 7 days per REST period, and 42 days for EREST. Water and feed intake event records were summed each day for each animal, generating daily intakes. Daily feed intakes were subsequently converted to daily dry matter intakes (DMI) using the percentage dry matter for each group. Daily WR within a group was calculated as

$$(1) \qquad WR_{ijk} = 1 - \left(\frac{WI_{ijk}}{bWI_{ij}}\right)$$

where WR_{ijk} represents the water restriction value for the jth animal and kth day/record from group i, WI_{ijk} represents the water intake value for the jth animal and kth day/record from REST or EREST in group i, and bWI_{ij} represents the average daily WI from BASE for the jth animal in the ith group. A value of zero would indicate no restriction (i.e., full water intake relative to the bWI) and a value of one would indicate no water consumed for the day. Occasionally, negative values were obtained at smaller levels of restriction if animals drank more water than intended. Only values between zero and one were used in the analysis. Summary information for water restriction rate by restriction period are presented in Table 2.1.

Respiration rate was defined as the number of breaths (one inhalation and exhalation) in a thirty second time span (breaths per 30 seconds; BP30S). On days where respiration rates were

collected, they were collected once in the morning and again in the afternoon by trained observers. During BASE, respiration rates were collected twice a day on the two days predicted to be the hottest per week. During REST and EREST, respiration rates were collected twice a day every day, except on days where processing occurred. Processing occurred once every week during REST and every other week during EREST. Respiration rate and DMI summary information are presented in Table 2.2. Body weights, in kilograms, were also periodically collected. In BASE and EREST, body weights were collected once every two weeks. During REST, body weight was collected once each week.

Genotyping and Quality Filtering

Blood for genotyping samples was obtained from the jugular vein of each animal in a 10 mL BD vacutainer tube with 1.5 mL of the anticoagulant citrate dextrose. Whole blood was centrifuged and the white blood cell layer was retrieved for a phenol:chloroform:isoamyl alcohol DNA extraction and ethanol precipitation. Genotyping on the GGP Bovine 150K array was performed by GeneSeek (Lincoln, NE). Groups were genotyped on different versions of the array, so only common loci between versions were utilized (138,892 SNPs). Markers were removed if call rate was less than or equal to 90% or minor allele frequency was less than or equal to 5%, yielding 123,912 SNPs for analysis. After quality filtering of markers, eight animals were removed for genotyping call rates less than 90%, leaving 819 genotyped animals.

Genetic Relatedness Matrix

The genetic relatedness matrix (GRM), $\mathbf{G}$, was computed in the BLUPf90 suite (Aguilar *et al.*, 2018; Misztal *et al.*, 2018) as described in VanRaden (2008). Briefly,

(2) $$\boldsymbol{G} = \frac{\boldsymbol{zz'}}{2\sum p_i(1-p_i)}$$

where $\boldsymbol{G}$ is the genomic relatedness matrix, $\boldsymbol{Z}$ is a matrix of alleles (expressed as -1, 0, and 1 for the homozygote, heterozygote, and alternative homozygote) centered around the mean allele effect and weighted for rarity, and p_i represents the frequency of the second allele at SNP i. The denominator scales $\boldsymbol{G}$ to be analogous to the pedigree GRM, $\boldsymbol{A}$ (Van Raden, 2008).

However, $\boldsymbol{G}$ tends to suffer problems with singularity (Aguilar *et al.*, 2010). Thus, $\boldsymbol{G}$ was blended with an equally sized identity matrix as follows to resolve potential singularity issues as follows

(3) $$0.99\boldsymbol{G} + 0.01\boldsymbol{I_{22}}$$

where $\boldsymbol{G}$ is the genomic relatedness matrix and $\boldsymbol{I_{22}}$ is an identity matrix with rows and columns equal to the number of genotyped animals and the dimensions of $\boldsymbol{G}$ (VanRaden, 2008; Aguilar *et al.*, 2010). The genetic relationship matrix utilized in subsequent analyses, $\boldsymbol{H^{-1}}$, was calculated as

(4) $$\boldsymbol{H^{-1}} = \boldsymbol{I} + \begin{bmatrix} 0 & 0 \\ 0 & \boldsymbol{G^{-1}} - \boldsymbol{I_{22}} \end{bmatrix}$$

where $\boldsymbol{G^{-1}}$ and $\boldsymbol{I_{22}}$ are as before and represent genotyped animals and $\boldsymbol{I}$ is an identity matrix with row and column dimensions equal to the number of genotyped animals plus non-genotyped animals with data. Several animals did not have genotypes and had data, but represent a small fraction of the total pool of animals. Using identity matrices was necessary as the pedigree relationships between animals was unknown.

Statistical Analysis

Dry Matter Intake Random Regression Model

Because examining the environmental sensitivity of DMI observed over water restricted environments was a core objective of this work, observations from BASE were not utilized and

WR was utilized as the environmental covariate in the random regression model. The random regression analysis for DMI was as follows:

(5) $$y_{ijk} = \eta + f_i + \beta_1 x_{ijk} + \beta_2 v_{ijk} + a_j + b_j x_{ijk} + g_j + h_j x_{ijk} + e_{ijk}$$

where, y_{ijk} is the kth DMI record for animal j and group i, η represents the overall population intercept, f_i represents the ith differential cohort effect ($i = 1, 2, \dots, 7$), β_1 represents the population slope of the covariate for WR, x_{ijk} represents the WR measurement for animal j in cohort i and day/record k, β_2 represents the slope of the covariate for weight, v_{ijk} represents the closest weight corresponding to the kth daily WR measurement for animal j in cohort i, a_j represents the additive genetic intercept for animal j, b_j represents the additive genetic slope for animal j, g_j represents the permanent environment (PE) intercept for animal j, h_j represents the PE slope for animal j, and e_{ijk} is the residual for the kth observation for animal j in cohort i. Effects for blocks besides cohort were not considered due to convergence issues.

The distributional assumptions were as follows. First,

(6) $$\boldsymbol{y}|\boldsymbol{a}, \boldsymbol{b}, \boldsymbol{f}, \boldsymbol{g}, \boldsymbol{h} \sim N(\boldsymbol{X\beta}, \boldsymbol{I}\sigma^2_{e_i})$$

where the vector of observations, $\boldsymbol{y}$, conditional on the cohort and random regression parameters, was normally distributed with mean $\boldsymbol{X\beta}$ in the mixed model equations and cohort-specific variance $\sigma^2_{e_i}$. Note the i subscript represents a variance unique to each cohort and a common variance is not assumed. Location parameters β_1 and β_2 have prior specifications as $\beta_1 \sim p(\beta_1)$ and $\beta_2 \sim p(\beta_2)$ where each are proportional to 1. This implies a flat prior specification on the location parameters. Second,

(7) $$\begin{bmatrix} \boldsymbol{a} \\ \boldsymbol{b} \end{bmatrix} \sim N_2 \left(\begin{bmatrix} 0 \\ 0 \end{bmatrix}, \begin{bmatrix} \sigma^2_a & \sigma_{ab} \\ \sigma_{ba} & \sigma^2_b \end{bmatrix} \otimes \boldsymbol{H} \right)$$

where $\begin{bmatrix} \boldsymbol{a} \\ \boldsymbol{b} \end{bmatrix}$ is the vector additive genetic effects for the intercept and slope. The additive genetic effects vector of location parameters is distributed bivariate normal with means of zero and a covariance matrix $\begin{bmatrix} \sigma_a^2 & \sigma_{ab} \\ \sigma_{ba} & \sigma_b^2 \end{bmatrix}$. The diagonals represent the additive genetic variance for the intercept and slope, and the off diagonals are the additive genetic covariance between the additive genetic intercept and slope. The covariance matrix is weighted by the Kronecker product of the genetic relatedness matrix, $\boldsymbol{H}$. The prior distribution specified for the additive genetic covariance parameters was specified under a flat Inverse Wishart prior, with

$$\begin{bmatrix} \sigma_a^2 & \sigma_{ab} \\ \sigma_{ba} & \sigma_b^2 \end{bmatrix} \sim IW(S, v), S = \begin{bmatrix} 0 & 0 \\ 0 & 0 \end{bmatrix} \quad (8)$$

and $v = -2$. Third,

$$\begin{bmatrix} \boldsymbol{g} \\ \boldsymbol{h} \end{bmatrix} \sim N_2 \left(\begin{bmatrix} 0 \\ 0 \end{bmatrix}, \begin{bmatrix} \sigma_g^2 & \sigma_{gh} \\ \sigma_{hg} & \sigma_h^2 \end{bmatrix} \otimes \boldsymbol{I} \right) \quad (9)$$

where $\begin{bmatrix} \boldsymbol{g} \\ \boldsymbol{h} \end{bmatrix}$ is the PE intercept and slope vector distributed bivariate normal with means of zero and covariance matrix $\begin{bmatrix} \sigma_g^2 & \sigma_{gh} \\ \sigma_{hg} & \sigma_h^2 \end{bmatrix}$. The diagonals represent the PE intercept and slope variances, and the off diagonals are the covariance between the PE intercept and slope. The Kronecker product with the identity matrix scales the covariance matrix to the size of $\begin{bmatrix} \boldsymbol{g} \\ \boldsymbol{h} \end{bmatrix}$. The prior distribution specified for the permanent environment covariance parameters was specified under a flat Inverse Wishart prior, where

$$\begin{bmatrix} \sigma_g^2 & \sigma_{gh} \\ \sigma_{hg} & \sigma_h^2 \end{bmatrix} \sim IW(S, v) \quad (10)$$

and S and v are as before. Fourth,

$$\boldsymbol{f} \sim N(0, \boldsymbol{I}\sigma_f^2) \quad (11)$$

where $\boldsymbol{f}$ is the vector of cohort effects distributed normally with a mean of zero and common cohort variance, σ_f^2. The prior distribution was specified

(12) $\sigma_f^2 \sim IG(\alpha = 1, \beta = 1).$

And finally,

(13) $\boldsymbol{e} \sim N(0, \boldsymbol{I}\sigma_{e_i}^2)$

where $\boldsymbol{e}$ is the vector of residuals with mean of zero and cohort-specific residual variance, $\sigma_{e_i}^2$, as previously discussed. The prior specifications for $\sigma_{e_i}^2$ were the same as σ_f^2.

Respiration Rate Random Regression Model

Similar to DMI, only observations during REST and EREST and from days with WR values greater than zero were utilized. However, respiration rate phenotypes and studentized residuals were not normally distributed. To confer normality, respiration rates were transformed using a base-ten logarithm transformation. Unlike the DMI model where DMI was measured once per day, respiration rates were measured twice per day. The model for respiration rate was as follows:

(14) $y_{ijkl} = \eta + f_i + \beta_1 x_{ijk} + a_j + b_j x_{ijk} + g_j + h_j x_{ijk} + e_{ijkl}$

Here all terms represent the same as the DMI model, except y_{ijkl} corresponds to the base-ten logarithmic transformation of the lth BP30S record for animal j and cohort i on the kth day, x_{ijk} is the daily WR measurement for animal j, and e_{ijkl} is the residual for an individual BP30S observation. All model distributional assumptions and prior specifications are the same as the DMI model.

Model Implementation and Assessment

The models for DMI and respiration rate were implemented in the BLUPF90 software suite (Aguilar *et al.*, 2018; Misztal *et al.*, 2018) with the THRGIBBS3f90 software to estimate variance and covariances from a Markov Chain Monte Carlo (MCMC) iterative procedure employing a Gibb's Sampler algorithm. Convergence was verified using trace plots of Gibb's samples and the Raftery-Lewis diagnostic (quantile of 0.025 and probability 0.95) from the Coda package in R (Plummer *et al.*, 2006; R Core Team, 2013). A total of 800,000 samples were collected after a 20,000 burn-in due to high autocorrelations between successive samples. A thinning of 40 was applied. This was done to reduce data dimensionality, as many computations involved functions of parameters, which will be discussed later. Generating posteriors for some functions was therefore computationally intensive and oftentimes intractable with 800,000 samples. The Coda package in R was used to determine the effective sample size and summarize posterior distributions of parameters with point estimates and 95% highest posterior density credible intervals (HPDCI). The effective sample size estimates the number of independent samples defining the posterior distribution and the 95% HPDCI represents the shortest interval of the posterior capturing 95% of the density.

Statistical Filtering

Statistical outliers for DMI and respiration rate observations were removed with studentized residuals (SR). Studentized residuals were assumed to follow a t-distribution with mean of zero and degrees of freedom (df) $n-1$, where n represents the number of observations or $SR \sim t_{df}$. The hypothesis test used to test each SR was as follows:

$$\mu_0: The\ observation\ is\ derived\ from\ the\ data\ distribution$$

$$\mu_1: The\ observation\ is\ not\ derived\ from\ the\ data\ distribution$$

The significance level was set at an alpha of 0.05. Bonferroni correction was utilized to account for multiple hypothesis testing, with the quantile significance threshold obtained using the qt function in R (R Core Team, 2013):

(15) $$\left|qt\left(\frac{\alpha}{2n}, df\right)\right|$$

where qt is an R function to find the quantile corresponding to the t-distribution with lower-tail probability $\frac{\alpha}{2n}$ (Bonferroni-corrected two-tailed test) and degrees of freedom as above. The null hypothesis was rejected for a SR with an absolute value greater than the Bonferroni-adjusted quantile. If the null hypothesis was rejected, the corresponding observation was subsequently removed from the analysis. Initially, there were 44,020 and 78,326 records for DMI and respiration rate, respectively. With an alpha of 0.05, the corresponding critical value thresholds were 4.87 and 4.98, resulting in a total of 44,000 and 78,272 observations remaining after outlier removal, respectively.

Variance Component Functions

The relationship between the additive genetic intercept (effect a in the random regression model), or baseline performance, and additive genetic slope (effect b) in the random regression model, or phenotypic plasticity, is a standard genetic correlation defined as:

(16) $$r_{ab} = \frac{\sigma_{ab}}{\sqrt{\sigma_a^2 \times \sigma_b^2}}$$

where r_{ab} is the genetic correlation between the additive genetic intercept and slope, σ_{ab} is the additive genetic covariance between the intercept and slope, and σ_a^2 and σ_b^2 are the additive genetic intercept and slope variances, respectively. Genetic correlations were computed from the

variance component estimates for each iteration of the MCMC chain to define a posterior density.

Genetic variances and genetic correlations can also be computed for individual levels of water restriction. However, computations involving the environmental covariate were limited to regions with adequate data. The scalar form to compute genetic variance for any given value of WR (in decimal form), is as follows:

(17) $$\sigma_u^2|x = var(a_j + b_j x) = \sigma_a^2 + x^2\sigma_b^2 + 2x\sigma_{ab}$$

where $\sigma_u^2|x$ is the additive genetic variance for a given value of WR, a_j is the additive genetic intercept, b_j is the additive genetic slope, σ_a^2 is the additive genetic variance for the intercept, σ_b^2 is the additive genetic variance for the slope, and σ_{ab} is the additive genetic covariance between the intercept and slope.

Likewise, the additive genetic covariance between two values of WR can also be computed. The additive genetic covariance represents the shared additive genetic background, or allelic effects, between the two environments. The additive genetic covariance between two environments is as follows:

(18) $$\sigma_{u|x,u|x'} = cov(a_j + b_j x, a_j + b_j x') = \sigma_a^2 + xx'\sigma_b^2 + (x + x')\sigma_{ab}$$

where $\sigma_{u|x,u|x'}$ is the additive genetic covariance between any two values of WR, x and x', and other terms are as described previously in equation 17.

Matrix algebra can be used to simultaneously solve for the genetic variances and covariances between many levels of WR simultaneously. The matrix notation is as follows:

(19) $$\boldsymbol{\phi Q \phi'}$$

where $\boldsymbol{\phi}$, for a first order (linear) random regression, is an $m\ x\ 2$ matrix containing a column of m ones (intercept) and a column with the m values of water restriction of interest (i.e., genetic

variances and covariances for m environments of interest), $\boldsymbol{Q}$ is the 2 x 2 covariance matrix for $\begin{bmatrix}\boldsymbol{a}\\ \boldsymbol{b}\end{bmatrix}$ (described previously), and $\boldsymbol{\phi Q \phi'}$ is the resulting m x m covariance matrix containing genetic covariances and variances for every level of WR specified in $\boldsymbol{\phi}$. Equation 19 was used with the parameter sample estimates from a given MCMC iteration. The equation was applied to each iteration, with the results all iterations defining posterior genetic variances and covariances for each level of WR.

Genetic correlations can thus then be obtained from scalar calculations as follows:

(20) $$r_{u|x,u|x'} = \frac{\sigma_{u|x,u|x'}}{\sqrt{(\sigma_u^2|x)(\sigma_u^2|x')}}$$

where $r_{u|x_1,u|x_1'}$ is the genetic correlation between any two levels of WR, $\sigma_u^2|x$ and $\sigma_u^2|x'$ are the additive genetic variances for two values of WR described previously in equation 17, and $\sigma_{u|x,u|x'}$ is the additive genetic covariance between the environments represented by x and x' as described in equation 18. Matrices were used to generate multiple genetic correlations simultaneously as follows:

(21) $$\boldsymbol{d^{-1}(\phi Q \phi')d^{-1}}$$

where $\boldsymbol{d^{-1}}$ is the inverse of a diagonal matrix containing the square root of the diagonals of the genetic covariance matrix, $\boldsymbol{\phi Q \phi'}$, and $\boldsymbol{\phi Q \phi'}$ is the covariance matrix for all pairwise combinations of m WR values defined previously. The result is an m x m correlation matrix containing the genetic correlations between each pair or WR values specified in $\boldsymbol{\phi}$. Like the covariance matrix, this was done for each iteration of the MCMC chain. The estimates from all iterations defined posterior genetic correlations between DMI or respiration rate at two different values of WR.

Permanent environment effects were included in the random regression with their own first order coefficients. Likewise, PE effects for specific values of WR were calculated as follows:

(22) $$\sigma^2_{pe}|x = \sigma^2_g + x^2\sigma^2_h + 2x\sigma_{gh}$$

where $\sigma^2_{pe}|x$ is the PE variance for a given value of WR (represented by x, identical to equation 17 and 18 for the genetic variance and covariance), σ^2_g, σ^2_h, and σ_{gh} are the PE intercept variance, slope variance, and covariance, respectively, and other terms are as described previously. Covariances, correlations, and matrices can be generated similarly to equations 17, 18, 19, and 20, but usually the PE variances are only of interest to calculate repeatability. The matrix interpretation is like equation 19, except the $2\ x\ 2$ covariance matrix for $\begin{bmatrix} \boldsymbol{g} \\ \boldsymbol{h} \end{bmatrix}$ is utilized.

Given genetic variance can be calculated for any specific value of WR, narrow-sense heritability can likewise be calculated. However, for both DMI and respiration rate, heterogeneous residuals by cohort were necessary. Given the residual variance is a part of the calculation for narrow-sense heritability, cohort-specific heritabilities for a given value of WR were calculated as follows:

(23) $$h^2_i|x = \frac{\sigma^2_u|x}{\sigma^2_f + \sigma^2_u|x + \sigma^2_{pe}|x + \sigma^2_{e_i}}$$

where $h^2_i|WR$ is the narrow-sense heritability for a given value of WR and cohort i (1…7), $\sigma^2_{e_i}$ is the cohort-specific residual variance for group i, and other terms are as described previously in equations 17-22. Diagonals from the genetic and PE covariance matrices can be extracted, if using matrix algebra, to compute heritabilities for many environments simultaneously. Likewise, cohort-specific repeatability for a given value of WR can be calculated as follows:

(24) $$r_i|x = \frac{\sigma^2_u|x + \sigma^2_{pe}|x}{\sigma^2_f + \sigma^2_u|x + \sigma^2_{pe}|x + \sigma^2_{e_i}}$$

where $r_i|x$ is the repeatability for a value of WR in cohort i and other terms are as described previously in equations 17-22. A repeatability and heritability were calculated for each group in each iteration of the MCMC chain to generate a posterior distribution as described previously.

Estimated Breeding Values for Traits Under Water Restriction

Estimated breeding values for any value of WR within the scope of the model can be generated. Furthermore, Spearman rank correlations between the EBVs for any pair of WR values can be generated to evaluate the impact of G×E on selection. Water restriction EBVs were calculated as follows in scalar notation:

(25) $$EBV_j|x = a_j + b_j x$$

where $EBV_j|x$ represents the EBV of animal j at a given value of WR, x, and $a_j + b_j$ represent the additive genetic intercept and slope of animal j. Breeding values for many environments can also be calculated with matrix operations as follows:

(26) $$\boldsymbol{\phi s}'$$

where $\boldsymbol{\phi}$ is interpreted as before and $\boldsymbol{s}'$ is the transpose of an $j\ x\ 2$ vector containing the additive genetic intercept and slope EBV predictions (a_j and b_j, respectively) for j animals in two columns. The result was an $m\ x\ j$ matrix of environment specific EBVs for all j animals in m environments. This matrix can be generated from the EBV predictions in a single iteration from the MCMC. A posterior for an environment specific EBV for the jth animal at the mth value of WR could thus be generated using the corresponding matrix indices from all MCMC iterations. Spearman rank correlations between the environment specific EBVs at specified pairwise values of WR were generated for each iteration of the MCMC chain to define a posterior density for the Spearman correlations.

Accuracy of Breeding Values

Accuracy of EBVs for the additive genetic intercept (a_j), the additive genetic slope (b_j), and for specified values of WR (equation 25) were calculated utilizing the Beef Improvement Federation (BIF) accuracy (BIF Guidelines, 2021a). The BIF accuracy is defined as follows:

$$Accuracy_{BIF} = 1 - \sqrt{\frac{PEV}{\widehat{\sigma_u^2}}} \quad (27)$$

where PEV is the prediction error variance and $\widehat{\sigma_u^2}$ is the point estimate for the additive genetic variance of the trait of interest. However, the posterior variance of an EBV was used in place of the prediction error variance. The BIF accuracy for the additive genetic intercept of an animal's EBV would be

$$Accuracy\ EBV_{int} = 1 - \sqrt{\frac{var(a_j)}{\widehat{\sigma_a^2}}} \quad (28)$$

The accuracy for the additive genetic slope is:

$$Accuracy\ EBV_{slope} = 1 - \sqrt{\frac{var(b_j)}{\widehat{\sigma_b^2}}} \quad (29)$$

Finally, the accuracy for the EBV at a given value of WR would be

$$Accuracy\ EBV_{WR} = 1 - \sqrt{\frac{var(EBV_j|x)}{\widehat{\sigma_{u|x}^2}}} \quad (30)$$

Terms are defined the same as in the previous equations.

Genome Wide Association Study

A genome wide association study (GWAS) was conducted for DMI and respiration rate, using the BLUPf90 software (Aguilar *et al.*, 2018; Misztal *et al.*, 2018). Unfortunately, BLUPf90 cannot model heteroscedasticity. Therefore, the same random regression models were fit, but

homoscedasticity was assumed, and a frequentist approach was utilized. Point estimates for variance components were obtained from the posteriors in the previously described Bayesian analyses fit with heteroscedastic residuals. Single nucleotide polymorphism effects, the corresponding prediction error variance, and p-values were computed with the BLUPF90 software in conjunction with PostGSf90. Probability values were generated for the intercept and slope for each SNP in the analysis.

Multiple testing correction was attempted using false discovery rate (Benjamini and Hochberg, 1995), but there were no significant SNPs at a threshold of 0.05. Therefore, the significance threshold was set at $-\log_{10}\left(\frac{\alpha}{2}\right) > 4.5$ (corrected for a two-tail test) to provide greater power at the expense of greater Type I error. Significant SNPs within ± 250 kb (McKay *et al.*, 2007) were considered part of the same QTL region centered on the SNP with the strongest signal. Removal of SNPs close together in the genome removes redundancy due to linkage disequilibrium (LD). Gene candidates within each 500 kb QTL region were identified using the GALLO package in R (R Core Team, 2013; Fonseca *et al.*, 2020) and the NCBI bovine GFF annotation file for the USDA ARS-UCD 1.2 genome assembly (Rosen *et al.*, 2020; accession GCF_002263795.1 from NCBI, 2021).

Associated genes for all traits (intercepts and slopes) were included in a network analysis using Network Analyst 3.0 (Xia *et al.*, 2014). Genes identified in the QTL regions for a given trait were used with data from the STRING database and a confidence score cutoff of 900 (Szklarczyk *et al.*, 2015) to create a protein-protein interaction (PPI) network. Enriched pathways were identified from the PPI network (Kanehisa and Goto, 2000). Multiple testing corrected enrichment p-values were obtained from Mann-Whitney-Wilcoxon tests for KEGG pathways and GO terms. Pathways and GO terms with an adjusted p-value of less than 0.05 were

reported. Candidate quantitative trait loci (QTL) were compared with previously reported trait associations within the animal QTLdb (Hu *et al.*, 2019).

Results and Discussion

Population Trends and Data

As might be expected, DMI appears to decrease as WR increases (Figure 2.1A). The trend appears to be linear between 0.00 and 0.50 WR. This is consistent with a study reporting the effect of WR in goats, where a linear trend was reported between 0.00, 0.25, and 0.50 WR (Alamer, 2009). However, as WR extends past 0.50, the relationship may not be completely linear, as DMI appears to stay relatively constant; however, data is also correspondingly scarce as the study was intentionally designed to cap WR at ~ 0.50 or 50%. In greater restriction periods, the mean daily WR was slightly below the target level (Table 2.1), likely due to bunks being under programmed (Allwardt *et al.*, 2017). Phenotypically, DMI daily means and variability appeared to vary by cohort (Table 2.2), possibly related to differences in weather conditions and the populations represented by each group.

Respiration rate does not appear to be strongly influenced by WR (Figure 2.1 B). There is a noticeable decline as WR approached 50%, but respiration rate appears to be stable at lower values of WR. There were clear differences and variability by cohort (Table 2.2), which likely corresponds to the time of year (Table A.1). Modeling the cohort differential effect and heteroscedasticity by cohort accounts for these differences. Weather data was available, but was too sparse for many regions of the weather covariates to accurately fit a regression as the relationship appeared non-linear (not shown). Like DMI, there appears to be a subsequent

increase in respiration rate as WR approaches one, but inference past ~50% WR is not recommended as data was sparse.

The decrease near 50% WR seems counterintuitive, as greater respiration rates usually indicate greater stress. However, positive correlations have been found between respiration rate and production traits, such as milk traits (Luo *et al.*, 2021). This is postulated to be a result of greater metabolic heat generation that must be expelled when metabolic production is greater (Kadzere *et al.*, 2002; West, 2003; Carabaño *et al.*, 2014). In this case, a lower respiration rate may be indicative of reduced metabolic heat generation as DMI decreased (Figure 2.1A).

Model Parameter Estimates

Dry Matter Intake

Estimates and 95% HPDCIs for the population intercept, population slope, and variance components of the DMI random regression model are presented in Table 2.3. Dry matter intake credible intervals for the PE intercept variance and covariance between the PE intercept and slope included zero (Table 2.3), indicating there is not much evidence to support a PE effect at a baseline environment or a relationship between the PE baseline and environmental sensitivity. This indicates environmental effects on DMI in optimal conditions are mostly random and/or temporary. Furthermore, the between-group variance point estimate was 1.99 (95% HPDCI: 0.29, 9.27; Table 2.3), indicating differences between groups were potentially substantial relative to the magnitude of other DMI variance components in Table 2.3. Clearly, heterogeneity of the residuals by cohort ($\sigma^2_{e_i}$) is important to account for, as many 95% HPDCIs do not overlap (Table 2.3). This indicates different temporary environmental effects occur naturally over time and scaling effects due to different environments need to be accounted for in analyses of G×E with

random regression, which is consistent with the argument of Schaeffer (2004). It is not clear what may have contributed to differences between cohorts, but weather, differences in animal behavior or their interactions, and/or management and personnel differences are possible. Of the possibilities, differences in weather conditions are the most likely contributors (Hill and Wall, 2017).

At the population level, the baseline DMI (η), was 10.27 kg (8.94 to 11.84 kg) and the population slope relating DMI to WR (β_1) was negative at -4.10 $\frac{\text{kg DMI}}{100\%\ \text{WR}}$ (-4.22 to -3.99 $\frac{\text{kg DMI}}{100\%\ \text{WR}}$; Table 2.3). At 25% WR, this would equate to an expected decrease of just over 1 kg daily DMI. Over the course of 100 days, as an example, this would equate to a decrease in 102.5 kg of DMI. Assuming a feed to gain ratio of 6:1, there would be an expected loss of ~ 17 kg of weight gain potential per animal. Over the course of many animals, this is clearly problematic if water is not readily available. The fixed slope represents the population mean environmental sensitivity as the environment changes (Schaeffer, 2004). A population is more phenotypically plastic as the population environmental sensitivity approaches zero (West-Eberhard, 2008). Given the population slope is highly negative (Table 2.3), selection to increase it is warranted to increase phenotypic plasticity.

The random coefficients in a random regression animal model (Quaas and Pollak, 1980), including the animal-specific intercept and slope, represent individual additive genetic deviations from the population expectation (Schaeffer, 2004). In other words, the additive genetic intercept for an animal is its additive genetic difference from the population baseline performance and the additive genetic slope for an animal is its additive genetic difference from the population environmental sensitivity. Notably, if the additive genetic slope variance is non-zero, then G×E effects must exist as the animal-specific slopes would inherently be different and relative BV

differences between animals would change (or BV rankings would change) as the environment changes. Thus, the additive genetic slope variance, which is the main selection component of phenotypic plasticity, is an indicator of G×E as well. This indicates selection potential for phenotypic plasticity and G×E effects are inherently tied together.

The additive genetic intercept variance was estimated at 2.08 kg DMI^2 (1.36 to 2.67 kg DMI^2; Table 2.3). Using empirical rule, this corresponds to a 95% probability interval of -2.88 to 2.88 kg DMI, or a difference of 5.77 kg DMI. This indicates selection potential for DMI at 0% WR is quite high. The slope variance was 3.16 $\frac{\text{kg DMI}^{\ 2}}{100\%\ \text{WR}}$ (1.64 to 4.76 $\frac{\text{kg DMI}^{\ 2}}{100\%\ \text{WR}}$; Table 2.3). Using empirical rule, this corresponds to a 95% probability interval of -3.56 to 3.56 $\frac{kg\ DMI}{100\%\ WR}$, or a difference of 7.12 $\frac{kg\ DMI}{100\%\ WR}$. Even with the large amount of uncertainty associated with slope variance, the difference in the 95% probability interval was still fairly sizeable at the lower end of the 95% HPDCI with a 5.12 $\frac{kg\ DMI}{100\%\ WR}$ difference using empirical rule. This slope difference seems rather large, but it is also based on 100% WR (a WR value of 1) rather than 1% WR (a WR value of 0.01). Given the population phenotypic slope was -4.10 $\frac{kg\ DMI}{100\%\ WR}$, there appears to be a reasonable amount of genetic variation to move the expectation of the phenotypic slope to 0 $\frac{kg\ DMI}{100\%\ WR}$ with stabilizing selection. This would result in a phenotypically plastic population on average, with differences due to genetic and environmental (residual) variation. Consequently, however, genetic variation would probably be similar after selection, meaning progeny would still be environmentally sensitive and G×E would still be relevant due to Mendelian sampling. Selection would then need to be mindful of maintaining phenotypic plasticity and identifying less plastic individuals. This may indicate a restricted or weighted selection index may be of use in selection for phenotypic plasticity.

Given the phenotypic slope is negative (β_1), selection should prioritize individuals with a positive EBV for the slope to increase overall plasticity. However, this assumes the genetic correlation between the baseline performance (intercept) and environmental sensitivity (slope) are favorable or zero. An unfavorable correlation would indicate economic selection indices are needed to balance the trade-off between reduced baseline performance or a less plastic population. It also likely means the outcome will be producer specific, as weightings in the index are likely different between producers. Therefore, there is likely a threshold point for producers at which point environmental sensitivity becomes too costly. It may also indicate more specialized seedstock production to meet very specific goals of specific clientele, which would imply differentially weighted indices.

In this case, the additive genetic covariance and correlation between the intercept and slope is negative (Table 2.3). This is important, as it indicates that increased DMI at ad libitum water intake, which is often seen as a result of selection to increase growth and performance, will increase the population's environmental sensitivity to WR and decrease phenotypic plasticity. Therefore, selection decisions for ad-libitum WI performance and environmental sensitivity will likely be more complex than a general, one-size-fits-all answer. In general, this supports the trend in beef and dairy cattle literature that selection to increase productivity in a neutral or favorable environment will increase sensitivity to unfavorable environments and reduce phenotypic plasticity (Ravagnolo and Misztal, 2000; Aguilar *et al.*, 2009; Brügemann *et al.*, 2011; Bradford *et al.*, 2016). However, Sungkhapreecha *et al.* (2021) estimated a moderate and favorable (positive) correlation between baseline production and environmental sensitivity. This indicates selection to increase production in baseline conditions will increase production in unfavorable conditions. Interestingly, this was in a population of Holsteins crossbred with a

tropically adapted Thai breed. This may indicate selection for performance under tropical conditions (i.e., selection for tropical adaptation) or introgression of genetic variation from tropically adapted breeds could, over time, change the genetic covariance between the intercept and slope to be favorable. It is possible selection for phenotypic plasticity may essentially be selection for performance under tropical conditions and, therefore, selection for phenotypic plasticity may favorably alter the genetic covariance between the intercept and slope.

Unfortunately, we were not able to concurrently model DMI with measures of feed efficiency or performance and must extrapolate from other literature. Previously, DMI has been shown to be positively correlated with average daily gain in a traditional animal model (Rolfe *et al.*, 2011; Santana *et al.*, 2014). While this represents the estimate of a genetic correlation averaged over environments, it is unlikely these feedlot populations faced issues with voluntary or involuntary WR. Therefore, the genetic correlations might be expected to be similar to DMI in ad-libitum WI conditions. If the extrapolation holds, this indicates selection to increase DMI in ad-libitum WI conditions would increase the environmental sensitivity on average. This would ultimately result in decreased phenotypic plasticity. However, DMI shares an unfavorable genetic correlation with feed efficiency traits (Rolfe *et al.*, 2011; Santana *et al.*, 2014), indicating selection for feed efficient cattle at ad libitum conditions may increase phenotypic plasticity in this population (if the extrapolations are appropriate). This is supported phenotypically in dairy cattle populations, where DMI decreased as WR increased to 0.50, but feed utilization efficiency appeared to increase (Burgos *et al.*, 2001). Selection for decreased DMI with ad libitum WI would move the population slope towards neutral, as previously discussed, hence the contribution towards increasing phenotypic plasticity. The discussions presented here will likely be important when making decisions on whether selection emphasis should be on maximizing

growth and production or efficiency, as environmental sensitivity does not appear to have been previously considered.

Respiration Rate

Parameter estimates for respiration rate are presented in Table 2.4, but are not interpreted save for the genetic correlation, as they are uninterpretable with log transformed data. The genetic correlations are invariant to logarithmic transformations, however. The genetic correlation between the intercept and slope for respiration rate was highly negative and almost unity at -0.98 (-0.99 to -0.97; Table 2.4). Selection for respiration rate at ad libitum WI is therefore almost completely analogous to selection for respiration rate sensitivity (slope) to WR and indicates the genetic background for both traits is almost entirely shared.

The population slope was negative, indicating selection to decrease respiration rate with ad libitum water availability will increase respiration rate in water restricted environments. This is strange behavior, as it would apparently move the population slope towards zero, reduce environmental sensitivity, and increase phenotypic plasticity. However, respiration rate has been shown to be moderately and positively genetically correlated with production traits (Luo *et al.*, 2021), which is postulated to contribute towards expelling excess heat generated from increased metabolism (Kadzere *et al.*, 2002; Carabaño *et al.* 2014; Al-Kanaan, 2016; Polsky and Keyserlingk, 2017; Luo *et al.*, 2021). Assuming this holds true in a random regression model, then respiration rate is an indicator of performance.

Thus, the relationship between the additive genetic intercept and slope in this study is unfavorable, as selection to increase either respiration rate or production traits correlated with respiration rate under ad libitum water availability will inevitably decrease the slope and decrease phenotypic plasticity. Thus, these results augment the results of Al-Kanaan (2016) and

Luo *et al.* (2021), indicating selection for production will increase respiration rate and subsequently increase environmental sensitivity. Overall, there is a clear, unfavorable relationship between selection in an environment with ad libitum water intake and water restricted environments for both DMI and respiration rate, which supports conclusions made by Ravagnolo and Misztal (2000), Aguilar *et al.* (2009), Brügemann *et al.* (2011), and Bradford *et al* (2016).

Genetic, and Permanent Environment Variance Trajectories as a Function of Water Restriction

Additive genetic and PE variance trajectories were only computed for DMI due to the issues with interpreting variance components of logarithmic-transformed data. Given that the variance of a $2 \; x \; 2$, linear covariance matrix is quadratic (equation 17), the additive genetic variance likely behaves non-linearly as WR increases. As seen in Figure 2.2A, genetic variance is maximized at ad libitum WI, but quickly decreases as WR increases to 0.50. To put it in perspective using empirical rule with 95% probability, the results for ad-libitum WI equate to an EBV interval difference of 5.73 kg DMI. This is the same as the interval for the additive genetic intercept presented previously as a value of zero for WR negates the slope variance and intercept and slope covariance contributions (equation 17). At 50% WR, the empirical rule with 95% probability equates to an EBV interval of -1.94 to 1.94 kg DMI or a difference of 3.88 kg DMI based on the point estimate. Clearly, there is still room for selection at 50% WR. However, the decreased genetic variance leads to slower genetic progress (Bourdon, 2000), which is reflected by EBV intervals.

Interestingly, the point estimate of the genetic variance for DMI with ad libitum WI was more than double of Ahlberg *et al.* (2019). However, the model presented here is inherently different, with additional random effects of group and PE (Table 2.3). Cohort was treated as a fixed effect (e.g., contemporary group), breed covariates were included, and residuals were treated as homogeneous in Ahlberg *et al.* (2019). Many of the studies in the review of DMI presented by Berry and Crowley (2013) present similar modeling differences under different environments, which implies a different scope of inference (Tempelman, 2010). Differences in the scope of inference contribute to differences in variance component estimates and, more importantly, functions of variance components like heritability and genetic correlations.

Unfortunately, the declining genetic variance (Figure 2.2A) indicates water restricted environments may have more limited potential for genetic selection. Given these limitations, this may push producers in arid environments towards seeking locally adapted breeds rather than phenotypic plasticity. The reduction in genetic variance is consistent with other random regression studies of G×E in different environments in beef and dairy cattle (e.g., Brügemann *et al.*, 2011; Bradford *et al.*, 2016). There are two reasons this reduction in genetic variance could occur. First, the number of loci contributing towards the phenotype may decrease. Second, the effects of the contributing loci are likely shrunk toward the mean. Though the reduction in variance could be due to both factors, the second theory is consistent with the behavior of random effects in mixed models and agrees more readily with infinitesimal model theory.

Random regression has previously been applied to model individual locus intercepts and slopes (Yang *et al.*, 2015), rather than animal genetic intercepts and slopes, which may provide a methodology to distinguish whether one of the two scenarios or a combination of both is correct. Using the same methodology discussed in this study, genetic variance can be calculated for

specific levels of WR. If the genetic variance of some loci converges to zero as WR increases, it would provide evidence for less loci contributing effects; however, this would most likely imply the locus slope effects are non-normally distributed. In this case Bayesian models allowing distributional flexibility (Meuwissen *et al.*, 2001; Habier *et al.*, 2011) or a weighted SNP frequentist model (Zhang *et al.*, 2016) would be appropriate. If the variance merely shrinks for all loci, but does not converge to zero, then it would provide evidence for a genetic architecture fitting the infinitesimal model assumptions, meaning standard mixed model methodology is appropriate. It is also possible that it is a combination of both scenarios.

The environment-specific PE variance, which represents repeatable (permanent) environmental effects influencing DMI, was also modeled along the WR continuum (Figure 2.2B). The PE appeared to be lowest at intermediate levels of WR. However, the PE variance 95% HPDCIs overlapped zero until approximately 40% WR, implying there was little evidence for a PE effect until high levels of WR were reached. This is indicative of most environmental factors being random and temporary; however, it is unclear what types of PE effects may influence DMI at greater WR levels.

Heritability Trajectories Across Water Restriction

Dry Matter Intake

Environment-specific heritability and repeatability estimates can be computed as a function of environment-specific variance components and are reported in Figure 2.3. However, the residual variance was heterogeneous by group, given the differences between the group-specific residual variances (Table 2.3). This is important, as heritability and repeatability trajectories must be reported for each group (BIF guidelines, 2021b; Figure 2.3). Heterogeneity

by group was clearly important, as heritability point estimates and 95% HPDCIs varied substantially (Figure 2.3 and A.1).

Point estimates for heritability in the baseline environment ranged from 0.20 to 0.33 across groups (Figures 2.3 and A.1), meaning DMI with ad libitum water intake is lowly to moderately heritable (95% HPDCIs across all groups; 0.11,0.53). Ahlberg *et al.* (2019), using a subset of the data in this study and a standard animal model, estimated the heritability of DMI with ad libitum WI at 0.67. Other estimates in the literature are similarly high (Koch *et al.*, 1963; Archer *et al.*, 1997). A review looking of 38 studies reported heritability estimates between 0.06 to 0.70 (Berry and Crowley, 2013). More recent estimates of DMI heritability range from 0.27 to 0.41 in several continental and British beef cattle breeds (Snelling *et al.*, 2011; Saatchi *et al.*, 2014), 0.40 to 0.46 in Nellore (Santana *et al.*, 2014; Polizel *et al.*, 2018), and 0.21 to 0.50 in a genetic evaluation including G×E comparing dairy cattle across different countries (Yao *et al.*, 2017). Our 95% HPDCIs of heritability with ad libitum WI (0.11 to 0.53 across groups; Figures 2.3 and A.1) overlapped substantially with the range reported by Berry and Crowley (2013), the ranges reported by Snelling *et al.* (2011), and the range reported by Saatchi *et al.* (2014).

Phenotypically, DMI has been shown to decrease as water availability decreases (Utley *et al.*, 1970; Meyer *et al.*, 2006). However, the change in phenotypic variance of DMI as WR increases has not been reported. Point estimates for heritability decreased as WR increased (Figures 2.3 and A.1); however, no other study to our knowledge has modeled DMI additive genetic variance as a function of water availability. As previously discussed, the PE variance did not contribute much to overall variation (Figure 2.2A; Table 2.3). Given the only variance components changing as a function of the environment were the PE and additive genetic variance, this indicated the shrinkage of genetic variance is largely responsible for the reduced

heritability. Consequently, the accuracy of phenotypic selection is reduced as WR increases, which would further slow genetic progress (Bourdon, 2000).

Repeatability is expected to be similar to heritability, given little evidence for PE variance (Figure 2.2B). Repeatabilities were not much greater than heritability (Figures 2.4 and A.2), but were expected to be at least as large as heritability (Bourdon, 2000). Interestingly, repeatability point estimates appeared to stabilize at 0.40 or greater WR. This is likely due to increased evidence for a non-zero PE effect at WR values of 0.40 or greater, which served to offset the declining genetic variance.

Respiration Rate

Respiration rate has been shown to be lowly heritable in a heat stressed environment (0.04 ± 0.01; Luo *et al.*, 2021) and slightly more heritable at a thermoneutral environment (0.1; Al-Kanaan, 2016), which mirrors the behavior presented here with ad libitum and restricted WI (Figures 2.5 and A.3). In an environment with ad libitum water access, heritabilities were similar to Al-Kanaan (2016) with point estimates close to 0.10. Similar to Al-Kanaan (2016) and Luo *et al.* (2021), point estimates for heritability decreased to less than 0.05 as the environmental stressor increased. In our case, as WR approached and surpassed 0.30, there was no evidence for a heritable component as the 95% HPDCIs overlapped zero (Figures 2.5 and A.3), indicating no ability to genetically improve the population. Likely, estimates near this threshold will be unstable as they rapidly approach zero. Given the similarity in point estimates and trends as Al-Kanaan (2016) and that Al-Kanaan (2016) used a random regression model with a temperature humidity index as the environmental covariate, this may point to WR and temperature humidity

indices being similar environmental descriptors or having similar effects on the genetic potential of respiration rate.

If respiration rate is considered an indicator of productivity (Kadzere *et al.*, 2002; West, 2003; Carabaño *et al.* 2014; Polsky and Keyserlingk, 2017; Luo *et al.*, 2021) due to the genetic correlation with production traits (Luo *et al.*, 2021), then the declining heritability for respiration rate mirrors the declining heritability of DMI as a symptom of declining genetic potential for production.

Repeatability trajectories (Figures 2.6 and A.4) were nearly identical to heritability trajectories (Figures 2.5 and A.3), so the PE variance was low if not entirely negligible (Bourdon, 2000). Like heritability, there appeared to be no evidence for respiration rate being repeatable as WR surpassed 0.20 and approached 0.30. Furthermore, given the point estimates and trajectories between groups were not greatly variable (Figures 2.6 and A.4), differences in temporary environment effects contributing towards heteroscedasticity were not as important for respiration rate as they were for DMI.

Genetic Correlations Across Different Levels of Water Restriction

Genetic correlations between DMI or respiration rate across different levels of WR are useful to determine the extent of G×E effects, as they reflect the potential for EBVs in one level of WR to be a predictor of EBVs at another value of WR and whether the additive genetic slope variance is great enough to cause sire reranking. Genetic correlations between DMI at different levels of WR are presented in Figure 2.7A and point estimates and 95% HPDCIs for select levels of WR are presented in Table A.2. In general, pairwise genetic correlations of DMI between two WR levels ranging from 0.00 to 0.30 tended to be very high (greater than 0.90), indicating EBVs

predicted using data from low WR levels tended to be excellent indicators of DMI EBVs predicted using data from moderate values of WR and vice-versa. In other words, using DMI EBVs from ad libitum water intakes are expected to be fairly accurate predictors of DMI EBVs under WR until high levels of WR (greater than 30%) are achieved. Dry matter intake genetic correlations between levels of WR ranging from 0.30 to 0.50 WR decayed slightly faster (Figure 2.7A), indicating EBVs generated at moderate values of WR are slightly weaker predictors of EBVs at high levels of WR in comparison (Figure 2.7A and Table A.2). Clearly, however, genetic correlations are lowest when comparing low or moderately low WR values to WR values greater than 0.40. In this case, DMI EBVs at ad libitum water intake are weaker predictors for DMI EBVs in heavily water restricted environments. This is similar to the conclusions of Bradford *et al.* (2016), who noted similar results for correlations between weaning weight and yearling weight at varying levels of a temperature humidity index. However, depending on the context, 0.80 may still be considered adequate, as it's difficult to determine at what level reduction in genetic correlations may meaningfully impact selection. Assuming 0.80 is adequate, this may indicate that environmental sensitivity to WR is not currently important to consider in selection decisions.

Currently, the relative change in genetic correlations between a trait in different environments is unknown. As discussed previously, if DMI or respiration rate are selected on under the baseline environmental conditions of ad libitum WI (the intercept), then the environmental sensitivity is expected to change. Assume this selection is in a direction which increases the environmental sensitivity. Under these conditions, the natural question is the degree to which between-environment genetic correlations are expected to change. Any change would imply a change in the genetic covariance between the intercept and slope for the trait (equation

18), assuming genetic variances remain constant (Crow, 1986). Genetic variation has been shown to be relatively stable over periods of selection (Yoo *et al.*, 1980; CDCB, 2021), which supports the notion of the covariance between the intercept and slope for a trait being the main driver of changes in the genetic correlations between a trait across different environments. If the genetic covariance between the intercept and slope does change, it likely means pleiotropic loci are moving towards fixation and new genetic variation does not have the same average pleiotropic effects. It could also mean new LD patterns between loci influencing the intercept and slope do not mimic the old LD patterns. If the genetic covariance between the intercept and slope does not change, however, then the genetic correlations between a trait across different environments would not be expected to change (assuming constant genetic variances). Thus, it remains unclear whether increasing or decreasing environmental sensitivity would change the genetic correlations between a trait across environments and correspondingly change G×E.

Selection in a singular environment or across a narrow range of environments, however, has been shown to decrease the between-environment genetic correlations outside of the range of environments where selection was practiced (Schou *et al.*, 2019). Interestingly, genetic correlations appear to remain very high over time within the narrow range of environments where selection occurs (Schou *et al.*, 2019). This is likely due to environments being very similar, which is reflected by the values of x and x' in equation 18. As the two environmental values converge, the covariance function converges to equation 17, which leads to a correlation of one. Overall, it is reasonable to suggest that continued selection for increased DMI under ad libitum WI conditions may decrease between-environment genetic correlations over time. If this occurs, environmental sensitivity will increase and between-environment genetic correlations will decrease, which will in turn decrease inter-environment predictability in future generations.

To our knowledge, no study has simulated the change in genetic correlations as selection under optimal environments occurs over many successive generations.

Genetic correlations between respiration rate using data from different levels of WR are presented in Figure 2.7B and point estimates and 95% HPDCIs are presented for select levels of WR in Table A.3. Respiration rate genetic variance decreased to near zero as WR approached 0.30 (as evidenced by the decreasing heritability in Figure 2.5), so correlations were only generated using data where WR was less than or equal to 0.25. In general, genetic correlations barely decreased as the distance between WR values increased and were uniformly high. This indicates selection on respiration rate at ad libitum intake will generally be a good predictor of respiration rate at moderate levels of WR, past which genetic variance is depleted.

Spearman Correlations Across Different Levels of Water Restriction

While genetic correlations between DMI or respiration rate at low and high levels of WR were generally very high, animal EBVs for either trait may re-rank as WR increases. If re-ranking is meaningful, then accuracy of selection will be lost. Spearman rank correlations between DMI EBVs at different levels of WR were generally high (Figure 2.8A). The lowest rank correlation point estimate observed was 0.80 (0.69, 0.90; Table A.2) between the EBVs at WR values of 0 and 0.50, which is consistent with the genetic correlations in Figure 2.7A. Rank correlations between the DMI EBVs at low and moderate levels of water restriction were nearly one, indicating animals in low to moderate WR environments tend to rank similarly. This corroborates well with the genetic correlations presented in Figure 2.7A.

Spearman rank correlations for respiration rate EBVs at different levels of WR were essentially identical to the genetic correlations between respiration rate at different levels of WR

(Figure 2.8B and 2.8B and Table A.3). Like the conclusions for respiration rate genetic correlations, EBV rankings for respiration rate in an environment with ad lib WI is a near perfect predictor of EBV rankings in moderately restricted environments. Water restriction values past 0.25 were not considered due to the depletion of genetic variance. In this case, the Spearman rank correlations seem to indicate a small loss in accuracy of selection between various levels of WR and minimal G×E effects. Therefore, elite animals under ad libitum WI conditions are likely to be elite animals in other environments. However, while sire reranking resulting from G×E may not be a concern, the rate of genetic progress is still certainly impacted due to the shrinkage of genetic variance.

Beef Improvement Federation Accuracies

Beef Improvement Federation accuracies were generally high for the EBVs of the additive genetic intercepts and slopes (Table 2.5). Accuracies for environment specific DMI EBVs increased as WR increased (Figure 2.2, 2.3, 2.9A). This is initially unexpected, but this study was purposely designed to include large amounts of water restricted data. Thus, parameter estimates are probably weighted towards the greatest density of data points close to 50% WR (Figure 2.1), which is intuitive. This would mean the posterior EBV variances should be lowest about the areas with the greatest data density. Interestingly, the BIF accuracy densities between 0.30 and 0.45 WR for DMI EBVs were non-normal, with a heavy skew towards lower accuracy. It is not entirely clear why the BIF accuracy densities were skewed in this region (Figure 2.9A).

Accuracies for the additive genetic intercept and slope EBVs for respiration rate were similar to those for DMI EBVs (Table 2.5), albeit with a lower additive genetic slope EBV mean accuracy. This may have been due to the lack of genetic variance at higher WR values where the

parameters were weighted, indicating future models should probably not exceed 0.30 WR. Accuracy of EBV prediction increased as WR increased (Figure 2.9B).

Genome Wide Association Study

Single nucleotide polymorphisms associated with the slope and intercept for DMI and respiration rate are presented in Table 2.6 and shown on Manhattan plots in Figures 2.10 and 2.11. Ten SNPs were associated with the DMI intercept, seven with the DMI slope, two with the respiration rate intercept, and one with the respiration rate slope. Utilizing a significance threshold of $-\log_{10}(p\ value) > 4.5$ with 123,912 SNPs, approximately four false positives are expected for the intercept and slope of DMI or respiration rate under the null hypothesis if SNPs are independent. However, not all SNPs are independent, as LD can create correlations which render the tests for each SNP non-independent (Nyholt, 2004). This likely means the expected number of false positives is lower, given many SNPs are close together on the array.

Variants Identified in Both the Intercept and Slope

Some SNPs were associated with both the intercept and slope within a trait. This was expected, because the correlation between the intercept and slope was large (Tables 2.3 and 2.4). For respiration rate, one SNP, rs109899758 (Table 2.6), was significantly associated with the intercept and slope (and had a large effect point estimate); however, it was unfortunately unmapped and therefore no gene candidates could be identified in the analysis.

For DMI, two SNPs, rs43381095 and rs43431165 (Table 2.6), were significantly associated with the intercept and slope. The rs43381095 QTL region overlapped with two gene candidates, DGKB and TRNAC-GCA. The latter has clear functions in translation and is

associated with the amino acid Cysteine. Given the broad scope of its role, it is unclear how it may mechanistically relate to DMI. The DGKB gene is a diacylglycerol kinase involved in phosphatidylinositol turnover (Sakane *et al.*, 2018). This may be the most likely of the two candidate genes, because phosphatidylinositol is part of a second-messenger system with direct signaling implications in metabolic pathways and cellular proliferation (Ramazzoti *et al.*, 2017). This may have implications for cellular energy states and signaling increased hunger and feed intake. However, given the diverse roles of the phosphatidylinositol second-messenger system, this is merely speculative.

The rs43431165 QTL region overlapped with seven gene candidates, DTD1, SCP2D1, LOC107133048, LOC112449285, SLC24A3, LOC112449287, and LOC112449288. Of the seven gene candidates, SLC24A3 and DTD1, or D-Aminoacyl-tRNA Deacylase 1, are the most likely candidates with known function. The first, SLC24A3, is a solute carrier involved in electrochemical neural transmission and smooth muscle contraction (Pizzagalli *et al.*, 2020). It could be argued this may involve digestive flowthrough via smooth muscle contractions, which might affect the rate of feed intake. The second, DTD1, has been associated with saturated and unsaturated fatty acid tissue levels in a previous human GWAS study (Andersen *et al.*, 2016). While the association with fatty acids represents a promising relationship with metabolism and feed intake, it is also unclear as to how a tRNA deacylase influences fatty acid tissue levels or metabolism.

Variants Associated with DMI Intercept

However, many SNPs were only associated with either the intercept or the slope. Thirteen SNPs were only associated with either the intercept or slope for DMI (Table 2.6). The

first variant for the DMI intercept, rs110689635, was associated one gene candidate, PAX1, which is a transcription factor and has previously been associated with embryonic development and thymus development to produce T-cells (Yamazaki *et al.*, 2020). It is unclear how this gene's function might affect DMI; however, it was also previously reported to be associated with body weight (Veerkamp *et al.*, 2012) and fat thickness at the 12th rib (Naserkheil *et al.*, 2020). Body weight and fat thickness are genetically correlated with DMI (Vallimont *et al.*, 2010; Ceacero *et al.*, 2016), which gives additional evidence that the variant rs110689635 may be related to DMI.

The second variant, rs134083327, was associated with two Cysteine tRNA genes and a gene of unknown function. It is unknown how the Cysteine tRNA genes may influence DMI under thermoneutral conditions. The rs41629087 variant was associated with several genes, including a gene involved in the SNARE complex and exocytosis and several Cystatin genes in the Cystatin gene superfamily. Cystatins are Cysteine proteinase inhibitors. The Cystatin genes play a role in a vast number of processes, including oncogenesis, various vascular diseases, and immune function (Ochieng and Chaudhuri, 2011). Its potential role with DMI remains unclear, but associations between DMI and variants near genes related to immune function may be common (e.g., Seabury *et al.*, 2017; Ghebrewold, 2018). It is, however, interesting that multiple loci involve Cysteine tRNAs and Cysteine proteinases. It is possible there is no relationship between the two, but it is interesting Cysteine-based biological systems are prominent across so many loci. This may indicate some unknown biological function or pathway that influences DMI.

The rs133281924 variant was associated with genes related to DNA transcription, translation, and complex metabolism-related signaling pathways, such as the mTOR pathway.

The most interesting candidate, however, was ATP6V1D, which is a protein involved in endocytosis, hydrogen ion transport (e.g., the electron transport chain in central metabolism), and the mTOR pathway (Sun, 2013). It is extensively involved in central metabolism, which could explain an association between the variant and DMI as it would regulate the energy balance and hunger signaling in the animal.

The rs109410618 variant was associated with several genes involved in DNA repair and transcription and translation. There was no clear association between the gene functions and DMI, however, given the broad functions these genes serve. Like the previous variant, rs109990182 associated genes and their functional relationship to DMI were ambiguous. One gene, ODAD2, is involved in ciliated movement in mucosal linings, however. While it was previously associated with airway disease (Legendre *et al.*, 2021), cilia lining the digestive system may have relationships to feed digestion/flowthrough or hunger signaling.

The SNP rs43076526 was associated with ALDH7A1, which is an important enzyme in alcohol metabolism (Wang *et al.*, 2014). While it may seem counterintuitive for alcohol metabolism to be relevant in cattle, various feeds may contain fermentation products and various fungi and bacteria in the rumen may ferment feeds and produce alcohols (Kristensen *et al.*, 2007). Assuming the fermentation products are absorbed, the animal would have a need to digest the alcohol products.

The last variant associated with the DMI intercept, rs42342704, was associated with several genes. Most genes had no known function or function that appeared to be related to DMI. Per QTLdb, rs42342704 has previously been associated with steak fatty acid content (Saatchi *et al.*, 2013) and muscle zinc content (Mateescu *et al.*, 2013). Fatty acid content and DMI may be indirectly related, as total DMI influences energy available for fat deposition. It is unclear,

however, what genomic feature may be influencing both. Muscle zinc content may be related to greater nutrient acquisition through feed, but it is difficult to posit a direct relationship.

Variants Associated with the DMI Slope

Five variants were associated exclusively with the DMI slope (Table 2.6). The first, rs42210470, was associated with the RRAGA gene. RRAGA is part of a general RAS signaling pathway and was examined as a target for differential expression in ruminal epithelium in a residual feed intake study (Elolimy *et al.*, 2019). There was no evidence for differential expression (Elolimy *et al.*, 2019) in high vs. low residual feed intake steers, but this association may provide additional evidence to support an association between RRAGA function and residual feed intake and/or feed intake environmental sensitivity.

The second variant, rs136988024, was associated with PPP2R5E, which is a serine phosphatase and regulates cell growth and cellular division (Cristóbal *et al.*, 2013). It directly regulates the mTOR pathway, which is implicated in cellular growth and may influence hunger signaling and feed intake (Cristóbal *et al.*, 2013). The third variant, rs134380542, was associated with several genes, but none had any clear function related to DMI.

The fourth variant, rs41686942, was associated with several potential gene candidates. Cystatin 3 and CST7 are Cystatin genes, similar to the cystatin genes discussed previously. The APMAP and ACSS1 genes could also play roles in DMI, however. The APMAP gene product is suspected to play a role in adipocyte differentiation and fatty acid/tissue production (Bogner-Strauss *et al.*, 2010) and the ACSS1 gene product converts acetate to acyl CoA, which is an essential step in fatty acid metabolism for energy production (Bräsen and Schönheit, 2004). Both fatty acid production and metabolism are inherently related to DMI and energy conversion

because volatile fatty acids and thus fatty acid production and metabolism are the primary product of digestion in the rumen (Baldwin and Allison, 1983). Therefore, both genes may affect the energy balance, which could be related to feed intake/hunger signaling. The last variant, rs133631786, was associated with several CD receptor and B-cell receptor genes, but there was no clear indicator for how these genes may be related to DMI.

Notably, Saatchi *et al.* (2014) identified ACSL6, which is similar to ACSS1 as it converts fatty acids to acyl CoA, as a pleiotropic gene candidate for DMI and mid-test metabolic body weight. The ACSL6 protein is heavily involved in central metabolism via fatty acid beta oxidation for energy production. A notable difference between the two studies is the interpretation of DMI in a traditional animal model vs. a random regression model intercept or slope. The variant effect point estimates represent the average effects of the variant across represented environments (Lillehammer *et al.*, 2007), but it is unlikely animals in the study were ever exposed to a WR environment. The correlation between the intercept and slope was large; it is feasible the variants may have effects in both ad libitum WI and WR environments, but it could not be detected in this study due to sample size or alleles segregating in different populations.

Variants Associated with the Respiration Rate Intercept and Slope

For respiration rate, one SNP was uniquely associated with the intercept (Table 2.6); however, there were no genes identified in the QTL region. This may indicate the causal mutation is in a sparse intergenic region, there may be assembly problems, or there may be missing annotations. No unique variants were identified for the respiration rate slope (Table 2.6).

Genome Wide Association Study Overview

As previously discussed, many different variants were associated with either the slope or intercept despite the large genetic correlation between the two. This is expected due to the sample size and the genetic correlation between the two being non-unity. Some may not have been detected for the other trait due to issues with power. However, some loci may only influence DMI in water restricted environments as they are influenced by different variation in the genome. The same phenomenon has been seen in random regression GWAS in dairy cattle populations, where higher order terms in the random regression model identified additional loci influencing different stages of production (Lillehammer *et al.*, 2007; Lillehammer *et al.*, 2009; Hayes *et al.*, 2009). In these random regression GWAS, the ability to detect loci was improved by utilizing repeated records and allowing for genetic covariance functions (van der Werf *et al.*, 1998). Therefore, our ability to detect loci was likely improved compared to a traditional animal model or simple repeated records model where genetic variance is assumed constant and environments are genetically independent.

Identification of Biological Pathways and Processes with Network Analysis

For DMI intercept, the KEGG pathway analysis revealed that SNARE interactions in the vesicular transport pathway were enriched in the PPI network (Table 2.7). The SNARE pathway involves the fusion of vesicles to the cellular membrane or lysosomes through endocytosis and exocytosis (Han *et al.*, 2017). These processes play roles in energy production and the cell life cycle (cell aging and death) and have been associated with metabolic diseases such as diabetes (Wirawan *et al.*, 2012). Dysfunctions in the pathway may result in decreased performance or energy production efficiency, which could influence feed intake. Enriched biological process GO

terms (Table 2.7) were comprised of metabolic pathways, including the phosphatidylinositol biosynthetic process and the lipoprotein biosynthesis process, as well as positive regulation of binding, protein oligomerization, and regulation of protein secretion. The SNARE pathway is likely related to the GO term regulation of protein secretion, as endocrine systems involve exocytosis of signaling molecules. Lipoproteins are also heavily involved in exocytosis, which work in conjunction with SNARE proteins and Clathrin for mediating secretion (Miller *et al.*, 2011; Bionaz *et al.*, 2020) and additionally transport many molecules throughout the body. Furthermore, phosphatidylinositol has been shown to be an important soluble signaling molecule in many pathways through similar PPI network analyses (Zewail *et al.*, 2003). An associated list of metabolic pathways includes cellular proliferation/growth, vesicle trafficking, glucose transport, lipid metabolism, protein synthesis/degradation, transcriptional regulation, and many other metabolic pathways (Fruman *et al.*, 1998; Zewail *et al.*, 2003; Ramazzoti *et al.*, 2017).

Combined, this information indicates that signaling molecules and exocytosis of signaling molecules are important in regulating metabolic pathways that ultimately affect DMI in ad libitum WI conditions. Protein secretion may be related to metabolic signaling through endocrine action, however, which would indicate these pathways could be related to the slope as well, based off the previous discussion of individual gene candidates.

The KEGG pathways associated with slope of DMI (Table 2.7) were mostly associated with amino acid metabolism, glycolysis and gluconeogenesis, and fatty acid metabolism. Amino acid metabolic pathways included most of the typical 20 amino acids and the central metabolic pathways included gluconeogenesis/glycolysis, pyruvate metabolism, beta-Alanine metabolism (a source of energy), propanoate (an important volatile fatty acid in beef cattle for energy production), and fatty acid metabolism. Each pathway converges during the Kreb's cycle for

energy production. Thus, any variant with an effect on energy production will likely affect energy balance and, subsequently, hunger signaling, which indicates a clear relationship between central metabolism pathways and DMI. Other pathways included drug and xenobiotic metabolism via cytochrome P450, ascorbate and aldarate metabolism, chemical carcinogenesis, and glyoxylate and dicarboxylate. However, the association between these pathways and DMI is more cryptic.

Conclusions

In general, the genetic correlation between the intercept and slope of DMI and respiration rate indicated that increased selection on either trait when ad libitum water is available affected the environmental sensitivity. Thus, it is probable that increasing DMI will increase the environmental sensitivity of the population. Notably, increasing respiration rate under ad libitum water intake increased environmental sensitivity due to its negative correlation with the slope. This is counterintuitive initially, but is a logical result under the proposed hypothesis of respiration rate as an indicator of productivity.

Genetic variance and heritability decreased substantially for DMI as WR increased. There was genetic variation for selection on DMI at large values of WR, but the selection potential was clearly reduced. Therefore, genetic progress under water restricted environments would be slower than predicted under ad libitum conditions. The genetic variance and heritability of respiration rate declined to essentially zero at moderate to high levels of WR, indicating there is no ability to practice selection under water restricted environments. This may be true for many traits, which would indicate that climate change presents a serious challenge for livestock genetic improvement.

Genetic correlations between DMI or respiration rate at different levels of WR tended to be very high. Genetic correlations between DMI at different values of WR were 0.80 between the most divergent environments. Genetic correlations between respiration rate at different values of WR were nearly one between 0% and 25% WR, where there was evidence that respiration rate was heritable. Similarly, Spearman rank correlations between the EBVs of DMI and respiration rate at different levels of WR were nearly identical. Therefore, DMI and respiration rate accuracy of selection for individuals under water restricted environments using ad libitum water intake EBVs would be expected to be very high because G×E effects are small. However, genetic progress in water restricted environments would be lessened due to the lack of genetic variance and shrinkage of EBVs. Furthermore, while rankings remain the same, selection for ad libitum intake production will continue to negatively impact the environmental sensitivity because of the negative correlation between the intercept and slope. It is also unclear whether continued selection under ad libitum production will lead to the degradation of genetic correlations between environments, which would increase G×E effects.

Finally, this study identified unique variants that contribute to performance under ad libitum WI or WR environments. Most variants and candidate genes were only identified for either the intercept or slope. However, many variants had candidate genes with similar function, such as direct relationships to central metabolism and energy balance/hunger signaling. This may indicate the variants may influence both the intercept and slope but were not identified for both given the small sample size. This would correspond with the generally high genetic correlations for DMI between different levels of WR.

Table 2.1 Water restriction observations (N), minimums, maximums, means, and quartiles for each restriction period are given for dry matter intake (DMI) and respiration rate. All values are a water restriction percentage.

Trait	N	Restriction	Min	1st Quartile	Median	Mean	3rd Quartile	Max
DMI	3,268	10	0.0	10.6	20.2	29.4	44.1	99.7
	4,295	20	0.0	13.6	22.0	27.4	36.1	99.2
	4,454	30	0.1	22.7	29.6	31.0	36.3	99.8
	4,450	40	0.3	31.7	38.8	38.5	44.5	99.7
	27,533	50	0.1	39.9	47.5	47.3	54.7	99.8
Respiration Rate	4,789	10	0.0	11.2	21.4	32.0	48.7	99.7
	6,809	20	0.0	13.4	21.5	26.1	33.9	97.2
	6,860	30	0.1	23.2	29.7	30.6	35.7	99.8
	6,757	40	0.3	31.8	38.7	37.8	54.5	99.8
	53,057	50	0.1	39.9	47.4	47.2	54.5	99.8

Table 2.2 Minimum, maximum, mean, median (Med.), first quartile (1st Q.), third quartile (3rd Q.), and standard deviation (SD) of daily dry matter intake (DMI; kg) and observed bi-daily respiration rates (breaths per 30 seconds; BP30S) by group.

Trait	Group	N	Min	1st Q.	Med.	Mean	3rd Q.	Max	SD
DMI (kg)	1	114	0.1	7.0	8.8	8.6	10.4	19.1	2.7
	2	114	0.2	7.2	8.5	8.6	9.9	18.4	2.3
	3	112	0.5	5.3	6.8	7.0	8.5	15.7	2.3
	4	105	0.1	7.7	9.1	9.1	10.5	17.8	2.1
	5	123	1.0	8.1	9.7	9.7	11.3	19.5	2.4
	6	120	2.7	8.5	9.6	9.7	10.8	21.5	1.8
	7	100	0.1	6.1	7.6	7.7	9.2	17.8	2.2
Respiration Rate (BP30S)	1	114	1	22	27	28.4	34	79	8.7
	2	114	1	11	13	14.3	16	60	5.7
	3	112	2	18	24	26.6	32	84	10.8
	4	105	2	24	30	32.1	38	130	11.3
	5	123	1	14	18	19.2	22	131	6.7
	6	120	1	12	14	16.5	20	60	6.9
	7	102	1	26	32	33.4	40	90	10.4

Table 2.3 Table of posterior point estimates for each model parameter, including lower and upper bounds of 95% highest posterior density credible intervals, and the effective sample sizes for dry matter intake (DMI). Point estimates were the medians of the posterior densities.

Parameter	Point Estimate	Lower	Upper	Effective Sample Size
η[1]	10.27	8.94	11.84	54
β_1[2]	-4.10	-4.22	-3.99	12,821
σ_f^2[3]	1.99	0.29	9.27	1,767
σ_a^2[4]	2.08	1.36	2.67	575
σ_{ab}[5]	-1.91	-2.80	-0.97	908
σ_b^2[6]	3.16	1.64	4.76	1,626
σ_g^2[7]	0.38	0.00	0.93	492
σ_{gh}[8]	-0.67	-1.47	0.06	806
σ_h^2[9]	2.18	0.75	3.62	1,795
$\sigma_{e_1}^2$[10]	5.01	4.84	5.18	20,000
$\sigma_{e_2}^2$	3.63	3.49	3.76	20,000
$\sigma_{e_3}^2$	3.16	3.04	3.27	19,583
$\sigma_{e_4}^2$	2.92	2.82	3.03	19,533
$\sigma_{e_5}^2$	4.06	3.92	4.20	20,000
$\sigma_{e_6}^2$	1.44	1.39	1.48	20,000
$\sigma_{e_7}^2$	3.45	3.32	3.57	20,000
r_{ab}[11]	-0.75	-0.88	-0.59	1,016

[1] Fixed intercept

[2] Fixed slope for water restriction

[3] Between group variance (block)

[4] Additive genetic intercept variance

[5] Additive genetic covariance between the intercept and slope

[6] Additive genetic slope variance

[7] Permanent environment intercept variance

[8] Permanent environment covariance between the intercept and slope

[9] Permanent environment slope variance

[10] Residual variance for group i

[11] Additive genetic correlation between the intercept and slope

Table 2.4 Table of posterior point estimates for each model parameter, including lower and upper bounds of 95% highest posterior density credible intervals, and the effective sample sizes for respiration rate. Point estimates were the medians of the posterior densities.

Parameter	Point Estimate	Lower	Upper	Effective Sample Size
η[1]	1.43	1.28	1.63	13
β_1 [2]	-0.16	-0.17	-0.16	17,346
σ_f^2[3]	3.93e-02	6.65e-03	1.82e-01	379
σ_a^2[4]	6.01e-03	4.73e-03	7.41e-03	1,999
σ_{ab}[5]	-1.29e-02	-1.53e-02	-1.05e-02	2,484
σ_b^2[6]	2.87e-02	2.39e-02	3.35e-02	2,983
σ_g^2[7]	9.01e-04	1.29e-04	1.75e-03	930
σ_{gh}[8]	-5.94e-04	-2.03e-03	4.15e-04	1,176
σ_h^2[9]	1.67e-03	5.14e-05	4.72e-03	1,093
$\sigma_{e_1}^2$ [10]	1.69e-02	1.65e-02	1.74e-02	20,000
$\sigma_{e_2}^2$	2.15e-02	2.08e-02	2.21e-02	20,000
$\sigma_{e_3}^2$	2.63e-02	2.54e-02	2.71e-02	20,000
$\sigma_{e_4}^2$	2.13e-02	2.08e-02	2.19e-02	20,000
$\sigma_{e_5}^2$	1.91e-02	1.86e-02	1.95e-02	18,428
$\sigma_{e_6}^2$	2.18e-02	2.13e-02	2.24e-02	18,972
$\sigma_{e_7}^2$	1.93e-02	1.87e-02	1.98e-02	19,569
r_{ab}[11]	-0.98	-0.99	-0.97	2,556

[1] Fixed intercept

[2] Fixed slope for water restriction

[3] Between group variance (block)

[4] Additive genetic intercept variance

[5] Additive genetic covariance between the intercept and slope

[6] Additive genetic slope variance

[7] Permanent environment intercept variance

[8] Permanent environment covariance between the intercept and slope

[9] Permanent environment slope variance

[10] Residual variance for group i

[11] Additive genetic correlation between the intercept and slope

Table 2.5 Beef Improvement Federation accuracies for the additive genetic intercept and slope estimated breeding values (EBV) for dry matter intake (DMI) and respiration rate, including the 95% density lower and upper bounds.

Trait	*Parameter*	*BIF Accuracy*	*Lower*	*Upper*
DMI EBV	Intercept	0.49	0.35	0.62
	Slope	0.60	0.51	0.65
Respiration Rate EBV	Intercept	0.45	0.27	0.59
	Slope	0.46	0.28	0.60

Table 2.6 Significant single nucleotide polymorphisms (SNP) associated with the intercept and slope of dry matter intake (DMI) and respiration rate (resp. rate) are reported with the genomic location and positive, base ten logarithm transformed p-values. The number of gene candidates in the linkage disequilibrium range (±250 kilobases) associated with each single nucleotide polymorphism (SNP) is listed. Asterisks indicate unmapped SNPs and/or no gene candidates. Bolded SNPs appeared in both the intercept and slope for the trait.

Trait	*SNP ID*	*Chr*	*Position*	$-log_{10}(p\ value)$	*Gene Candidates*
DMI Intercept	**rs43381095**	4	22,867,751	5.26	2
	rs43431165	13	38,935,644	5.15	7
	rs110689635	13	41,066,076	5.13	1
	rs134083327	12	10,040,464	4.96	3
	rs41629087	13	42,303,504	4.89	13
	rs133281924	10	79,350,337	4.77	16
	rs109410618	4	103,409,974	4.76	7
	rs109990182	13	36,931,090	4.71	7
	rs43076526	7	27,252,564	4.70	10
	rs42342704	10	87,957,986	4.61	7
DMI Slope	rs42210470	8	25,384,913	5.47	5
	rs43431165	13	38,935,644	5.16	7
	rs136988024	10	76,021,126	5.12	8
	rs134380542	4	114,746,432	4.76	4
	rs43381095	13	22,867,741	4.58	2
	rs41686942	13	42,395,432	4.57	11
	rs133631786	3	12,627,278	4.51	10
Resp. Rate Intercept	**BovineHD3000041474**	*	*	12.51	*
	rs43127418	6	1,687,796	4.55	0
Resp. Rate Slope	**BovineHD3000041474**	*	*	12.45	*

Table 2.7 Pathways and biological process (BP) gene ontologies associated with dry matter intake (DMI) intercept and slope quantitative trait loci. Bolded terms indicate BP gene ontologies.

Trait	*Pathway or BP Gene Ontology*
DMI Intercept	SNARE interactions in vesicular transport
	Positive regulation of binding
	Phosphatidylinositol biosynthetic process
	Protein oligomerization
	Regulation of protein secretion
DMI Slope	Histidine metabolism
	Glycolysis/Gluconeogenesis
	beta-Alanine metabolism
	Pyruvate metabolism
	Metabolic pathways
	Phenylalanine metabolism
	Propanoate metabolism
	Tyrosine metabolism
	Valine, leucine, and isoleucine degradation
	Drug metabolism - cytochrome P450
	Chemical carcinogenesis
	Ascorbate and aldarate metabolism
	Fatty acid degredation
	Tryptophan metabolism
	Arginine and proline metabolism
	Lysine degradation
	Glyderolipid metabolism
	Fatty acid biosynthesis
	Glyoxylate and dicarboxylate metabolism
	Glucagon signaling pathway
	Carbon metabolism
	AMPK signaling pathway
	Insulin signaling pathway
	Regulation of translational initiation

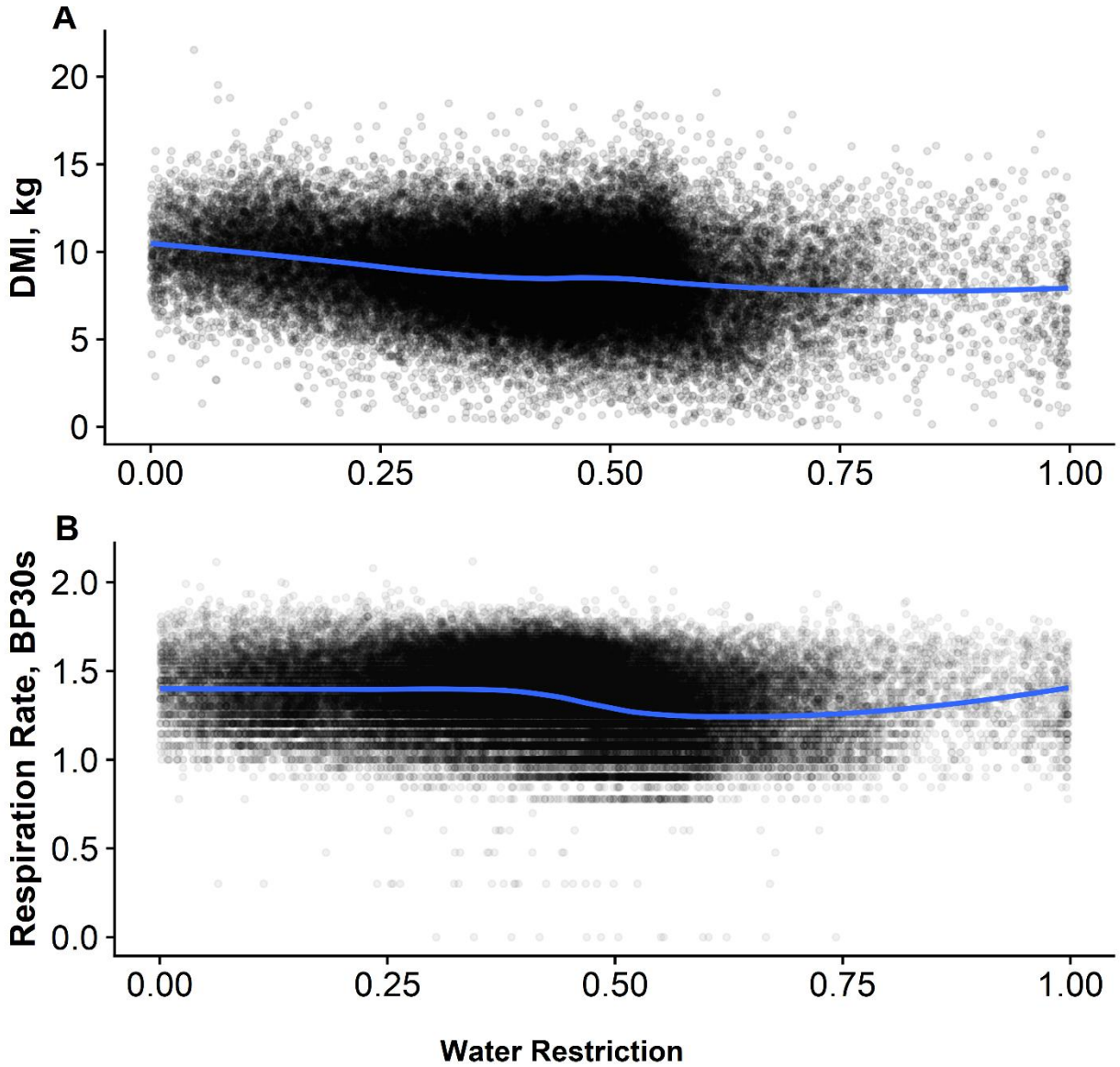

Figure 2.1 Scatterplot of daily dry matter intake (DMI; A) in kilograms and respiration rate (B), measured in breaths per 30 seconds (BP30S), at varying levels of water restriction. A locally weighted scatterplot smoothing line (blue) was fit to determine the relative population trajectory.

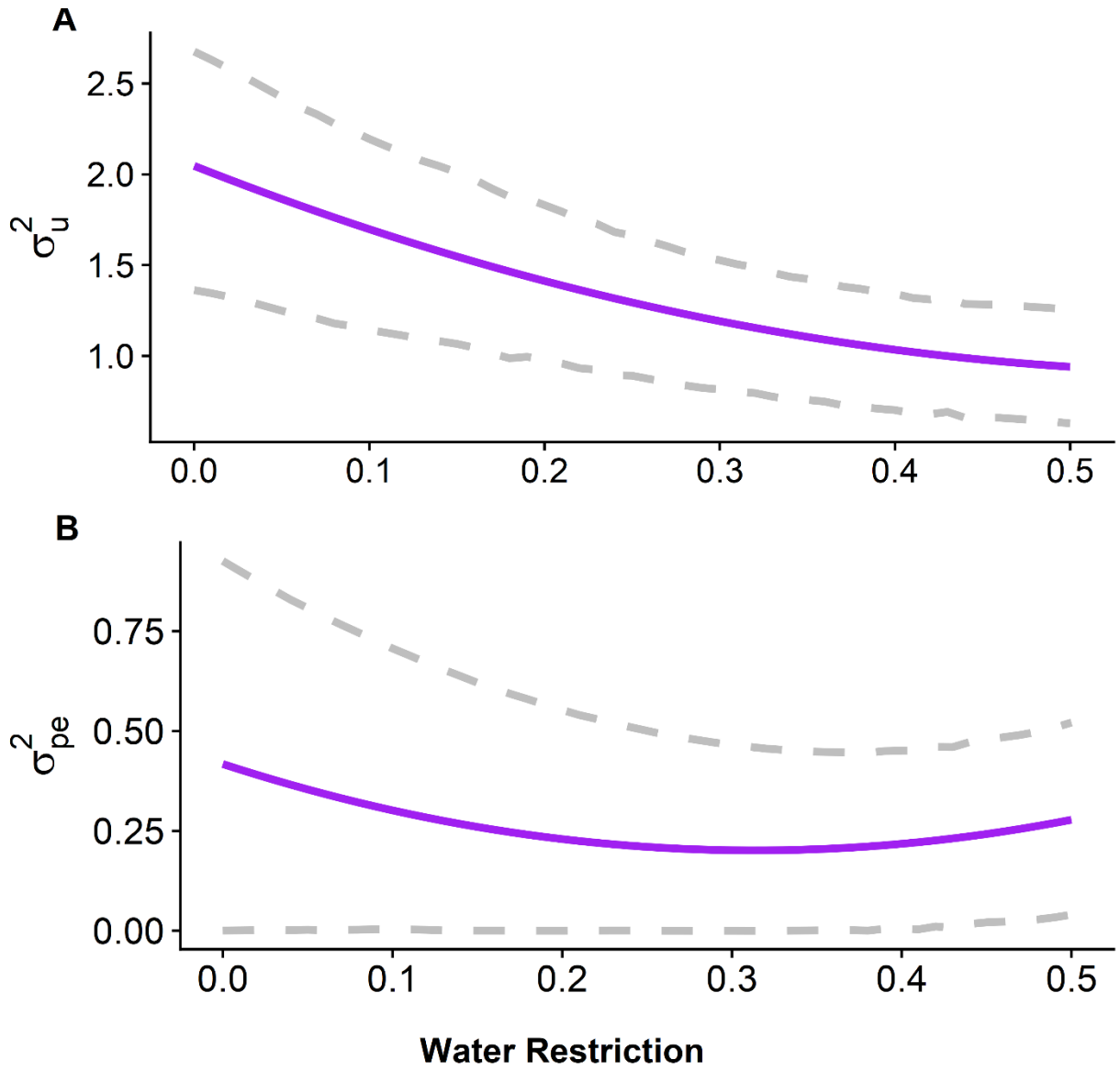

Figure 2.2 The posterior means (purple line) for additive genetic variance (A) and permanent environment variance (B) of dry matter intake by water restriction level. The gray dashed lines represent the upper and lower bounds of the 95% highest posterior density credible intervals.

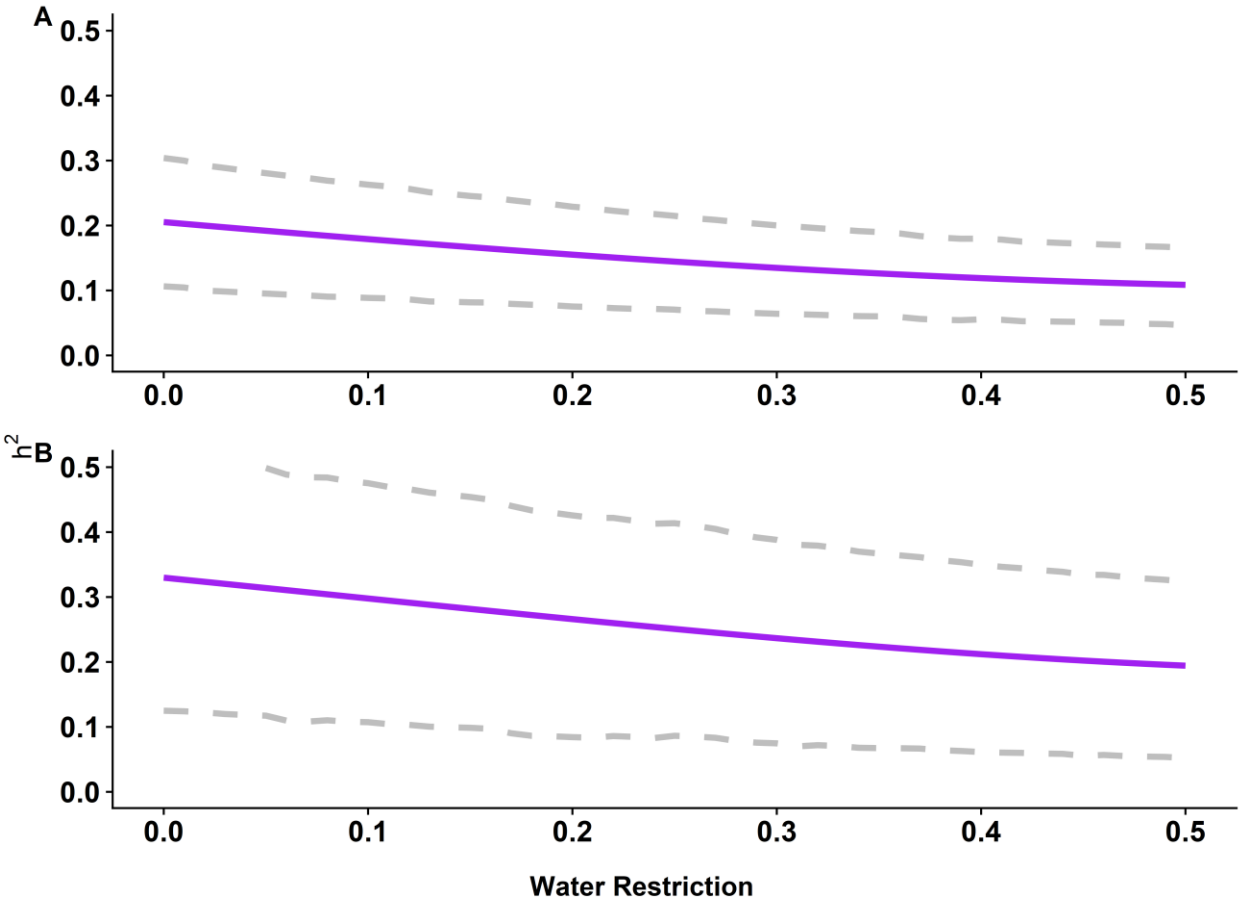

Figure 2.3 Heritability of dry matter intake as water restriction increases for groups 1 (A) and 6 (B). Groups 1 and 6 represent the groups with the highest and lowest point estimate for the residual variance, respectively. The purple line indicates posterior mean point estimates for each value of water restriction and the gray, dashed lines are the 95% highest posterior density credible intervals for each value of water restriction.

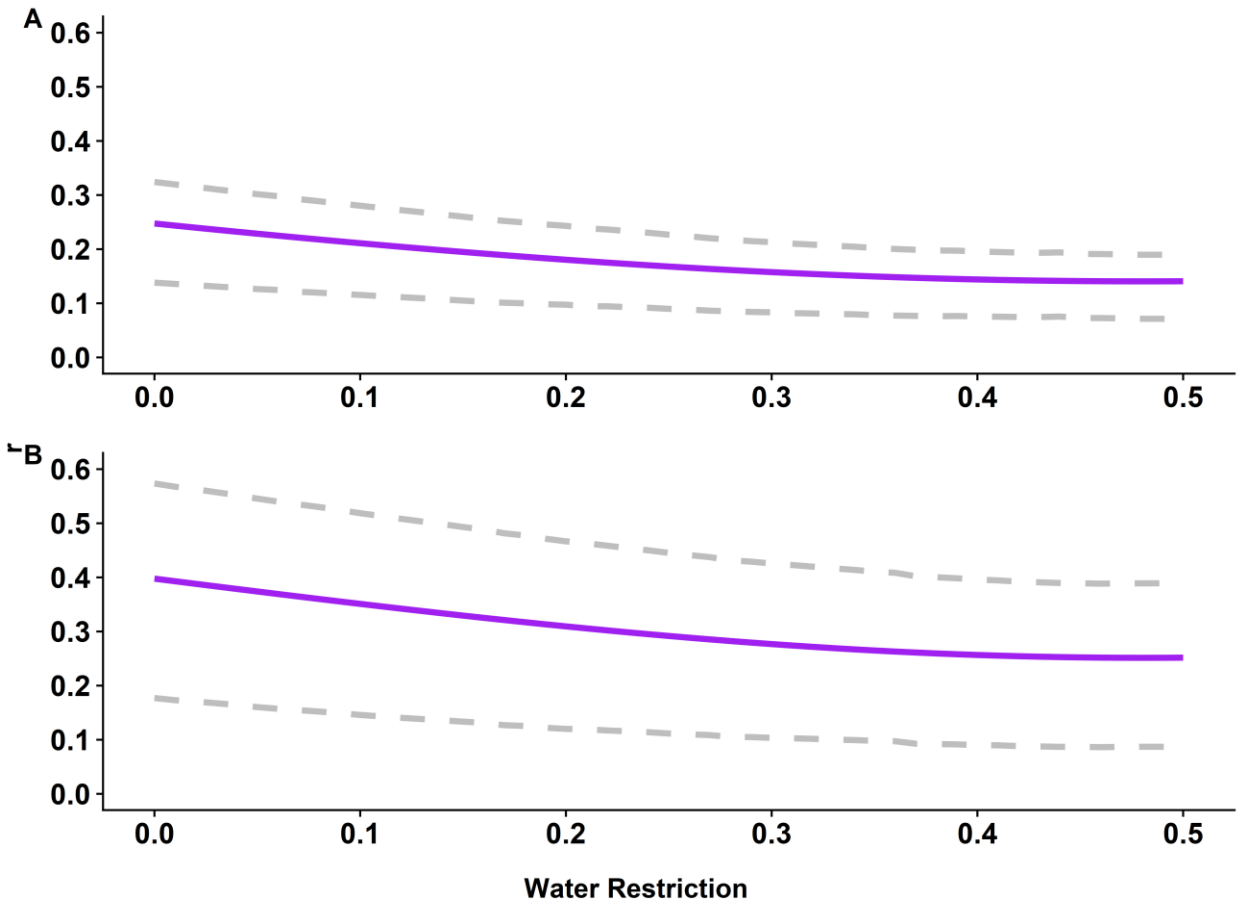

Figure 2.4 Repeatability of dry matter intake as water restriction increases for groups 1 (A) and 6 (B). Groups 1 and 6 represent the groups with the highest and lowest point estimate for the residual variance, respectively. The purple line indicates posterior mean point estimates for each value of water restriction and the gray, dashed lines are the 95% highest posterior density credible intervals for each value of water restriction.

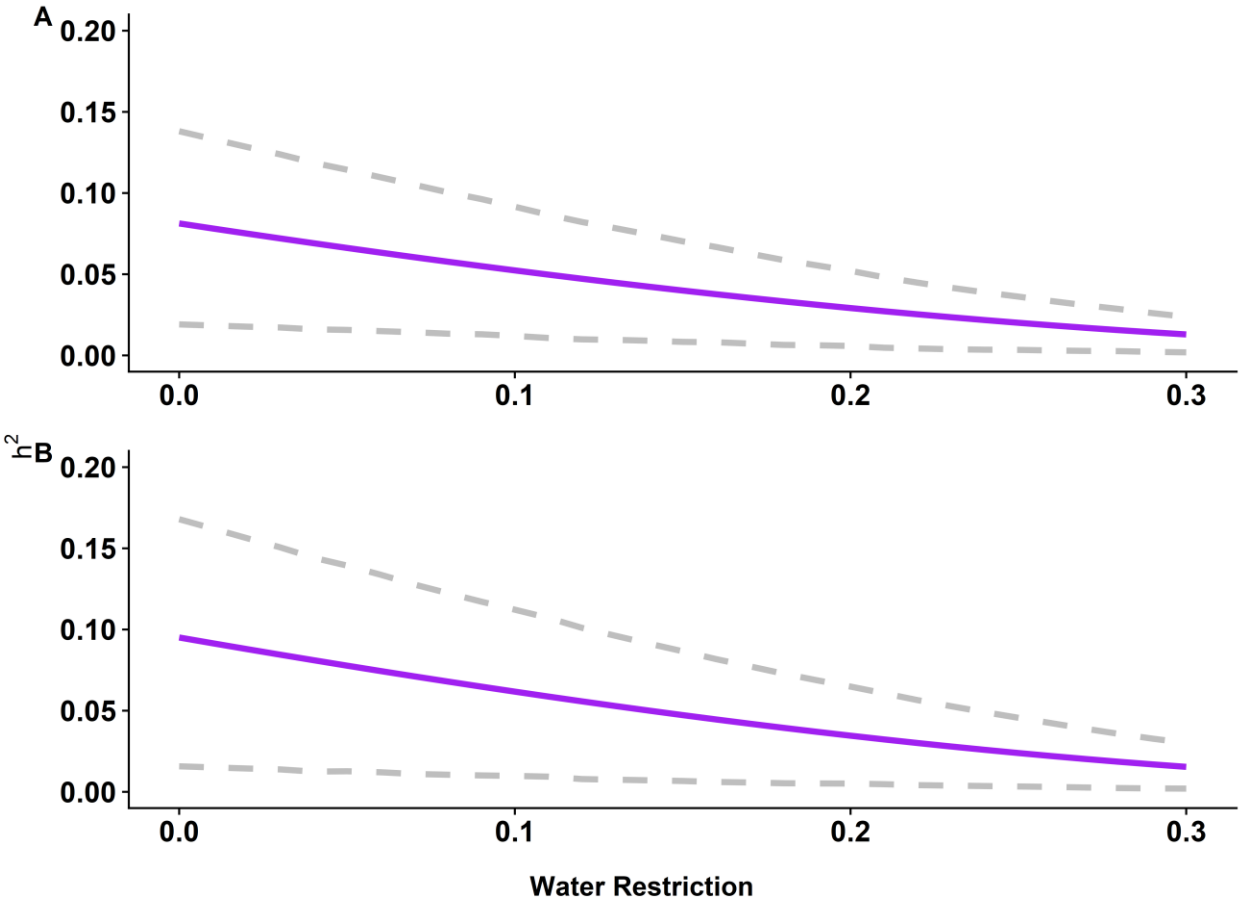

Figure 2.5 Heritability of respiration rate as water restriction increases for groups 3 (A) and 1 (B). Groups 3 and 1 represent the groups with the highest and lowest point estimate for the residual variance, respectively. The purple line indicates posterior mean point estimates for each value of water restriction and the gray, dashed lines are the 95% highest posterior density credible intervals for each value of water restriction.

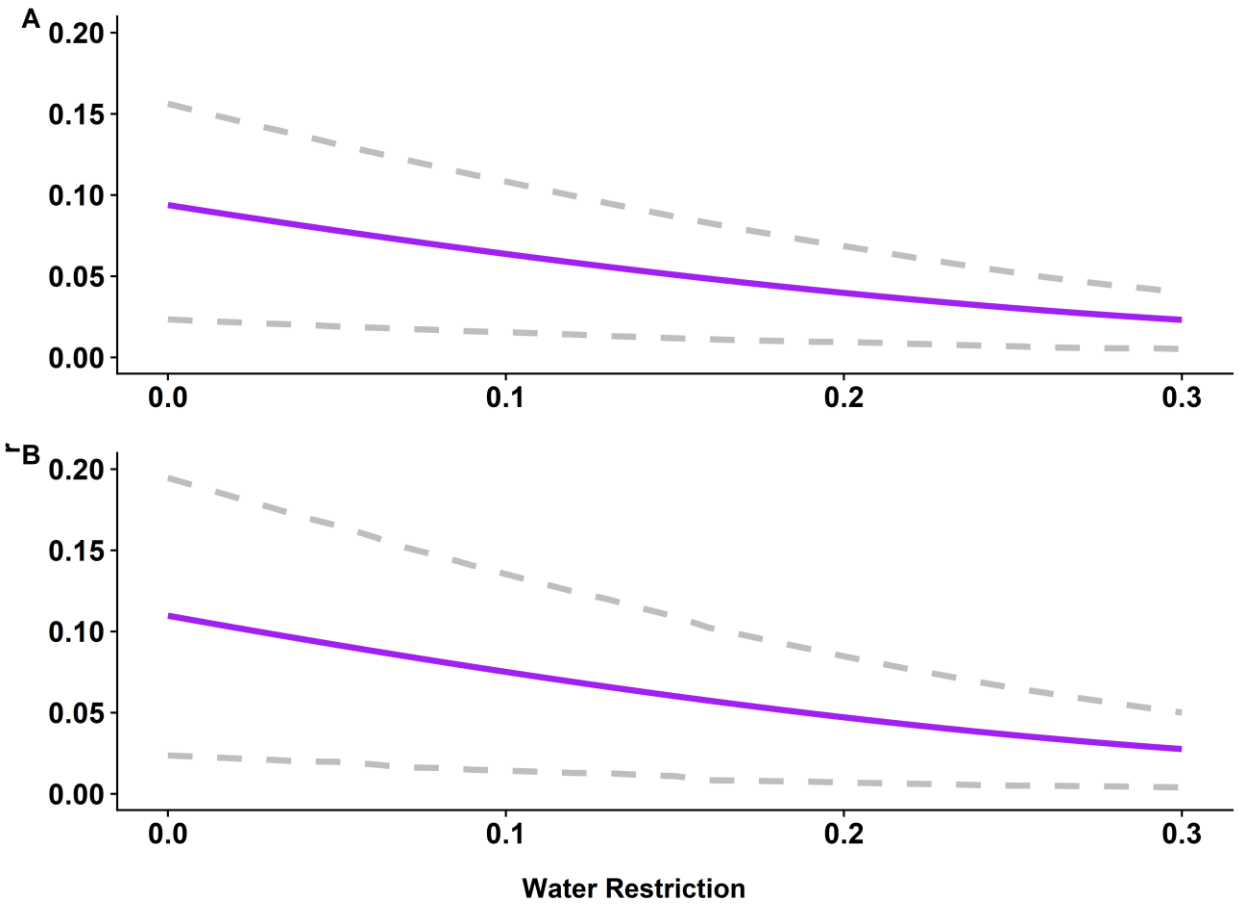

Figure 2.6 Repeatability of respiration rate as water restriction increases for groups 3 (A) and 1 (B). Groups 3 and 1 represent the groups with the highest and lowest point estimate for the residual variance, respectively. The purple line indicates posterior mean point estimates for each value of water restriction and the gray, dashed lines are the 95% highest posterior density credible intervals for each value of water restriction.

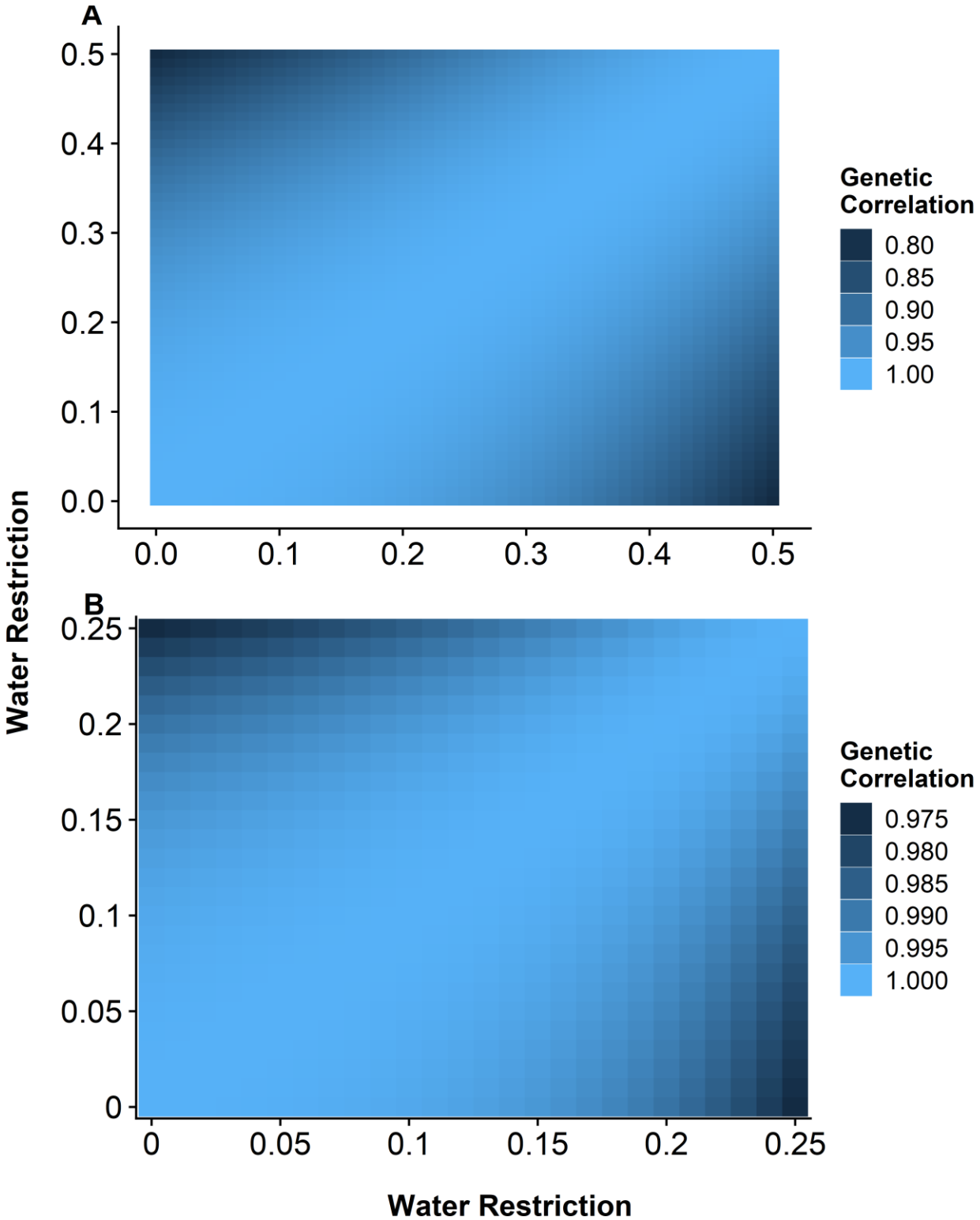

Figure 2.7 Genetic correlation point estimates between dry matter intake across various levels of water restriction (A) and respiration rate across various levels of water restriction (B).

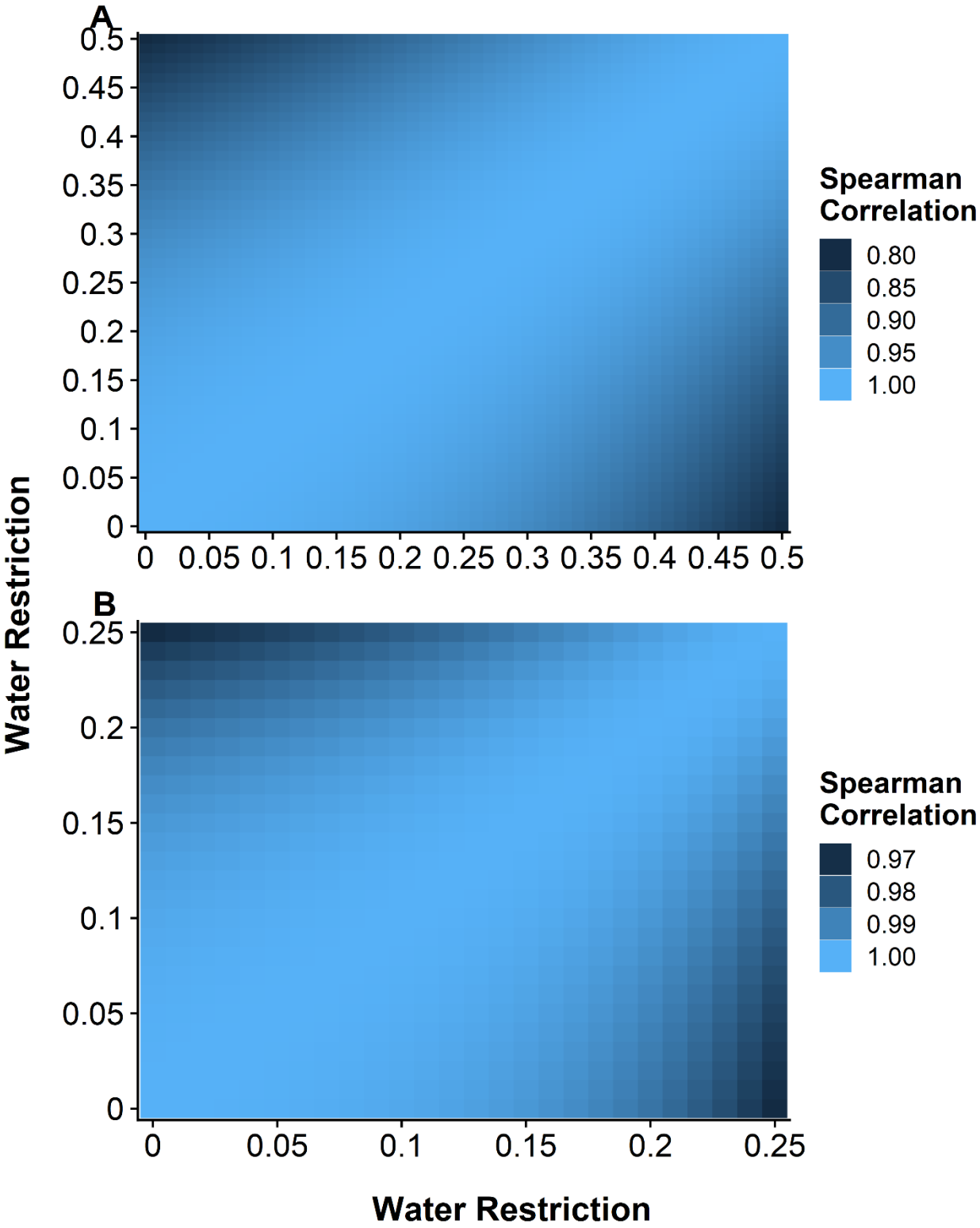

Figure 2.8 Spearman rank correlations between estimated breeding values for dry matter intake at different levels of water restriction (A) or respiration rate at different levels of water restriction (B).

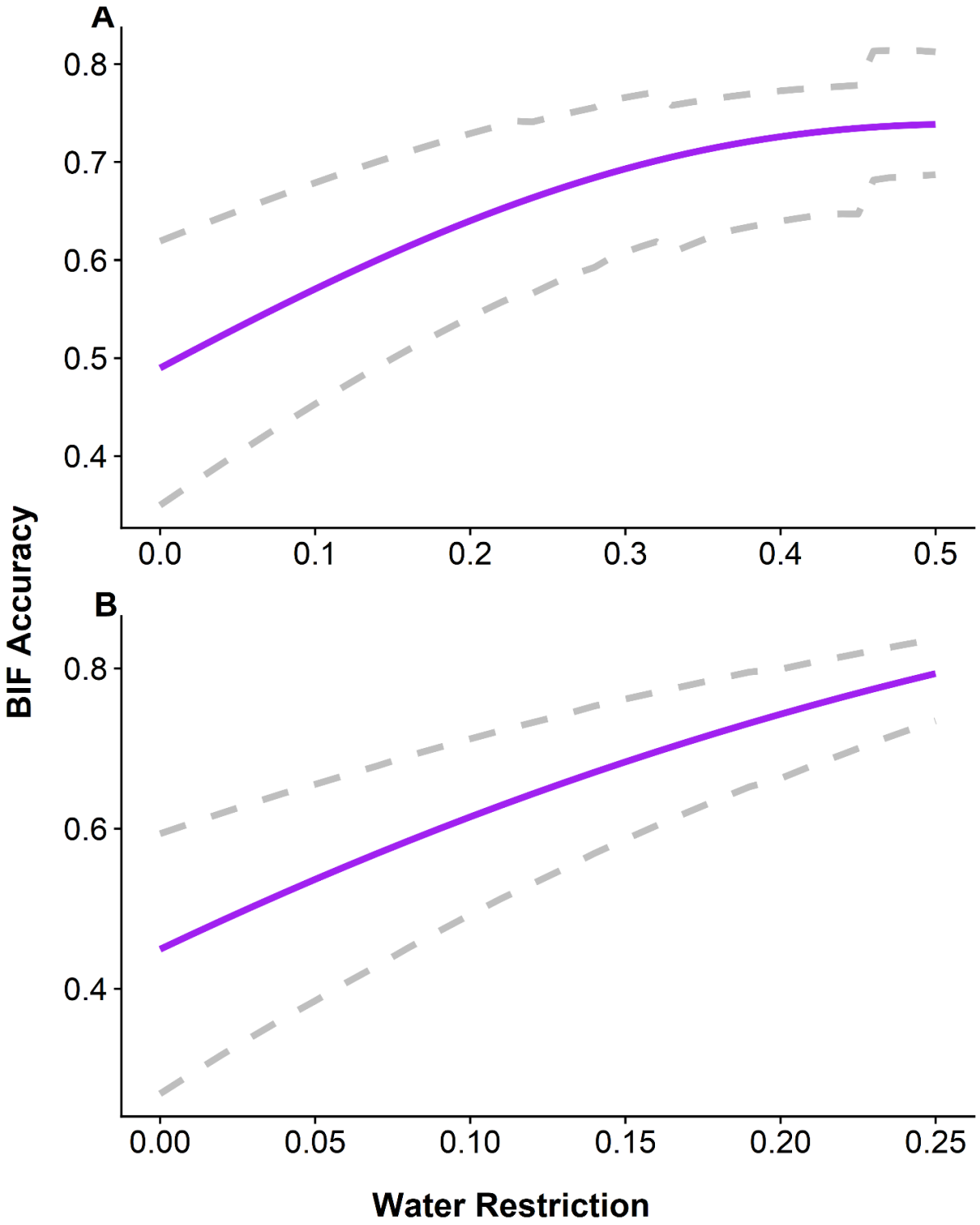

Figure 2.9 Mean Beef Improvement Federation accuracy represented by the purple line for dry matter intake (A) and respiration rate (B) as water restriction increases. The gray, dashed lines represent the 95% highest density credible interval.

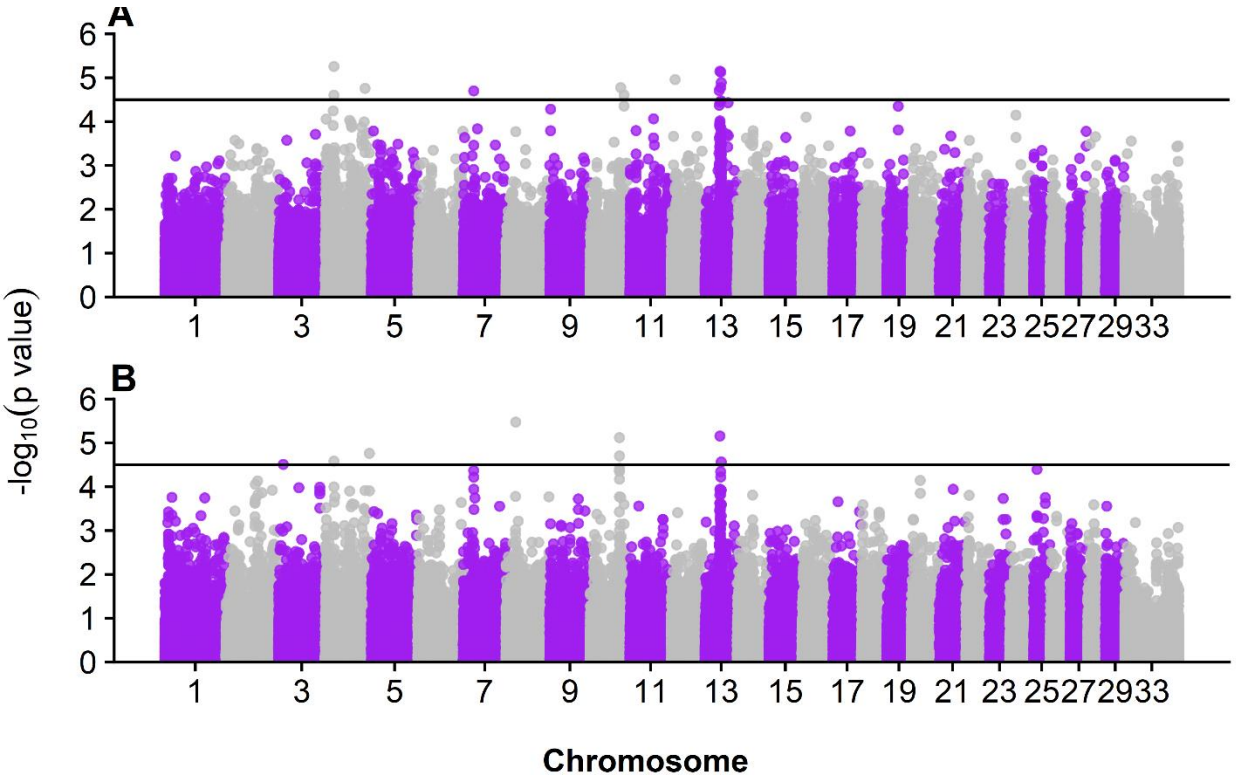

Figure 2.10 Manhattan plot showing the positive, base-ten logarithm transformed probability values for the dry matter intake intercept (A) and slope (B). Chromosome 33 corresponds to unmapped markers.

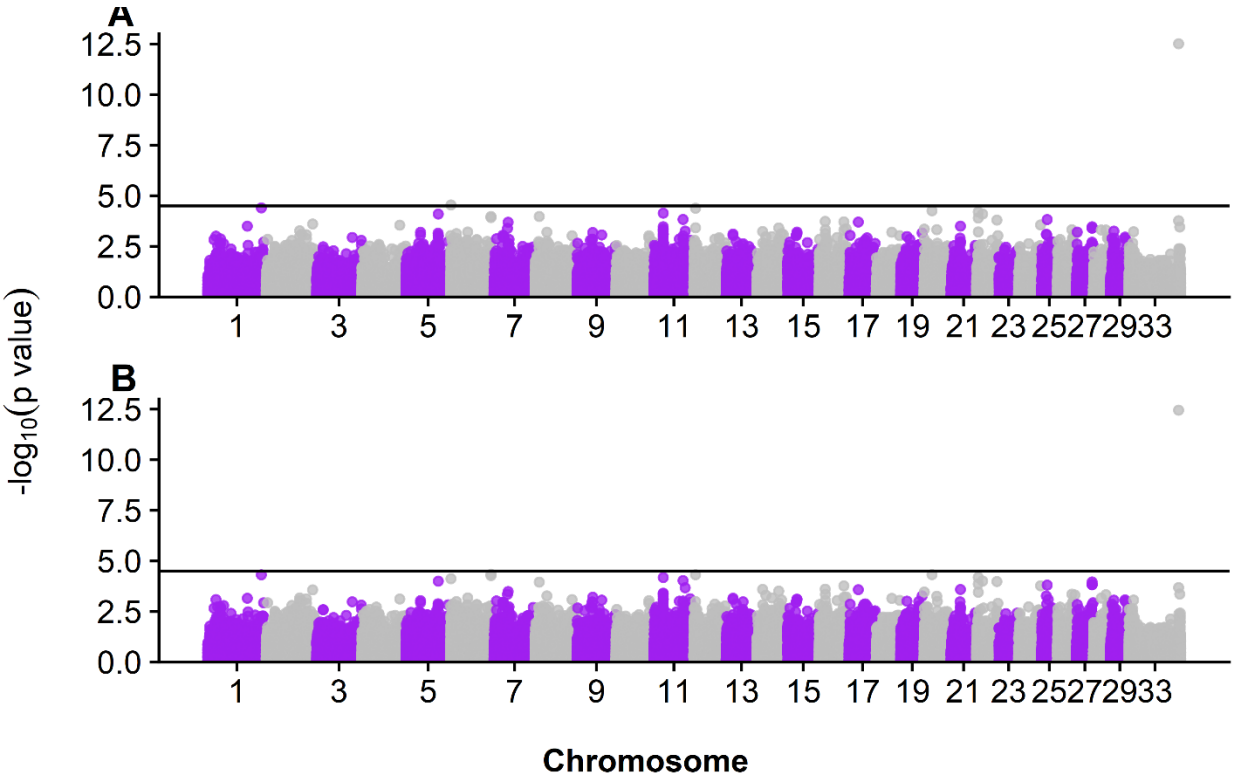

Figure 2.11 Manhattan plot showing the positive, base-ten logarithm transformed probability values for respiration rate intercept (A) and slope (B). Chromosome 33 corresponds to unmapped markers.

References

Aguilar, I., I. Misztal, and S. Tsuruta. 2009. Genetic components of heat stress for dairy cattle with multiple lactations. J. Dairy Sci. 92:5702-5711.

Aguilar, I., I. Misztal, D. L. Johnson, A. Legarra, S. Tsuruta, T. J. Lawlor. 2010. Hot topic: a unified approach to utilize phenotypic, full pedigree, and genomic information for genetic evaluation of Holstein final score. J. Dairy Sci. 93:743-752.

Aguilar, I., S. Tsuruta, Y. Masuda, D. A. Lourenco, A. Legarra, and I. Misztal. 2018. BLUPF90 suite of programs for animal breeding with focus on genomics. In: Proc. 11th World Cong. Genet. Appl. Livest. Prod., Auckland, New Zealand:751.

Ahlberg, C. M., K. Allwardt, A. Broocks. K. Bruno, A. Taylor, L. Mcphillips, C. R. Krehbiel, M. Calvo-Lorezno, C. J. Richards, S. E. Place, U. Desilva, D. L. Vanoverbeke, R. G. Mateescu, L. A. Kuehn, R. Weaber, J. Bormann, and M. M. Rolf. 2019. Characterization of water intake and water efficiency in beef cattle. J. Anim. Sci. 97:4770-4782.

Al-Kanaan, A. J. J. 2016. Heat stress response for physiological traits in dairy and dual purpose cattle populations on phenotypic and genetic scales. PhD Diss. Univ. Kassel, Germany.

Alamar, M. A. 2009. Effect of water restriction on lactation performance of Aardi goats under heat stress conditions. Small Rumin. Res. 84:76-81.

Allwardt, K., C. Ahlberg, A. Broocks, K. Bruno, A. Taylor, S. Place, C. Richards, C. Krehbiel, M. Calvo-Lorenzo, U. DeSilva, D. VanOverbeke, R. Mateescu, C. Goad, and M. M. Rolf. 2017. Technical note: Validation of an automated system for monitoring and restriction water intake in group-house beef systems. J. Anim. Sci. 95:4213-4219.

Andersen, M. K., E. Jørsboe, C. H. Sandholt, N. Grarup, M. E. Jørgensen, N. J. Færgeman, P. Bjerregaard, O Pedersen, I. Moltke, T. Hanse,n and A. Albrechtsen. 2016. Identification of novel genetic determinants of membrane fatty acid composition among Greenlanders. PLoS Genet. 12:e1006119.

Archer, J. A., P. F. Arthur, R. M. Herd, P. F. Parnell, and W. S. Pitchford. 1997. Optimum postweaning test for measurement of growth rate, feed intake, and feed efficiency in British breed cattle. J. Anim. Sci. 75:2024-2032.

Baldwin, R. L, and M. J. Allison. 1983. Rumen metabolism. J. Anim. Sci. 57:461-477.

Banos, G., and A. Sigurdsson. 1996. Application of contemporary methods for the use of international data in national genetic evaluations. J. Dairy Sci. 79:1117-1125.

Beef Improvement Federation Guidelines. 2021a. Accuracy. http://guidelines.beefimprovement.org/index.php/Accuracy (Accessed 8 June 2021.)

Beef Improvement Federation Guidelines. 2021b. Heterogeneous variance. Available from http://guidelines.beefimprovement.org/index.php/Heterogeneous_varianceBenjamini, Y., and Y. Hochberg. 1995. Controlling the false discovery rate: A practical and powerful approach to multiple testing. J. R. Stat. Soc. Ser. B Methodol. 57:289-300.

Berry, D. P., and J. J. Crowley. 2013. Cell biology symposium: genetics of feed efficiency in dairy and beef cattle. J. Anim. Sci. 91:1594-1613.

Bionaz, M., E. Vargas-Bello-Pérez, and S. Busato. 2020. Advances in fatty acids nutrition in dairy cows: from gut to cells and effects on performance. J. Anim. Sci. and Biotechnol. 11:110.

Bogner-Strauss, J. G., A. prokesch, F. Sanchez-Cabo, D. Rieder, H. Hackl, K. Duszka, A. Krogsdam, B. D. Camillo, E. Walenta, A. Klatzer, A. Lass, M. Pinent, W. Wong, F.

Eisenhaber, and Z. Trajanoski. 2010. Reconstruction of gene association network reveals a transmembrane protein required for adipogenesis and targeted by PPARγ. Cell. Mol. Life Sci. 67:4049-4064.

Bourdon, R. M. 2000. Factors affecting the rate of genetic change. In: Understanding animal breeding. Prentice Hall, Upper Saddle River, NJ. P. 200.

Bradford, H. L., B. O. Fragomeni, J. K. Bertrand, D. A. L. Lourenco, and I. Misztal. 2016. Genetic evaluations for growth heat tolerance in Angus cattle. J. Anim. Sci. 94:4143-4150.

Bräsen, C., and P. Schönheit. 2004. Regulation of acetate and acetyl-CoA converting enzymes during growth on acetate and/or glucose in the halphilic arcaheon Haloarcula marismortui. FEMS Microbiol. Lett. 241:21-26.

Brew, M. N., R. O. Meyer, M. J. Hersom, J. N. Carter, M. A. Elzo, G. R. Hansen, and D.G. Riley. 2011. Water intake and factors affecting water intake of growing beef cattle. Livest. Sci. 140:297-300.

Brotherstone, S., and M. Goddard. 2005. Artificial selection and maintenance of genetic variance in the global dairy cow population. Phil. Trans. R. Soc. B. 360:1479-1488.

Brügemann, K., E. Gernand, U. U. von Borstel, and S. König. 2011. Genetic analyses of protein yield in dairy cows applying random regression models with time-dependent and temperature x humidity-dependent covariates. J. Dairy Sci. 94:4129-4139.

Burgos, M. S., M. Senn, F. Sutter, M. Kreuzer, and W. Langhans. 2001. Effect of water restriction on feeding and metabolism in dairy cows. Am. J. Physiol. Regulatory Integrative Comp. Physiol. 280:R418-R427.

Ceacero, T. M., M. E. Z. Mercadante, J. N. S. G. Cyrillo, R. C. Canesin, S. F. M. Bonilha, and L. G. de Albuquerque. 2016. Phenotypic and genetic correlations of feed efficiency traits with growth and carcass traits in Nellore cattle selected for postweaning gain. PLoS One 11:e0161366.

Carabaño, M. J., K. Bachagha, M. Ramón, and C. Díaz. 2014. Modeling heat stress effect on Holstein cows under hot and dry conditions: Selection tools. J. Dairy Sci. 97:7889-7904.

The Council of Dairy Cattle Breeding. 2020. Genotypic and phenotypic trends. https://queries.uscdcb.com/eval/summary/trend.cfm (Accessed 8 June 2020.)

Cristóbal, I., C. Cirauqui, R. Castello-Cros, L. Garcia-Orti, M. J. Calasanz, and M. D. Odero. 2013. Downregulation of PPP2R5E is a common event in acute myeloid leukemia that affects the oncogenic potential of leukemic cells. Haematologica: 98:e103-e104.

Crow, J. F. 1986. Basic concepts in population, quantitative, and evolutionary genetics. W.H. Freeman, New York.

Elolimy, A. A., E. Abdel-Hamied, L. Hu, J. C. McCann, D. W. Shike, and J. J. Loor. 2019. Rapid communication: Residual feed intake in beef cattle is associated with differences in protein turnover and nutrient transporters in ruminal epithelium. J. Anim. Sci. 97:2181-2187.Federation of Animal Science Societies. 2010. Guide for the care and use of agricultural animal in research and teaching. Responses of Cattle to thermal heat loads. http:// aaalac.org/about/Ag_Guide_3rd_ed.pdf

Fonseca, P. A., A. Suárez-Vega, G. Marras, and A. Cánovas. 2020. GALLO: an R package for genomic annotation and integration of multiple data sources in livestock for positional candidate loci. GigaScience 9:giaa149.

Fruman, D. A., R. E. Meyers, and L. C. Cantley. Phosphoinositide kinases. Annu. Rev. Biochem. 67:481-507.

Golher, D. M., G. H. M. Patel, S. H. Bhoite, M. I. Syed, G. J. Panchbhai, and P. Thirumurugan. 2020. Factors influencing water intake in dairy cows: a review. Int. J. Biometeorol. 65:617-625.

Grandin, T. 2016. Evaluation of the welfare of cattle housed in outdoor feedlot pens. Vet. Anim. Sci. 1:23-28.

Habier, D., R. L. Fernando, D. Kizilkaya, and D. J. Garrick. 2011. Extension of the Bayesian alphabet for genomic selection. BMC Bioinform. 12:168.

Han, J., K. Pluhackova, and R. A. Böckmann. 2017. The multifaceted role of SNARE proteins in membrane fusion. Front. Physiol. 8:5.

Hayes, B. J., P. J. Bowman, A. J. Chamberlain, K. Savin, C. P. van Tassell, T. S. Sonstegard, and M. E. Goddard. 2009. A validated genome wide association study to breed cattle adapted to an environment altered by climate change. PloS ONE 4:e6676.

Hill, D. L., and E. Wall. 2017. Weather influences feed intake and feed efficiency in a temperate climate. J. Dairy Sci. 100:2240-2257.

Hu, Z., C. A. Park, and J. M. Reecy. 2019. Building a livestock genetic and genomic information knowledgebase through integrative developments of animal QTLdb and CorrDB. Nucleic Acids Res. 47:D701-D710.

Kadzere, C. T., M. R. Murphy, N. Silanikove, and E. Maltz. 2002. Heat stress in lactating dairy cows: a review. Livest. Prod. Sci. 77:59-91.

Kanehisa, M., and S. Goto. 2000. KEGG: Kyoto Encyclopedia of Genes and Genomes. Nucleic Acids Res. 28:27-30.

Koch, R. M., L. A. Swiger, D. Chambers, and K. E. Gregory. 1963. Efficiency of feed use in beef cattle. J. Anim. Sci. 22:486-494.

Kristensen, N. B., A. Storm, B. M. L. Raun, B.A.Røjen, and D. L. Harmon. 2007. Metabolism of silage alcohols in lactating dairy cows. J. Dairy Sci. 90:1364-1377.

Legendre, M., L. Zaragosi, and H. M. Mitchison. 2021. Motile cilia and airway disease. Semin. Cell Dev. Biol. 110:19-33.

Lillehammer, M., M. Árnyasi, S. Lien, H. G. Olsen, E. Sehested, J. Ødegård, and T. H. E. Meuwissen. 2007. A genome scan for quantitative trait locus by environment interactions for production traits. J. Dairy. Sci. 90:3482-3489.

Lillehammer, M., B. J. Hayes, T. H. E. Meuwissen, and M. E. Goddard. 2009. Gene by environment interactions for production traits in Australian dairy cattle J. Dairy Sci. 8:4008-4017.

Luo, H., L. F. Brito, X. Li, G. Su, W. Xu, X. Yan, H. Zhang, G. Guo, L. Liu, and Y. Wang. 2021. Genetic parameters for rectal temperature, respiration rate, and drooling score in Holtein cattle and their relationships with various fertility, production, body conformation, and health traits. J. Dairy Sci. 104:4390-4403.

Mateescu, R. G., D. J. Garrick, R. G. Tait, A. J. Garmyn, Q. Duan, Q. Liu, M. S. Mayes, A. L. Van Eenennaam, D. L. VanOverbeke, G. G. Hilton, D. C. Beitz, and J. M. Reecy. 2013. Genome-wide association study of concentrations of iron and other minerals in longissimus muscle of Angus cattle. J. Anim. Sci. 8:3593-3600.

McKay, S. D., R. D. Schnabel,B. M. Murdoch, L. K. Matukumalli, W. Coppieters, D. Crews, E. D. Neto, C. A. Gill, C. Gao, H. Mannen, P. Stothard, Z. Wang, C. P. Van Tassell, J. L.

Williams, J. F. Taylor, and S. S. Moore. 2007. Whole genome linkage disequilibrium maps in cattle. BMC Genom. Data 8:74.

Meuwissen, T. H. E., B. J. Hayes, and M. E. Goddard. 2001. Prediction of total genetic value using genome-wide dense marker maps. Genetics 157:1819-1829.

Meyer, U., W. Stahl, and G. Flachowsky. 2006. Investigations on the water intake of growing bulls. Livest. Sci. 103:186-191.

Miller, S. E., D. A. Sahlender, S. C. Graham, S. Höning, M. S. Robinson, A. A. Peden, and D. J. Owen. 2011. The molecular basis for the endocytosis of small R-SNAREs by the Clathrin adaptor CALM. Cell 147:1118-1131.Misztal, I., S. Tsuruta, D. A. Lourenco, Y. Masuda, I. Aguilar, A. Legarra, and Z. Vitezica. 2018. Manual for BLUPF90 family programs. Univ. Georgia. Available from http://nce.ads.uga.edu/wiki/doku.php?id=documentation

Mota, R. R., R. J. Tempelman, P. S. Lopes, I. Aguilar, F. F. Silva, and F. F. Cardoso. 2016. Genotype by environment interaction for tick resistance of Hereford and Braford beef cattle using reaction norm models. Genet. Sel. Evol. 48.

Nardone, A., B. Ronchi, N. Lacetera, M. S. Ranieri, and U. Bernabucci. 2010. Effects of climate changes on animal production and sustainability of livestock systems. Livest. Sci. 130:57-69.

Naserkheil M., A. Bahrami, D. and H. Mehrban. 2020. Integrating single-step GWAS and bipartite networks reconstruction provides novel insights into yearling weight and carcass traits in Hanwoo beef cattle. Animals 10.

Nyholt, D. R. 2004. A simple correction for multiple testing for single-nucleotide polymorphisms in linkage disequilibrium with each other. Am. J. Hum. Genet. 74:765-769.

Ochieng, J., and G. Chaudhuri. 2011. Cystatin superfamily. J. health Care Poor Underserved 21:51-70.

Pizzagalli, M. D., A. Bensimon, and G. Superti-Furga. 2020. A guide to plasma membrane solute carrier proteins. The FEBS J. 288:2784-2835.

Polizel, G. H. G., L. Grigoletto, M. Carvalho, and P. Rossi Jr. 2018. Genetic correlations and heritability estimates for dry matter intake, weight gain and feed efficiency of Nellore cattle in feedlot. Livest. Sci. 214:209-210.

Polsky, L., and M. A. G. von Keyserlingk. 2017. Invited review: Effects of heat stress on dairy cattle welfare. J. Dairy Sci. 100:8656-8657.

Plummer, M., N. Best, K. Cowles, and K. Vines. 2006. CODA: Convergence diagnosis and output analysis for MCMC. R News 6:7-11. https://journal.r-project.org/archive/

Quaas, R. L., and E. J. Pollak. 1980. Mixed model methodology for farm and ranch beef cattle testing programs. J. Anim. Sci. 51: 1277-1287.

R Core Team. 2013. R: a language and environment for statistical computing. Vienna, Austria: R Foundation for Statistical Computing. Available from http://www.r-project.org/

Ramazzotti, G., I. Faneza, R. Fiume, A. M. Billi, L. Manzoli, S. Mongiorgi, S. Ratti, J. A. McCubrey, P. Suh, L. Cocco, and M. Y. Follo. 2017. PLC-β and cell differentiation: an insight into myogenesis and osteogenesis. Adv. Biol. Regul. 63: 1-5.

Ravagnolo, O., and I. Misztal. 2000. Genetic component of heat stress in dairy cattle, parameter estimation. J. Dairy Sci. 83:2126-2130.

Rolfe, K. M., W. M. Snelling, M. K. Nielsen, H. C. Freetly, C. L. Ferrell, and T. G. Jenkins. 2011. Genetic and phenotypic parameter estimates for feed intake and other traits in growing beef cattle, and opportunities for selection. J. Anim. Sci. 89:3452-3459.

Rosen, B. D., D. M. Bickhart, R. D. Schnabel, S. Koren, C. G. Elsik, E. Tseng, T. N. Rowan, W. Y. Low, A. Zimin, C. Couldrey, R. Hall, W. Li, A. Rhie, J. Ghurye, S. D. McKay, F. Thibaud-Nissen, J. Hoffman, B. M. Murdoch, W. M. Snelling, T. G. McDaneld, J. A. Hammond, J. C. Schwartz, W. Nandolo, D. E. Hagen, C. Dreischer, S. J. Schultheiss, S. G. Schroder, A. M. Phillippy, J. B. Cole, C. P. Van Tasell, G.. Liu, T. P. L. Smith, J. F. Medrano. 2020. De novo assembly of the cattle reference genome with single-molecule sequencing. GigaScience. 9:giaa021.

Saatchi, M., D. J. Garrick, R. G. Tait, M. S. Mayes, M. Drewnoski, J. Schoonmaker, C. Diaz, D. C. Beitz, and J. M. Reecy. 2013. Genome-wide association and prediction of direct genomic breeding values for composition of fatty acids in Angus beef cattle. BMC Genomics 14:730.

Saatchi, M., J. E. Beever, J. E. Decker, D. B. Faulkner, G. C. Freetly, S. L. Hansen, H. Yampara-Iquise, K. A. Johnson, S. D. Kachman, M. S. Kerley, J. Kim, D. D. Loy, E. Marques, H. L. Neilbergs, E. J. Pollak, R. D. Schnabel, C. M. Seabury, D. W. Shike, W. M. Snelling, M. L. Spangler, R. L. Weaber, D. J. Garrick, and J. F. Taylor. 2014. QTLs associated with dry matter intake, metabolic mid-test weight, growth, and feed efficiency have little overlap across 4 beef cattle studies. BMC Genom. 15:1004.

Sakane, F., S. Mizuno, D. Takahashi, and H. Sakai. 2018. Where do substrates of diacylglycerol kinases come from? Diacylglycerol kinases utilize diacylglycerol species supplied from phosphatidylinositol turnover-independent pathways. Adv. Bio. Regul. 67: 101-108.

Santana, M. H. A, G. A. Oliveira Jr., R. C. Gomes, S. L. Silva, P. R. Leme, T. R. Stella, E. C. Mattos, P. Rossi Jr., F. S. Baldi, J. P. Eler, and J. B. S. Ferraz. 2014. Genetic parameter

estimates for feed efficiency and dry matter intake and their association with growth and carcass traits in Nellore cattle. Livest. Sci. 167:80-85.

Schaeffer, L. R. 2004. Application of random regression models in animal breeding. Livest. Prod. Sci. 86:35-45.

Schou, M. F., A. A. Hoffmann, and T. N. Kristensen. 2019. Genetic correlations and their dependence on environmental similarity-Insights from livestock data. Evolution. 73:1672–1678.

Seabury, C. M., D. L. Oldeschulte, M. Saatchi, J. E. Beever, J. E. Decker, Y. A. Halley, E. K. Bhattarai, M. Molaei, H. C. Freetly, S. L. Hansen, H. Yampara-Iquise, K. A. Johnson, M. S. Kerley, J. kim, D. D. Loy, E. Marques, H. L. Neibergs, R. D. Schnabel, D. W. Shike, M. L. Spangler, R. L. Weaber, D. J. Garrick, and J. F. Taylor. 2017. Genome-wide association study for feed efficiency and growth traits in U.S. beef cattle. BMC Genom. 18:386.

Sgrò, C. M., and A. A. Hoffman. 2004. Genetic correlations, tradeoffs, and environmental variation. Heredity. 93: 241-248.

Snelling, W. M., M. F. Allan, J. W. Keele, L. A. Kuehn, R. M. Thallman, G. L. Bennett, C. L. Ferrell, T. G. Jenkins, H. C. Freetly, M. K. Nielsen, and K. M. Rolfe. 2011. Partial-genome evaluation of postweaning feed intake and efficiency of crossbred beef cattle. J. Anim. Sci. 89:1731-1741.

Sun, S. 2013. mTOR kinase inhibitors as potential therapeutic drugs. Cancer Lett. 340:1-8.

Sungkhapreecha, P., I. Misztal, J. Hidalgo, Y. Steyn, S. Buaban, M. Duangjinda, and W. Boonkum. 2021. Changes in genetic parameters for milk yield and heat tolerance in the Thai Holstein crossbred dairy population under different heat stress levels and over time. J. Diary Sci. 104:12703-12712.

Szklarczyk, D., A. Franceschini, S. Wyder, K. Forslund, D. Heller, J. Huerta-Cepas, M. Simonovic, A. Roth, A. Santos, K. P. Tsafou, M. Kuhn, P. Bork, L. J. Jensen, and C. von Mering. 2015. STRING v10: protein-protein interaction networks, integrated over the tree of life. Nucleic Acids Res. 43:D447-D452.

Tempelman, R. J. 2010. Addressing scope of inference for global evaluation of livestock. R. Bras. Zootec. 39.Utley, P. R., N. W. Bradley, and J. A. Boling. 1970. Effect of restricted water intake on feed intake, nutrient digestibility and nitrogen metabolism in steers. J. Anim. Sci. 31:130-135.

Vallimont, J. E., C. D. Dechow, J. M. Daubert, M. W. Dekleva, J. W. Blum, C. M. Barlieb, W. Liu, G. A. Varga, A. J. Heinrichs, and C. R. Baumrucker. 2010. Genetic parameters of feed intake, production, and selected type traits of Holstein cows in commercial tie-stalls barns. J. Dairy Sci. 93:4892-4901.

Van Der Werf, J. H., M. E. Goddard, and K. Meyer. 1998. The use of covariance functions and rando regressions for genetic evaluation of milk production based on test day records. J. Dairy Sci. 81:3300-3308.

VanRaden, P. M. 2008. Efficient methods to compute genomic predictions. J. Diary Sci. 91:4414-4423.

Veerkamp, R. F., M. P. Coffey, D. P. Berry, Y. de Haas, E. Strandberg, H. Bovenhuis, M. P. L. Calus, and E. Wall. 2012. Genome-wide associations for feed utilization complex in primiparous Holstein-Fresian dairy cows from experimental research herds in four European countries. Animal 11:1738-1749.

Via, S., and R. Lande. 1985. Genotype-environment interaction and the evolution of phenotypic plasticity. Evolution. 39:505–522.

Wang, H., L. Tong, J. Wei, W. Pan, L. Li, Y. Ge, L. Zhou, Q. Yuan, C. Zhou, and M. Yang. 2014. The ALDH7A1 genetic polymorphisms contribute to development of esophageal squamous cell carcinoma. Tumor Biol. 35:12665-12670.

West, J. W. 2003. Effects of heat-stress on production in dairy cattle. J. Dairy Sci. 86:2131-2144.

West-Eberhard, M. J. 2008. Phenotypic plasticity. In: Encyclopedia of ecology. 1st ed. Elsevier, Amsterdam, Netherlands. p. 2701-2707.

Winchester, C. F., and M. J. Morris. 1956. Water intake rates of cattle. J. Anim. Sci. 15:722-740.

Wirawan, E., T. V. Gerghe, S. Lippens, P. Agostinis, and P. Vandenabeele. 2012. Autophagy: for better or for worse. Cell Res. 22:43-61.

Xia, J., M. J. Benner, and R. E. W. Hancock. 2014. NetworkAnalyst – integrative approaches for protein-protein interaction network analysis and visual exploration. Nucleic Acids Res. 42:W167-W174.

Yamazaki, Y., R. Urrutia, L. M. Franco, S. Giliani, K. Zhang, A. M. Alazami, A. K. Dobbs, S. Masneri, A. Joshi, F. Otaizo-Carrasquero, T. G. Myers, S. Ganesan, M. P. Bondioni, M. L. Ho, C. Marks, H. Alajlan, R. W. Mohammed, F. Zou, C. A. Valencia, A. H. Filipovich, F. Facchetti, B. Boisson, C. Azzari, B. K. Al-Saud, H. Al-Mousa, J. L. Casanova, R. S. Abraham, and L. D. Notarangelo. 2020. PAX1 is essential for development and function of the human thymus. Sci. Immunol. 5:44.

Yang, W., C. Chen, J. P. Steibel, C. W. Ernst, R. O. Bates, L. Zhou, and R. J. Tempelman. 2015. A comparison of alternative random regression and reaction norm models for whole genome predictions. J. Anim. Sci. 93:2678-2692.

Yao, C., G. de los Campos, M. J. VandeHaar, D. M. Spurlock, L. E. Armentano, M. Coffey, Y. de Haas, R. F. Veerkamp, C. R. Staples, E. E. Connor, Z. Wang, M. D. Hanigan, R. J. Tempelman, K. A. Weigel. 2017. Use of genotype × environment interaction model to accommodate genetic heterogeneity for residual feed intake, dry matter intake, net energy in milk, and metabolic body weight in dairy cattle. J. Dairy Sci. 100:2007-2016.

Yoo, B. H., F. W. Nicholas, and K. A. Rathie. 1980. Long-term selection for a quantitative character in large replicate populations of Drosophila melanogaster. Theor. Appl. Genet. 57:113-117.

Zewail, A., M. W. Xie, Y. Xing, L. Lin, P. F. Zhang, W. Zou, J. P. Saxe, and J. Huang. 2003. Novel functions of the phosphatidylinositol metabolic pathway discovered by a chemical genomics screen with wortmannin. Proc. Natl. Acad. Sci. 100:3345-3350.

Zhang, X., D. Lourenco, I. Aguilar, A. Legarra, and I. Misztal. 2016. Weighting strategies for single-step genomic BLUP: An iterative approach for accurate calculation of GEBV and GWAS. Front. Genet. 7:151.

Chapter 3 - Phenotypic Plasticity and Genetic Architecture of Dry Matter Intake and Respiration Rate Under a Temperature Humidity Index

Abstract

Climate change is expected to cause rising temperatures and climate instability. This warming and instability will lead to greater and more extreme fluctuations in temperatures cattle are exposed to or may live in. This exacerbates problems with diverse climates germplasm or progeny may be utilized in. Therefore, selection for phenotypically plastic cattle, which perform more stably despite varying environmental conditions, may be warranted. Random regression methodology was utilized to model the linear change in dry matter intake (DMI) and respiration rate as the temperature humidity index (THI) increased, with the intercept representing the thermoneutral inflection point and the slope representing the environmental sensitivity to THI. Estimated breeding values (EBV) for an additive genetic intercept and slope were specified with a covariance structure, which allowed for environment-specific genetic variances and heritabilities to be computed. Genetic-by-environment interactions (G×E) could subsequently be evaluated with genetic correlations between DMI or respiration rate at different levels of THI and Spearman correlations between DMI or respiration rate EBVs at different levels of THI. Finally, genetic architecture of phenotypic plasticity was dissected in a genome wide association study (GWAS) on the intercept and slope of DMI and respiration rate to determine putative biological processes and gene ontologies contributing to each. The population slope was negative at -0.046 lbs DMI per unit increase in THI, indicating DMI decreases on average as THI increase. The log-transformed population slope for respiration rate was positive, indicating

respiration increases as THI increases. The point estimate for the genetic correlation between the intercept and slope of DMI and respiration rate were -0.78 and -0.72, respectively. However, the uncertainty associated with the respiration rate genetic correlation between the intercept and slope was large, such that there was no evidence that the intercept and slope were different traits. The negative correlation indicates selection that increases DMI (i.e., correlated traits, like average daily gain) in thermoneutral environments will increase the environmental sensitivity and decrease phenotypic plasticity. However, selection that decreases DMI in thermoneutral environments, such as correlated feed efficiency traits, may increase phenotypic plasticity. The heritability of DMI in thermoneutral environments ranged from approximately 0.30 to 0.40 across groups, but quickly dropped as THI increased before stabilizing THI values of 80 or greater. There was little to no evidence for respiration rate being a heritable trait, except at a few levels of THI. Unfortunately, genetic-by-environment interaction effects were also large, as the genetic correlations between DMI at various THI levels and the Spearman correlations between DMI estimated breeding values at various THI levels rapidly dropped as the distance between THI values increased. These genetic and Spearman correlations dropped as low as 0.42 and 0.39, respectively, when comparing DMI at a thermoneutral THI to 85 THI. This clearly indicates performance at a given level of THI is unlikely to be a good indicator of performance under different THI conditions. The GWAS revealed the DMI slope was primarily associated with metabolic signaling in this study. However, respiration rate QTL were highly different between the slope and intercept. In thermoneutral conditions, respiration rate appeared to be associated with heart function and heart disease. The environmental sensitivity, however, was strongly associated with metabolic signaling, supporting respiration rate as an indicator of production and performance.

Introduction

Climate change is expected to cause continued warming and climate instability (Nardone *et al.*, 2010; IPCC, 2007). It is expected that warming will continue for decades, despite efforts to curb emissions (IPCC, 2007). Cattle are known to be negatively affected by heat stress (Fuquay, 1981; Nardone *et al.*, 2010), which can be measured by a temperature humidity index (THI). Given the impending changes due to climate change, selection for cattle resistant to the effects of heat stress may be prudent.

Furthermore, the beef industry is spread out across a diverse set of environments where THI likely varies substantially. Beef and dairy sires are often utilized in artificial insemination (AI) across the country and globe (Banos and Sigurdsson, 1996; Brotherstone and Goddard, 2005). Commercial users who do not practice AI purchase bulls from multiplier herds that are derived from AI sires. To further compound the issue, animals entering the food chain will likely need to be transported to feedlots, many of which are in hot, arid environments (Grandin, 2016), further diversifying the environments for which animals must be able to thrive.

Tolerance, or phenotypic plasticity, as a trait can be captured as environmental sensitivity and represents an animal's ability to maintain their phenotypic performance despite stressful environmental conditions (West-Eberhard, 2008). Environmental sensitivity is a measure of genetic-by-environment interactions (G×E), where the genetic merit of an individual is a function of the environment and can be computed as the slope of a reaction norm. Environmental sensitivity remains an understudied area. Furthermore, the genetic architecture contributing to environmental sensitivity has not been characterized. Thus, the objectives of this study were to characterize the genetic parameters of dry matter intake (DMI) and respiration rate with respect

to THI, the influence of G×E on selection, and the genetic architecture of environmental sensitivity using random regression.

Materials and Methods

Study Population

The study design, ration, and processing details for a subset of the animals in this study were previously described in Ahlberg *et al.* (2019). Seven cohorts of animals, composed of 830 steers, were on trial between May 2014 and May 2018 (Table B.1). Animals were sourced from sale barns in the south, great plains, and Oklahoma State University herds. Animals with observable *Bos indicus* or dairy characteristics were removed from the study due to known differences in adaptation to tropical conditions (Winchester and Morris, 1956; Brew *et al.*, 2011). Animals were on trial at the Willard Sparks feedlot at Oklahoma State University. All procedures involving animals were approved by Institutional Animal Care and Use Committee at Oklahoma State University (protocol AG13-18) in compliance with the Federation of Animal Science Societies (FASS, 2010) guidelines.

Pre-Processing, Pen Assignment, and Acclimation Procedures

Upon arrival, animals underwent processing, including vaccination and implantation with Compudose (Elanco Animal Health, Greenfield, IN), an estradiol 17ß (E2 ß) implant as part of the normal feedlot processing procedure. Subsequently, animals spent a variable amount of time in standard feedlot pens acclimating to the facility and feedlot conditions before pen assignment. After the acclimation period ended, animals were sorted into a heavy or light group by weight as a proxy for size. Half of each weight group was randomly assigned to one of four pens, with

approximately 35 steers per pen. Splitting by size was necessary, as animals were fed water and feed using the Insentec (Hokofarm Group, The Netherlands) system. Feed bunk gates set lower to allow access for smaller steers failed to exclude unrecorded access to the larger animals when bunks were full, necessitating allocation by size. Following pen assignment, animals were subjected to a 21-day acclimation period to the pen conditions and Insentec system. Animals who failed to learn to utilize the system were removed from the study. Data for the acclimation period was not included.

Ration Information

For the duration of the trial, rations consisted of roughly 51.36% wet corn sweet bran, 15% cracked corn, 28.44% prairie hay, and 5.20% mineral supplement. Ration dry matter (DM) and gross energy composition were estimated by Dairy One, Inc. (Ithaca, New York). Diets were similar in composition between cohorts, but slight variations did occur. The gross energy values for groups 1-7 ranged between 18.26 to 19.91 MJ/kg of DM. Likewise, ration average DM percentages ranged from 70 to 74 percent (dry matter percentages within a group had little variation; not shown) across cohorts. The first three cohorts were fed under a slick bunk protocol, where feed was steadily increased as animals were able to clear bunks. Cohorts 4-7 were fed using an ad libitum protocol.

Trial Design, Phenotype Collection, and Quality Filtering

The trial was conducted for 70 days after the acclimation period and animals were provided feed and ad libitum water. Animals were processed every other week, where body weights were obtained. Feed intake (FI) events were continuously recorded by the Insentec

system on an individual animal basis by weighing the difference between the start and end weights of the feed bunk and associating it with the animal's electronic identification (eID) tag. Feed intake event records were filtered to remove erroneous data. Records with end weights greater than the start weight, start or end values outside of the margin of error of the programmed bunk values, and events with lengths shorter than 5s or greater than 3600s were removed. Records pertaining to the preceding day, day of, and day after an animal was treated for illness were removed. All records during processing days, days where equipment malfunctioned, or any event which may have interfered with animal FI were removed. Feed intake records were summed into daily values intakes for each animal and were converted to DMI according to the average feed dry matter percentage for the corresponding group. Summaries of DMI by cohort are presented in Table 3.1.

Respiration rates were collected twice a day, two times per week on the two days predicted to be the hottest for the week. Respiration rates were measured as the number of breaths in a 30s period (breaths per 30s; BP30S). Respiration rates were collected once in the morning and once in the afternoon by trained observers and times were recorded (Table 3.1). Body weights were also collected weekly.

Weather Data Collection and Temperature Humidity Index Calculations and Filtering

Weather data was obtained from the Oklahoma Mesonet Stillwater tower in five-minute intervals for the duration of the study (Brock *et al.*, 1995; McPherson *et al.*, 2007). The equation used to calculate THI was

(1) $$THI = (1.8 \times T_{db} + 32) - \left(0.55 - 0.55 \times \frac{RH}{100}\right) \times (1.8 \times T_{db} - 26)$$

where T_{db} is the dry-bulb temperature in Celsius, and RH is the relative humidity expressed as a percentage (NOAA, 1976). Equation 1 was specifically developed for livestock (Bohmanova *et al.*, 2007) and is commonly used in other repeatability and random regression studies looking at THI (Ravagnolo and Misztal, 2000; Aguilar *et al.*, 2009; Brügemann *et al.*, 2011; Al-Kanaan, 2016; Bradford *et al.*, 2016; Sungkhapreecha *et al.*, 2021). Respiration rates were paired with the five-minute interval THI value closest to the collection time and the maximum THI value for a given day was paired with daily DMI values for analysis.

The onset of heat stress was determined visually with the aid of scatterplots plotting DMI or respiration rate against THI. A locally weighted scatterplot smooth (LOESS) line was used to determine the inflection point where heat stress began to impact performance. For this study, a THI of 70 was identified as the threshold for where heat stress began.

A THI value of 70 was considered a thermoneutral environment and THI values greater than 70 were considered heat-stressed environments. Respiration rate and DMI records associated with a THI of less than 70 were removed. Corresponding DMI and respiration rate summaries after record pruning can be found in Table 3.1. Unfortunately, respiration rate records for two groups of steers (n = 234) were never observed with THI values of 70 or greater and were subsequently removed from the analysis. Summaries of THI ranges by group for each trait after record pruning are presented in Table 3.2. For downstream analyses as a covariate, 70 was subtracted from each THI observation to center THI around the thermoneutral point, but figures and tables represent the actual THI value. Centering THI around 70 THI moved the interpretation of intercepts from 0 THI to 70 THI.

Genotyping and Quality Filtering

Blood was collected on each animal from the jugular vein and collected in 10 mL BD vacutainer tubes with 1.5 mL of anticoagulant citrate dextrose. The whole blood was centrifuged and DNA was extracted from the white blood cell layer using a phenol:chloroform:isoamyl alcohol extraction and ethanol precipitation protocol. Samples were subsequently sent to GeneSeek (Linoln, NE), where they were genotyped on the GGP Bovine 150K array. Groups were genotyped on different versions of the array, however, so only loci in common between all versions were kept, resulting in 138,892 single nucleotide polymorphisms (SNP) for analysis. Genotypes were further filtered for call rates less than 90% or minor allele frequency less than 5%. Filtering resulted in 14,980 SNPs being removed, leaving 123,912 SNPs in the analysis. Furthermore, animals with a call rate less than 90% were removed, leaving 819 animals with genotypes. However, not all genotyped animals had phenotypic records.

Genetic Relatedness Matrix

The genetic relatedness matrix (GRM), $\mathbf{G}$, was computed with the BLUPf90 suite (Aguilar *et al.*, 2018; Misztal *et al.*, 2018) utilizing equation three in VanRaden (2008). The GRM constructed from genotypes was constructed as

$$\boldsymbol{G} = \frac{\boldsymbol{zz'}}{2\sum p_i(1-p_i)} \quad (2)$$

where $\boldsymbol{G}$ is the genomic relatedness matrix, $\boldsymbol{Z}$ is a matrix of alleles (expressed as -1, 0, and 1 for the homozygote, heterozygote, and alternative homozygote) centered around the mean allele effect and weighted for rarity, and p_i is the minor allele frequency for genotype i. The denominator scales the genomic relatedness matrix, $\boldsymbol{G}$ to the numerator relationship matrix, $\boldsymbol{A}$.

The GRM utilized in subsequent models, $\boldsymbol{H^{-1}}$, was constructed according to Aguilar *et al.* (2010). The genomic relatedness matrix, $\mathbf{G}$, and an equivalently sized identity matrix were blended with weights of 0.99 and 0.01, respectively, to resolve issues with singularity. In mathematical notation, $\boldsymbol{G}$ was blended as

(3) $$0.99\boldsymbol{G} + 0.01\boldsymbol{I_{22}}$$

where $\boldsymbol{G}$ is the genomic relatedness matrix and $\boldsymbol{I_{22}}$ is an identity matrix with rows and columns equal to the number of genotyped animals (VanRaden, 2008; Aguilar *et al.*, 2010). Then, $\boldsymbol{H^{-1}}$ was computed with the blended $\boldsymbol{G}$ using

(4) $$\boldsymbol{H^{-1}} = \boldsymbol{I} + \begin{bmatrix} 0 & 0 \\ 0 & \boldsymbol{G^{-1}} - \boldsymbol{I_{22}} \end{bmatrix}$$

where $\boldsymbol{I}$ is an identity matrix with dimensions equal to the number of animals in the analysis. An identity matrix was used instead of the numerator relationship matrix, $\boldsymbol{A}$, given no pedigree information was available.

Statistical Analysis

Dry Matter Intake Random Regression Model

Random regression models were utilized to incorporate THI into the genetic evaluation. The random regression model for DMI was specified as follows:

(5) $$y_{ijk} = \eta + f_i + \beta_1 x_{ijk} + \beta_2 v_{ijk} + a_j + b_j x_{ijk} + g_j + h_j x_{ijk} + e_{ijk}$$

where, y_{ijk} is the kth DMI record for animal j in group i, η represents the overall population intercept, f_i represents the ith differential cohort effect ($i = 1,2, \ldots,7$), β_1 represents the population slope of the covariate for THI, x_{ijk} represents the kth THI measurement for animal j in cohort i, β_2 represents the slope of the covariate for weight, v_{ijk} represents the closest weight

corresponding to the kth daily THI measurement, a_j represents the additive genetic intercept for animal j, b_j represents the additive genetic slope for animal j, g_j represents the permanent environment (PE) intercept for animal j, h_j represents the PE slope for animal j, and e_{ijk} is the residual for the kth observation.

The distributional assumptions of the model were as follows. First,

(6) $$\boldsymbol{y}|\boldsymbol{a},\boldsymbol{b},\boldsymbol{f},\boldsymbol{g},\boldsymbol{h} \sim N(\boldsymbol{X\beta}, \boldsymbol{I}\sigma^2_{e_i})$$

where the vector of observations, $\boldsymbol{y}$, conditional on all random effects, was normally distributed with mean $\boldsymbol{X\beta}$ and with a residual variance, $\sigma^2_{e_i}$, unique to each ith cohort. Second,

(7) $$\begin{bmatrix}\boldsymbol{a}\\ \boldsymbol{b}\end{bmatrix} \sim N_2\left(\begin{bmatrix}0\\0\end{bmatrix}, \begin{bmatrix}\sigma^2_a & \sigma_{ab}\\ \sigma_{ba} & \sigma^2_b\end{bmatrix} \otimes \boldsymbol{H}\right)$$

where $\begin{bmatrix}\boldsymbol{a}\\ \boldsymbol{b}\end{bmatrix}$ is the vector of additive genetic effects for the intercept and slope. The vector is distributed bivariate normal with means of zero and a covariance $\begin{bmatrix}\sigma^2_a & \sigma_{ab}\\ \sigma_{ba} & \sigma^2_b\end{bmatrix}$. The diagonals represent the additive genetic variance for the intercept and slope, and the off diagonals are the additive genetic covariance between the additive genetic intercept and slope. The covariance matrix is weighted by the Kronecker product of the genetic relatedness matrix, $\boldsymbol{H}$. The prior distribution specified for the additive genetic covariance parameters was specified under a flat Inverse Wishart prior, with

(8) $$\begin{bmatrix}\sigma^2_a & \sigma_{ab}\\ \sigma_{ba} & \sigma^2_b\end{bmatrix} \sim IW(S, v) \text{ and } S = \begin{bmatrix}0 & 0\\ 0 & 0\end{bmatrix}$$

and $v = -2$. Third,

(9) $$\begin{bmatrix}\boldsymbol{g}\\ \boldsymbol{h}\end{bmatrix} \sim N_2\left(\begin{bmatrix}0\\0\end{bmatrix}, \begin{bmatrix}\sigma^2_g & \sigma_{gh}\\ \sigma_{hg} & \sigma^2_h\end{bmatrix} \otimes \boldsymbol{I}\right)$$

where $\begin{bmatrix} \boldsymbol{g} \\ \boldsymbol{h} \end{bmatrix}$ is the vector of PE effects distributed bivariate normal with means of zero and covariance $\begin{bmatrix} \sigma_g^2 & \sigma_{gh} \\ \sigma_{hg} & \sigma_h^2 \end{bmatrix}$. The diagonals represent the PE variances for the intercept and slope, and the off diagonals are the covariance between the PE intercept and slope. The Kronecker product with the identity matrix weights the covariance matrix to the size of $\begin{bmatrix} \boldsymbol{g} \\ \boldsymbol{h} \end{bmatrix}$. The prior distribution specified for the permanent environment covariance parameters was specified under a flat Inverse Wishart prior, where

(10) $$\begin{bmatrix} \sigma_g^2 & \sigma_{gh} \\ \sigma_{hg} & \sigma_h^2 \end{bmatrix} \sim IW(S, v)$$

And S and v are as before. Fourth,

(11) $$\boldsymbol{f} \sim N(0, \boldsymbol{I}\sigma_f^2)$$

where $\boldsymbol{f}$ is the vector of group effects distributed normally with a mean of zero and common group variance, σ_f^2. The prior distribution was specified

(12) $$\sigma_f^2 \sim IG(\alpha = 1, \beta = 1)$$

And finally,

(13) $$\boldsymbol{e} \sim N(0, \boldsymbol{I}\sigma_{e_i}^2)$$

where $\boldsymbol{e}$ is the vector of residuals with mean of zero and cohort-specific heteroscedastic variance, $\sigma_{e_i}^2$. The prior specifications for $\sigma_{e_i}^2$ were the same as σ_f^2.

Respiration Rate Random Regression Model

Respiration rate was likewise evaluated. Unfortunately, respiration rates were non-normally distributed. Normality was conferred with a base-ten logarithmic transformation. The model for respiration rate was specified as follows:

(14) $$y_{ijk} = \eta + f_i + \beta_1 x_{ijk} + a_j + b_j x_{ijk} + g_j + h_j x_{ijk} + e_{ijk}$$

where y_{ijk} represents the kth log-transformed respiration rate observation for the jth animal and ith cohort, β_1 is the population phenotypic slope regression coefficient for the centered THI covariate, x_{ijk} is the kth centered THI measurement for a given animal, and e_{ijk} is the residual for each observation. Other terms are as previously described in the DMI random regression model and the same model distributional assumptions are assumed.

Model Implementation and Assessment

Models for DMI and respiration rate were fit in the BLUPf90 software suite (Aguilar *et al.*, 2018; Misztal *et al.*, 2018) with the THRGIBBS3f90 software. Variance components, location parameter estimates, and random effect predictions were obtained from a Markov Chain Monte Carlo (MCMC) iterative procedure employing a Gibb's sampler algorithm. Convergence and diagnostics were assessed with the Coda package in the R statistical computing environment (Plummer *et al.*, 2006; R Core Team, 2013). The Raftery-Lewis diagnostic function with a quantile of 0.025 and probability 0.95 and trace plots were analyzed for convergence. Priors for all parameters were specified with noninformative priors, as no prior information was available. The location parameters were specified as flat, improper uniform priors in the THRGIBBS3f90 software by default. Variance components without a correlation structure utilized flat, improper inverse gamma priors. The random regression coefficients, which had a correlation structure as previously shown, utilized an Inverse-Wishart prior. After a burn-in of 20,000 samples, 800,000 MCMC iterate samples were obtained from the full conditional densities of all parameters. Samples were thinned by 40, resulting in 20,000 samples, as autocorrelations between successive samples were large and downstream computations burdens would require extensive computing

resources for little to no gain in defining the posterior densities. The amount of information defining the posterior distributions can be shown with the effective sample size, which determines the number of independent samples defining the posterior distribution. The Coda package (Plummer *et al.*, 2006) was utilized to determine the effective sample size for each parameter. Uncertainty was represented with 95% highest posterior density credible intervals (HPDCI) using the Coda package.

Statistical Filtering

Outliers were identified and removed using studentized residuals (SR). Studentized residuals were assumed to follow a t-distribution with degrees of freedom (df) $n-1$, where n represents the number of observations, such that $SR \sim t_{df}$. The hypotheses used to test the SRs were as follows:

$$\mu_0 : The\ observation\ is\ derived\ from\ the\ data\ distribution$$

$$\mu_1 : The\ observation\ is\ not\ derived\ from\ the\ data\ distribution$$

The significance level was set at an alpha of 0.05. Multiple testing was corrected using a Bonferroni correction and the quantile corresponding the Bonferroni significance threshold was obtained with the qt function in R (R Core Team, 2013) as follows:

$$\left| qt\left(\frac{\alpha}{2n}, df\right)\right| \quad (15)$$

Where qt is an R function to find the quantile of a t-distribution with probability $\frac{\alpha}{2n}$ (Bonferroni-corrected two-tailed test) and degrees of freedom as above. The null hypothesis was rejected if the absolute value of the studentized residual exceeded the quantity corresponding to the Bonferroni-corrected threshold. Initially, 26,206 records were available for DMI and 8,861 for

respiration rate. After removing statistical outliers, 26,160 records were available for DMI and 8,852 for respiration rate.

Variance Component Functions

With random regression, the (co)variance structures can be utilized in functions with the environmental covariate, THI, to answer a large array of questions. Posterior densities for any functions of variance components were obtained by applying the following functions to estimates in each iteration of the MCMC. First, the genetic relationship between the additive genetic intercept and additive genetic slope in the random regression model can be defined as a genetic correlation in the following equation:

(16) $$r_{ab} = \frac{\sigma_{ab}}{\sqrt{\sigma_a^2 \times \sigma_b^2}}$$

where r_{ab} is the genetic correlation between the additive genetic intercept and slope, σ_{ab} is the additive genetic covariance between the intercept and slope, and σ_a^2 and σ_b^2 are the additive genetic intercept and slope variances, respectively.

Genetic variances, covariances, and genetic correlations can also be computed for individual levels of water restriction. The scalar form to compute genetic variance for any given value of THI is as follows:

(17) $$\sigma_u^2|x = var(a_j + b_j x) = \sigma_a^2 + x^2\sigma_b^2 + 2x\sigma_{ab}$$

where $\sigma_u^2|x$ is the additive genetic variance for a given value of THI, a_i is the additive genetic intercept, b_i is the additive genetic slope, σ_a^2 is the additive genetic variance for the intercept, σ_b^2 is the additive genetic variance for the slope, and σ_{ab} is the additive genetic covariance between the intercept and slope. It is worth noting the values of x correspond to the centered values of THI. In this case, a value of zero (the intercept) corresponds to 70 THI and a value of 20

corresponds to 90 THI due to the centering previously applied. Therefore, 70 must be added back to the THI value post-analysis for graphical representation.

Likewise, the additive genetic covariance between two environments can be calculated as follows:

(18) $$\sigma_{u|x,u|x'} = cov\left(a_j + b_j x, a_j + b_j x'\right) = \sigma_a^2 + xx'\sigma_b^2 + (x + x')\sigma_{ab}$$

where $\sigma_{u|x,u|x'}$ is the additive genetic covariance between any two values of THI, x and x', and other terms are as described previously in the model statements. However, matrix algebra simplifies the process and allows for simultaneous calculation of all desired variances and covariances across levels of THI. The additive genetic (co)variance for all value of THI (centered at 70) of interest is

(19) $$\boldsymbol{\phi Q \phi'}$$

Where $\boldsymbol{\phi}$, in the case of a linear order random regression, is an $m\ x\ 2$ matrix composed of an intercept column (i.e., a vector with every value as one and length m) and a column of m centered THI values of interest. The matrix $\boldsymbol{Q}$ is the $2\ x\ 2$ genetic covariance matrix for the intercept and slope (for a first order model).

Genetic correlations between any pair of environments can likewise be computed in scalar notation:

(20) $$r_{u|x,u|x'} = \frac{\sigma_{u|x,u|x'}}{\sqrt{\left(\sigma_u^2|x\right)\left(\sigma_u^2|x'\right)}}$$

Where $r_{u|x,u|x'}$ is the genetic correlation between any two environments and other terms are as described previously in equations 17 and 18. Matrix notation simplifies this process immensely and a genetic correlation matrix between DMI or respiration rate across all values of THI can be computed as:

(21) $\boldsymbol{d^{-1}(\phi Q \phi')d^{-1}}$

where, $\boldsymbol{d^{-1}}$ represents the inverse of a diagonal matrix composed of the square root of the additive genetic variances (i.e., the square root of the diagonals) from the covariance matrix, $(\boldsymbol{\phi Q \phi'})$, in equation 19. The output is a genetic correlation matrix with dimensions corresponding to the number of THI values specified, m.

Permanent environment variances were evaluated as well and can be calculated much in the same manner as equations 17 and 19. The PE variance for a value of THI can be computed in scalar notation as:

(22) $\sigma^2_{pe}|x = \sigma^2_g + x^2\sigma^2_h + 2x\sigma_{gh}$

where $\sigma^2_{pe}|x$ is the PE variance for a given environment, σ^2_g, σ^2_h, and σ_{gh} are the PE intercept variance, slope variance, and covariance, respectively, from the model specification and x is a value of THI. The matrix notation is the similar to equation 19, but with the covariance matrix corresponding to the PE random regression covariance structure for $\begin{bmatrix}\boldsymbol{g}\\ \boldsymbol{h}\end{bmatrix}$.

In both the respiration rate and DMI models, heritability must be calculated for each cohort, given each cohort has a cohort-specific residual variance. Heritability for a given value of THI can be calculated as follows:

(23) $h^2_i|x = \frac{\sigma^2_u|x}{\sigma^2_f+\sigma^2_u|x+\sigma^2_{pe}|x+\sigma^2_{e_i}}$

where $h^2_i|x$ is the narrow-sense heritability for a given value of THI and cohort i, $\sigma^2_{e_i}$ is the cohort specific residual variance, σ^2_f is the between-cohort variance, and other terms are as described previously in equations 17-22. Repeatability can likewise be calculated, given the inclusion of PE effects in the model:

(24) $r_i|x = \frac{\sigma^2_u|x+\sigma^2_{pe}|x}{\sigma^2_f+\sigma^2_u|x+\sigma^2_{pe}|x+\sigma^2_{e_i}}$

where $r_i|x$ is the repeatability for a given value of THI and cohort i, other terms are as described previously in equation 23.

Estimated Breeding Values for Traits in Heat Stressed Environments

Estimated breeding values (EBV) for either DMI or respiration rate at any value of the centered THI covariate can be generated within the scope of the model. However, estimates in sparse regions may be unreliable or unstable. Environment-specific EBVs were calculated as follows:

(25) $$EBV_j|x = a_j + b_j x$$

where $EBV_j|x$ represents the breeding value for a given value of the centered THI environmental covariate and other terms are as described previously in the model statements. Like previous functions, matrix notation can simplify the calculations:

(26) $$\boldsymbol{\phi s}'$$

where $\boldsymbol{\phi}$ is interpreted as before in equation 19 and $\boldsymbol{s}'$ is the transpose of an $j\ x\ 2$ vector containing the additive genetic intercept and breeding value for all j animals, resulting in an $m\ x\ j$ matrix of EBVs for each animal for each value of THI.

Accuracy of Estimated Breeding Values

Beef Improvement Federation accuracies (BIF Guidelines, 2021a) can be computed for the additive genetic intercept, slope, or THI-specific EBVs. The BIF accuracy was computed as follows:

(27) $$Accuracy_{BIF} = 1 - \sqrt{\frac{PEV}{\widehat{\sigma_u^2}}}$$

where PEV is the prediction error variance for an EBV and $\widehat{\sigma_u^2}$ is the point estimate of the additive genetic variance of the trait. However, the posterior variance of an EBV was used in place of the prediction error variance. The BIF accuracy for the additive genetic intercept of an animal's EBV would be

$$Accuracy\ EBV_{int} = 1 - \sqrt{\frac{var(a_j)}{\widehat{\sigma_a^2}}} \quad (28)$$

The accuracy for the additive genetic slope would be similar:

$$Accuracy\ EBV_{slope} = 1 - \sqrt{\frac{var(b_j)}{\widehat{\sigma_b^2}}} \quad (29)$$

Finally, the accuracy for the EBV at a given value of WR would be

$$Accuracy\ EBV_{WR} = 1 - \sqrt{\frac{var(EBV_j|x)}{\widehat{\sigma_{u|x}^2}}} \quad (30)$$

Terms are as before in the models and all previous equations.

Genome Wide Association Study

Genome wide association studies (GWAS) were conducted for the DMI and respiration rate intercept and slope traits. The DMI and respiration rate random regression models detailed previously were fit in the BLUPF90 program in the BLUPF90 software suite (Aguilar *et al.*, 2018; Misztal *et al.*, 2018), yielding probability values obtained with PostGSF90 to conduct hypothesis testing. Point estimates for variance components used in the BLUPF90 program were obtained from the same models for each trait described previously, but fit as homoscedastic, in THRGIBBS3F90. Homoscedastic models were used as the program needed to compute

probability values for PostGSF90 cannot model heteroscedasticity. A significance threshold was set at $-\log_{10}\frac{\alpha}{2} > 5$. Each SNP was tested with the following hypothesis set:

$$H_0: SNP\ effect\ equal\ to\ zero$$

$$H_1: SNP\ effect\ not\ equal\ to\ zero$$

The null hypothesis was rejected if the positive, log-transformed p-value exceeded 5.

Significant SNPs within ± 250 kb were considered to represent the same QTL region due to linkage disequilibrium (LD; McKay *et al.*, 2007). Significant SNPs were subsequently ordered according to their $-\log_{10}(p\ value)$ and an iterative function was applied to this ordered list to remove SNPs in the same LD window (in the same 500 kb region from the SNP with the greatest signal). Utilizing the LD pruned list of significant SNPs, gene candidates within each QTL region were identified with the GALLO package in R (R Core Team, 2013; Fonseca *et al.*, 2020) and the bovine GFF annotation file for the USDA ARS-UCD 1.2 genome assembly (Rosen *et al.*, 2020) from NCBI (accession GCF_002263795.1).

Gene candidates for each trait and sub-component (intercept and slope) were evaluated separately using Network Analyst 3.0 (Xia *et al.*, 2014). A protein-protein interaction (PPI) network was created within Network Analyst 3.0 with data from the STRING interactome database and a confidence score cutoff of 900 (Szklarczyk *et al.*, 2015). The PPI network was utilized to identify enriched KEGG pathways and biological process gene ontology (GO) terms (Kanehisa and Goto, 2000). Multiple testing corrected enrichment p-values were obtained from Mann-Whitney-Wilcoxon tests for KEGG pathways and GO terms generated in Network Analyst 3.0. Pathways and GO terms with an adjusted p-value of less than 0.05 were reported. If there were many pathways and terms enriched, the top ten were presented. Candidate

quantitative trait loci (QTL) were also compared to existing studies in the literature using QTLdb (Hu *et al.*, 2019).

Results and Discussion

Population Trends

Scatterplots with locally weighted smoothing (LOESS) curves comparing DMI and respiration rate across various levels of THI post outlier filtering can be seen in Figure 3.1. Dry matter intake appeared to have a small, linear, and negative population phenotypic trajectory (Figure 3.1A). The phenotypic decrease of approximately 1-2 kg DMI when moving from 70 THI to 85 THI was less than the decreases seen in dairy cattle, where DMI would decrease by four kg from 68-78 THI (Bouraoui *et al.*, 2002; West, 2003; Hill and Wall, 2017). Values at the extreme end of THI may have started to decrease non-linearly, but not enough data was obtained at extreme THI values to warrant the exploration of higher order models. Even though the changes in daily DMI seemed small, a loss of two kg of DMI per day would likely lead to meaningful losses in potential weight gain over the finishing or grower production stage, which would likely impact profitability.

Respiration rate clearly increased as THI increased, as expected (Figure 3.1B). The increase appeared linear throughout the range represented in this study, with a slight perturbance around 75 – 77.5 THI. The trend presented in Figure 3.1B is similar to the respiration rate trend reported for dairy cattle in Al-Kanaan (2016) in the same THI range. The trend in Al-Kanaan (2016) was slightly steeper, however. This may be due to the high production potential of dairy cattle, as increased production is known to increase metabolic heat and thus the need to expel it through respiration (Kadzere *et al.*, 2002; West, 2003; Carabaño *et al.*, 2014). This may increase

their sensitivity to THI because metabolic and environmental heat are additive, which would in turn lead to a greater rate of change in respiration rate. Thus, given the ties between DMI and production (Kertz *et al.*, 1991), production and metabolic heat (Kadzere *et al.*, 2002; West, 2003; Carabaño *et al.*, 2014), and the need to expel it through respiration or other means (Kadzere *et al.*, 2002; West, 2003; Carabaño *et al.*, 2014), there is a clear link for the biological mechanisms of environmental sensitivity. Individuals which must expel more metabolic heat may be more likely to become stressed as the environment makes it more difficult to expel the metabolic heat.

The THI range in this study is relatively narrow and the effects of THI on respiration rate may not be linear as THI increases to 90 or greater. However, given the modeling choices and results of Ravagnolo and Misztal (2000), Aguilar *et al.* (2009), and Bradford *et al.* (2016) for other traits, the assumption of linearity appears to be commonplace in heat stress literature with threshold characteristics. Similar thresholds to those used in this study were identified for the onset of heat stress in these studies. Brügemann *et al.* (2011) utilized a non-linear model, but the hottest year on record had a maximum mean monthly THI under 70, indicating very different THI ranges and therefore very different trends and modeling needs. Ravagnolo and Misztal (2000), Aguilar *et al.* (2009), and Bradford *et al.* (2016) utilized a threshold approach, where linearity was assumed once THI surpassed a certain threshold (generally after 70-75 THI) and values below the threshold were treated as the threshold value. In other words, values below the threshold were considered to have a neutral effect or flat slope. Al-Kanaan (2016), who also evaluated respiration rate in response to THI and utilized a non-linear random regression model, but over a large THI range (35-85). Even so, the trend in Al-Kanaan (2016) appeared linear within the same range presented in this study.

Model Parameter Estimates

Dry Matter Intake

Point estimates and 95% HPDCIs for the population fixed intercept, population fixed slope, and variance components of the DMI random regression model are presented in Table 3.3. In general, there did not appear to be much evidence for PE effects, as the 95% HPDCIs included zero for all PE covariance and variance parameters. The differences between groups were non-zero, with a between-group variance point estimate of 0.57 (95% HPDCI 0.10, 3.92; Table 3.3). However, there were few groups to inform the between-group variance, as indicated by the large amount of uncertainty in the HPDCI.

The population intercept point estimate was 5.79 $kg\ DMI$ (95% HPDCI 4.88, 6.66 $kg\ DMI$), which indicates gain potential under thermoneutral conditions. Assuming a feed to gain ratio of 6:1, this corresponds to nearly 1 kg of weight gain per day in thermoneutral conditions on average in the population. The population slope point estimate was -0.046 $\frac{kg\ DMI}{1\ unit\ THI}$ (95% HPDCI -0.053, -0.039 $\frac{kg\ DMI}{1\ unit\ THI}$), indicating losses are occurring due to heat stress. This decrease is expected, but not as large as estimates that were 10 times greater in dairy cattle (Bouraoui *et al.*, 2002; West, 2003; Hill and Wall, 2017). At 85 THI (15 units greater than thermoneutral), this corresponds to a decrease of 0.69 $kg\ DMI$ per day for the population median. While it may not seem like much, this would correspond to 69 $kg\ DMI$ intake potential lost over a 100-day period in the feedlot. Using the same feed to gain ratio, this corresponds to 11.5 kg of weight gain potential lost per animal. Therefore, selection for plasticity may be warranted to decrease losses to heat stress or increase predictability based on thermoneutral conditions.

The additive genetic intercept variance was quite large with a point estimate of 2.01 $kg\ DMI^2$ (95% HPDCI 1.54, 2.49 $kg\ DMI^2$; Table 3.3) relative to other variance components (Table 3.3), indicating DMI is heritable under thermoneutral conditions. Using the point estimate and empirical rule, 95% of the EBVs are expected to fall within the interval of -2.84 to 2.84 $kg\ DMI$ at thermoneutrality, or an interval difference of 5.67 $kg\ DMI$. The additive genetic slope variance, which was used to determine environmental sensitivity genetic variance to THI, is difficult to interpret, due to dependencies on the scale of the covariate. For example, a THI value of 10 greater than the onset of heat stress (80 before centering to the threshold of 70 THI) would yield a multiplier of 100 to the slope variance. The point estimate of the additive genetic slope was 0.0078 $\frac{kg\ DMI^2}{1\ unit\ THI^2}$. Using empirical rule again, 95% of EBVs would be expected to be within the interval of -0.177 to 0.177 $\frac{kg\ DMI}{1\ unit\ THI}$. The population slope point estimate and 95% HPDCI had a much lesser magnitude, which clearly demonstrates the ability to reduce the population average environmental sensitivity of DMI with selection. This may indicate the magnitude of G×E effects are likely large because of the greater additive genetic slope variance. Furthermore, selection alone to reduce the environmental sensitivity of DMI ignores any potential genetic relationship to the intercept, or general performance in environments without heat stress. Thus, the genetic correlation should be an important part of selection decisions if there is an unfavorable relationship.

The genetic covariance between the slope and intercept was negative with a point estimate of -0.10 (95% HPDCI -0.13, -0.07; Table 3.3), indicating selection for increased DMI (i.e., production) prior to the onset of heat stress will strongly increase the environmental sensitivity. The environmental sensitivity would increase as the slope would be expected to decrease further (Schaeffer, 2004). The strength of the relationship between the intercept, or

performance in thermoneutral conditions, and the slope, or environmental sensitivity is measured by the genetic correlation between the two, which had a point estimate of -0.74 (95% HPDCI -0.86, -0.69), indicating selection to increase DMI in thermoneutral conditions will strongly decrease the slope. This is unfavorable, as the population trajectory slope is already negative, indicating environmental sensitivity would increase and, to increase phenotypic plasticity, selection towards a population trajectory slope of zero is required (West-Eberhard, 2008). This matches the conclusions for other traits evaluated under the same THI function in random regression models (Ravagnolo and Misztal, 2000; Aguilar *et al.*, 2009; Brügemann *et al.*, 2011; Bradford *et al.*, 2016).

However, while DMI has previously been shown to have a positive genetic correlation with average daily gain, negative genetic correlations between DMI and feed efficiency traits have previously been reported (e.g., Santana *et al.* 2014). If selection for reduced DMI, or increased feed efficiency, in thermoneutral conditions occurs, phenotypic plasticity would be expected to increase based off the genetic correlation between the intercept and slope for DMI (Table 3.3). Unfortunately, the genetic correlations referenced between DMI and average daily gain/feed efficiency were conducted in standard animal models, meaning the genetic correlations represent the average genetic relationship across all environments not accounted for in the model (i.e., averaged over the residual). While the postulated relationships between selection for feed efficiency/average daily gain and DMI environmental sensitivity are promising, the relationships should be validated in the context of random regression models. This remains a missing source of information needed to make accurate selection decisions.

Respiration Rate

Estimates for variance components and location parameters reflect the base-ten logarithm transformed respiration rate data. Therefore, only 95% HPDCIs overlapping zero, which implied little evidence for an effect, signs of covariances, and the genetic correlation between the slope and intercept will be discussed. Like DMI, there did not appear to be evidence for PE effects, as the PE covariance between the slope and intercept overlapped zero and the lower bounds of the credible intervals appear to not meaningfully differ from zero (Table 3.4). However, in the case of the intercept and slope, it is difficult to tell whether credible intervals fall meaningfully close to zero due to the logarithmic transformation and the software constraining the variances to be bounded at zero. Regardless, the lower bounds of the credible intervals for the PE effects appear to be two or more magnitudes smaller than other variance components, implying their contribution is likely negligible (Table 3.4).

The genetic correlation between the additive genetic intercept and slope for respiration rate was also highly negative, with a point estimate of -0.72 (Table 3.4). However, the 95% HPDCI ranged from -1.0 to -0.20 (Table 3.4), indicating there is almost no certainty about the value of the genetic correlation, other than it is negative. Even so, selection to decrease respiration rates in thermoneutral conditions would be expected to increase environmental sensitivity to heat stress. Initially, a negative correlation may be considered confusing or uninterpretable. However, recent work has shown that respiration rate is lowly to moderately, positively correlated genetically with production traits in a heat-stressed environment (Luo *et al.*, 2021). Put simply, selection to increase production would be expected to increase respiration rate. This means respiration rate serves as a positive indicator trait of performance. Given the trends observed for DMI and respiration rate in response to THI in this study, this information

may augment the argument postulation that increased DMI is correlated with increased ADG. If ADG represents production, then increased DMI, which was unfavorably associated with environmental sensitivity, may be an indicator of respiration rate and vice-versa. This would explain the seemingly paradoxical relationship between the additive genetic intercept and slope for respiration rate. If respiration rate, a proxy for ADG or production, is increased under thermoneutral conditions, then it would be expected to decrease as THI increased based on the genetic correlation in Table 3.4. This increases environmental sensitivity, as ADG or production would also be expected to decrease as respiration rate decreases. This needs to be validated in a multivariate random regression approach, however.

There is also a biological explanation, as respiration rate is postulated to help expel the extra metabolic heat generated from increased production (e.g., milk yield), creating the positive genetic correlations described between respiration rate and production traits (Kadzere *et al.*, 2002; Carabaño *et al.* 2014; Al-Kanaan, 2016; Polsky and Keyserlingk, 2017; Luo *et al.*, 2021). In other words, selection to increase the genetic component of respiration rate would be expected to increase the genetic potential for production traits. Therefore, given a positive phenotypic trajectory (Table 3.4), selection to increase respiration rate, or production, in thermoneutral conditions is expected to increase environmental sensitivity and decrease phenotypic plasticity.

Respiration rate and DMI intercepts, or selection in thermoneutral environments, both share (potentially) unfavorable genetic correlations with their respective slopes, or the environmental sensitivity. In the case of DMI, however, selection for decreased DMI (and reduced average daily gain) appears to be correlated with increased feed efficiency (Santana *et al.*, 2014). In the context of this study, selection for feed efficiency in thermoneutral conditions would be expected to reduce the environmental sensitivity and increase phenotypic plasticity.

This creates a dilemma for DMI selection. With respiration rate, it is unclear whether selection for increased production, at the expense of reduced phenotypic plasticity, is optimal. Likely, the optimal between productivity and plasticity will vary across producers and location. To our knowledge, no economic study has ever been conducted with random regression results to determine the optimal selection program. This remains a gap in the literature which will need to be filled to adequately construct economic indices and may require producer inputs and a dynamic index to fully address. One emerging tool, iGenDec, may provide the interface needed to customize indices to producer-specific conditions.

Environmental Genetic and Permanent Environment Variance Trajectories

Additive genetic and PE variance trajectories are shown and discussed for DMI only, as variance components for log-transformed data have limited interpretability. Genetic variance decreased substantially as THI increased (Figure 3.2). Genetic variance appeared to minimize and stabilize, with credible intervals indicating greatly reduced genetic variance relative to thermoneutral conditions, just past 80 THI. A THI of 80 may be a critical threshold for genetic selection potential for the represented population based on this dataset. It is also possible 80 THI is another inflection point where the trend may become non-linear. However, relatively little data was available past 80 THI in this study, so it is difficult to determine whether the lack of genetic variance is simply due to sparsity of data and estimate instability or if genetic variance is truly low. Based on Al-Kanaan (2016), who utilized the same THI function, THI was roughly linear from 70-85 THI in dairy cattle. The genetic variance trajectory here follows a similar trend as Brügemann *et al.* (2011) for milk protein and Bradford *et al.* (2016) for weaning and yearling weight under THI, but disagrees with the trend reported by Ravognolo and Misztal (2000) in a

repeatability model. However, Aguilar *et al.* (2009) reported the genetic variance from the repeatability model was likely inflated as dairy cattle were managed to prevent lactations overlapping with high THI values.

In low-stress THI environments, there appears to be little evidence to suggest there is a PE effect, given the 95% HPDCI's contain zero (Figure 3.2), which agrees with the earlier conclusions about the parameters in Table 3.3. As THI increases, there is evidence for PE effects; but, as THI surpasses 80, the evidence for PE effects decreased again, demonstrating the uncertainty associated with estimates just past 80 THI. The 95% HPDCI upper boundary for the PE variance implies the PE effects are small compared to the residual variance and other variance components (Table 3.3), even when there is evidence for non-zero effects. The genetic variance is also smaller at this point, however, which means repeatability would be expected to be different from heritability at moderate levels of heat stress.

Heritability and Repeatability Trajectories Across THI

Dry Matter Intake

Heritability estimates for DMI in thermoneutral conditions were moderate to high, with point estimates lying between 0.30 and 0.40 (Figure 3.3 and B.1). Previously, with a subset of this data and a frequentist model, DMI heritability was estimated to be 0.67 (Ahlberg *et al.*, 2009). In a review of 38 studies, DMI estimates ranged from 0.06 to 0.70 (Berry and Crowley, 2013). Other estimates of DMI heritability ranged from 0.27 to 0.41 in taurine beef cattle (Snelling *et al.*, 2011; Saatchi *et al.*, 2014), 0.40 to 0.46 in Nellore cattle (Santana *et al.*, 2014; Polizel *et al.*, 2018), and 0.21 to 0.50 in a G×E study utilizing countries as different environments in dairy cattle (Yao *et al.*, 2017). The 95% HPDCIs of heritability estimates in

thermoneutral environments easily fell within these ranges. Heritability decreased as THI increased (Figure 3.3). This is expected as the PE variance and genetic variance decrease, while the residual variance and group variance are assumed constant as THI increases. Residual variances as a function of THI were modeled and tested, but there the differences for heteroscedasticity as a function of THI were minimal compared to heteroscedasticity by group (data not shown). Similar to the genetic variance trend, heritability appears to stabilize at approximately 80 THI and no further decreases were seen in this study. However, there was evidence for non-zero heritabilities past 80 THI, implying evidence for non-zero additive genetic variance, unlike Figure 3.2.

Repeatability trajectories mirrored the heritability trajectories (Figure 3.4 and B.2). This is to be expected, given little evidence for variance attributable to PE effects. Point estimates were slightly greater than heritability point estimates, but the 95% HPDCIs substantially overlapped between the repeatability and heritability trajectories.

Respiration Rate

Overall, there was little evidence for a heritable component of respiration rate at many values of THI, especially in thermoneutral environments (Figure 3.5 and B.3). There was evidence for small non-zero heritabilities at moderate THI levels. Point estimates of heritability tended to be very low, ranging from ~0.02 to 0.04 across groups (Figure 3.5 and B.3). Point estimates are nearly identical with estimates recently reported by Luo *et al.* (2021), who reported a point estimate of 0.04 with standard error of 0.01. Al-Kanaan (2016) reported a similar heritability trend in a random regression model with THI, where heritability point estimates increased between 70 and 80 THI. However, the point estimates reported by Al-Kanaan (2016)

were slightly greater, ranging from approximately 0.04 to 0.06. Overall, respiration rate is either not heritable or extremely lowly heritable in this study.

However, there was increased evidence to suggest repeatability was greater than zero past approximately 72 THI (Figure 3.6 and B.4). Beyond this threshold, repeatability point estimates tended to increase as THI approached 80. However, PE effects were small (Table 3.4 and Figure 3.6). While the same trend was observed in Al-Kanaan (2016), they noted a much larger repeatability ranging from approximately 0.22 to 0.28 in the same THI range. Granted, this was a study conducted for dairy cattle, so the PE effects are likely different than beef cattle.

Genetic Correlations Between Traits Across Different Levels of the Temperature Humidity Index

Genetic correlations between DMI or respiration rate at different levels of THI, in combination with the corresponding slope variance, are useful to determine the current extent and functional form of G×E effects. Genetic-by-environment effects imply that as the environment, or THI in this case, changes, the genetic value of the individual changes (Kang, 1997). Whereas the non-intercept genetic random regression parameter (slope only in the linear case) variances let us predict the magnitude and direction of change in EBVs trajectories across the environment (THI), the genetic correlation measures how predictable these changes are. In other words, genetic correlations inform whether there is a strong, linear relationship to predict outcomes across environments or whether the relationships, if any exist, are linearly independent (Crow, 1986). This information is important to breeders in evaluating whether animals who perform well in a given range of THI are expected to predictively perform well at other values of THI.

Given the genetic correlations between the intercept and slope for DMI and respiration rate are most likely considered unfavorable when selection emphasizes production in thermoneutral environments, the environmental sensitivity of animals is expected to increase. One question that remains unexplored in this study is whether increasing the environmental sensitivity through selection of traits in thermoneutral environments will cause genetic correlations to deteriorate. For this to happen, the magnitude of the covariance between the intercept and slope would have to decrease. In the absence of new variation from mutations or population introgression, this would imply selection has moved pleiotropic genetic variants towards fixation while the environmental sensitivity-specific genetic variation is not under selection (or under less powerful selection; Via and Lande, 1985; Falconer and Mackay, 1996; Sgrò and Hoffman, 2004; Schou *et al.*, 2019). The current genetic correlations offer a snapshot of the genetic-by-environment in the population and its effects on the accuracy of selection across environments.

In general, genetic correlations between DMI in thermoneutral environments and environments with significant heat stress were low (Figure 3.7A and Table B.2). Point estimates for genetic correlations between DMI at 70 THI and 85 THI dropped as low as 0.42 (Table B.2), indicating EBVs in evaluations under thermoneutral conditions are likely to be very poor selection metrics of genetic performance in environments under significant heat stress. Uncertainties between DMI at across THI were moderately high (Table B.2), but clearly indicated genetic correlations were decreasing. Using the same function to calculate THI, Bradford *et al.* (2016) noted very similar genetic correlation decreases with weaning weight and yearling weight at different levels heat stress in Angus cattle. However, this contradicts the results of Ravagnolo and Misztal (2000), who reported strong genetic correlations across a

similar THI range (with the same THI function) for milk production in dairy cattle. Santana *et al.* (2015) observed similar declines in weaning weight genetic correlations in the THI range presented here for Brangus and tropical composites, but observed high genetic correlations in Nellore cattle. This would suggest Nellore cattle are, unsurprisingly, adapted to tropical conditions. Unless selection to reduce environmental sensitivity is practiced in taurine cattle, which will likely lead to a loss in productivity as previously discussed (Table 3.3; Santana *et al.*, 2014), utilizing locally adapted breeds may currently be the best option.

It would appear that G×E effects across environments with different THI impact selection accuracy and estimation of breeding values for DMI. Simulations to determine the impact of ignoring G×E over successive generations will likely be needed to determine the exact loss in genetic progress. However, the decline in genetic correlations may be severe enough to warrant consideration of G×E effects with random regression methodology in current evaluations.

Genetic correlations for respiration rate are presented in Figure 3.7B. Uncertainties for genetic correlations involving THI values closer to thermoneutral and high THI overlapped one or zero (Table B.3), implying no predictability between environments or respiration rate was the same trait in the two environments. The large uncertainties associated with genetic correlations are not surprising, however, given the little evidence for a heritable component or instability of the heritability estimates (Figure 3.5). Likely these estimates are not meaningful, which is implied by the large uncertainties. In general, genetic correlations declined rapidly as differences between environments increased. While large measures of uncertainty were observed here due to the lack of a heritable component, which led to instability in the estimates, Al-Kanaan (2016) previously reported high genetic correlations in dairy cattle between respiration rates in the same THI range.

Spearman Correlations Between Estimated Breeding Values Across Different Levels of the Temperature Humidity Index

Spearman correlations between EBVs of traits in different environments can inform whether G×E effects are severe enough to cause re-ranking between animals. For DMI, Spearman correlations between EBVs at different levels of THI were generally lower than the genetic correlations (Figure 3.8A), indicating a significant number of animals' EBVs are reranking as THI increases. In general, as the difference between THI increased, the corresponding Spearman correlations decreased (Figure 3.8A). The lowest Spearman correlation point estimate for DMI was observed between 70 and 85 THI, with a value of 0.39 (95% HPDCI 0.26, 0.52; Table B.2). This indicates selection across environments for DMI is likely highly inaccurate. For respiration rate, uncertainties were generally very large and tended to overlap zero or one (Table B.3), similar to the genetic correlations and with similar conclusions and reasoning.

Overall, the Spearman correlations further corroborate the importance of considering THI G×E effects in taurine breeds, as it likely impacts selection accuracy in extreme evaluations. Given the degree of reranking, G×E should be considered in national evaluation. The impact of ignoring G×E in traditional animal models, such as what are currently used in industry, remains unclear and remains an area of exploration.

Beef Improvement Federation Accuracies

Beef Improvement Federation accuracies were moderate to moderately high for the EBVs of the additive genetic intercept and slope of DMI (Table 3.5). Respiration rate accuracies of intercept and slope EBVs were low (Figure 3.9B). However, due to the lack of genetic variance

and heritability for respiration rate (Table 3.4; Figure 3.5), respiration rate EBV accuracies were invalid and have no interpretation. Interestingly, the densities of the accuracy estimates were bi or sometimes tri-modal for DMI (not shown). This likely reflects differences in data availability for different groups. These multi-modal densities are what caused the skew seen in the 95% density range values in Table 3.5.

For DMI, accuracy of DMI EBVs at different levels of THI tended to increase as THI increased, up until approximately 80 THI (Figure 3.9A). This at least partially reflects the amount of data available as THI increased (Figure 3.1A). Most likely, this phenomenon of increasing accuracy is observed due to variance component estimates being biased towards regions with more data, which may decrease the variance of the EBV posteriors used to calculate BIF accuracy.

Genome Wide Association Study

A significance threshold of $-\log_{10}(p\ value) > 5$ was utilized to detect associated SNPs, with approximately one false positive expected per trait when testing 123,912 SNPs. However, not all SNPs were independent due to LD, meaning the expected number of false positives is likely less (Nyholt, 2004). Single nucleotide polymorphisms associated with the DMI intercept and slope are presented in Table 3.6 and in Figure 3.10. Four SNPs that were not within LD range of each other were associated with the intercept, and seven were associated with the slope (Table 3.6). However, three SNPs were identified for both the intercept and slope, indicating a shared genetic background, which supports the strong genetic correlation between the intercept and slope previously discussed. Fifty-nine candidate genes were identified in the QTL regions associated with the intercept and 79 were identified in the QTL regions associated with the slope

(Table 3.6). Unfortunately, some SNPS were unmapped and candidate genes could not be identified. None of the SNPs associated with the DMI intercept or slope have previously been reported in QTLdb for other traits (Hu *et al.*, 2019), indicating potentially novel QTL were identified in this study.

Variants Associated with the DMI Intercept and Slope

The first of the SNPs associated with both the intercept and slope, rs110000217, had many gene candidates with diverse functions. The PIP4P1 gene is involved in the phosphatidylinositol pathway, which has functions in metabolic signaling (Fruman *et al.*, 1998; Zewail *et al.*, 2003; Ramazzoti *et al.*, 2017). The second variant, rs43076526, was near an alcohol dehydrogenase, ALDH7A1, which breaks down alcohols into compounds that enter fatty acid metabolism (Wang *et al.*, 2014). These products may come from the fermentation byproducts of various fungi and bacteria (Kristensen *et al.*, 2007). Once absorbed, the alcohol byproducts from fermentation would be broken down for energy in fat metabolism pathways. The third variant was, unfortunately, not mapped. Only one other variant was associated with the DMI intercept, but there were no nearby genes with a function that was intuitively related.

Variants Associated with the DMI Slope

The first of the four variants uniquely associated with the DMI slope, rs41584168, was near two genes, but neither had functions that would intuitively lend themselves as candidates. The second variant, rs42893659, was near many putative genes, but no functions were identified. The third variant, rs42754402, was near two tRNA genes and the GRIA2 gene. The GRIA2 gene plays a role in modulating brain chemistry (Mead and Stephens, 2003), but it is unclear how it

may be related to DMI. The final variant was unmapped. Overall, there were few gene candidates for the DMI slope or intercept with known function that were intuitively related to the traits.

Variants Associated with the Respiration Rate Intercept

Single nucleotide polymorphisms associated with the respiration rate intercept and slope are presented in Table 3.7 and Figure 3.11. Only two SNPs were found to be associated with the intercept, whereas 12 were associated with the slope (Table 3.7), potentially illustrating the increased power associated with utilizing a random regression model. Under a typical animal model, it is likely that only SNPs strongly associated with the average environment or across the entire environment would be identified (Lillehammer *et al.*, 2007). In this case, the identification of QTL associated with respiration rate may have been less successful had a standard animal model been used.

One SNP associated with the respiration rate intercept, rs42195584, has previously been identified in QTLdb and was associated with teat thickness and conception rate (Vallée *et al.*, 2016; Jiang *et al.*, 2019). The rs42195584 variant was near troponin genes, genes related to immune processes and lymphocyte function, exocytosis for hormone release, and a phosphatase gene in the MAPK pathway. The phosphatase gene helps regulate cell growth and proliferation (Zhang and Liu, 2002). The troponin genes may be related to respiratory function through diaphragm contractions, the immune-related functions could be related to respiratory distress and inflammatory signals, and the phosphatase gene may be related to increased respiration for cellular growth. The phosphatase gene in the MAPK pathway, DUSP8, may be the most likely as

it is related to metabolism and supports the hypothesis that respiration rate is related to metabolic traits like average daily gain, because it may help shed metabolic heat.

The second SNP associated with the respiration rate intercept, rs41638833, was only in the vicinity of one gene, MECOM, which is a transcriptional regulator and protooncogene regulating cellular growth and proliferation (Makondi *et al.*, 2017). The MECOM gene is involved in the MAPK pathway (Makondi *et al.*, 2017), which explains its role in cellular growth and proliferation. As previously discussed, this may further support the hypothesis of respiration rate being genetically related to production through shedding heat generated through metabolism.

Variants Associated with the Respiration Rate Slope

Twelve SNPs were associated with the respiration rate slope (Table 3.7). However, only 11 were mapped. The first, rs43548481, was near the FBXO8 gene, which has been associated with cardiomyopathies and, previously, cardiovascular disease in a human GWAS (Shendre *et al.*, 2017). This may indicate a relationship between respiration rate and susceptibility to heart problems in feedlot populations. The second, rs41572817, was associated with a tRNA gene, but given the broad role of tRNAs in many biological processes, it is unclear how it may be related to respiration rate. The third, rs135406674, was associated with DPP6, which has been associated with ventricular fibrillation (Postema *et al.*, 2011). This condition leads to cardiac death, which supports the purported relationship between respiration rate and cardiac issues in the feedlot. It may be that higher performing feedlot cattle (i.e., cattle with a greater amount of fat deposition) struggle with greater insulative effects, greater heart strain to maintain blood flow, and dispelling heat though increased blood flow to the skin (Vroman *et al.*, 1983). Cattle with greater body fat deposition essentially mimic obesity in humans and suffer from greater

incidence of heart problems and cardiac failure (Krafsur *et al.*, 2019). The phenomenon of increased cardiac failure under heat stressed conditions and an inability to shed body heat is also observed in humans (Cui and Sinoway, 2015) and may explain why respiration rate is associated with heart disease as respiration rate is used to shed body heat.

The rs110929815 variant was in the vicinity of nine genes. Many of the gene candidates had no known function. Amongst the candidates with known function, there was no intuitive relationship between the function and respiration rate slope. The rs136072282 and rs42299083 variants were only in the vicinity of one known gene each, but the gene candidate for the first variant had no known function and the gene candidate for the second variant, FAM110B, had a relatively ambiguous function related to tumor progression. While it was in the vicinity of six genes, the genes corresponding to the rs137234036 variant were also mostly of unknown function, except for two. The two with known function were described as a scaffolding protein in dendritic cells and an RNA guanine-N7 methyltransferase. No clear relationship between the functions of these genes and respiration rate is apparent.

Variant rs110434146 was near several genes. Some of the gene functions included development of collagen in connective tissues, regulation of the cell cycle and cellular proliferation with oncogenic potential, and muscle fiber function with known relationships to muscular dystrophy. The SNTB1 gene may be directly related to respiration rate because it is associated with muscular dystrophy and muscular dystrophy is commonly associated with respiratory failure or difficulty (Mauro and Aliverti, 2016). The SNTB1 gene product is involved in muscle tissue scaffolding, signaling, and leads to necrosis when absent, even though it comprises a very small percentage of muscle tissue (Aartsma-Rus *et al.*, 2006). While truncations and frameshift mutations can cause severe and acute muscular dystrophy disease

because of complete functional loss in the resulting protein, point mutations tend to lead to a less severe disease with a slow progression over many years in humans (Aartsma-Rus *et al.*, 2006). Thus, it may be reasonable to suggest similar variation may exist in cattle populations. Point mutations may lead to partial loss of function in the resulting protein, which may reduce severity of symptoms generally associated with muscular dystrophy (i.e., respiratory difficulty in this case). It may also be that the effects are only noticeable or important under stressful cardiac/respiratory conditions like those observed in the feedlot.

The next variant, rs110136264, was located near several genes, with ANAPC13 being the most likely candidate. The ANAPC13 gene helps regulate cell cycle progression (Peters, 2002), which indicates clear oncogenic properties. This may also support the hypothesis relating respiration rate slope to performance, as cell cycle progression may indicate cellular proliferation and growth. The rs110590148 variant was near one gene candidate with known function, FANCC, which is involved in DNA repair. In the marrow, specifically, it can lead to bone marrow failure and anemia (Pulliam-Leath *et al.*, 2009). Anemia-related mutations likely change hypoxic signals, which may in turn influence respiration rate. The last variant associated with the respiration rate slope, rs135187770, was near many genes. Several genes could be likely candidates, but OBSCN, which affects muscular function and development, may be the most likely based on its relationship to cardiac hypertrophy and cardiac failure (Perry *et al.*, 2014). Thus far, multiple loci with genes related to cardiac and muscular function and metabolism have been implicated, which adds a large amount of support for the hypotheses that they're related to respiration rate.

Genome-Wide Association Overview

There were many different types of genes associated with the respiration rate intercept and slope. However, some general categories of genes appeared to be highly prevalent across many loci. Many genes were related to cellular proliferation and growth, which supports the previous hypothesis relating respiration rate to metabolic functions and growth traits. Other types of candidate genes included those associated with muscular function and cardiac function or cardiac disease. This may indicate respiration rate has a relationship to heart disease in feedlot cattle. Specifically, loci associated with the slope were mere commonly associated with cardiac and respiratory function genes. It may be that the variants have relatively small effects, but increased stress placed upon the cardiovascular and respiratory systems to eliminate excess body heat combined with increased cardiovascular stress leads to more cardiac failure events. Thus, respiration rate may be an indicator of increased cardiac failure or other types of cardiac problems given it's an indicator of the increased stress placed upon the cardiovascular system. This is especially true for environmentally sensitive individuals.

Identification of Biological Pathways and Processes with Network Analysis

Dry Matter Intake

The KEGG pathways and biological process gene ontologies associated with the DMI intercept and slope are reported in Table 3.8. Primarily, candidate genes for DMI at 70 THI had enriched pathways involving DNA replication and DNA repair (Table 3.8). This is perhaps an indicator of cellular division and growth signaling, which requires energy and would likely lead to increased feed intake to supplement the energy demands. This may also be related to mTOR related pathways previously identified, which translate cellular energy balances into signals

regulating feed intake and cellular proliferation (Cota *et al.*, 2006). In other words, pathways and functions related to cellular proliferation and growth likely feed into typical large, metabolic signaling pathways that translate cellular energy states into feed intake signaling.

Gene ontologies, however, were more associated with metabolic processes. One metabolic process was the energy reserve metabolic process ontology, which involves generation of adenosine triphosphate from glycogen and nitrogen metabolism (Table 3.8). Generation of adenosine triphosphate is core in central metabolism and has shown relationships with appetite control (Minokoshi *et al.*, 2004). Overall, this data indicates DMI in thermoneutral environments seems to be mostly controlled by regulation of energy balances and energy balance signaling. Alcohol metabolic processes were indicated. Alcohol products may come from the fermentation byproducts, as previously discussed, and could be used in fat metabolism pathways for energy production (Kristensen *et al.*, 2007).

The KEGG pathways associated with the slope QTL were much more varied, including metabolic pathways, such as gastric acid secretion and lipolysis in adipocytes, as well as many different signaling pathways including cAMP signaling, Ras signaling, phospholipase D signaling, and secretion of the renin hormone. Gastric acid secretion is affected by heat stress in pigs (Ou *et al.*, 2016), which may explain the genetic relationship with the environmental sensitivity to heat stress. Therefore, heat stress may affect the ability to digest feed by affecting gastric acid secretions, which would likely impact DMI. Phospholipase D is involved in the phosphatidylinositol second messenger system, which is associated with cellular proliferation, vesicle trafficking, glucose transport, lipid metabolism, protein metabolism, and many other metabolic pathways (Fruman *et al.*, 1998; Zewail *et al.*, 2003; Ramazzoti *et al.*, 2017). The phosphatidylinositol pathway is also associated with the activation of the mTOR pathway, which

was previously discussed to be related to feed intake (Cota *et al.*, 2006). Because these signals tied to the mTOR pathway were identified for both the intercept and slope, this indicates the intercept and slope for DMI may be influenced by similar mechanisms (i.e., signaling).

Likewise, cAMP signaling is heavily associated with glucose and lipid metabolism (Ravnskjaer *et al.*, 2016), Ras signaling is associated with lipid metabolism (Slack, 2017), and sphingolipid signaling is associated with lipid biosynthesis (Gault *et al.*, 2011). Similar gene ontologies were seen, with more signaling and central metabolism elements (Table 3.8). These all play key roles in energy production or are involved in cellular energy states. Therefore, it is likely they influence the mTOR pathway and other pathways involved with regulating hunger. This provides evidence that variants associated with the additive genetic slope and intercept both influence energy production through metabolic signaling in response to cellular energy states. However, variation unique to the environmental sensitivity may be attributable to digestion and metabolic pathways being directly influenced by heat stress. It may be the QTL identified for the slope are signaling events in metabolic pathways that only have an effect when affected by THI or heat stress, though the exact mechanism is unclear.

In addition to metabolic signaling in response to cellular energy states, key central metabolism pathways in energy production were identified. Beta oxidation, a process by which fat is converted into adenosine triphosphate, was also identified for the DMI Slope. Saatchi *et al.* (2014) identified an acyl-CoA synthetase (ACSL6) subunit associated with DMI, which is also involved in the beta oxidation pathway. This likely means variants associated with DMI are not only regulatory or signaling in nature, but also affect enzymatic function in core pathways and therefore affect an animal's ability to efficiently produce energy from feed intake. Changes in energy generation efficiency and the energy balance of the cell likely affect hunger signaling,

which would influence feed intake. Therefore, while different pathways and ontologies were identified for the intercept and slope, many seem to share a similar theme related to central metabolism. It is perhaps unclear whether certain variants may only be related to production at 70 THI or environmental sensitivity to THI, or whether random regression merely increased the power to find variants which may affect both traits.

Respiration Rate

The intercept of respiration rate was mostly associated with KEGG pathways involving heart disease and heart contraction (Table 3.9). Heart function, cardiomyocyte contractile ability, and rhythm is an important part in the synchronous control of respiration rate and meeting the oxygenation requirements of cells to fuel oxidative metabolism (Hayano *et al.*, 1996; Brinkman *et al.*, 2021). This may indicate alleles associated with heart function, which synchronously influence respiration rate, play an important role in supporting metabolic processes. This provides direct evidence to support the genetic correlations between respiration rate and metabolism/production discussed previously. Cardiomyopathies may similarly affect oxygenation potential. This is a population of feedlot cattle, where heart disease is historically a problem (Neary *et al.*, 2015) and thus these could represent feedlot-specific signals for heart disease or general ties between cardiovascular and respiratory function.

Cattle suffering from heart conditions may be more at risk for high altitude disease as well (Neary *et al.*, 2016), which is an affliction that is economically important in mountainous regions like Colorado, Wyoming, and Montana (Jennings *et al.*, 2019). The pulmonary hypertension characterizing high altitude disease develops because of long-term hypoxic conditions (Hecht *et al.*, 1962), which place greater stress on the cardiovascular and respiratory

systems. Therefore, ability to sufficiently meet oxygenation demands may directly be related to susceptibility to this disease. Feedlot cattle are also likely under greater cardiovascular stress and therefore the feedlot may mimic hypoxic conditions because cattle are pushed to rapidly gain weight. This weight gain mimics obesity in humans, putting cattle under greater cardiovascular strain and making them more susceptible to heart disease (Krasfur *et al.*, 2019). Assuming high altitude-driven hypoxia and cardiovascular stress in feedlot cattle lead to similar physiological responses and pathologies, variants may have similar impacts in both cardiovascular challenging environments. In other words, high altitudes present hypoxic conditions that create cardiovascular challenges and feedlot cattle suffer from obesity-related effects that create or exacerbate cardiovascular challenges. In both cases variants with a small or negligible impact on heart disease (as a binary trait) under normal or mild conditions may have larger effects because of the additional cardiovascular stress. This is supported for high altitude environments by Zeng (2016) who previously identified gene candidates related to cardiomyopathies, congenital heart defects, and general heart function in a GWAS evaluating high altitude disease with pulmonary arterial pressures measurements. These gene candidates are similar to pathways and gene candidates identified for respiration rate in this study, which supports the postulation that variants affecting cardiac function in the feedlot environment may influence cardiac function in hypoxic conditions. High pulmonary arterial pressure measurements, which are prevalent in conditions where cattle experience high altitude, are also associated with lung problems, cardiac problems, and cardiac failure in feedlot cattle (Krasfur *et al.*, 2019). Problems with respiration rate in thermoneutral conditions may therefore be related to high altitude disease/pulmonary arterial pressure, but more work would be needed to determine whether respiration rate of feedlot cattle in thermoneutral conditions is associated with high-altitude disease. If confirmed, it may

indicate respiration rate EBVs in thermoneutral environments are an indicator of genetic susceptibility to high altitude disease.

The slope, or environmental sensitivity, of respiration rate appeared to be more innately related to metabolism and metabolic signaling, (Table 3.9). Core pathways and gene ontologies involved signaling pathways/signal transduction, including the phosphatidylinositol signaling system, and lipid metabolism previously identified with the DMI intercept and slope. These are innately embedded in metabolic pathways which regulate food intake (Fruman *et al.*, 1998; Zewail *et al.*, 2003; Cota *et al.*, 2006; Ramazzoti *et al.*, 2017). This supports the previously discussed hypothesis that respiration rate is linked to metabolism and production by helping shed metabolic heat associated with increased production (Kadzere *et al.*, 2002; Carabaño *et al.* 2014; Polsky and Keyserlingk, 2017). One final association of interest was response to hypoxia, which is similarly associated with other pathways and gene ontologies identified in the intercept, indicating the respiration rate response environmental sensitivity, or slope, also has some relationship to maintaining adequate oxygenation.

Conclusions

There was a clear, inverse relationship between selection for DMI in thermoneutral environments and phenotypic plasticity in this study. Genetic variance and the heritability of DMI clearly declined until THI reached approximately 80. Unfortunately, G×E effects appear to be large in this study, as the genetic correlations between DMI at various levels of THI and Spearman correlations between DMI EBVs at various THI levels decreased quite rapidly as the distance between the pairwise THI environments increased. This indicates EBVs at a given level of THI would not be a good indicator of performance in environments where THI is different.

Biologically, the environmental sensitivity of DMI was associated with many metabolic signaling pathways and some pathways involved in digestion and central metabolism.

Unfortunately, there was only evidence for respiration rate being heritable at moderate values of THI. Non-zero heritability point estimates were similar to previous literature estimates and were very low. Interestingly, heart disease and function appeared to be related to respiration rate in thermoneutral conditions. This is likely related to cellular signals for hypoxia or increased oxygenic needs for oxidative metabolism. Given this is a study in a feedlot population, it may also have relationships to high-altitude disease, which is manifests similar pathologies and physiological responses under hypoxic conditions. The environmental sensitivity was mostly associated with metabolic processes and metabolic signaling, which supports the hypothesis of respiration rate's association with production and efficiency.

Table 3.1 Minimum, maximum, mean, median (Med.), first quartile (1st Q.), third quartile (3rd Q.), and standard deviation of daily dry matter intake (DMI; kg) and observed twice daily respiration rates (breaths per 30 seconds; BP30S) by group.

Trait	Group	N	Min	1st Q.	Mean	Median	3rd Q.	Max	SD
DMI (kg)	1	114	0.1	9.0	10.2	10.3	11.6	18.9	2.2
	2	114	0.6	6.5	8.1	8.0	9.7	15.5	2.5
	3	112	0.4	8.9	10.2	10.4	11.7	19.9	2.3
	4	105	2.4	9.6	10.7	10.7	11.8	16.7	1.7
	5	123	1.0	10.4	11.7	11.7	13.0	22.8	2.2
	6	120	1.6	8.9	10.3	10.3	11.8	18.4	2.2
	7	100	2.8	10.3	11.5	11.5	12.8	18.9	2.1
Respiration Rate (BP30S)	1	114	13	28	34.0	31	35	84	10.7
	3	112	11	20	29.5	28	37	68	11.4
	4	105	3	38	47.2	46	56	110	12.6
	6	120	2	28	37.9	37	48	72	12.1
	7	118	12	22	28.3	28	32	60	7.9

Table 3.2 Temperature humidity index number of observations (N), minimums, maximums, means, and quartiles for each group are given for dry matter intake (DMI) and respiration rate.

Trait	Group	N	Min	1st Quartile	Median	Mean	3rd Quartile	Max
DMI	1	7,038	70.3	77.8	81.0	79.9	82.7	85.0
	2	114	71.0	71.0	71.0	71.0	71.0	71.0
	3	5,432	70.4	75.7	80.0	78.8	81.9	84.0
	4	5,964	74.7	82.0	83.8	83.1	84.8	87.1
	5	1,467	70.0	71.4	72.6	73.0	74.5	78.2
	6	4,380	70.5	74.5	76.6	77.3	79.7	84.6
	7	1,765	70.6	72.8	74.3	74.4	76.4	78.5
Respiration Rate	1	1,368	70.6	72.0	73.5	74.3	76.2	79.5
	3	1,789	70.2	71.2	72.9	72.6	73.6	75.8
	4	4,501	72.9	76.3	77.7	77.6	79.1	81.4
	5	958	70.8	71.5	75.1	74.5	77.7	79.4
	7	236	70.1	70.1	71.0	71.0	71.9	71.9

Table 3.3 Table of posterior point estimates for each model parameter, including lower and upper bounds of 95% highest posterior density credible intervals, and the effective sample sizes for dry matter intake (DMI). Point estimates were the medians of the posterior densities.

Parameter	Estimate	Lower	Upper	Effective Size
η[1]	5.79	4.88	6.66	205
β_1[2]	-0.046	-0.053	-0.039	12,509
σ_f^2[3]	0.85	0.10	3.92	1,754
σ_a^2[4]	2.01	1.54	2.49	1,287
σ_{ab}[5]	-0.10	-0.13	-0.07	1,204
σ_b^2[6]	0.0078	0.0061	0.0096	2,983
σ_g^2[7]	0.27	0.00	0.59	635
σ_{gh}[8]	-0.0066	-0.03	0.00	520
σ_h^2[9]	0.0007	0.0000	0.0020	882
$\sigma_{e_1}^2$[10]	2.80	2.71	2.90	17,861
$\sigma_{e_2}^2$	3.22	1.86	4.71	19.459
$\sigma_{e_3}^2$	2.68	2.57	2.78	20,000
$\sigma_{e_4}^2$	2.07	2.00	2.15	20,000
$\sigma_{e_5}^2$	3.07	2.84	3.31	19,517
$\sigma_{e_6}^2$	2.23	2.13	2.33	20,000
$\sigma_{e_7}^2$	2.33	2.17	2.49	20,000
r_{ab}[11]	-0.78	-0.86	-0.69	890

[1] Fixed intercept

[2] Fixed slope for the temperature humidity index

[3] Between group variance (block)

[4] Additive genetic intercept variance

[5] Additive genetic covariance between the intercept and slope

[6] Additive genetic slope variance

[7] Permanent environment intercept variance

[8] Permanent environment covariance between the intercept and slope

[9] Permanent environment slope variance

[10] Residual variance for group i

[11] Additive genetic correlation between the intercept and slope

Table 3.4 Table of posterior point estimates for each model parameter, lower and upper bounds of 95% highest posterior density credible intervals, and the effective sample sizes for respiration rate. Point estimates were the medians of the posterior densities.

Parameter	Estimate	Lower	Upper	Effective Size
η[1]	1.41	1.31	1.50	194
β_1[2]	0.027	0.026	0.029	8,666
σ_f^2[3]	3.11e-03	1.96e-04	4.39e-02	1,934
σ_a^2[4]	5.84e-04	1.65e-04	1.07e-03	2,123
σ_{ab}[5]	-4.63e-05	-1.02e-04	2.70e-06	1,910
σ_b^2[6]	8.64e-06	1.99e-06	1.74e-05	2,060
σ_g^2[7]	9.87e-05	5.5e-08	3.87e-04	605
σ_{gh}[8]	-1.04e-05	-1.02e-04	2.70e-06	604
σ_h^2[9]	2.70e-06	2.72e-08	7.62e-06	1,016
$\sigma_{e_1}^2$[10]	9.55e-03	8.89e-03	1.03e-02	19,513
$\sigma_{e_3}^2$	2.18e-02	2.03e-02	2.33e-02	18,656
$\sigma_{e_4}^2$	1.07e-02	1.03e-02	1.11e-02	18,456
$\sigma_{e_5}^2$	1.31e-02	1.19e-02	1.44e-02	16,306
$\sigma_{e_7}^2$	1.71e-02	1.41e-02	2.04e-02	20,000
r_{ab}	-0.66	-1.0	-0.20	861

[1] Fixed intercept

[2] Fixed slope for the temperature humidity index

[3] Between group variance (block)

[4] Additive genetic intercept variance

[5] Additive genetic covariance between the intercept and slope

[6] Additive genetic slope variance

[7] Permanent environment intercept variance

[8] Permanent environment covariance between the intercept and slope

[9] Permanent environment slope variance

[10] Residual variance for group i

Table 3.5 Beef Improvement Federation accuracy median point estimates for the additive genetic intercept and slope of dry matter intake (DMI) and respiration rate estimated breeding values (EBV), including the 95% highest density lower and upper bounds.

Trait	*Parameter*	*BIF Accuracy*	*Lower*	*Upper*
DMI EBV	Intercept	0.51	0.17	0.56
	Slope	0.35	0.08	0.43
Respiration Rate EBV	Intercept	0.067	-0.04	0.15
	Slope	0.021	-0.09	0.10

Table 3.6 Significant single nucleotide polymorphisms (SNP) associated with the intercept and slope of dry matter intake (DMI) are reported with the genomic location and positive, base-ten logarithm transformed p-values. The number of gene candidates in the linkage disequilibrium range (± 250 kilobases) associated with each single nucleotide polymorphism (SNP) is listed. Asterisks indicate unmapped SNPs and/or no gene candidates. Bolded SNPs appeared in both the intercept and slope for the trait.

Trait	*SNP ID*	*Chr*	*Position*	$-log_{10}(p\ value)$	*Gene Cand.*
DMI Intercept	**rs110000217**	10	26,664,869	10.23	42
	rs43076526	7	27,252,564	6.80	10
	rs109277986	10	95,128,964	5.60	7
	BovineHD3000041486	*	*	8.31	*
DMI Slope	**rs110000217**	10	26,664,869	9.70	42
	rs43076526	7	27,252,564	6.14	10
	rs41584168	8	89,280,421	6.00	2
	rs42893659	21	20,058,560	5.44	22
	rs42754402	17	41,730,827	5.40	3
	BovineHD3000039754	*	*	5.13	*
	BovineHD3000041486	*	*	14.27	*

Table 3.7 Significant single nucleotide polymorphisms (SNP) associated with the intercept and slope of respiration rate are reported with the genomic location and positive, base-ten logarithm transformed p-values. The number of gene candidates in the linkage disequilibrium range (±250 kilobases) associated with each single nucleotide polymorphism (SNP) is listed. Asterisks indicate unmapped SNPs and/or no gene candidates. Bolded SNPs appeared in both the intercept and slope for the trait.

Trait	*SNP ID*	*Chr*	*Position*	$-log_{10}(p\ value)$	*Gene Cand.*
Resp. Rate Intercept	rs42195584	29	49,798,274	5.41	13
	rs41638833	1	98,103,554	5.01	1
Resp. Rate Slope	rs43548481	8	6,504,304	7.04	4
	rs41572817	11	18,547,348	6.44	2
	rs135406674	4	115,979,151	6.29	1
	rs110929815	28	39,213,609	6.10	9
	rs136072282	16	13,562,207	6.06	1
	rs42299083	14	24,162,163	5.82	1
	rs137234036	21	23,432,860	5.62	6
	rs110434146	14	81,977,771	5.47	4
	rs110136264	1	134,679,711	5.05	4
	rs110590148	8	81,613,969	5.02	7
	rs135187770	7	28,43,253	5.01	11
	BovineHD3000043087	*	*	5.22	*

Table 3.8 Pathways and biological process (BP) gene ontologies associated with dry matter intake (DMI) intercept and slope quantitative trait loci. Bolded terms indicate BP gene ontologies.

Trait	*Pathway or BP Gene Ontology*
DMI Intercept	Base Excision Repair
	DNA replication
	Mismatch repair
	Establishment of organelle localization
	Nitrogen compound metabolic process
	Alcohol metabolic process
	Energy reserve metabolic process
DMI slope	Natural killer cell mediated cytotoxicity
	Phospholipase D signaling pathway
	Sphingolipid signaling pathway
	Ras signaling pathway
	Gastric acid secretion
	Regulation of lipolysis in adipocytes
	cAMP signaling pathway
	Taste transduction
	Renin secretion
	Regulation of binding
	Lipid biosynthetic process
	Inflammatory response
	Stress activated protein kinase
	Carbohydrate transport
	JAK-STAT cascade
	Fatty Acid Oxidation
	Actin filament-based process
	Cell development

Table 3.9 Pathways and biological process (BP) gene ontologies associated with respiration rate intercept and slope quantitative trait loci. Bolded terms indicate BP gene ontologies.

Trait	*Pathway or BP Gene Ontology*
Resp. Rate Intercept	Cardiac muscle contraction
	Adrenergic signaling in cardiomyocytes
	Hypertrophic cardiomyopathy
	Dilated cardiomyopathy
	Cellular aromatic compound metabolic process
Resp. Rate Slope	Lysosome
	Endocytosis
	Inositol phosphate metabolism
	Phosphatidylinositol signaling system
	Nucleosome assembly
	Peroxisome organization
	Protein modification by small protein conjugation
	Negative regulation of signal transduction
	Cell maturation
	Cellular carbohydrate metabolic process
	Neuron development
	Protein tetramerization
	Tyrosine phosphorylation of STAT proteins
	Response to hypoxia

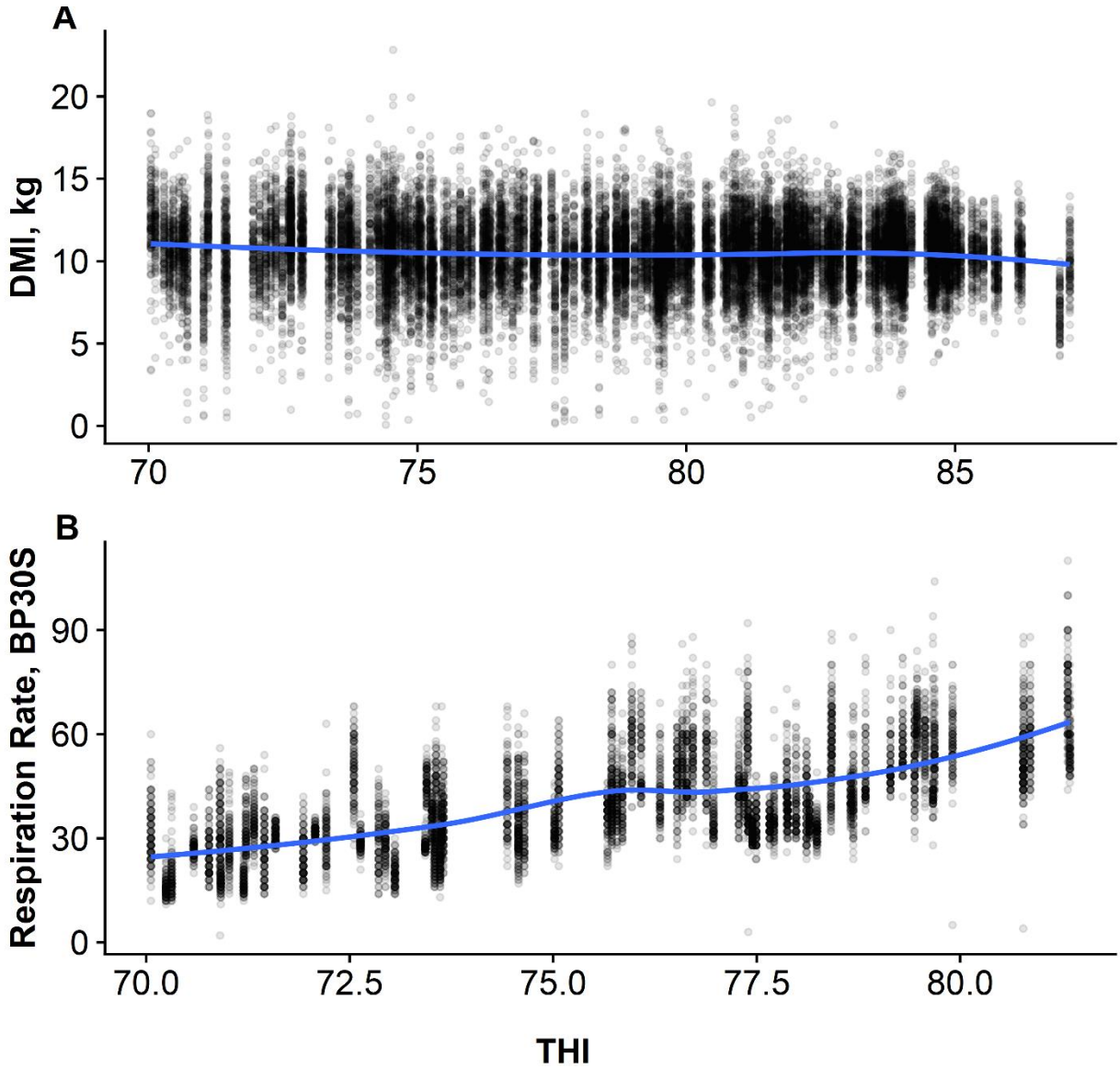

Figure 3.1 Scatterplot of daily dry matter intake (DMI; A) in kilograms and respiration rate (B), measured in breaths per 30 seconds (BP30S), at varying levels of the temperature humidity index (THI). A locally weighted scatterplot smoothing line (blue) was fit to determine the relative population trajectory.

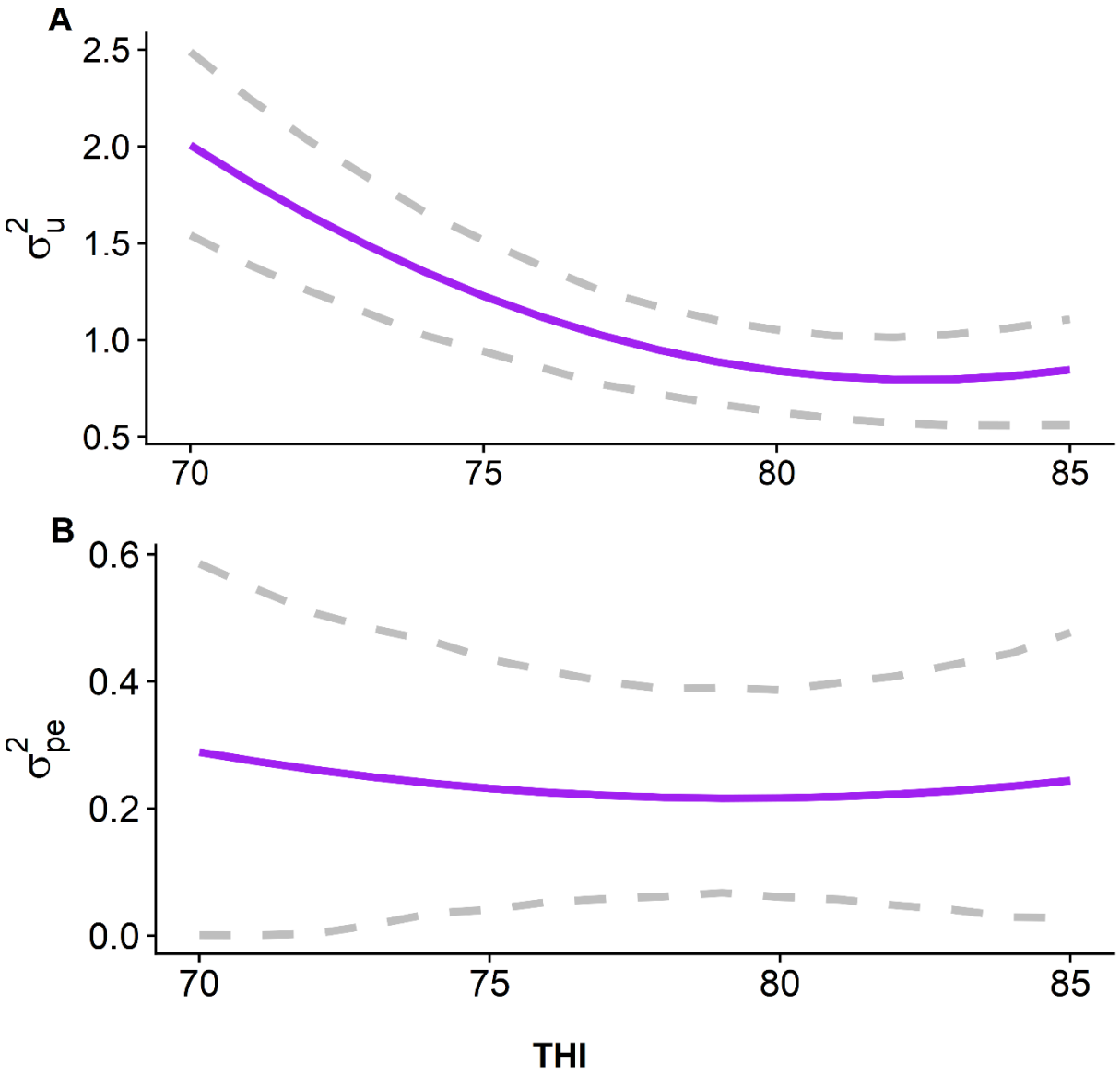

Figure 3.2 The posterior means (purple line) for additive genetic variance (A) and permanent environment variance (B) of dry matter intake by temperature humidity index (THI) level. The gray dashed lines are 95% highest posterior density credible intervals.

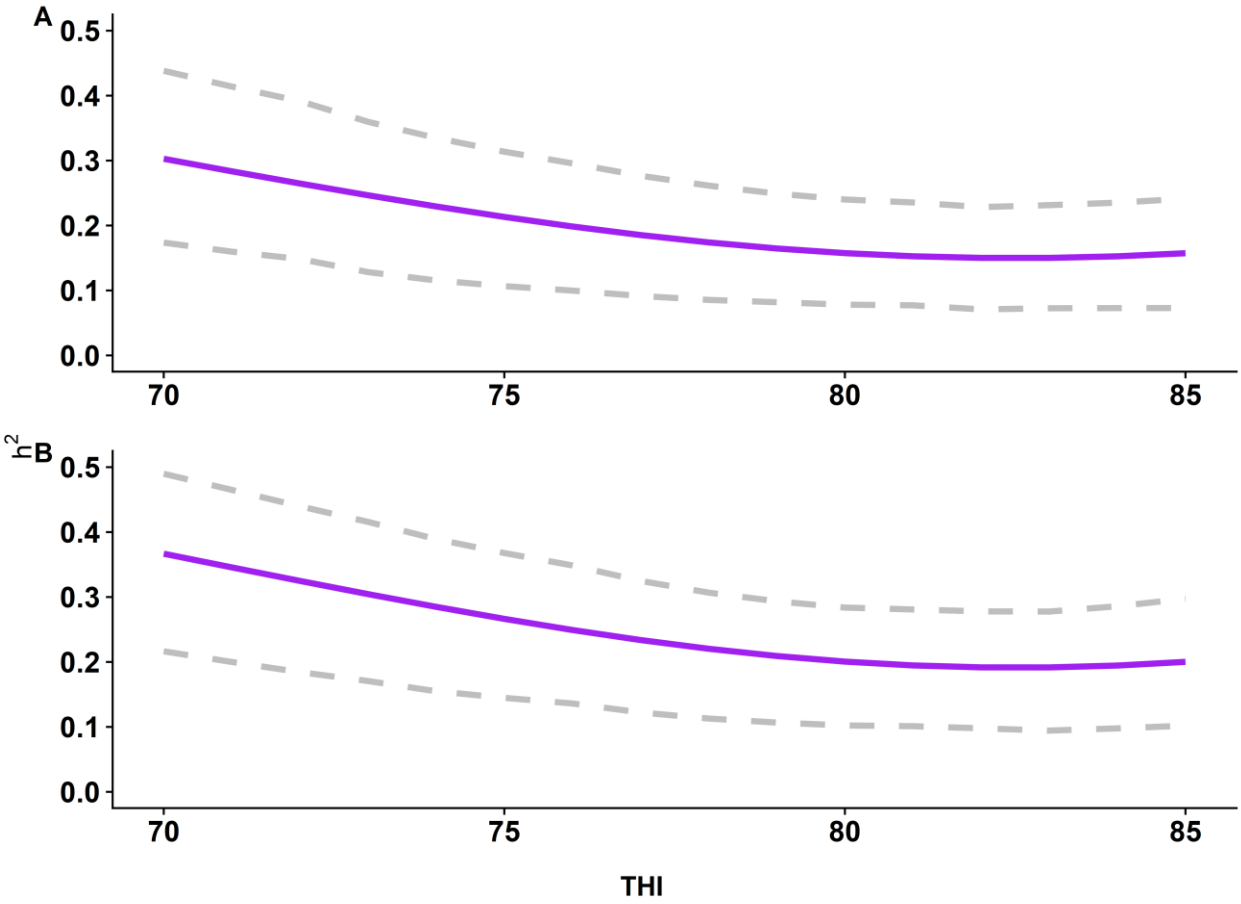

Figure 3.3 Heritability of dry matter intake as the temperature humidity index (THI) increases for group 2 (A) and 4 (B). Groups 2 and 4 represent the groups with the highest and lowest point estimate for the residual variance, respectively. The purple line indicates posterior mean point estimates for each value of water restriction and the gray, dashed lines are the 95% highest posterior density credible intervals for each value of THI.

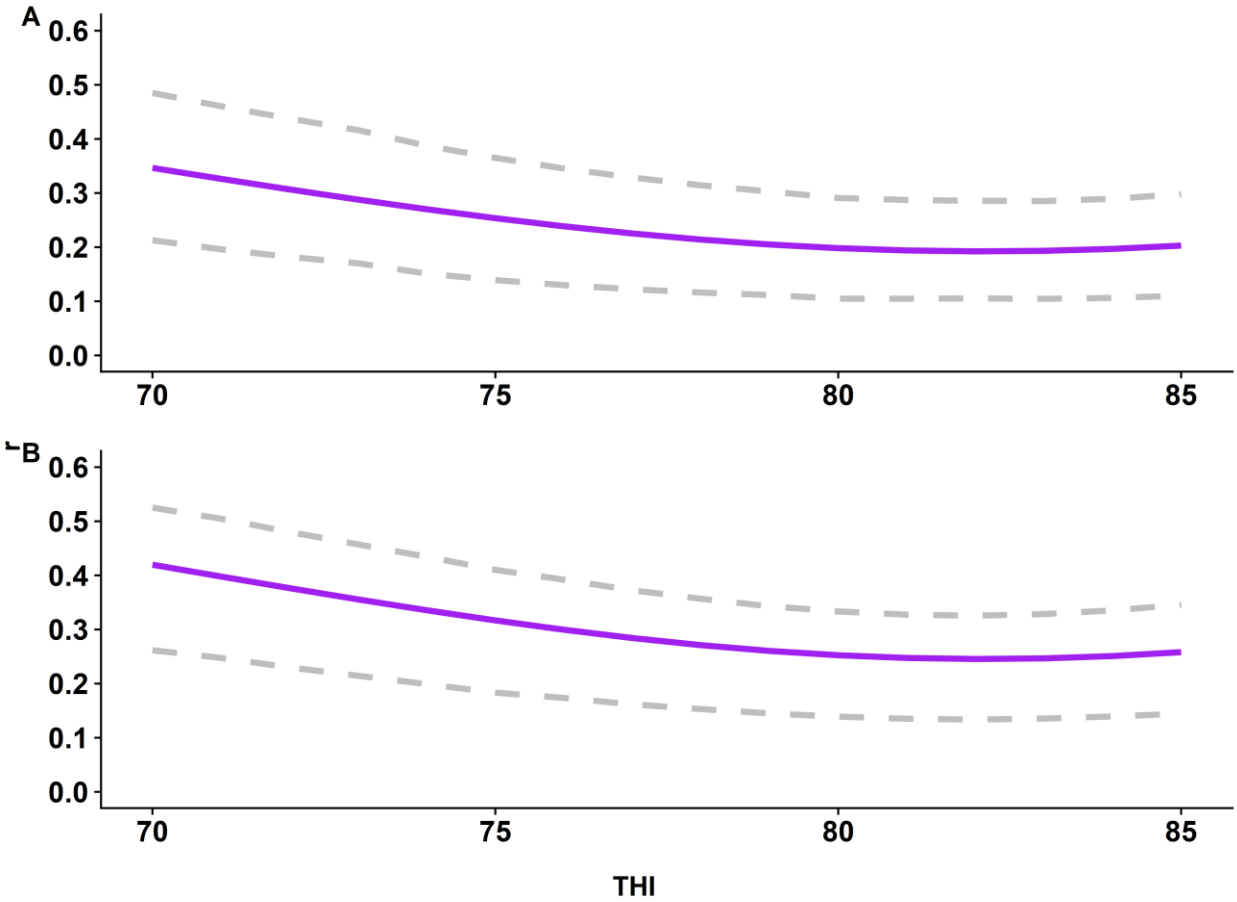

Figure 3.4 Repeatability of dry matter intake as the temperature humidity index (THI) increases for groups 2 (A) and 4 (B). Groups 2 and 4 represent the groups with the highest and lowest point estimate for the residual variance, respectively. The purple line indicates posterior mean point estimates for each value of water restriction and the gray, dashed lines are the 95% highest posterior density credible intervals for each value of THI.

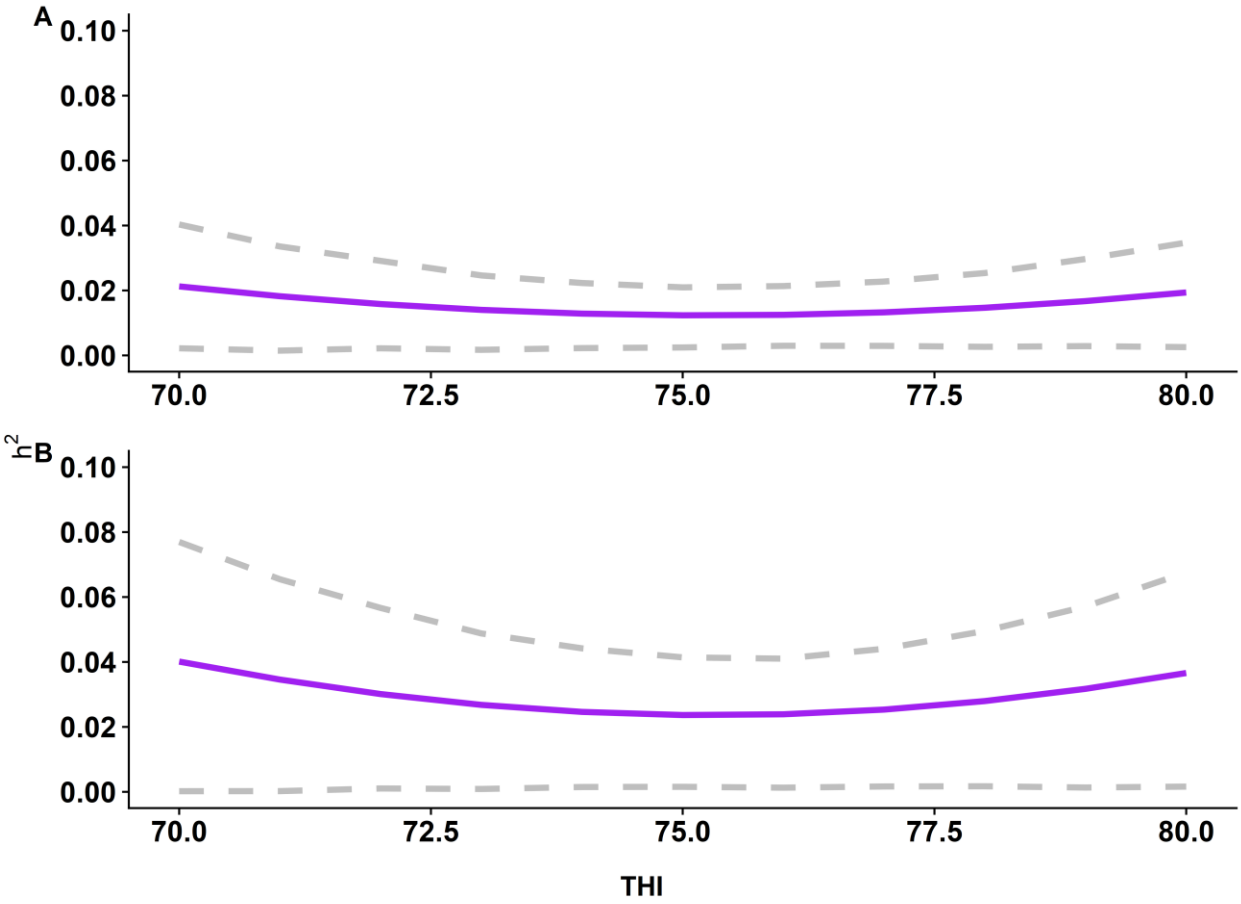

Figure 3.5 Heritability of respiration rate as the temperature humidity index (THI) increases for group 3 (A) and 1 (B). Groups 3 and 1 represent the groups with the highest and lowest point estimate for the residual variance, respectively. The purple line indicates posterior mean point estimates for each value of water restriction and the gray, dashed lines are the 95% highest posterior density credible intervals for each value of THI.

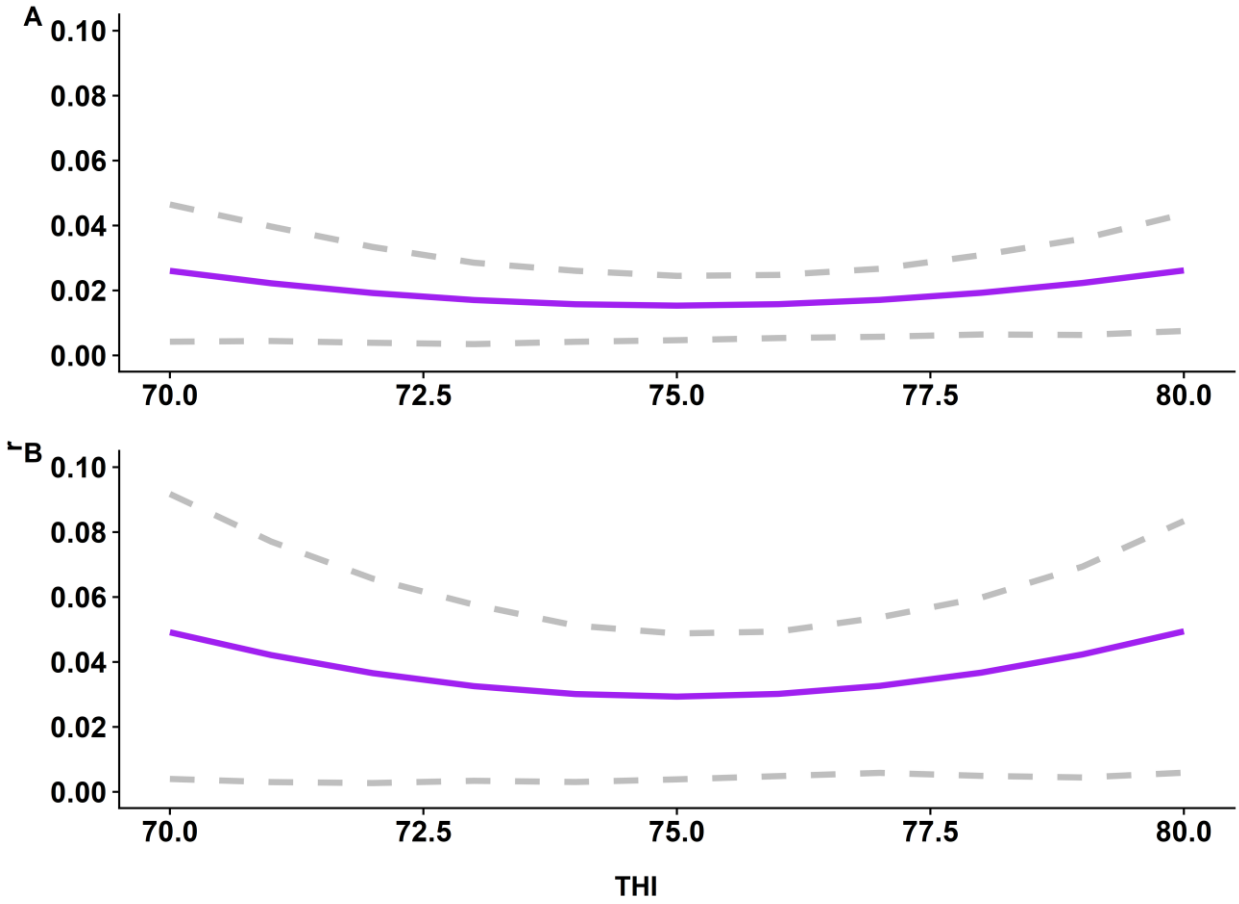

Figure 3.6 Repeatability of respiration rate as the temperature humidity index (THI) increases for groups 3 (A) and 1 (B). Groups 3 and 1 represent the groups with the highest and lowest point estimate for the residual variance, respectively. The purple line indicates posterior mean point estimates for each value of water restriction and the gray, dashed lines are the 95% highest posterior density credible intervals for each value of THI.

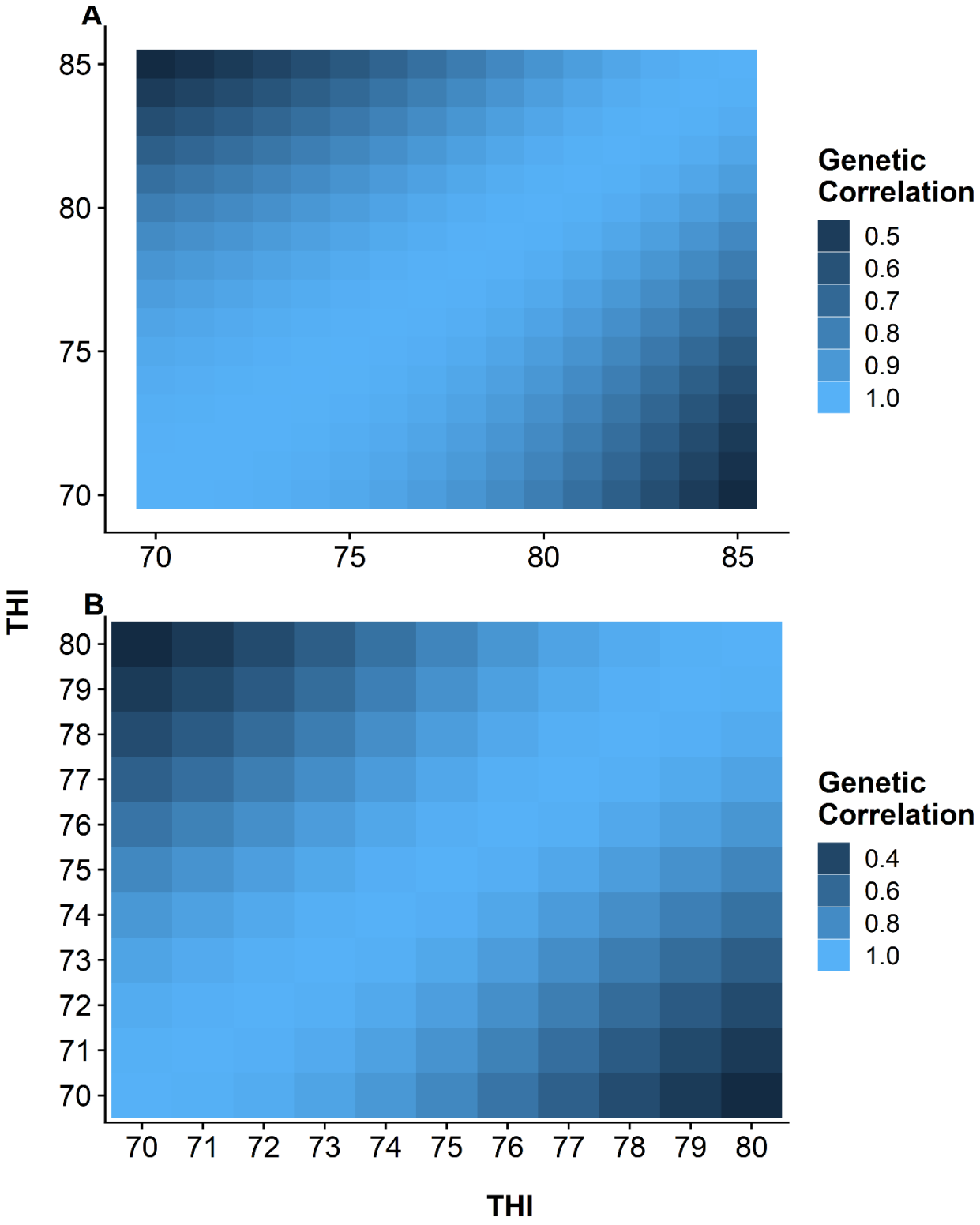

Figure 3.7 Genetic correlations between dry matter intake (A) or respiration rate (B) at different values of the temperature humidity index (THI).

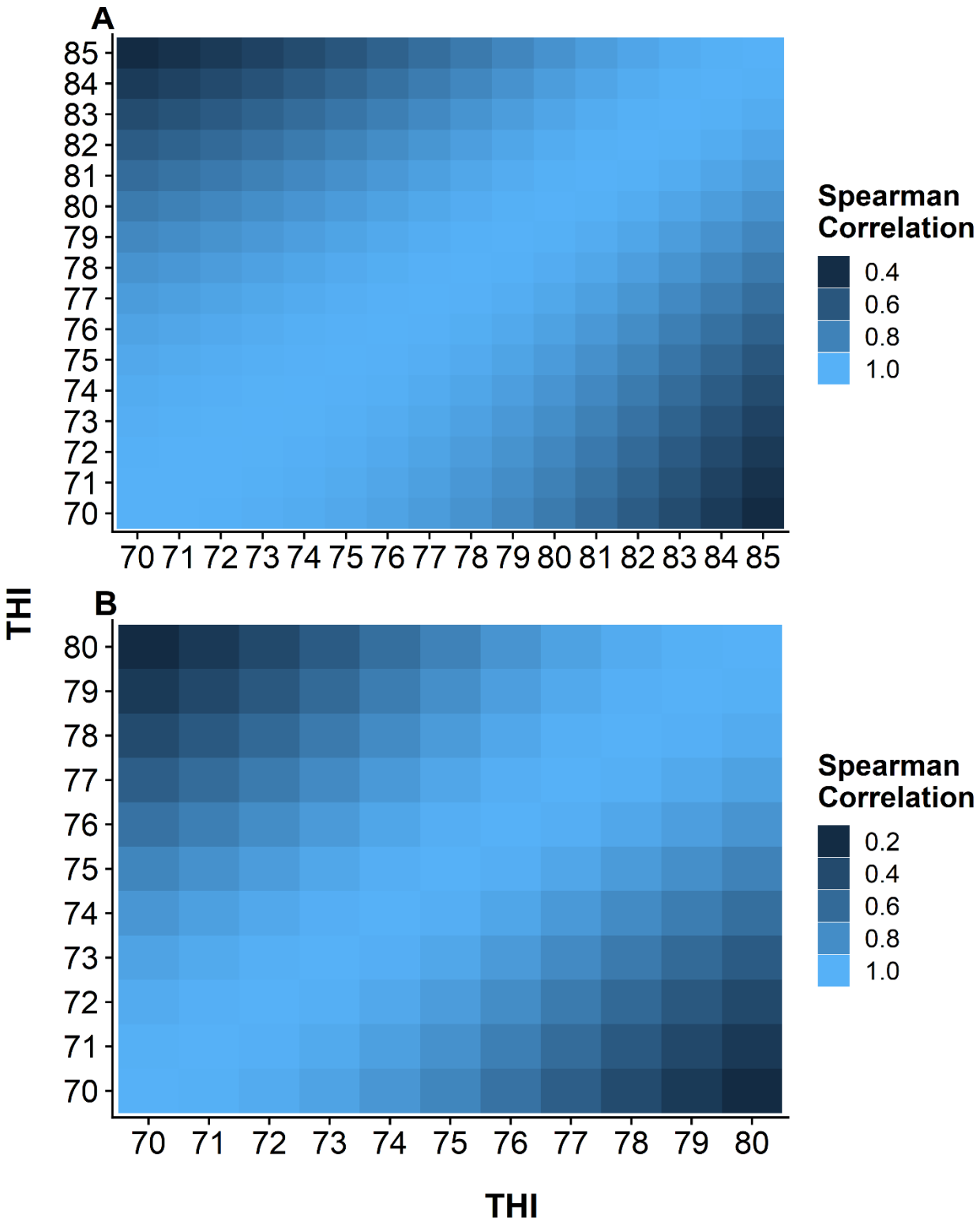

Figure 3.8 Spearman correlations between estimated breeding values of dry matter intake (A) or respiration rate (B) at different values of the temperature humidity index (THI).

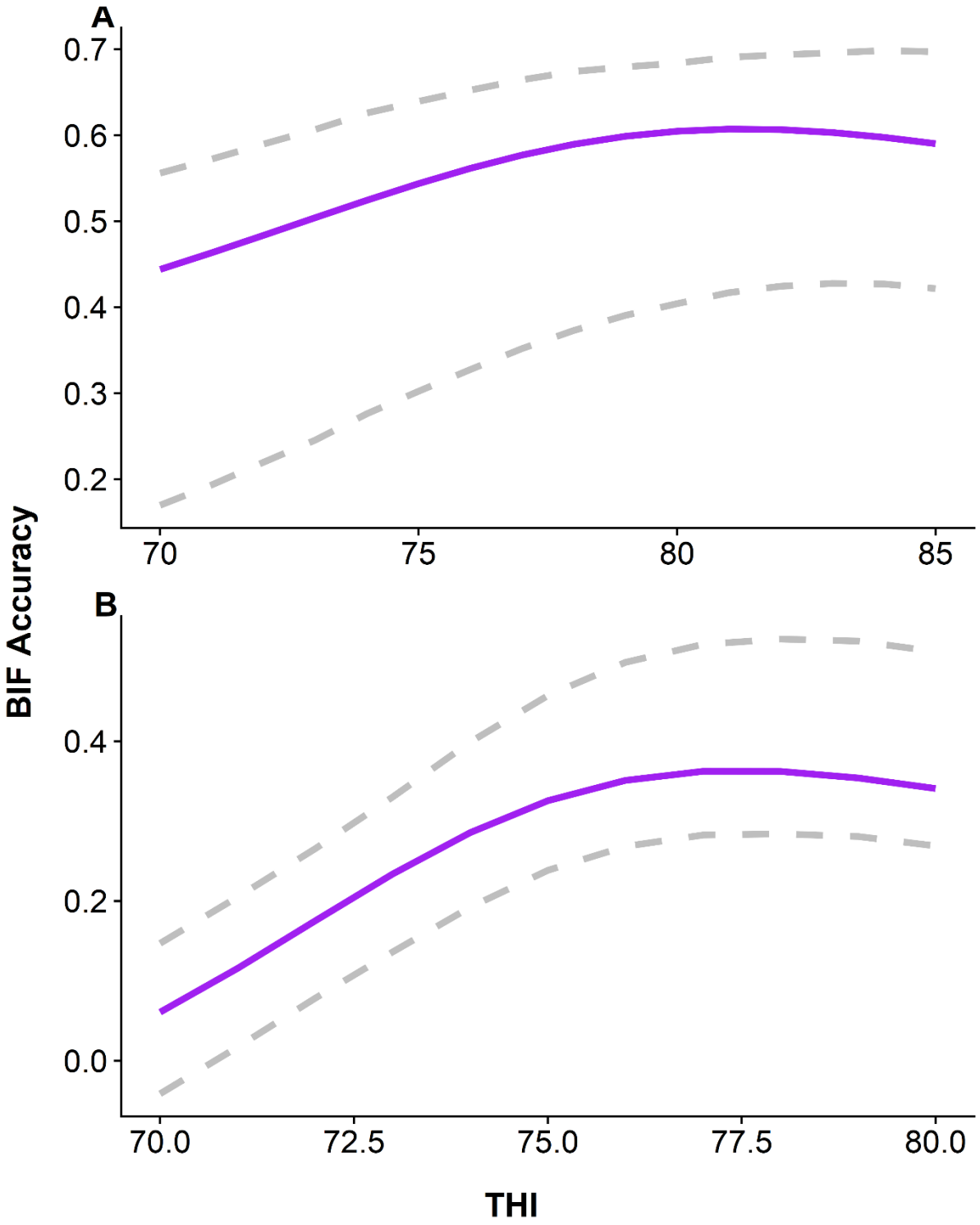

Figure 3.9 Mean Beef Improvement Federation accuracy represented by the purple line for dry matter intake (A) and respiration rate (B) as temperature humidity index (THI) increases. The gray, dashed lines represent the 95% highest density credible interval.

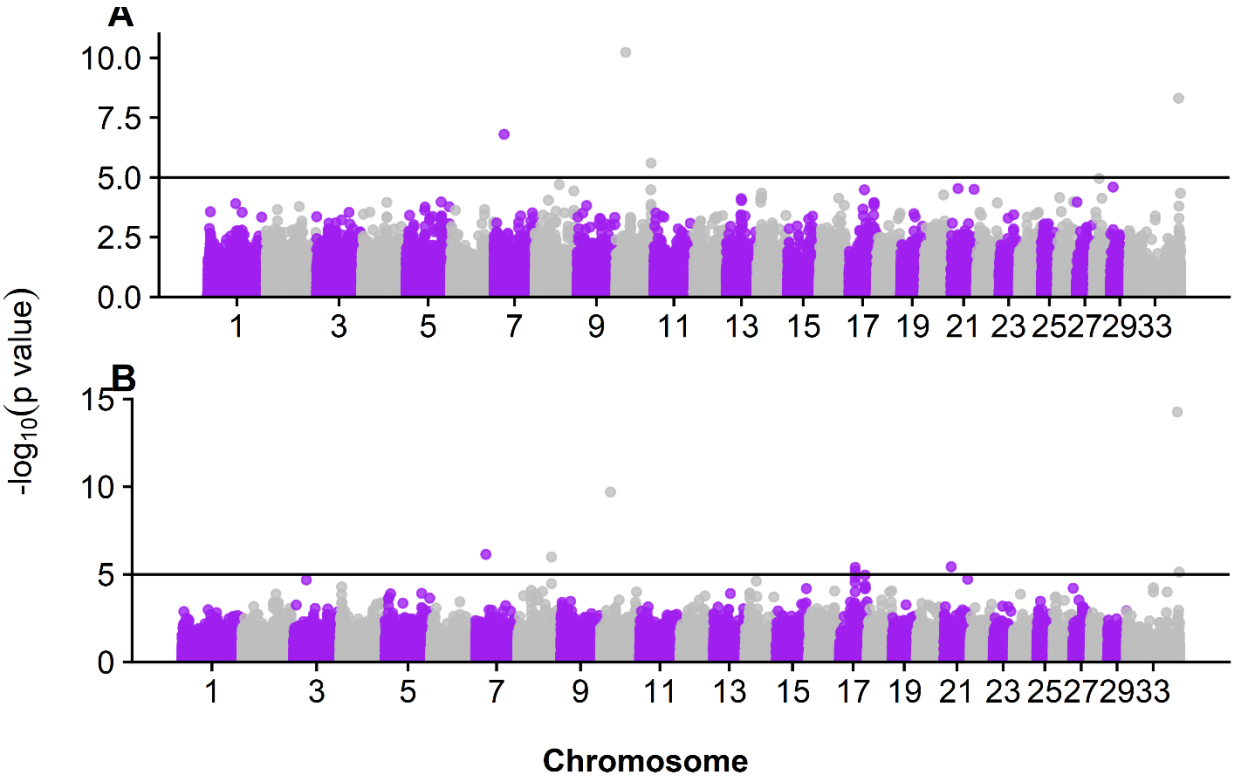

Figure 3.10 Manhattan plot showing the positive, base-ten logarithm transformed probability values for the dry matter intake intercept (A) and slope (B). Chromosome 33 corresponds to unmapped markers.

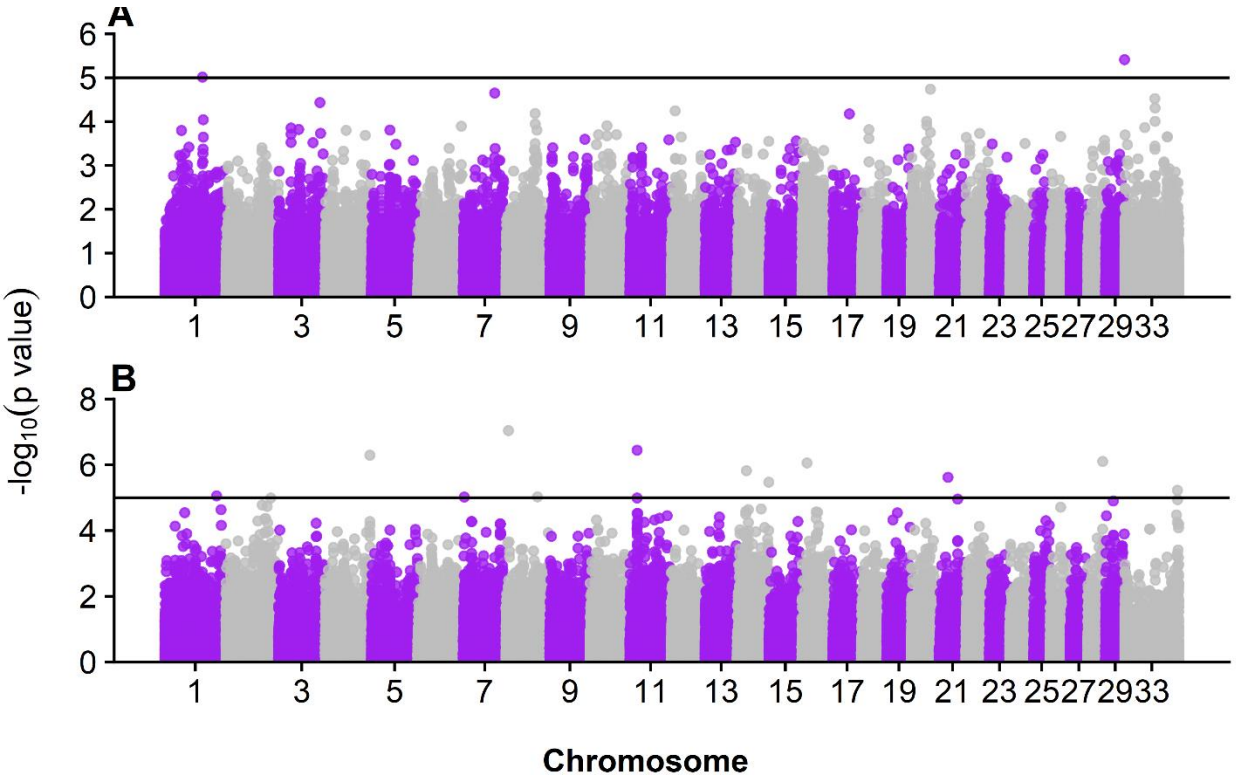

Figure 3.11 Manhattan plot showing the positive, base-ten logarithm transformed probability values for the respiration rate intercept (A) and slope (B). Chromosome 33 corresponds to unmapped markers.

References

Aartsma-Rus, A., J. C. T. Van Deutekom, I. F. Fokkema, G. B. Van Ommen, and J. T. D. Dunnen. 2006. Entries in the Leiden Duchenne muscular dystrophy mutation database: Aan overview of mutation types and paradoxical cases that confirm the reading-frame rule. Muscle Nerve 34:135-144.

Aguilar, I., I. Misztal, and S. Tsuruta. 2009. Genetic components of heat stress for dairy cattle with multiple lactations. J. Dairy Sci. 92:5702-5711.

Aguilar, I., I. Misztal, D. L. Johnson, A. Legarra, S. Tsuruta, T. J. Lawlor. 2010. Hot topic: a unified approach to utilize phenotypic, full pedigree, and genomic information for genetic evaluation of Holstein final score. J. Dairy Sci. 93:743-752.

Aguilar, I., S. Tsuruta, Y. Masuda, D. A. Lourenco, A. Legarra, and I. Misztal. 2018. BLUPF90 suite of programs for animal breeding with focus on genomics. In: Proc. 11th World Cong. Genet. Appl. Livest. Prod., Auckland, New Zealand:751.

Ahlberg, C. M., K. Allwardt, A. Broocks. K. Bruno, A. Taylor, L. Mcphillips, C. R. Krehbiel, M. Calvo-Lorezno, C. J. Richards, S. E. Place, U. Desilva, D. L. Vanoverbeke, R. G. Mateescu, L. A. Kuehn, R. Weaber, J. Bormann, and M. M. Rolf. 2019. Characterization of water intake and water efficiency in beef cattle. J. Anim. Sci. 97:4770-4782.

Al-Kanaan, A. J. J. 2016. Heat stress response for physiological traits in dairy and dual purpose cattle populations on phenotypic and genetic scales. PhD Diss. Univ. Kassel, Germany.Banos, G., and A. Sigurdsson. 1996. Application of contemporary methods for the use of international data in national genetic evaluations. J. Dairy Sci. 79:1117-1125.

Beef Improvement Federation Guidelines. 2021a. Accuracy. http://guidelines.beefimprovement.org/index.php/Accuracy (Accessed 10 August 2021.)

Beef Improvement Federation Guidelines. 2021b. Heterogeneous variance. http://guidelines.beefimprovement.org/index.php/Heterogeneous_variance (Accessed 10 August 2021.)

Berry, D. P., and J. J. Crowley. 2013. Cell biology symposium: genetics of feed efficiency in dairy and beef cattle. J. Anim. Sci. 91:1594-1613.

Bohmanova, J., I. Misztal, and J. B. Cole. 2007. Temperature-humidity indices as indicators of milk production losses due to heat stress. J. Dairy Sci. 90:1947-1956.

Bouraoui R., M. Lahmar, A. Majdoub, M. Djemali, and R. Belyea. 2002. The relationship of temperature-humidity index with milk production of dairy cows in a Mediterranean climate. Anim. Res. 51:479-491.

Bradford, H. L., B. O. Fragomeni, J. K. Bertrand, D. A. L. Lourenco, and I. Misztal. 2016. Genetic evaluations for growth heat tolerance in Angus cattle. J. Anim. Sci. 94:4143-4150.

Brew, M. N., R. O. Myer, M. J. Hersom, J. N. Carter, M. A. Elzo, G. R. Hansen, and D. G. Riley. 2011. Water intake and factors affecting water intake of growing beef cattle. Livest. Sci. 140:297-300.

Brinkman, J. E., F. Toro, and S. Sharma. Physiology, respiratory drive. https://www.ncbi.nlm.nih.gov/books/NBK482414/ (Accessed 10 August 2021.)

Brock, F. V., K. C. Crawford, R. L. Elliott, G. W. Cuperus, S. J. Stadler, H. L. Johnson, and M. D. Eilts. 1995. The Oklahoma Mesonet: A technical overview. J. Atmos. Oceanic Technol. 12:5-19.

Brotherstone, S., and M. Goddard. 2005. Artificial selection and maintenance of genetic variance in the global dairy cow population. Phil. Trans. R. Soc. B. 360:1479-1488.

Brügemann, K., E. Gernand, U. U. von Borstel, and S. König. 2011. Genetic analyses of protein yield in dairy cows applying random regression models with time-dependent and temperature x humidity-dependent covariates. J. Dairy Sci. 94:4129-4139.

Carabaño, M. J., K. Bachagha, M. Ramón, and C. Díaz. 2014. Modeling heat stress effect on Holstein cows under hot and dry conditions: Selection tools. J. Dairy Sci. 97:7889-7904.

Cota, D., K. Proulx, K. A. B. Smith, S. C. Kozma, G. Tomas, S. C. Woods, and R. J. Seeley. 2006. Hypothalamic mTOR signaling regulates food intake. Science 312:927-930.

Crow, J. F. 1986. Basic concepts in population, quantitative, and evolutionary genetics. W.H. Freeman, New York.

Cui, J., and l. I. Sinoway. 2015. Cardiovascular responses to heat stress in chronic heart failure. Curr. Heart Fail. Rep. 11:139-145.

Falconer, D. S., and T. F. Mackay. 1996. Introduction to Quantitative Genetics. 4th ed. Rev. Pearson, New York City, NY.

Federation of Animal Science Societies. 2010. Guide for the care and use of agricultural animal in research and teaching. Responses of Cattle to thermal heat loads. http:// aaalac.org/about/Ag_Guide_3rd_ed.pdf

Fonseca, P. A., A. Suárez-Vega, G. Marras, and A. Cánovas. 2020. GALLO: an R package for genomic annotation and integration of multiple data sources in livestock for positional candidate loci. GigaScience 9:giaa149.

Fruman, D. A., R. E. Meyers, and L. C. Cantley. Phosphoinositide kinases. Annu. Rev. Biochem. 67:481-507.

Fuquay, J. W. 1981. Heat stress as it affects animal production. J. Anim. Sci. 52:164-174.

Gault, C. R., L. M. Obeid, and Y. A. Hannun. 2011. An overview of sphingolipid metabolism: from synthesis to breakdown. Adv. Exp. Med. Biol. 688:1-23.

Grandin, T. 2016. Evaluation of the welfare of cattle housed in outdoor feedlot pens. Vet. Anim. Sci. 1:23-28.

Ghebrewold, R. 2018. Genome-wide association study for the relationship between temperature and feed intake in beef cattle. MS Thesis. Univ. Nebraska, Lincoln.

Hayano, J., F. Yasuma, A. Okada, S. Mukai, and T. Fujinami. 1996. A phenomenon improving pulmonary gas exchange and circulatory efficiency. Circulation 94:842-847.

Hecht, H. H., H. Kuida, R. L. Lange, J. L. Thorne, and A. M. Brown. 1962. Clinical features and hemodynamic observations in altitude-dependent right heart failure of cattle. Am. J. Med. 32:171-183.

Hill, D. L., and E. Wall. 2017. Weather influences feed intake and feed efficiency in a temperate climate. J. Dairy Sci. 100:2240-2257.

Hu, Z., C. A. Park, and J. M. Reecy. 2019. Building a livestock genetic and genomic information knowledgebase through integrative developments of animal QTLdb and CorrDB. Nucleic Acids Res. 47:D701-D710.

Intergovernmental Panel on Climate Change. 2007. The intergovernmental panel on climate change 4th assessment report. Jackson Inst., Univ. College, London.

Jennings, K. J., G. M. Krasfur, R. D. Brown, T. N. Holt, S. J. Coleman, S. E. Speidel, R. M. Enns, K. R. Stenmark, and M. G. Thomas. 2019. Characterizing the impact of altitude

and finishing system on mean pulmonary arterial pressure and carcass characteristics in Angus cattle. Transl. Anim. Sci. 3:1669-1672.

Jiang, J., L. Ma, D. Prakapenka, P. M. VanRaden, J. B. Cole, and Y. Da. 2019. A large-scale genome-wide association study in U.S. Holstein cattle. Front. Genet. 10:412

Kadzere, C. T., M. R. Murphy, N. Silanikove, and E. Maltz. 2002. Heat stress in lactating dairy cows: a review. Livest. Prod. Sci. 77:59-91.

Kanehisa, M., and S. Goto. 2000. KEGG: Kyoto Encyclopedia of Genes and Genomes. Nucleic Acids Res. 28:27-30.

Kang, M. S. 1997. Using genotype-by-environment interaction for crop cultivar development. Adv. Agron. 62:199-252.

Kertz, A. F., L. F. Reutzel, and G. M. Thomson. 1991. Dry matter intake from parturition to midlactation. J. Dairy Sci. 74:2290-2295.

Krasfur, G. M., J. M. Neary, F. Garry, T. Holt, D. H. Gould, G. L. Mason, M. G. Thomas, R. M. Enns, R. M. Tuder, M. P. Heaton, R. D. Brown, and K. R. Stenmark. 2019. Cardiopulmonary remodeling in fattened beef cattle: a naturally occurring large animal model of obesity-associated pulmonary hypertension with left heart disease. Pulm. Circ. 9:1-13.

Kristensen, N. B., A. Storm, B. M. L. Raun, B. A. Røjen, and D. L. Harmon. 2007. Metabolism of silage alcohols in lactating dairy cows. J. Dairy Sci. 90:1364-1377.Lillehammer, M., M. Árnyasi, S. Lien, H. G. Olsen, E. Sehested, J. Ødegård, and T. H. E. Meuwissen. 2007. A genome scan for quantitative trait locus by environment interactions for production traits. J. Dairy. Sci. 90:3482-3489.

Luo, H., L. F. Brito, X. Li, G. Su, W. Xu, X. Yan, H. Zhang, G. Guo, L. Liu, and Y. Wang. 2021. Genetic parameters for rectal temperature, respiration rate, and drooling score in Holtein cattle and their relationships with various fertility, production, body conformation, and health traits. J. Dairy Sci. 104:4390-4403.

Makondi, P. T., C. Chu, P. Wei, and Y. Chang. 2017. Prediction ofn ovel target genes and pathways involved in irinotecan-resistant colorectal cancter. PLoS One 12:e0180616.

Mauro, A. L, and A. Aliverti. 2016. Physiology of respiratory distrubances in muscular dystrophies. Breathe 12:318-327.

McKay, S. D., R. D. Schnabel,B. M. Murdoch, L. K. Matukumalli, W. Coppieters, D. Crews, E. D. Neto, C. A. Gill, C. Gao, H. Mannen, P. Stothard, Z. Wang, C. P. Van Tassell, J. L. Williams, J. F. Taylor, and S. S. Moore. 2007. Whole genome linkage disequilibrium maps in cattle. BMC Genom. Data 8:74.

McPherson, R. A., C. Fiebrich, K. C. Crawford, R. L. Elliott, J. R. Kilby, D. L. Grimsley, J. E. Martinez, J. B. Basara, B. G. Illston, D. A. Morris, K. A. Kloesel, S. J. Stadler, A. D. Melvin, A. J. Sutherland, and H. Shrivastava. 2007. Statewide monitoring of the mesoscale environment: A technical update on the Oklahoma Mesonet. J. Atmos. Oceanic Technol. 24:301-321.

Mead, A. N., and D. N. Stephens. 2003. Involvement of AMPA receptor GluR2 subunits in stimulus-reward learning: Evidence from Glutamate receptor gria2 knock-out mice. J. Neuroscience 23:9500-9507.

Minokoshi, Y., T. Alquier, N. Furukawa, Y. B. kim,A. Lee, B. Xue, J. Mu, F. Foufelle, P . Ferré, M. J. Birnbaum, B. J. Stuck, and B. B. Kahn. 2004. AMP-kinase regulates food intake by responding to hormonal and nutrient signals in the hypothalamus. Nature 428:569-574.

Misztal, I., S. Tsuruta, D. A. Lourenco, Y. Masuda, I. Aguilar, A. Legarra, and Z. Vitezica. 2018. Manual for BLUPF90 family programs. Univ. Georgia. Available from http://nce.ads.uga.edu/wiki/doku.php?id=documentation

Nardone, A., B. Ronchi, N. Lacetera, M. S. Ranieri, and U. Bernabucci. 2010. Effects of climate changes on animal production and sustainability of livestock systems. Livest. Sci. 130:57-69.

National Oceanic and Atmospheric Administration. 1976. Livestock hot weather stress. US Dept. Commerce, Natl. Weather Serv. Central Reg., Reg. Operations Manual Lett. C-31-76. US Govt. Printing Office, Washington, DC.

Neary, J. M., C. W. Booker, B. K. Wildman, and P. S. Morley. 2016. Right-sided congestive heart failure in North American feedlot cattle. J. Vet. Intern. Med. 30:326-334.

Nyholt, D. R. 2004. A simple correction for multiple testing for single-nucleotide polymorphisms in linkage disequilibrium with each other. Am. J. Hum. Genet. 74:765-769.

Ou, J. Z, J. J. Cottrell, N. Ha, N. Pillai, C. K. Yao, K. J. Berean, S. A. Ward, D. Grando, J. G. Muir, C. J. Harrison, U. Wijesiriwardana, F. R.Dunshea, P. R. Gibson, and K. Kalantar-zadeh. 2016. Potential of in vivo real-time gastric gas profiling: a pilot evaluation of heat-stress and modulating dietary cinnamon effect in an animal model. Sci. Rep. 6:33387.

Perry, N. A., M. A. Ackermann, M. Shriver, L. R. Hu, and A. Kontrogianni-Konstantopoulos. 2014. Obscurins: Unassuming giants enter the spotlight. IUBMB Life 65:479-486.

Peters. J. 2002. The anaphase-promoting complex: Proteolysis in mitosis and beyond. Mol. Cell 9:931-943.

Plummer, M., N. Best, K. Cowles, and K. Vines. 2006. CODA: Convergence diagnosis and output analysis for MCMC. R News 6:7-11. https://journal.r-project.org/archive/

Polizel, G. H. G., L. Grigoletto, M. Carvalho, and P. Rossi Jr. 2018. Genetic correlations and heritability estimates for dry matter intake, weight gain and feed efficiency of Nellore cattle in feedlot. Livest. Sci. 214:209-210.

Polsky, L., and M. A. G. von Keyserlingk. 2017. Invited review: Effects of heat stress on dairy cattle welfare. J. Dairy Sci. 100:8656-8657.

Postema, P. G., I. Christiaans, N. Hofman, M. Alders, T. T. Koopmann, C. R. Bezzina, P. Log, K. Zeppenfeld, P. G. A. Volders, and A. A. M. Wilde. 2011. Founder mutations in the Netherlands: familiar idiopathic ventricular fibrillation and DPP6. Neth. Heart J. 19:290-296.

Pulliam-Leath, A. C., S. L. Ciccone, G. Nalepa, X. Li, Y. Si, L. Miravalle, D. Smith, J. Yuan, J. Li, P . Anur, A. Orazi, G. H. Vance, F. Yang, H. Hanenberg, G. C. Bagby, D. W. Clapp. 2009. Genetic disruption of both Fancc and Fancg in mice recaptiulates the hematopoietic manifestations of Fanconi anemia. Blood 116:2915-2920.

R Core Team. 2013. R: a language and environment for statistical computing. Vienna, Austria: R Foundation for Statistical Computing. Available from http://www.r-project.org/

Ramazzotti, G., I. Faneza, R. Fiume, A. M. Billi, L. Manzoli, S. Mongiorgi, S. Ratti, J. A. McCubrey, P. Suh, L. Cocco, and M. Y. Follo. 2017. PLC-β and cell differentiation: an insight into myogenesis and osteogenesis. Adv. Biol. Regul. 63: 1-5.

Ravagnolo, O., and I. Misztal. 2000. Genetic component of heat stress in dairy cattle, parameter estimation. J. Dairy Sci. 83:2126-2130.

Ravnjskjaer, K., A. Madiraju, and M. Montminy. 2016. Role of the cAMP pathway in glucose and lipid metabolism. Handb. Exp. Pharmacol. 233:29-49.

Rosen, B. D., D. M. Bickhart, R. D. Schnabel, S. Koren, C. G. Elsik, E. Tseng, T. N. Rowan, W. Y. Low, A. Zimin, C. Couldrey, R. Hall, W. Li, A. Rhie, J. Ghurye, S. D. McKay, F. Thibaud-Nissen, J. Hoffman, B. M. Murdoch, W. M. Snelling, T. G. McDaneld, J. A. Hammond, J. C. Schwartz, W. Nandolo, D. E. Hagen, C. Dreischer, S. J. Schultheiss, S. G. Schroder, A. M. Phillippy, J. B. Cole, C. P. Van Tasell, G.. Liu, T. P. L. Smith, J. F. Medrano. 2020. De novo assembly of the cattle reference genome with single-molecule sequencing. GigaScience. 9:giaa021.

Saatchi, M., J. E. Beever, J. E. Decker, D. B. Faulkner, G. C. Freetly, S. L. Hansen, H. Yampara-Iquise, K. A. Johnson, S. D. Kachman, M. S. Kerley, J. Kim, D. D. Loy, E. Marques, H. L. Neilbergs, E. J. Pollak, R. D. Schnabel, C. M. Seabury, D. W. Shike, W. M. Snelling, M. L. Spangler, R. L. Weaber, D. J. Garrick, and J. F. Taylor. 2014. QTLs associated with dry matter intake, metabolic mid-test weight, growth, and feed efficiency have little overlap across 4 beef cattle studies. BMC Genom. 15:1004.

Santana, M. H. A, G. A. Oliveira Jr., R. C. Gomes, S. L. Silva, P. R. Leme, T. R. Stella, E. C. Mattos, P. Rossi Jr., F. S. Baldi, J. P. Eler, and J. B. S. Ferraz. 2014. Genetic parameter estimates for feed efficiency and dry matter intake and their association with growth and carcass traits in Nellore cattle. Livest. Sci. 167:80-85.

Santana, M. L. Jr., A. B. Bignardi, J. P. Eler, and J. B. S. Ferraz. 2015. Genetic variation of the weaning weight of beef cattle as a function of accumulated heat stress. J. Anim. Breed. Genet. 133:92-104.

Schaeffer, L. R. 2004. Application of random regression models in animal breeding. Livest. Prod. Sci. 86:35-45.

Schou, M. F., A. A. Hoffmann, and T. N. Kristensen. 2019. Genetic correlations and their dependence on environmental similarity-Insights from livestock data. Evolution. 73:1672–1678.

Shendre, A., M. R. Irvin, H. Wiender, D. Zhi, N. A. Limdi, E. T. Overton, and S. Shrestha. 2017. Local ancestry and clinical cardiovascular events among African Americans from the atherosclerosis risk in communities study. J. Am. Heart Assoc. 6:e004739.

Sgrò, C. M., and A. A. Hoffman. 2004. Genetic correlations, tradeoffs, and environmental variation. Heredity. 93: 241-248.

Slack, C. 2017. Ras signaling in aging and metabolic regulation. Nutr. Healthy Aging 4:195-205.

Snelling, W. M., M. F. Allan, J. W. Keele, L. A. Kuehn, R. M. Thallman, G. L. Bennett, C. L. Ferrell, T. G. Jenkins, H. C. Freetly, M. K. Nielsen, and K. M. Rolfe. 2011. Partial-genome evaluation of postweaning feed intake and efficiency of crossbred beef cattle. J. Anim. Sci. 89:1731-1741.

Sungkhapreecha, P., I. Misztal, J. Hidalgo, Y. Steyn, S. Buaban, M. Duangjinda, and W. Boonkum. 2021. Changes in genetic parameters for milk yield and heat tolerance in the Thai Holstein crossbred dairy population under different heat stress levels and over time. J. Diary Sci. 104:12703-12712.

Szklarczyk, D., A. Franceschini, S. Wyder, K. Forslund, D. Heller, J. Huerta-Cepas, M. Simonovic, A. Roth, A. Santos, K. P. Tsafou, M. Kuhn, P. Bork, L. J. Jensen, and C. von

Mering. 2015. STRING v10: protein-protein interaction networks, integrated over the tree of life. Nucleic Acids Res. 43:D447-D452.

Vallée, A., J. Daures, J. A. M. van Arendonk, and H. Bovenhuis. 2016. Genome-wide association study for behavior, type traits, and muscular development in Charolais beef cattle. J. Anim. Sci. 94: 2307-2316.

VanRaden, P. M. 2008. Efficient methods to compute genomic predictions. J. Diary Sci. 91:4414-4423.

Via, S., and R. Lande. 1985. Genotype-environment interaction and the evolution of phenotypic plasticity. Evolution. 39:505–522.

Vroman, N. B., E. R. Buskirk, and J. L. Hodgson. 1983. Cardiac output and skin blood flow in lean and obese individuals during exercise in the heat. J. Appl. Physiol. Respir. Environ. Exerc. Physiol. 55:69-74.

Wang, H., L. Tong, J. Wei, W. Pan, L. Li, Y. Ge, L. Zhou, Q. Yuan, C. Zhou, and M. Yang. 2014. The ALDH7A1 genetic polymorphisms contribute to development of esophageal squamous cell carcinoma. Tumour Biol. 35:12665-12670.

West, J. W. 2003. Effects of heat-stress on production in dairy cattle. J. Dairy Sci. 86:2131-2144.

West-Eberhard, M. J. 2008. Phenotypic plasticity. In: Encyclopedia of ecology. 1st ed. Elsevier, Amsterdam, Netherlands. p. 2701-2707.

Winchester, C. F., and M. J. Morris. 1956. Water intake rates of cattle. J. Anim. Sci. 15:722-740.

Xia, J., M. J. Benner, and R. E. W. Hancock. 2014. NetworkAnalyst – integrative approaches for protein-protein interaction network analysis and visual exploration. Nucleic Acids Res. 42:W167-W174.Yao, C., G. de los Campos, M. J. VandeHaar, D. M. Spurlock, L. E. Armentano, M. Coffey, Y. de Haas, R. F. Veerkamp, C. R. Staples, E. E. Connor, Z. Wang, M. D. Hanigan, R. J. Tempelman, K. A. Weigel. 2017. Use of genotype × environment

interaction model to accommodate genetic heterogeneity for residual feed intake, dry matter intake, net energy in milk, and metabolic body weight in dairy cattle. J. Dairy Sci. 100:2007-2016.

Zeng, X. 2016. Angus cattle at high altitude: pulmonary arterial pressure, estimated breeding value and genome-wide association study. PhD Diss. Colo. State Univ. Fort Collins, Colorado.

Zewail, A., M. W. Xie, Y. Xing, L. Lin, P. F. Zhang, W. Zou, J. P. Saxe, and J. Huang. 2003. Novel functions of the phosphatidylinositol metabolic pathway discovered by a chemical genomics screen with wortmannin. Proc. Natl. Acad. Sci. 100:3345-3350.

Zhang, W., and H. T. Liu. 2002. MAPK signal pathways in the regulation of cell proliferation in mammalian cells. Cell Res. 12:9-18.

Appendix A - Chapter 2 Supplementary Figures

Table A.1 Trial date ranges and the number of animals are detailed for each group.

Group	Dates
1	05/25/14 - 10/11/14
2	11/07/14 - 03/26/15
3	05/05/15 - 09/21/15
4	06/03/16 - 10/20/16
5	01/10/17 - 05/29/17
6	09/07/17 - 01/24/18
7	02/27/18 – 07/16/18

Table A.2 Posterior means and 95% HPDCIs of genetic correlations between select levels of water restriction (WR; above the diagonal) and Spearman rank correlations between estimated breeding values for select levels of WR (below the diagonal) for dry matter intake.

	0.00	0.25	0.50
0.00		0.96 (0.94, 0.99)	0.78 (0.65, 0.91)
0.25	0.96 (0.94, 0.98)		0.92 (0.87, 0.97)
0.50	0.80 (0.69, 0.90)	0.92 (0.88, 0.97)	

Table A.3 Posterior means and 95% HPDCIs of genetic correlations between select levels of water restriction (WR; above the diagonal) and Spearman rank correlations between estimated breeding values for select levels of WR (below the diagonal) for respiration rate. Correlations past 0.25 WR were not included due to zero genetic variance and instability of estimates.

	0.00	0.25	0.50
0.00		0.98 (0.95, 0.99)	N/A
0.25	0.97 (0.94, 0.99)		N/A
0.50	N/A	N/A	

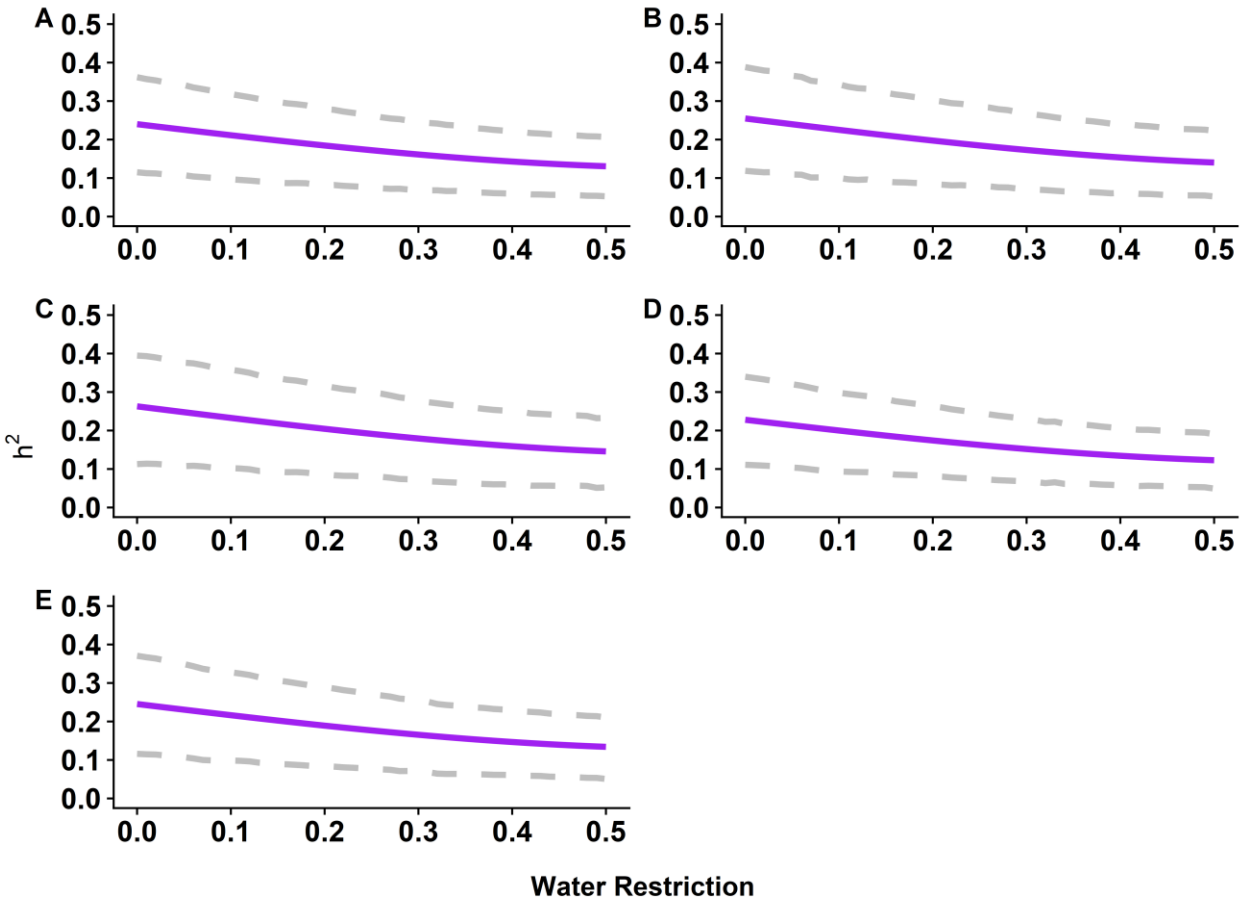

Figure A.1 Heritability of dry matter intake as water restriction increases for groups 2-5 (A-D) and 7 (E). The purple line indicates posterior mean point estimates for each value of water restriction and the gray, dashed lines are the 95% highest posterior density credible intervals for each value of water restriction.

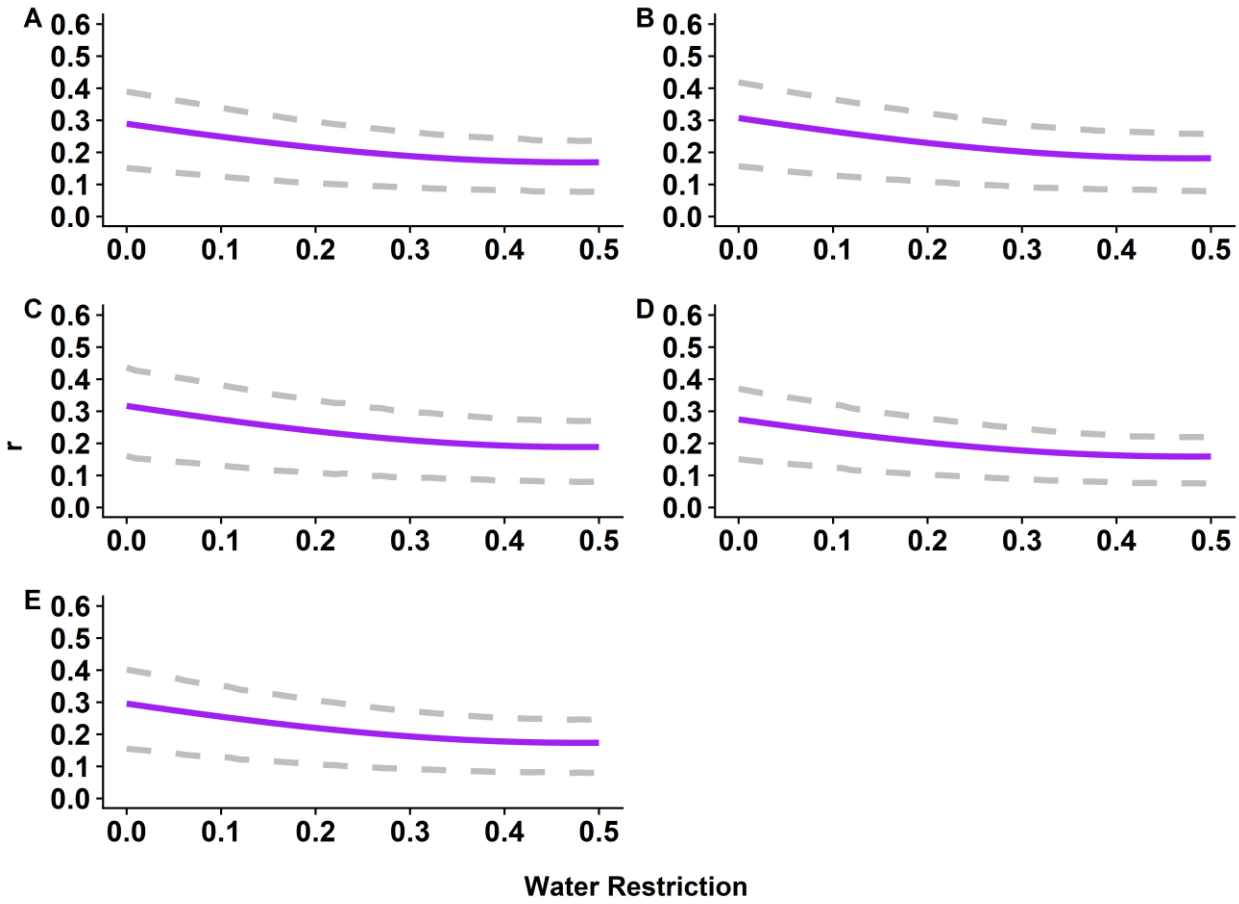

Figure A.2 Repeatability of dry matter intake as water restriction increases for groups 2-5 (A-D) and 7 (E). The purple line indicates posterior mean point estimates for each value of water restriction and the gray, dashed lines are the 95% highest posterior density credible intervals for each value of water restriction.

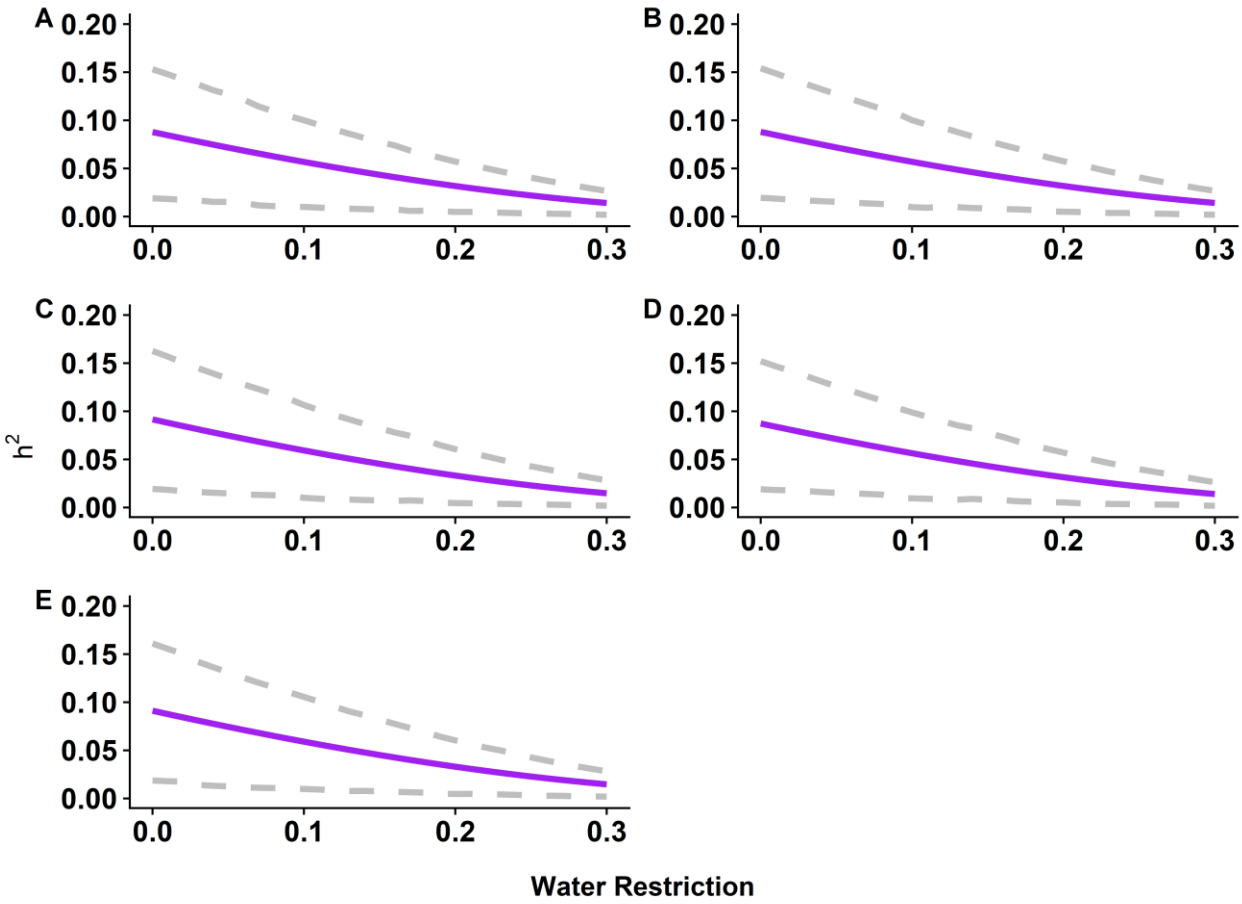

Figure A.3 Heritability of respiration rate as water restriction increases for groups 2 (A) and 4-7 (B-E). The purple line indicates posterior mean point estimates for each value of water restriction and the gray, dashed lines are the 95% highest posterior density credible intervals for each value of water restriction.

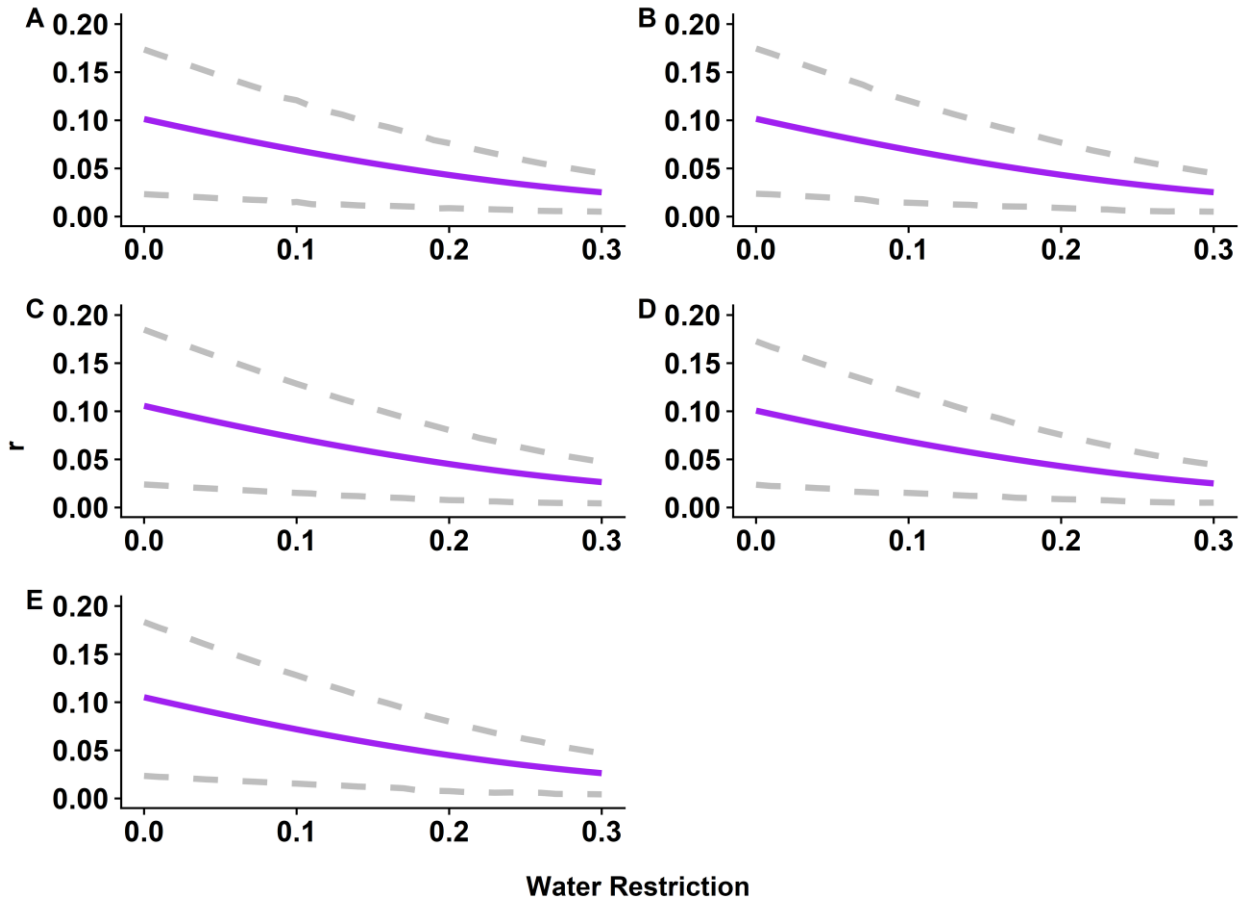

Figure A.4 Repeatability of respiration rate as water restriction increases for groups 2 (A) and 4-7 (B-E). The purple line indicates posterior mean point estimates for each value of water restriction and the gray, dashed lines are the 95% highest posterior density credible intervals for each value of water restriction.

Appendix B - Chapter 3 Supplementary Figures

Table B.1 Trial date ranges and the number of animals are detailed for each group.

Group	Dates
1	05/25/14 - 08/02/14
2	11/07/14 - 01/15/15
3	05/05/15 - 07/13/15
4	06/03/16 - 08/11/16
5	01/10/17 - 03/20/17
6	09/07/17 - 11/15/17
7	02/27/18 – 05/07/18

Table B.2 Posterior means and 95% HPDCIs of genetic correlations between select levels of temperature humidity index (THI; above the diagonal) and Spearman rank correlations between estimated breeding values for select levels of THI (below the diagonal) for dry matter intake.

	70	75	85
70		0.92 (0.89, 0.95)	0.42 (0.26, 0.57)
75	0.96 (0.95, 0.98)		0.73 (0.65, 0.82)
85	0.39 (0.26, 0.52)	0.60 (0.50, 0.69)	

Table B.3 Posterior means and 95% HPDCIs of genetic correlations between select levels of temperature humidity index (THI; above the diagonal) and Spearman rank correlations between estimated breeding values for select levels of THI (below the diagonal) for respiration rate. Correlations past 80 THI were not included due to a lack of records.

	70	75	80
70		0.84 (0.56, 1.00)	0.23 (-0.30, 0.78)
75	0.81 (0.52, 0.98)		0.76 (0.54, 1.00)
80	0.20 (-0.32, 0.73)	0.78 (0.49, 0.98)	

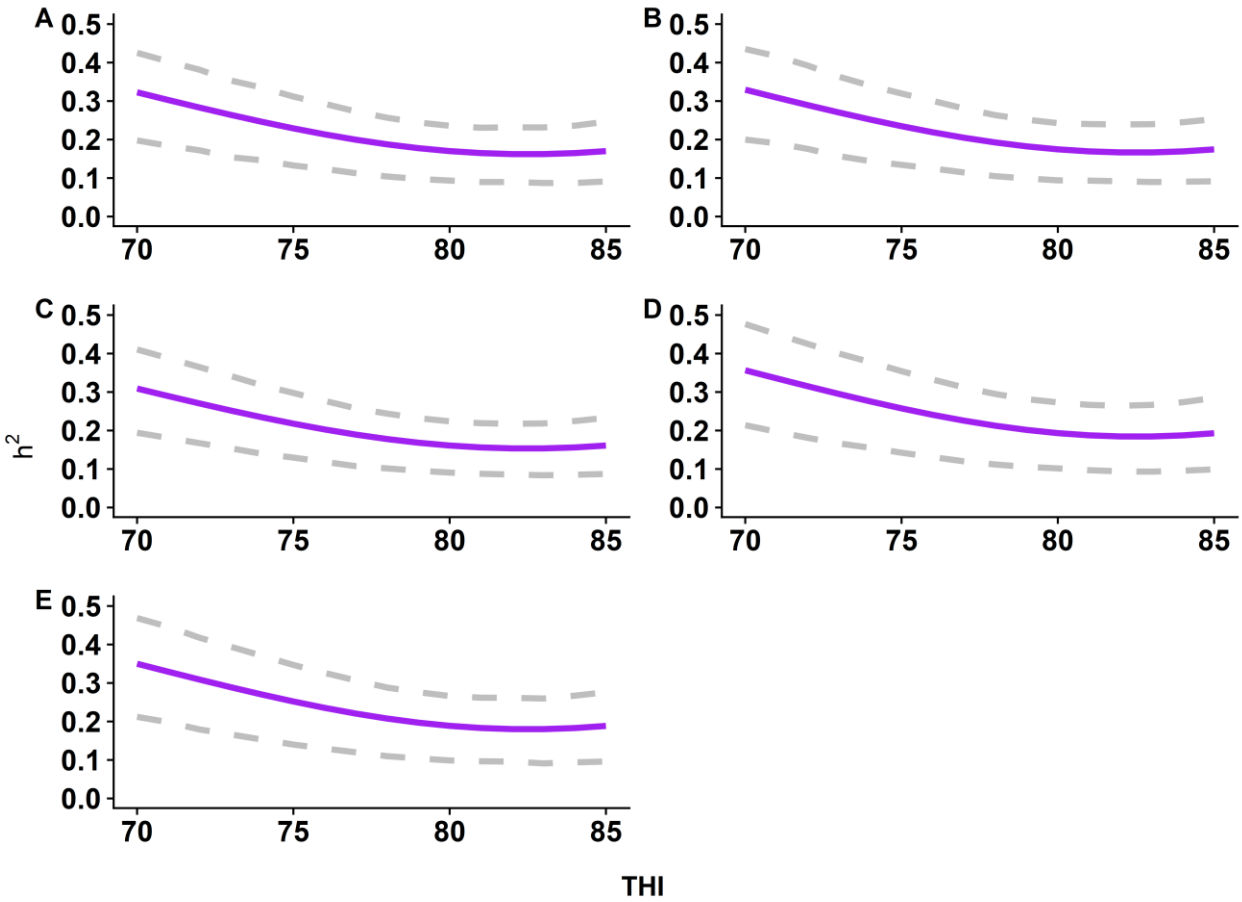

Figure B.1 Heritability of dry matter intake as the temperature humidity index (THI) increases for groups 1 (A), 3 (B), and 5-7 (C-E). The purple line indicates posterior mean point estimates for each value of water restriction and the gray, dashed lines are the 95% highest posterior density credible intervals for each value of THI.

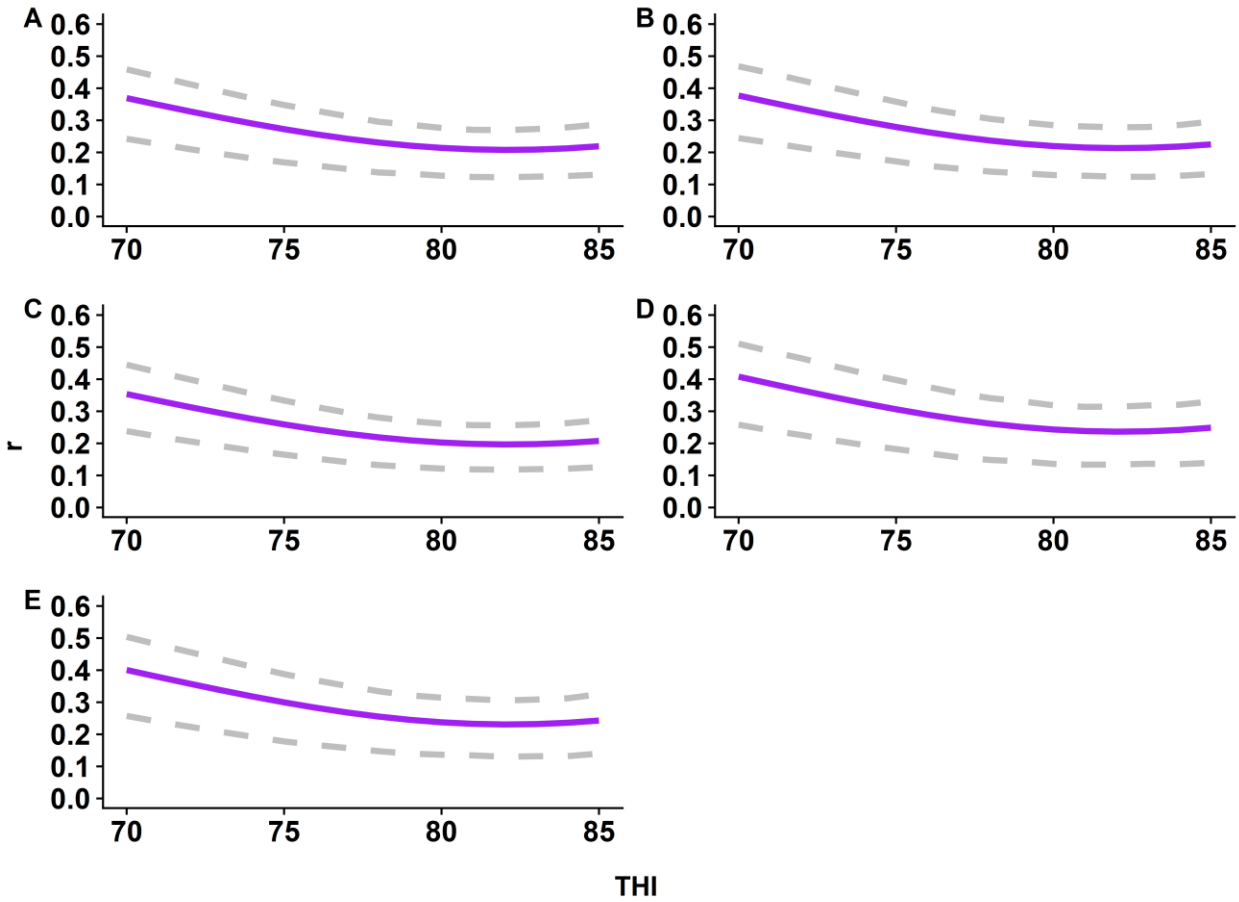

Figure B.2 Repeatability of dry matter intake as the temperature humidity index (THI) increases for groups1 (A), 3 (B), and 5-7 (C-E). The purple line indicates posterior mean point estimates for each value of water restriction and the gray, dashed lines are the 95% highest posterior density credible intervals for each value of THI.

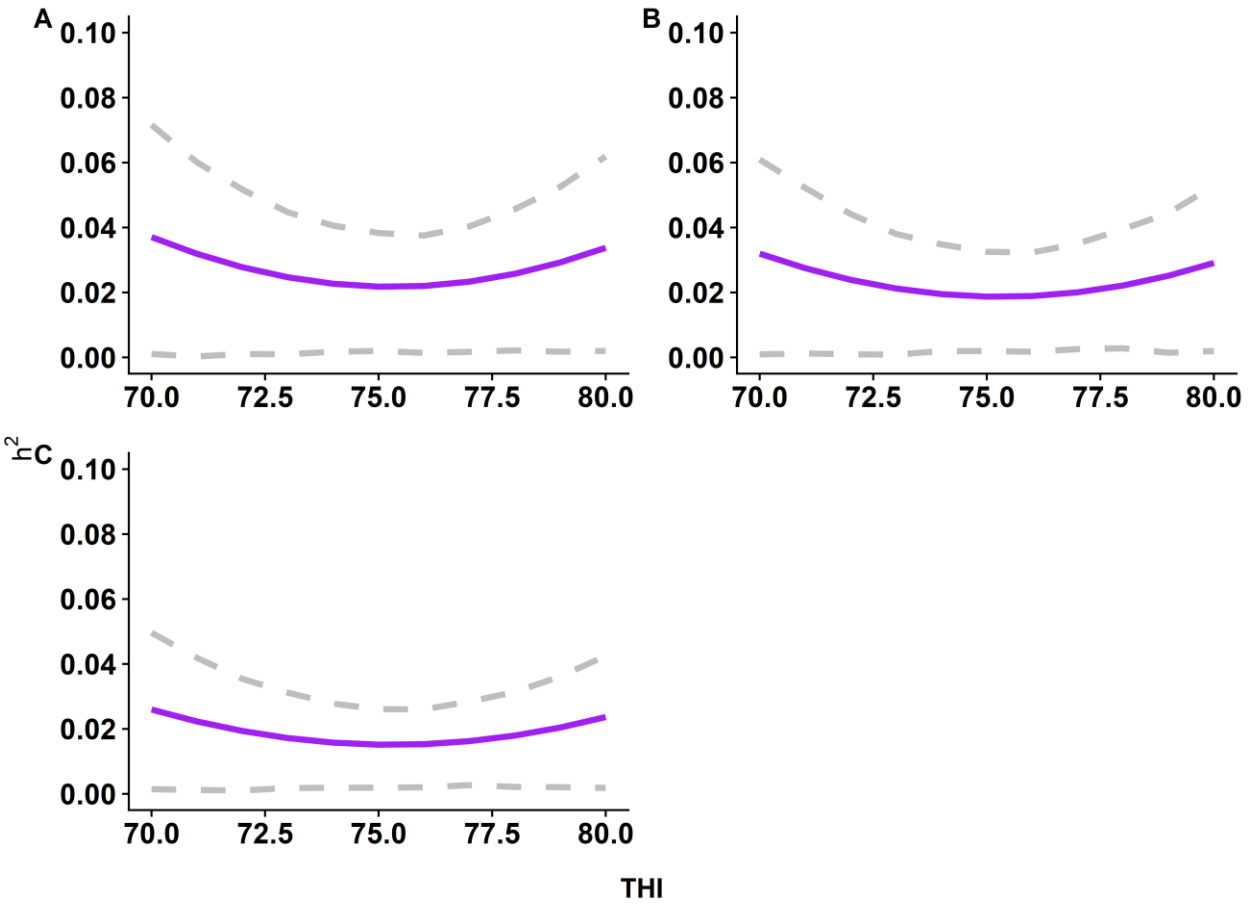

Figure B.3 Heritability of respiration rate as the temperature humidity index (THI) increases for groups 4 (A), 5 (B), and 7 (C). The purple line indicates posterior mean point estimates for each value of water restriction and the gray, dashed lines are the 95% highest posterior density credible intervals for each value of THI.

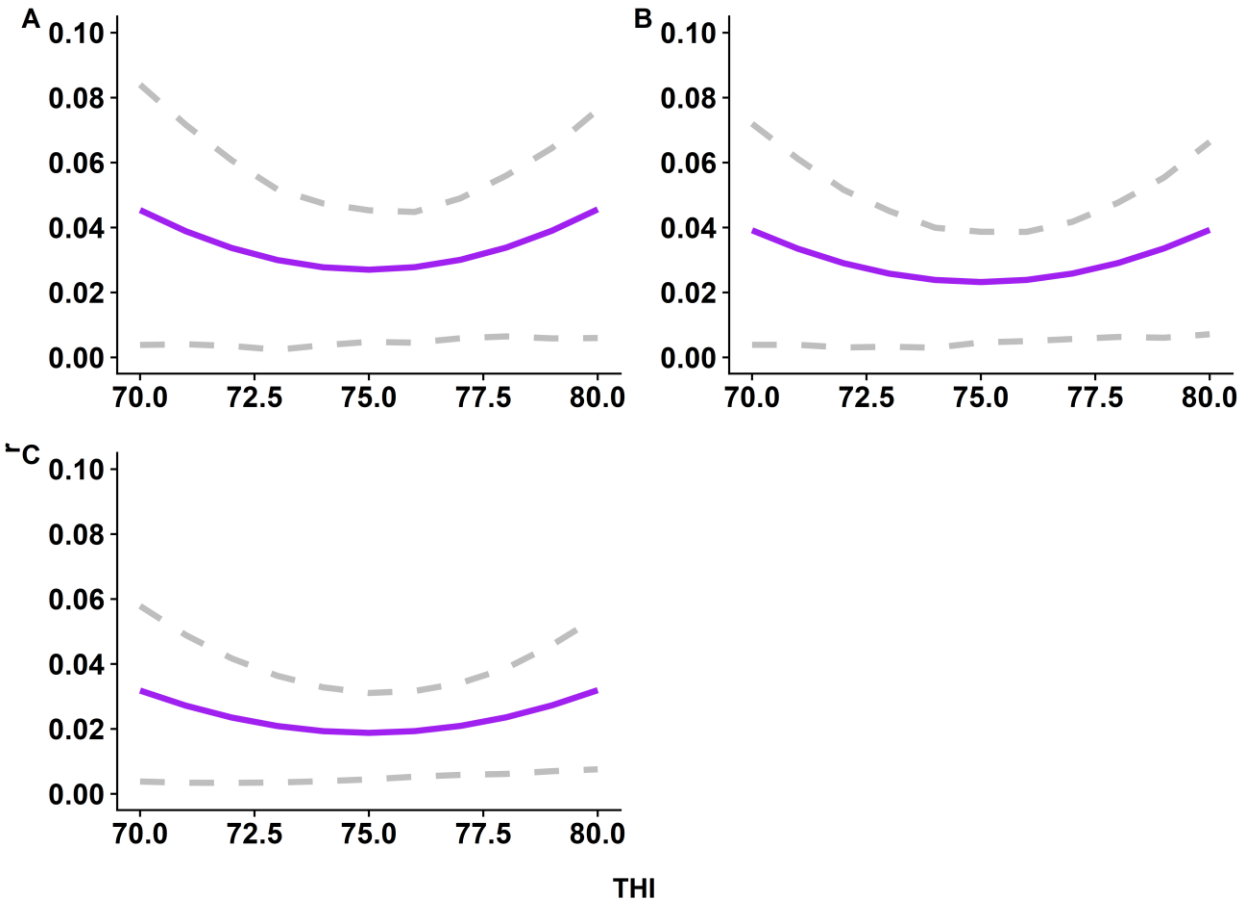

Figure B.4 Repeatability of respiration rate as the temperature humidity index (THI) increases for groups 4 (A), 5 (B), and 7 (C). The purple line indicates posterior mean point estimates for each value of water restriction and the gray, dashed lines are the 95% highest posterior density credible intervals for each value of THI.